



THE UNIVERSITY OF
NEWCASTLE
AUSTRALIA

**ARC CORROSION & ODOUR
LINKAGE PROJECT
(LP0882016)**

**Identification of controlling factors for the
corrosion rate of concrete.
(SP1B)**

**Dr Tony Wells
Centre for Infrastructure Performance and Reliability
The University of Newcastle**

Final Report



Table of Contents

Contents

1	Introduction	7
1.1	Background.....	7
1.2	Objectives.....	9
1.3	Outline of report.....	9
2	Project Overview.....	10
3	Activity 1: Survey of available corrosion data.....	12
3.1	Introduction.....	12
3.2	Industry data.....	12
3.2.1	Sydney Water Historical Data	12
3.2.2	Melbourne Water Historical data	34
3.3	Data in Scientific Literature.....	39
3.4	Summary of Activity 1 outcomes.....	40
4	Activity 2: Concrete characterisation	41
4.1	Introduction.....	41
4.2	Objectives.....	41
4.3	Concrete characterisation methodologies.....	42
4.3.1	Mineralogical and pore size distribution	42
4.3.2	Concrete aggregate content and density determination	42
4.3.3	Acid neutralisation capacity (ANC) curves determination.....	43
4.4	Concrete characterisation results	45
4.4.1	Mineralogical analysis	45
4.4.2	Pore size distribution (PSD)	47
4.4.3	Aggregate content and density results.....	48
4.4.4	Acid neutralisation capacity results	49
4.5	Summary of Activity 2 outcomes.....	58
5	Activity 3: Sp1B Field Corrosion Trials	60
5.1	Introduction.....	60
5.2	Objectives.....	60
5.3	Methodology.....	60
5.3.1	Field samples.....	60
5.3.2	Field sites	62

5.3.3	Recovery of field samples	68
5.3.4	Photogrammetric evaluation of the amount of corrosion product formed and the amount of sound concrete lost.....	69
5.3.5	pH survey of samples.....	74
5.3.6	pH profiling	75
5.3.7	Collection of Environmental data for the three field sites.....	76
5.4	Field study results.....	78
5.4.1	Environmental observations	78
5.4.2	Analysis of recovered coupons	85
5.4.3	Calculation of acid consumed during the corrosion of the field samples	123
5.5	Summary of Activity 3 outcomes.....	128
6	Activity 4: Modelling the corrosion of concrete sewer pipe.....	130
6.1	Introduction.....	130
6.2	Objectives.....	131
6.3	A physical representation of the corrosion process	132
6.3.1	Timeline for the corrosion of concrete sewer pipe.....	132
6.3.2	Time dependence of the corrosion rate function	138
6.3.3	The spatial nature of the corrosion process	139
6.4	Phenomenological model of concrete sewer pipe corrosion	145
6.4.1	Framework for the 1D model.....	145
6.4.2	Operation of the 1D model	149
6.4.3	1D modelling results	150
6.5	Factors impacting the rate of corrosion	152
6.5.1	Impact of H ₂ S concentration in the sewer headspace	152
6.5.2	Impact of sewer gas temperature.....	158
6.5.3	Impact of humidity.....	159
6.5.4	Impact of sewer pipe wall temperature.	165
6.5.5	Impact of position around the sewer circumference.....	168
6.6	Concrete sewer pipe service life estimation.....	169
6.6.1	Introduction	169
6.6.2	Time to initiation of corrosion losses (t_{in})	170
6.6.3	Calculation of the corrosion rate (CR).....	173
6.6.4	An example calculation of the service life of a concrete sewer pipe	178
6.7	Summary of Activity 4 outcomes.....	184
7	Practical Outcomes and Conclusion.....	189

8	Recommendations for future work.....	191
9	Appendices.....	192
10	References.....	286

Executive Summary

This report outlines the findings of sub-project 1B (Sp1B) "Identification of controlling factors for the corrosion rate of concrete" which is part of the Sewer Corrosion and Odour Research (SCoRe) project funded by the ARC Linkage grant (LP0882016) and various Australian water utilities. The work for Sp1B was conducted by Dr Tony Wells at the Centre for Infrastructure Performance and Reliability (CIPAR), The University of Newcastle, Australia, with in-kind and other support provided by Sydney Water Corporation, Melbourne Water, Water Corporation and SA Water.

The aim of sub-project Sp1B was to develop a more complete physical and quantitative understanding of the corrosion of reinforced concrete sewer pipe such as used extensively in sewer networks in Australian cities. The research program included field and laboratory work and from the insights gained from this work tools were developed to improve prediction of the expected service life of concrete sewer pipes under given environmental conditions. Specifically the sub-project sought to:

1. Determine the relationship between sewer headspace temperature, humidity and H₂S concentration and the instantaneous corrosion rate of concrete using laboratory and in-situ field studies.
2. Identify the factors controlling sewer pipe corrosion.
3. Develop a mathematical model to predict the corrosion of concrete as a function both of period of exposure and environmental and operational conditions.
4. Develop a simplified rational methodology based on (3) for use by the water utilities.

The primary outcomes are:

- Field trials were conducted in situ in sewers in Sydney, Melbourne and Perth providing data and information for the corrosion behaviour of new and previously corroded concrete sewer pipe samples.
- The field trial results allowed a comprehensive picture of the complete corrosion cycle from pipe installation to pipe failure to be developed for the first time.
- The main features of the concrete sewer pipe corrosion cycle include:
 - For the first 6-24 months after installation (the incubation period) no corrosion losses occur. Initially the pipe surface is too alkaline to support microbial activity but with time acidic gases in the sewer slowly neutralise the alkaline components, allowing corrosion to commence.
 - The incubation period at a given location, t_{in} , is a function of average sewer gas humidity (RH%, %), temperature (T, °C) and H₂S concentration ([H₂S], ppm):

$$t_{in}(\text{years}) = 1.24e - 10 \times [H_2S]^{-0.8} \times \frac{(0.0955 \times RH\% - 9.8044)}{(1 - 0.01245 \times RH\%)} \times e^{(56,000/(8.314 \times (T+273)))} + 0.91 \quad (1)$$

- If sewer gas humidity and temperature are not known t_{in} can be estimated via:

$$t_{in} (\text{years}) = 1.62 - 0.083 \times \ln[H_2S] \quad (2)$$

- In the latter stages of the incubation period the surface pH falls below 9 and fungal and bacterial colonies begin to populate the pipe surface.
- Eventually chemical attack will reduce the pipe surface to pH=6 at which stage damaging corrosion commences, with concomitant loss of concrete.
- This stage involves the escalating production of acids (particularly sulphuric acid) generated by biological activity.
- Once this stage is reached the loss of concrete occurs at a reasonably uniform rate for the remainder of the life of the pipe. The corrosion rate, CR (mm/yr)), at a given sewer location is given by:

$$CR \text{ (mm/yr)} = 458000 \times [H_2S]^{0.5} \times \frac{(1 - 0.01245 \times RH\%)}{(0.0955 \times RH\% - 9.8044)} \times e^{(-30,000 / (8.314 \times (T + 273)))} \quad (3)$$

- Analysis of field, historical industry and literature data has confirmed the general applicability of Eqn. (3). It also shows that the uncertainty is +/- 1.5mm/yr.
- If sewer gas humidity and temperature are not known a first estimate of the rate of corrosion can be obtained by substituting RH=95% and T=22°C to give:

$$CR \text{ (mm/yr)} = 0.56 \times [H_2S]^{0.5} \quad (4)$$

- Eqn. (4) can be significantly in particularly if the actual humidity is in excess of 95%.

A service life prediction tool created in Excel has been developed from Eqns. (1) and (3) for use by industry partners. It predicts the likely service life of sewer pipe for a given set of temperature, humidity and H_2S gas concentration conditions. The same Excel file can be used to define the optimal sewer operating conditions to produce acceptable corrosion levels (as specified by the user).

The main report provides details on which the above observations and models are based. It also provides an outline of the improved scientific understanding gained during the project of the processes that occur during sewer corrosion and the main influencing factors. In addition it gives details of recommended further work. In brief these are:

Because of difficulties encountered with the Sydney field trials the data pool used to construct the model was limited. The model represented by Eqns (1)-(4) can be improved to become more accurate and responsive to influencing factors by increasing the data base, preferably through further, controlled, long-term exposure trials at more varied locations and during which corrosion losses, temperature, humidity and H_2S concentration are measured.

- Since corrosion losses are heavily impacted by humidity levels continuous monitoring of in-situ humidity levels would be desirable. Also, it would be desirable for model accuracy improvement to improve understanding of the link between concrete moisture content and humidity cycling.
- Further investigation of the effect of the position around the sewer wall on corrosion is considered desirable.

1 Introduction

1.1 Background

Concrete sewer pipe corrodes as the result of chemical (abiotic) and biological processes. Biological processes, (microbial induced corrosion or MIC); are responsible for the majority of the degradation of the concrete matrix. Microbial induced corrosion (MIC) of reinforced concrete sewer pipe is currently considered one of the most serious and costly problems currently affecting the world's sewerage infrastructure. Globally, the losses due to MIC breakdown of sewer piping are estimated to be in the order of billions of dollars per year [1]. In Germany alone the estimated cost for the repair of MIC degraded sewer pipe is in excess of \$50 billion [2]. In Flanders, Belgium, biogenic corrosion of sewers represents approximately 10% of the total sewage treatment cost [3]. Throughout the Los Angeles county district an estimated 200km of corroded pipe needs to be replaced at a cost of more than \$500 million dollars [4]. In Australia the total value of wastewater assets is approximately \$40billion of which 70% is tied up in ~110,000 km of sewer piping and channel that service the residential and industrial sectors of the community. The annual repair cost to redress MIC damage to this system is tens to hundreds of millions of dollars per year.

The incidence of corrosion of concrete sewer pipe was first studied towards the end of the 19th century in the USA by Olmsted and Hamlin [5] who noted that a white pasty material formed on corroded sections of concrete sewer pipe. They concluded that sulphuric acid was the corrosive agent but the link between the occurrence of the acid and the presence of H₂S in the sewer system was not recognized until some decades later [6]. At this time it was believed that the oxidation of H₂S to form H₂SO₄ was a purely chemical process which occurred in the presence of oxygen in the sewer headspace [7]. In the 1940's a conceptual understanding of the biological nature of the concrete corrosion process was established through systematic work undertaken in Australia and the USA [8, 9], [10] when the bacterium "Thiobacillus concretivorous", (later renamed Acidithiobacillus Thiooxidans, (Kelly and Wood [11])), was identified amongst the acidic corrosion products.

MIC of concrete sewers was not regarded as a significant issue until the 1980's when a manifold increase in the corrosion rates in sewers in the USA [12] and Europe [13] was observed. At this time government authorities were imposing tighter limits on the nature and toxicity of industrial wastewaters to be discharged to the sewer system (via the US Clean Water Act and EPA pre-treatment programs). This led to significantly lower levels of biologically toxic metals such as lead, chromium, mercury, arsenic and cadmium in the sewer system and as a consequence bacterial levels (and consequently MIC) increased dramatically [4]. Increases in MIC were also linked to increased sewage temperature, (due to increasing use of hot water in domestic situations) and increased use of sulphate containing detergents. Increases in bacterial activity also accompanied the general increase in sewer line lengths (and hence sewage residence times) that have accompanied the growth of suburban populations [14]. The increase in the severity of the MIC problem has led to a renewed interest in the

processes involved. This new work has revealed the complexity of the corrosion cycle as well as the involvement of many species of bacteria [15, 16] and fungi [13, 15, 17].

The challenges posed by the increasing influence of MIC has resulted in an increased research effort to improve understanding and quantification of mechanisms underlying the sewer corrosion processes [18-21] including the bacterial population dynamics and kinetics involved [16, 22-24]. Much of the research however has involved laboratory experimentation and has focussed on examining individual facets of the corrosion process. Consequently practical management of sewer corrosion is still hindered by a limited understanding of the in-sewer processes causing sewer corrosion and how those processes evolve with time.

Part of the problem when attempting to model sewer corrosion processes is that they vary over time in a complex fashion. Conditions on the exposed pipe surface change as chemical (abiotic) and biotic processes alter the surface chemistry. In turn surface conditions help determine the nature and magnitude of corrosive activities taking place. This was recognized in the three stage model first proposed by Islander et al. [25] in which concrete sewer pipe corrosion is presented as initially proceeding by chemical (abiotic) acidification of the pipe surface followed by MIC driven by a succession of evolving microbial communities (Figure 1). While the general concept of the Islander model is accepted little quantitative assessment of the Islander model or the corrosion process as a whole, has been undertaken [26]. As a result, management of sewer corrosion is still hindered by a limited understanding of several key in sewer processes [27].

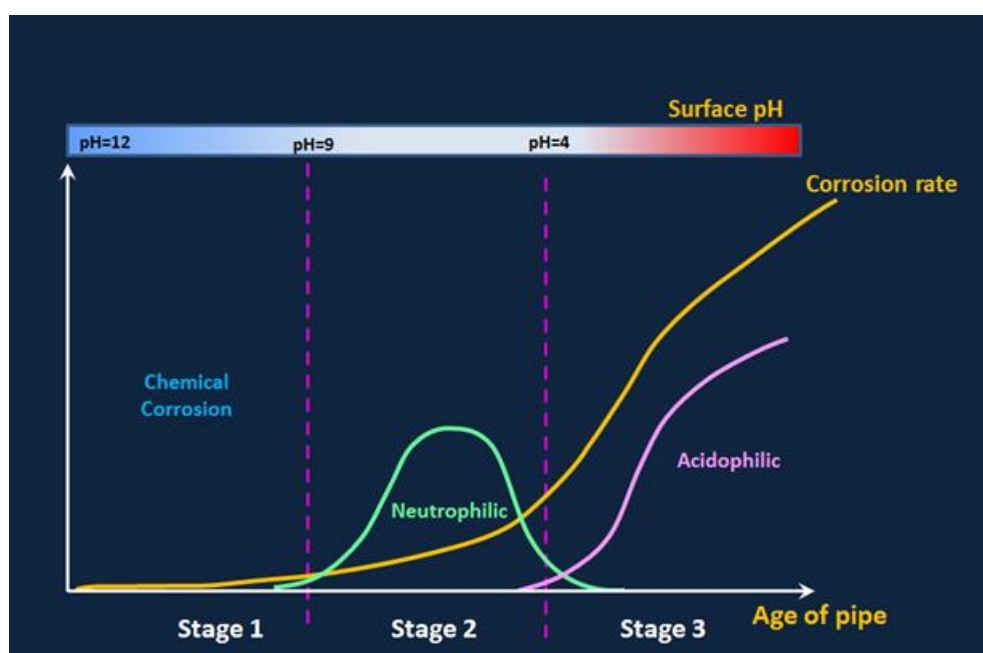


Figure 1. The three stage corrosion of concrete sewer pipe as originally proposed by Islander.
(adapted from [25]).

To predict the service life of a concrete sewer pipe on a scientific basis it is desirable to have an adequate quantitative understanding of the overall process and the various sub-processes involved. However, to date only a limited number of studies have examined the initial stages of sewer pipe corrosion process [26] or even the overall process [16]. The present report details the findings of a 5 year in-field and laboratory study of sewer pipe corrosion reports on advances made in the understanding the process as a whole and details the corrosion models developed as a result.

1.2 Objectives

The objectives of the sub-project Sp1B were as follows:

1. Determine the relationship between H₂S concentration in the gas space, temperature, humidity and the instantaneous corrosion rate of concrete using both laboratory and in-situ field studies.
2. Identify the controlling factors for the sewer pipe corrosion process.
3. Use the insights and data thus made available to develop a mathematical model to predict the corrosion of concrete versus time of exposure and as a function of environmental and operational conditions.
4. Develop a rational methodology that can be used by the industry to estimate the expected remaining service life of concrete sewers under given conditions.

1.3 Outline of report

The report is organised as follows. First, the overall project methodology is described. This is followed by a summary of the methodology and findings of the survey of existing corrosion data, concrete characterisation work undertaken at the University of Newcastle Civil Engineering laboratories and the in-situ field work program. The report then describes insights gained into the overall as well as the individual corrosion processes. This is followed by a description of the development of the corrosion model based on the new knowledge gained about the corrosion cycle. Finally a short Discussion, Conclusions and Recommendation for further work are presented.

During the course of the present work, some 20 Quarterly Project Reports, 8 Detailed Technical Sub-project Research Reports and one Final Report were delivered. These contain all the technical details of the sub-project. Findings of this study were also published in a number of journal and conference papers in the general scientific literature [27-30]. A summary of the main findings of this project are also available through the SCORe project knowledge management system. Readers are referred to these reports and publications for detailed scientific and technical information arising from the project.

2 Project Overview

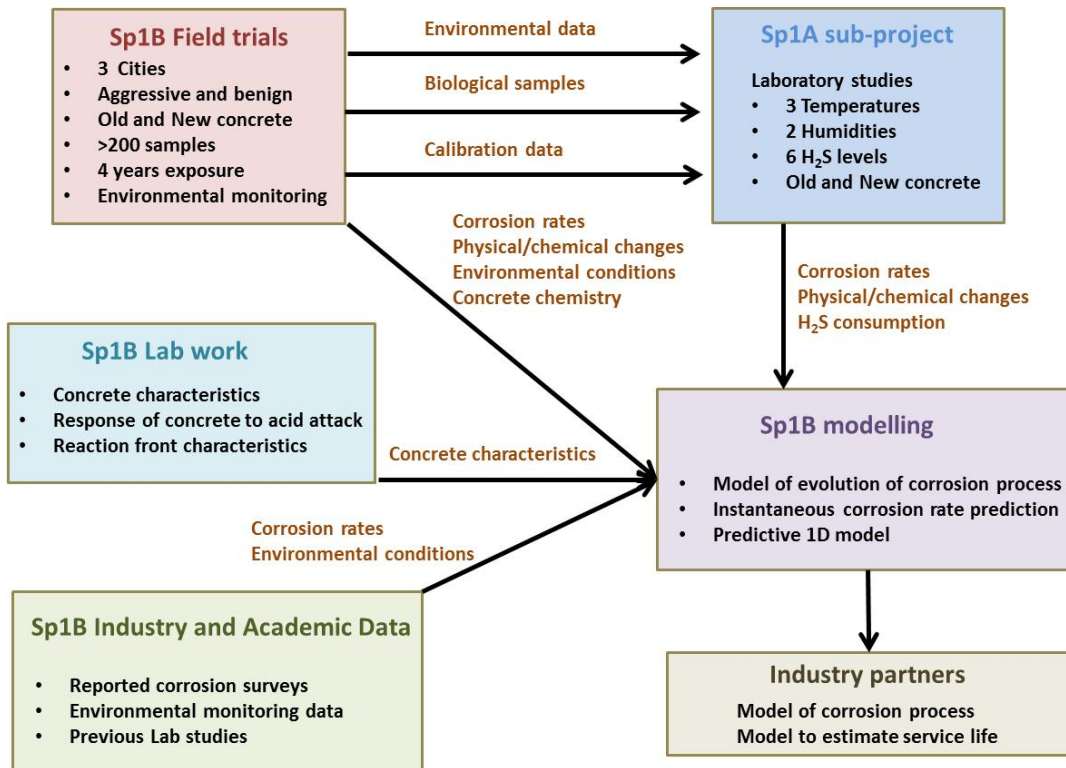


Figure 2. Organisation of information flow for the Sp1B sub-project.

The structure of the sub-project Sp1B is illustrated in Figure 2. The majority of the work shown was conducted by Tony Wells at The University of Newcastle in conjunction with the project's industry partners. The SP1A sub-project work, consisting of a laboratory based experimental program was run in parallel with the field trials and undertaken by personnel at the University of Queensland. Readers are directed to reports from subproject SP1A for further information.

A summary of the activities leading to the development of the corrosion and service life models is given below:

Activity 1: Survey of corrosion data available from Industry and scientific literature sources.

An important source of data for the corrosion modelling was historical data sourced from the scientific literature and the project's industry partners. The industry data principally took the form of corrosion pin measurements (Melbourne Water) and sewer traverses (Sydney Water). Historical records of environmental conditions were also gathered where possible. Sewer conditions (H₂S levels) were determined from a sewer simulation program (SEWEX) where necessary.

A detailed discussion of the data obtained follows in Section 3 of this report.

Activity 2: Concrete characterisation.

A number of laboratory experiments were conducted as part of the Sp1B sub-project to determine the characteristics of the concrete materials used in this study that impact on the corrosion process. Characteristics examined included density, aggregate content, bulk and surface chemistry, mineralogy and acid neutralisation capacity.

A detailed discussion of the methodology employed in Activity 2 and the results obtained follows in Section 4 of this report.

Activity 3: In situ field study of sewer pipe corrosion.

The aim of this activity was to study the dynamics of concrete sewer pipe corrosion at the initial stages of pipe's service life and also later in the life of the pipe when corrosion was well advanced. Sites across Australia were selected to provide a good range of sewer conditions (H_2S gas concentrations, temperature and humidity) and samples were placed in the sewers for up to 4 years. Samples were retrieved periodically and examined to assess changes in chemistry and mineralogy as well as any loss of concrete suffered over the exposure period. Environmental conditions at the field sites were also monitored throughout the trial period.

A detailed discussion of the methodology employed in Activity 3 and the results obtained follows in Section 5 of this report.

Activity 4: Development of corrosion models.

The ultimate aim of the SP1B sub-project was to develop a model of sewer pipe corrosion that would enable the service life of concrete sewer pipes to be determined for a given set of local sewer conditions. To achieve this it was necessary to develop a physical understanding of how the process evolves over time from the moment the sewer pipe is installed to its moment of failure. The data obtained through activities 1-3 as well as some data generated by the Sp1A sub-project were used to accomplish this. Once a detailed understanding of the process was obtained a phenomenological model of the process was constructed and a methodology for determining the service life of concrete sewer pipe developed.

A detailed discussion of the methodology employed in Activity 4 and the results obtained follows in Section 6 of this report.

3 Activity 1: Survey of available corrosion data

3.1 Introduction

To serve as an input into the modelling process and to complement the findings of the field and laboratory trials data was obtained also from industry reports and from the scientific literature. The industry data was collected from a number of sources, principally from work conducted at Sydney Water and Melbourne Water. Generally it was found that while there was a large pool of corrosion data available there was little corresponding environmental data available to correlate with the losses observed. The following text summarises the findings of the search for historical corrosion records.

NOTE ON CORROSION RATE

In the following and throughout this report the term 'corrosion rate' is the rate of change of corrosion loss (or pit depth) obtained from two successive readings of corrosion loss divided by the time period between the readings. For example the loss of concrete identified at a given location in a sewer in 1997 was observed to be 5 mm and in 2004 at the same location the loss was observed to be approximately 50 mm. Thus the corrosion rate **during this period** for this location is estimated as:

$$\text{Corrosion rate} = \frac{(50 - 5)}{(2004 - 1997)} = 6.4 \text{ mm/yr} \quad (5)$$

In general the corrosion rate estimated from Eqn. (5) will change with time. Note that the corrosion rate given by Eqn. (5) is not the same as the '**average corrosion rate**' often quoted in the corrosion or other literature. For example, for a sewer that started operation in 1990 (when the corrosion loss would have been zero) the '**average corrosion rate**' at year 2004 is $(50 - 0) / (2004 - 1990) = 3.57 \text{ mm/yr}$. This calculation assumes, without justification, that the corrosion process is a linear function of time. In contrast, Eqn. (5) makes no reference to the original starting time. It is concerned only with the '**current**' rate of corrosion. Unless stated otherwise in the text, the meaning of '**corrosion rate**' is that given by Eqn. (5).

3.2 Industry data

3.2.1 Sydney Water Historical Data

3.2.1.1 Introduction

Data sourced from Sydney Water forms the most comprehensive of the data sets obtained from industry. The corrosion data principally is sourced from a series of traverse inspections carried out at regular (5-10 year) inspections of several of the major sewer networks located in the Sydney catchment area. There was also (relatively speaking) a significant amount of environmental data, although as will be discussed shortly, even in the Sydney system, the level of environmental data available is still not sufficiently detailed for accurate modelling of the

corrosion process. The main body of traverse work has been undertaken in the North Georges River Submain (NGRS) and the Southern and Western Suburbs Ocean Outfall Sewer (SWSOOS) sewer lines.

The industry data retrieved will now be discussed for the different sewer systems.

3.2.1.2 Corrosion Loss Observations

North Georges River Submain (NGRS)

The North Georges River Submain (NGRS) services south western Sydney from Fairfield through to Arncliffe (Figure 3). The NGRS is normally divided into two parts: (1) Tangerine St, Fairfield to the Salt Pan Creek Aqueduct (Sections 11 – 4) and (2) the exit of the Salt Pan Creek aqueduct through to the Eve St Merging Chamber at Arncliffe (Sections 3-1). Sections 4 to 11 have been in service for 40-50 years being progressively commissioned from Padstow to Fairfield between 1963 and 1966. Sections 1-3 are considerably older being commissioned from 1944 (sections 1, 2) to 1949 (section 3). Since 1997 a number of traverses of the NGRS have been undertaken (Table 1). Corrosion depths were determined visually along the length of the traverse and generally rounded off to the nearest 5 or 10mm. To determine the rate of corrosion taking place it is necessary to compare the losses observed at a single location at different times.

By comparing the corrosion losses observed in each of the traverses it is possible to build up a picture of pipe corrosion rates down the length of the sewer. Raw corrosion data is listed in Appendix I. Figure 4 shows corrosion losses plotted against location (starting at the furthest upstream location – section 11 manhole 1 -Tangerine St) for the years 1997, 2004, 2009 and 2011.

Table 1. Corrosion data sources for the North Georges River Submain (Sydney).

Date	Section											
	1	2	3	Salt Pan Aqueduct	4	5	6	7	8	9	10	11
1997	[31]	[31]	[31]	[32]	[33]	[33]	[33]	[33]	[33]	[33]	[33]	[33]
2004	[34]	[34]	[34]		[35]	[35]	[35]	[35]	[35]	[35]	[35]	[35]
2009	[36]	[36]	[36]			[36]	[36]	[36]	[36]			[36]
2011					[37]	[37]	[37]	[37]	[37]	[37]	[37]	

The corrosion losses observed in the different traverses (Figure 4) showed a considerable degree of variation from manhole to manhole indicating that local effects (such as possibly local air flow characteristics, pipe wall temperature and localised wastewater turbulence) probably have a significant influence on corrosion activity. It is also apparent that the rate of increase in corrosion depth has been accelerating over time. Over the first 40-60 years of the life of the NGRS pipeline, (from the time of installation (1940's for sections 1-3 and ~mid 1960's for sections 4-11) to 1997 when the first traverse was completed), the total loss of concrete was generally of the order of 2 to 10 mm. Between 1997 and 2004 total losses had climbed to between 10 to 20 mm and 5 years later had climbed further to between 20 to 40-50 mm.

To further illustrate the increase in NGRS corrosion rates over time a site to site comparison of corrosion losses was undertaken to produce a “down the line” map of corrosion rates for the NGRS for the time periods: (Installation) to 1997; 1997-2004; 2004-2009 and 2009 to 2011 (Figure 5). Corrosion rates are also listed in Appendix II. (Note that as more sections of the NGRS were lined they have been excluded from the corrosion survey). It is clear that during the initial stages of the pipe life corrosion rates were low (an average 0.2mm/yr). This period includes the era before the introduction of the clean water act (1970) which had the effect of lowering the levels of bio toxic materials in wastewater streams (in particular heavy metals) which inhibited the activity of H₂S producing bacteria. During this period virtually none of the NGRS was lined. As a result the entire sewer pipe surface was available for the absorption of H₂S. After 1997 progressively more of the NGRS was lined (starting with the most aggressive corrosion locations) until by 2011 only a small proportion of the system remained unlined (in sections 6 and 8).

While the lining process protected the more susceptible sewer locations from further corrosion it also reduced the amount of surface area available for H₂S absorption. In removing this H₂S sink H₂S levels were raised contributing to an acceleration of corrosion at the remaining unlined sites. Consequently corrosion rates at exposed sites increased from 0.2 mm/yr prior to 1997 to 1.4 mm/yr during the 1997-2004 period to 4.1 mm/yr during the 2009-2011 period despite the lining (and subsequent removal from consideration) of the most aggressive corrosion sites during each of those periods.

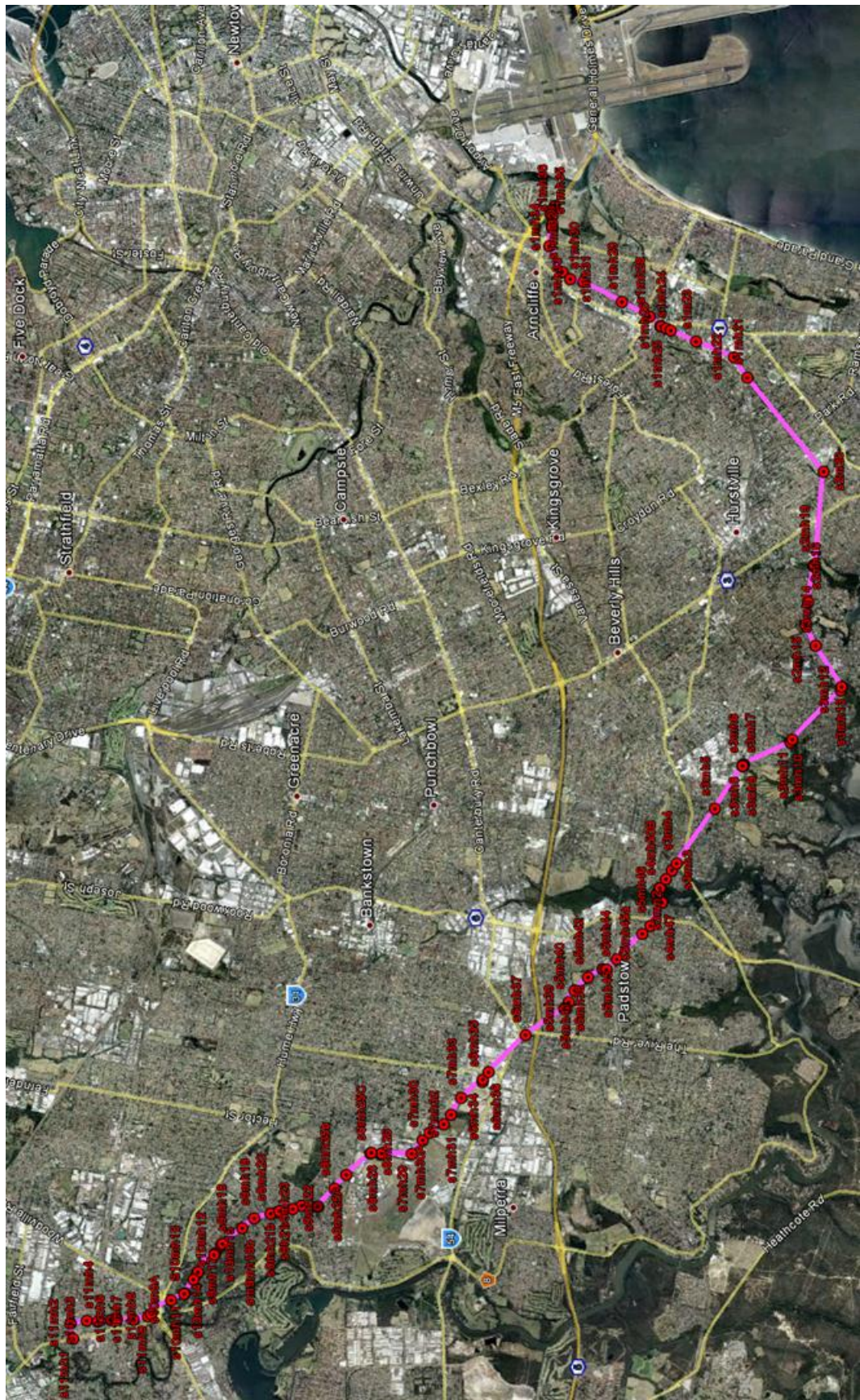


Figure 3. NGRS location (Sydney) with associated manhole positions.

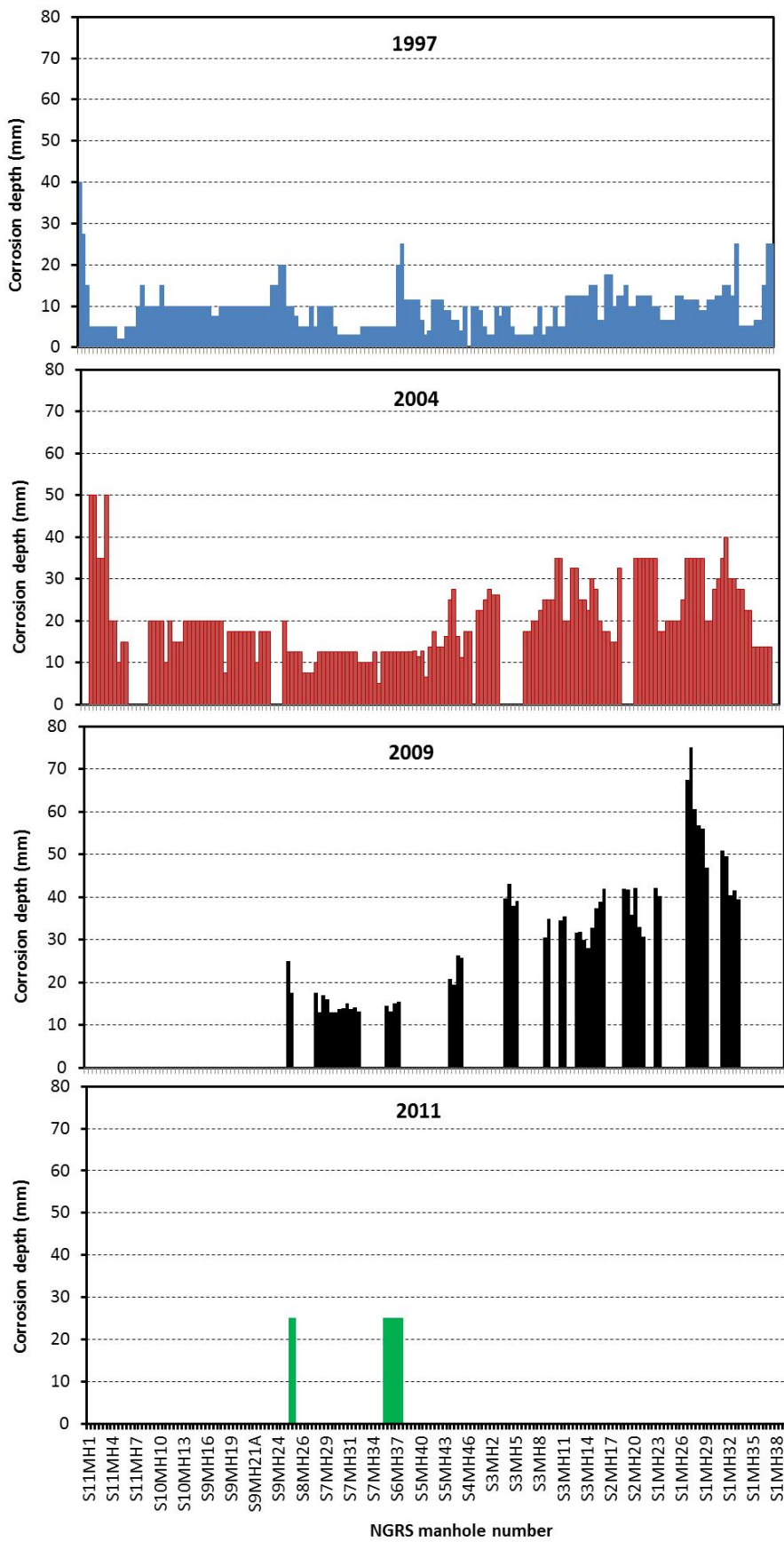


Figure 4. NGRS corrosion losses reported in the 1997, 2004, 2007 and 2011 traverses.

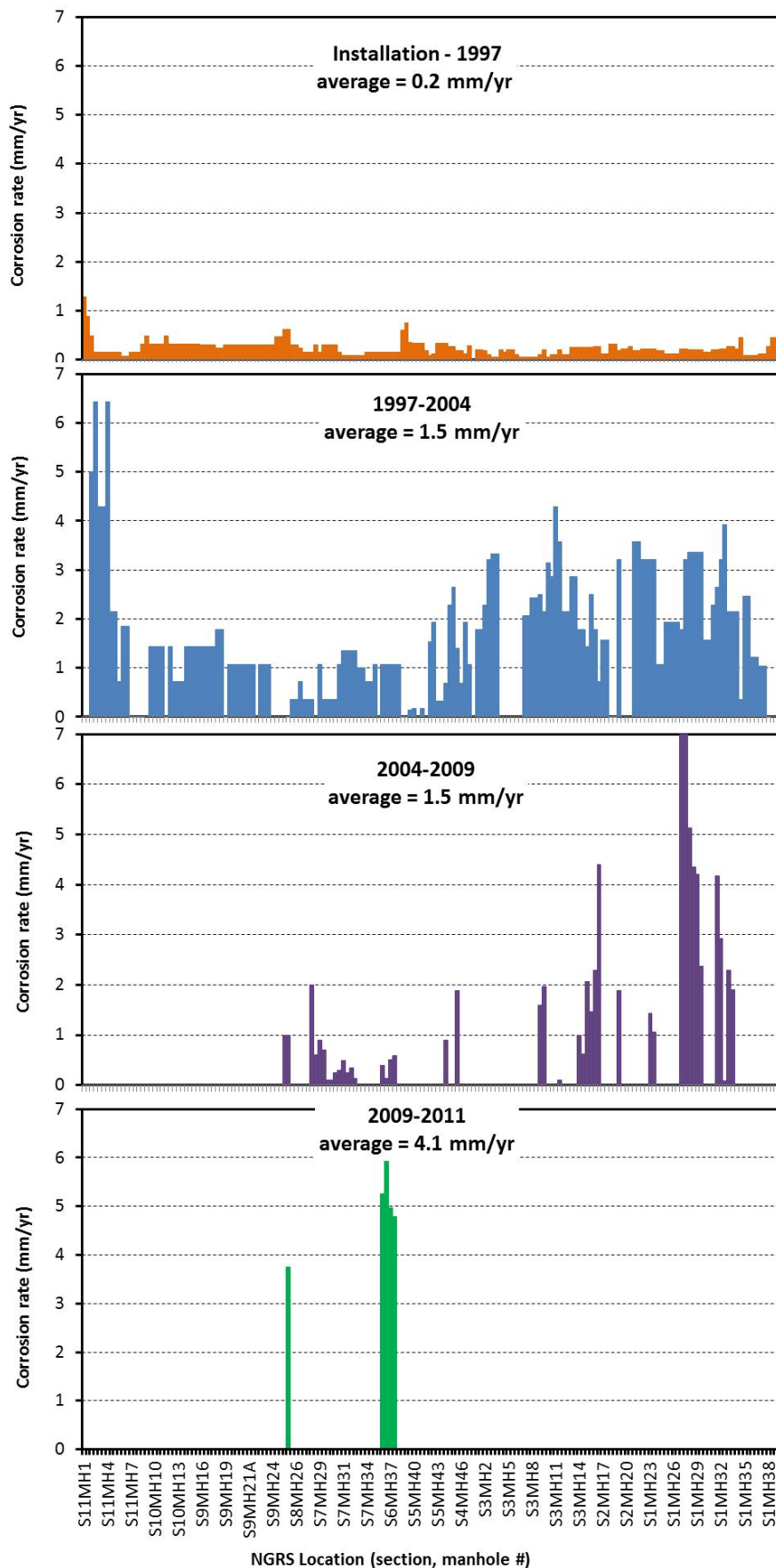


Figure 5. NGRS corrosion rates as a function of location.

Sydney Southern and Western Suburbs Ocean Outfall Sewers (SWSOOS)

The Southern and Western Suburbs Ocean Outfall (SWSOOS) system takes wastewater from the NGRS and also services southern Sydney. It runs between the Eve St merging chamber in Arncliffe through a set of silt traps past Sydney Airport and a set of syphons before proceeding to the Malabar treatment plant (Figure 6). The bulk of the original sewer (SWSOOS1) was constructed in various stages between 1898 and 1916. SWSOOS2 was added in 1941 to facilitate the growing volume of wastewater produced by the growing Western Sydney population.

The SWSOOS lines are normally divided into the sections to the west of the Syphon (where SWSOOS1 and SWSOOS2 run side by side) and those to the east where the two lines separate. SWSOOS2 is made of two sewers running side by side (SWSOOS2N and SWSOOS2S). Traverses of both SWSOOS1 and 2 have been undertaken several times since 1997 (see Table 2 and Table 3). A limited number of SWSOOS2 corrosion loss observations for the period 1966 to 1997 were also sourced from Appendix E of [38].

Table 2. Corrosion data sources for Sydney SWSOOS1 line.

SWSOOS1 Section			
Date	Eve St to Silt Traps	Silt traps to Syphon	Syphon to Malabar STP
1997	[39]	[39]	[40]
2007	[41]	[42]	
2009			[43]
2012			[44]

Table 3. Corrosion data sources for Sydney SWSOOS2 line.

SWSOOS2 North and South Section				
Date	Eve St to Silt Traps	Silt traps to Syphon	Syphon to Barwon Crescent	Barwon Crescent to Malabar STP
1997	[39]	[39]	[38]	[38]
2007	[41]	[42]	[45]	

Raw corrosion loss data and corrosion rate data for the SWSOOS1 and 2 (North and South Cell) lines are listed in Appendix III to Appendix IX. Corrosion losses are plotted against location (from the Eve St Merge to the Malabar treatment facility) for SWSOOS1 (1997, 2007, 2009 and 2012 - Figure 7) and SWSOOS2 south and north lines (1997 and 2007 - Figure 8 and Figure 9 respectively). Earlier losses for SWSOOS2 are plotted in Figure 10.

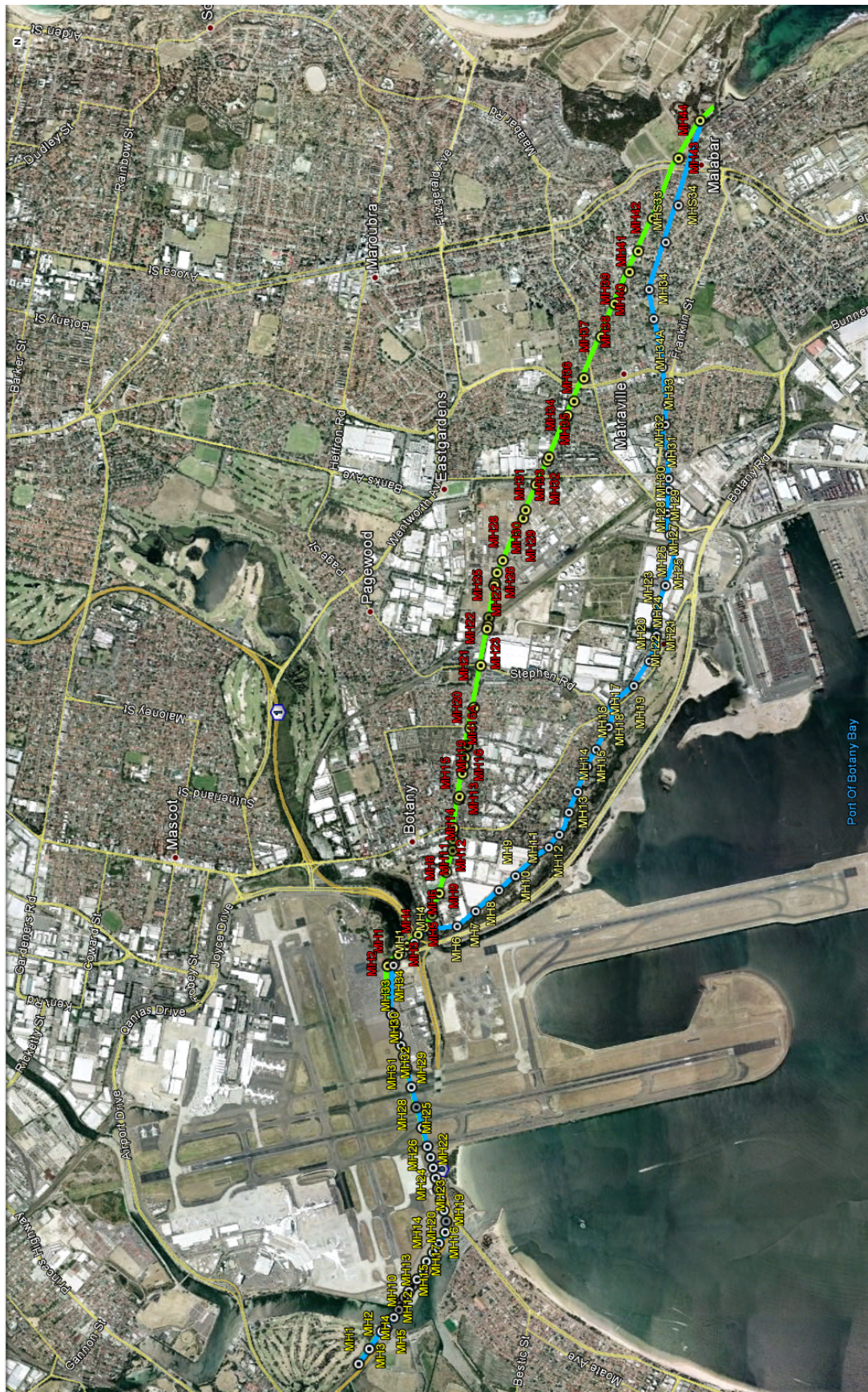


Figure 6. Location of SWSOOS1 (green) and SWSOOS2 (blue) with manhole locations.

Once again the increase in losses over time is apparent. For example losses incurred in the SWSOOS 1 line over the period between the pipe installation (1898 to 1910) to 1997 were in the order of 0-25 mm with average losses of 10mm observed along the length of SWSOOS1. During the next 10 to 15 years losses observed in the unlined sections of the same sewer increased to 20-50mm and as high as 100mm representing a significant increase in corrosion rates. This trend is repeated in the two SWSOOS2 lines (Figure 8 and Figure 9) with average loss incurred along the two sewers from installation to 1997 (~55 years) ranging between of 17 (N) to 22mm (S) increasing over the next 10 years to average losses of 38mm (S) to 40mm (N) over the next 10 years in unlined section of the sewers.

Examination of (scarce) early observations of pipe losses (Figure 10) indicate that for SWSOOS2 at least there was little or no corrosion activity in the system until at least 1970 – the period at which clean water acts were introduced into the country (see earlier discussion). After 1970 an increase in corrosion losses is observed over time with a number of the sites showing an accelerating increase in losses even prior to 1997.

Figure 11 to Figure 14 show the corrosion rates for different periods for the SWSOOS1 and SWSOOS2 lines. As was the case for the NGRS, corrosion rates in all sewer lines increased over time. This again despite the fact that over the study period significant sections of pipe in the more corrosive locations were being progressively lined and thereby excluded from following surveys. The increase in losses is consistent with trends observed for the NGRS and again indicates that lining of the sewer increases rates of corrosion in the remaining unlined sections. By 2007 rates of corrosion in the remaining unlined sections of SWSOOS1 and 2 were of the order of 2-4mm/year (compared to ~4mm/yr for the NGRS in the 2009-2011 period).

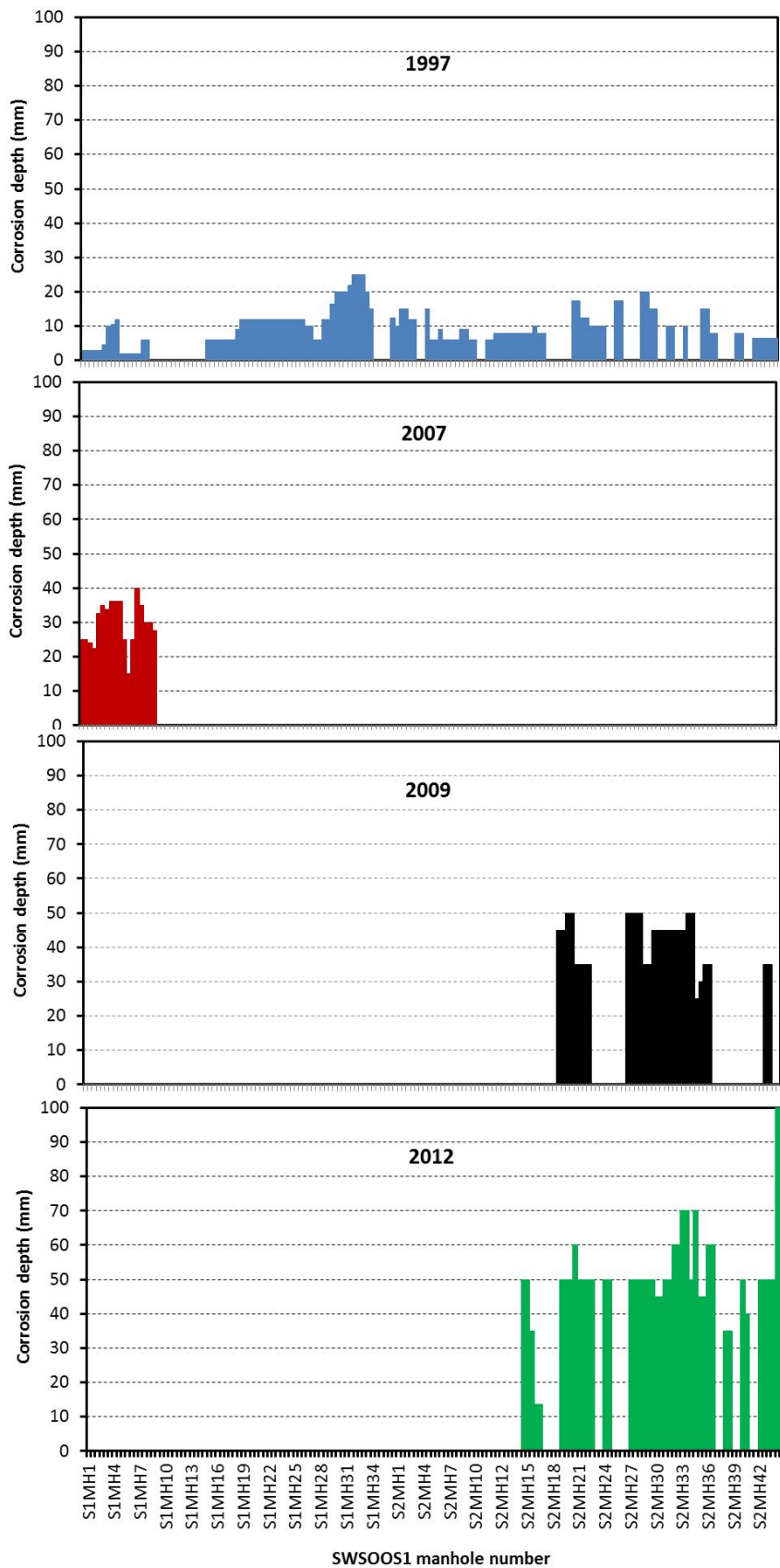


Figure 7. Corrosion losses observed along the SWSOOS1 line.

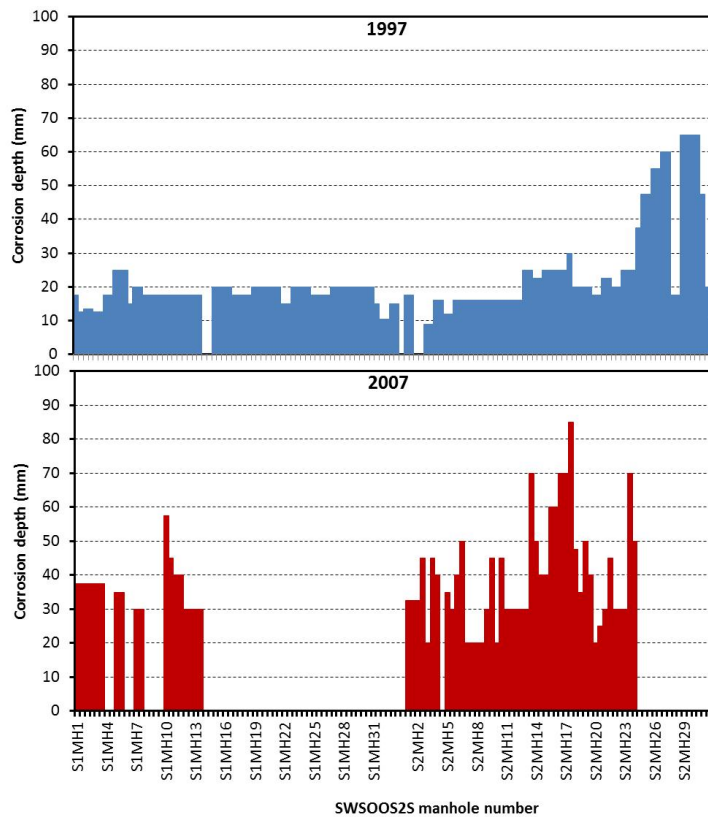


Figure 8. Corrosion Losses observed along the SWSOO52S (south) line.

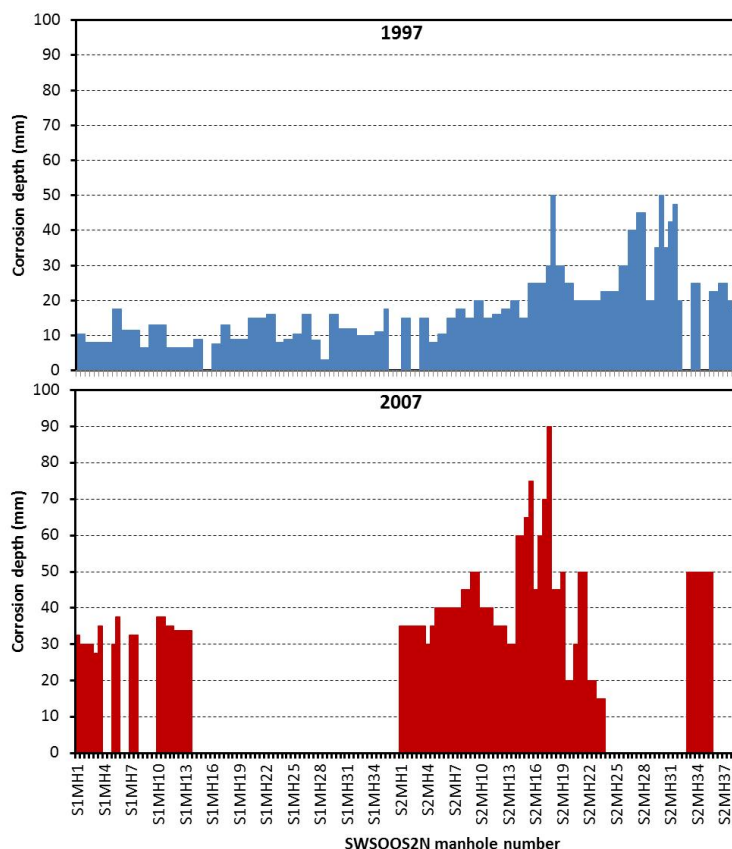


Figure 9. Corrosion losses observed along the SWSOO52S (north) line.

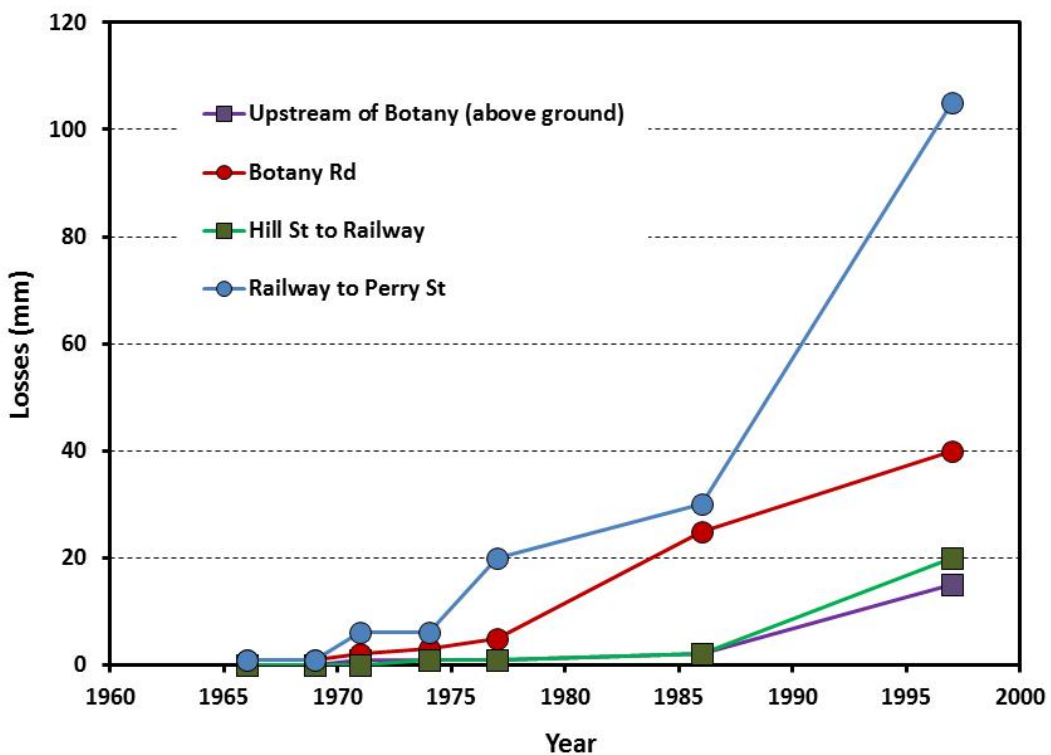


Figure 10. Observed early losses at selected SWSOOS2 sites.

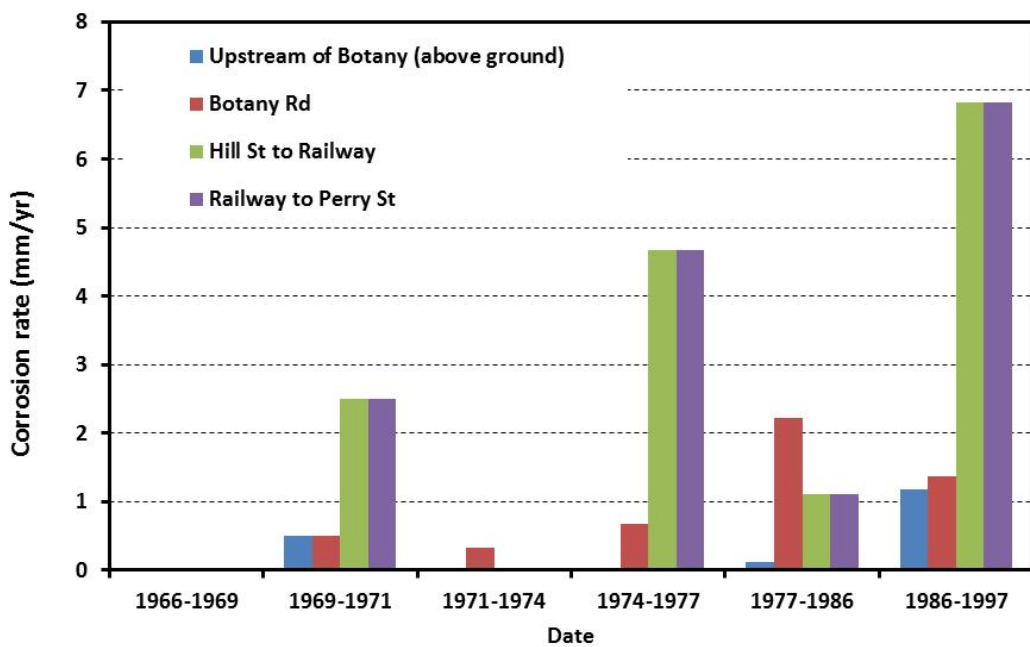


Figure 11. Calculated early corrosion rates at selected SWSOOS2 sites.

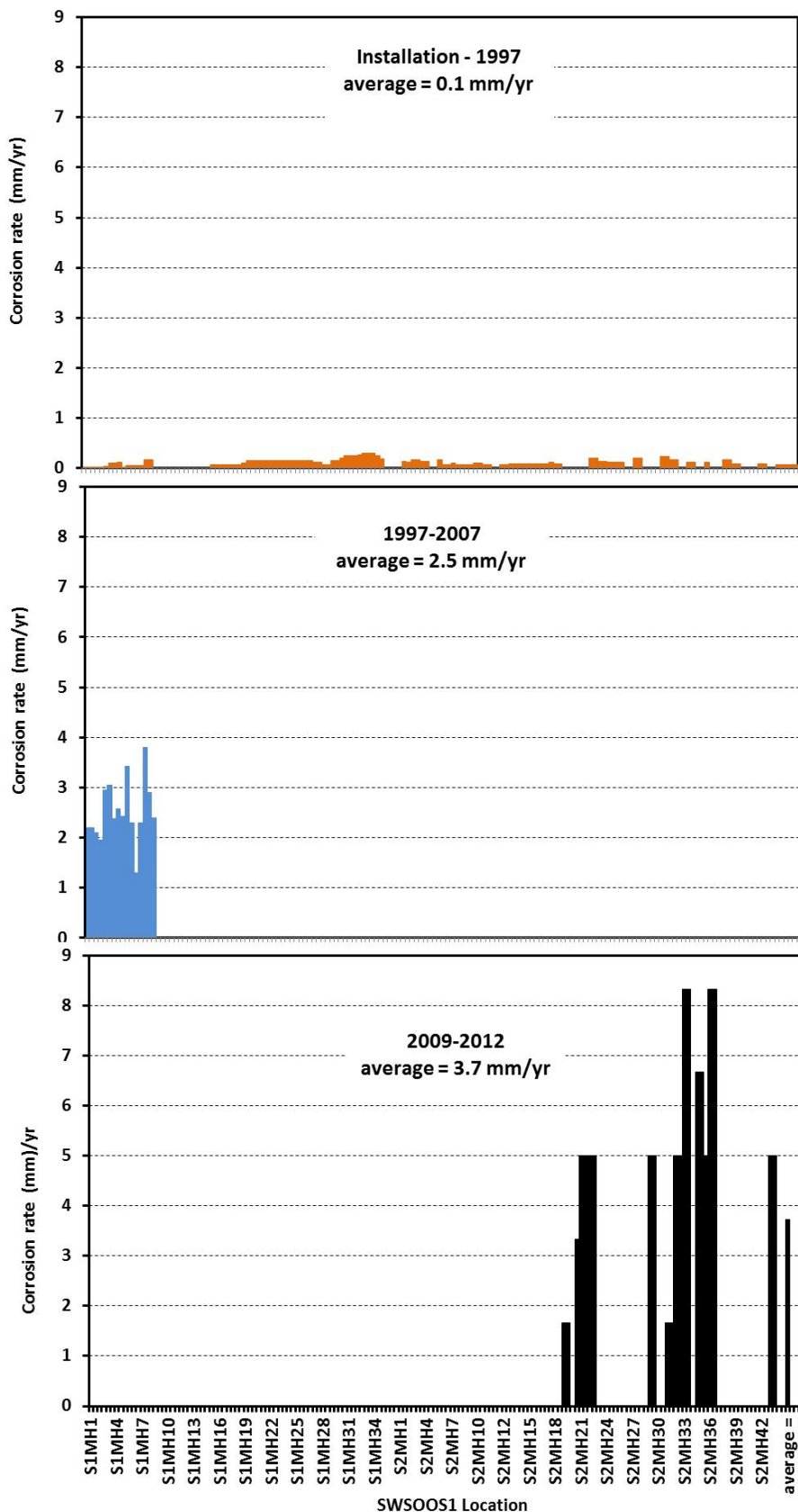


Figure 12. Calculated corrosion rates along the SWSOOS1 line.

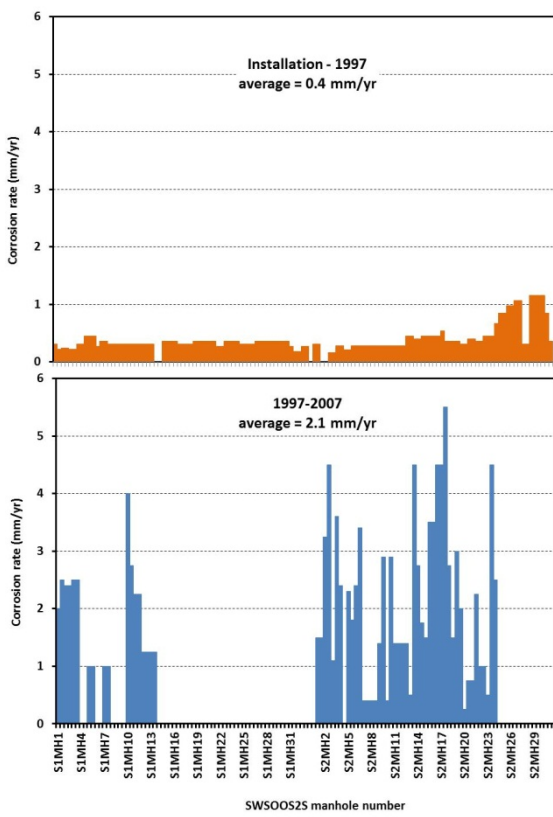


Figure 13. Calculated rates of corrosion for the SWSOOS2 (south) line.

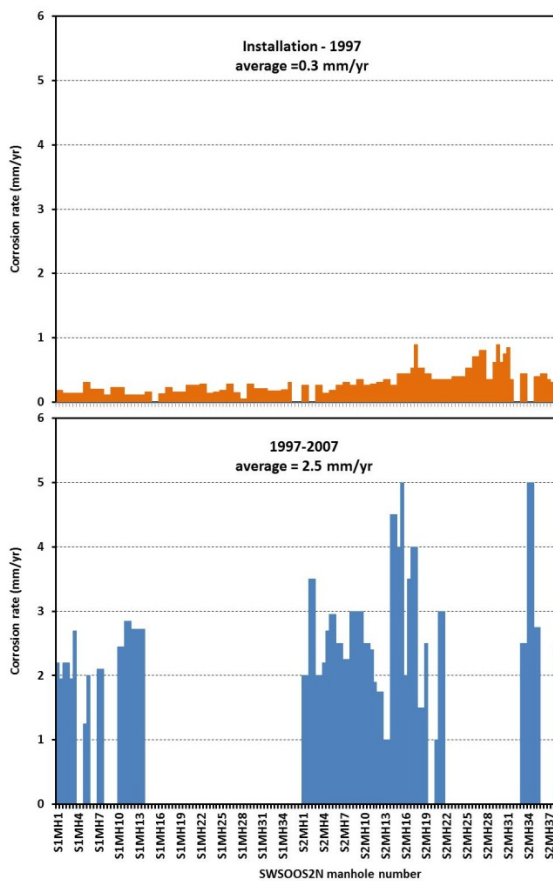


Figure 14. Calculated rates of corrosion for SWSOOS2 (north) line.

Northern Suburbs Ocean Outfall Sewer (NSOOS)

The Northern Suburbs Ocean Outfall (NSOOS) system services 416 sq. km of the northern suburbs of Sydney. The system has its upstream end located near to Wentworthville station and discharges into the ocean at Blue Fish Point. It crosses beneath Middle Harbour and Lane Cove River, and passes through Manly, Mosman, North Sydney, Lane Cove, Hunter's Hill, Ryde, Ermington, Rydalmer, Dundas, Parramatta, Baulkham Hills and Blacktown (see Figure 15). The bulk of the original sewer was constructed in various stages between 1916 and 1933. The areas between Parramatta and Blacktown were constructed between 1933 and 1970.

Traverses of the NSOOS were undertaken in 1997 and various sections re-examined between 2007 and 2010 (see Table 4).

Table 4. Corrosion data sources for the Sydney NSOOS line.

Date	NSOOS Section			
	1-2	3-5	6-7	8
1993	[46]	[46]	[46]	[46]
2007	[47]			
2008		[48]		
2009			[49]	
2010				[50]

Raw corrosion loss data and corrosion rate data for the NSOOS line are listed in Appendix X and Appendix XI. Corrosion losses are plotted against location in Figure 16 while calculated average corrosion rates are plotted in Figure 17. Corrosion losses incurred from the time of construction (1916-1930) to 1993 were generally of the order of 10-20mm. Over all sections an additional 10-30 mm loss was incurred in the following approximately 15 years. This increase in corrosion activity is illustrated in Figure 17. Average corrosion rates for the period before the first inspection were in the order of 0-0.5mm/yr (average = 0.2mm/yr). Subsequent to 1993 however corrosion rates as high as ~7mm/yr were observed with an average over the whole NSOOS line of approximately 1.5mm/yr. The increase in losses is consistent with trends observed for the NGRS and SWSOOS lines.

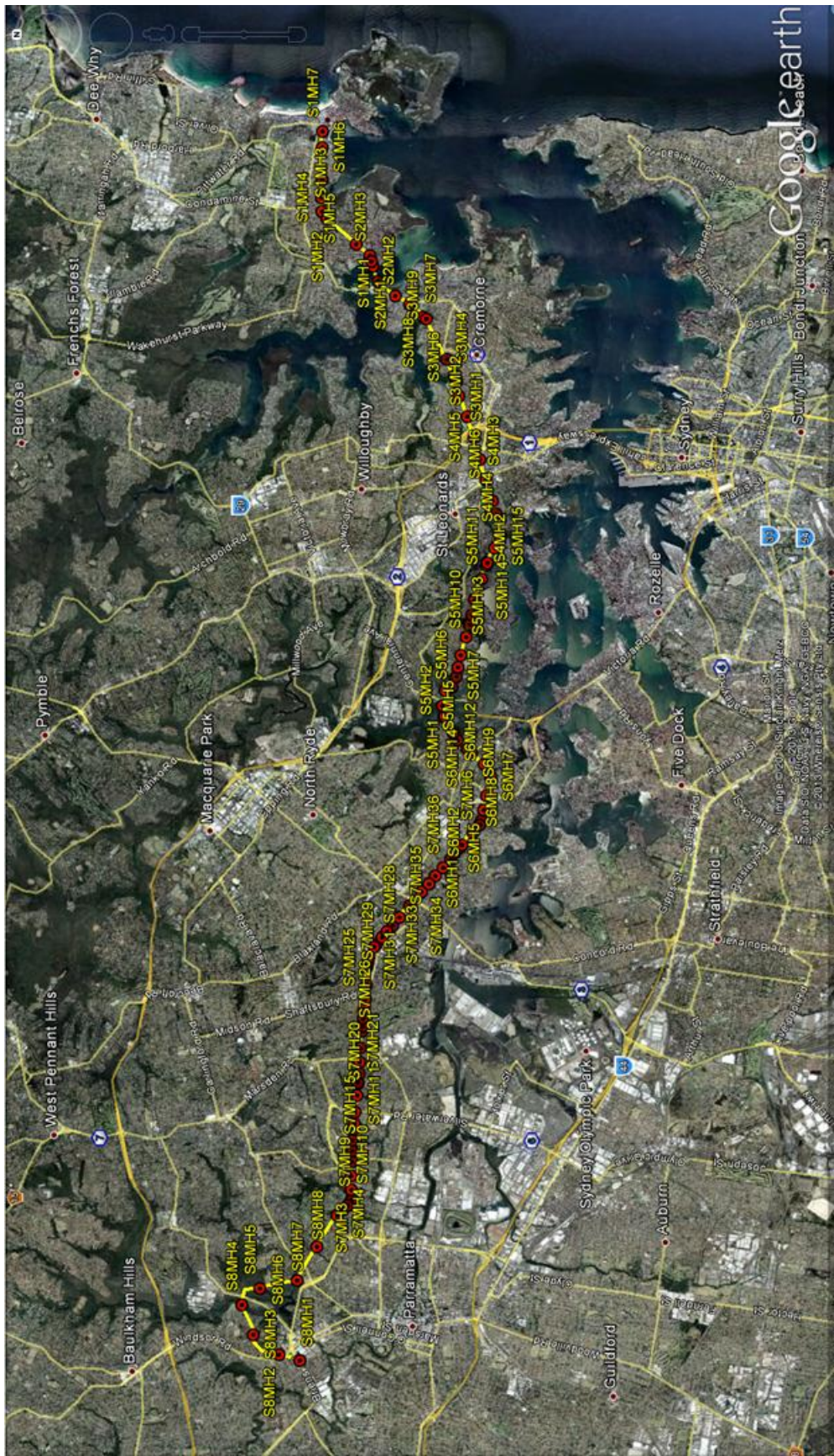


Figure 15. Route taken by NSOOS sewer line. Manhole locations are shown in red.

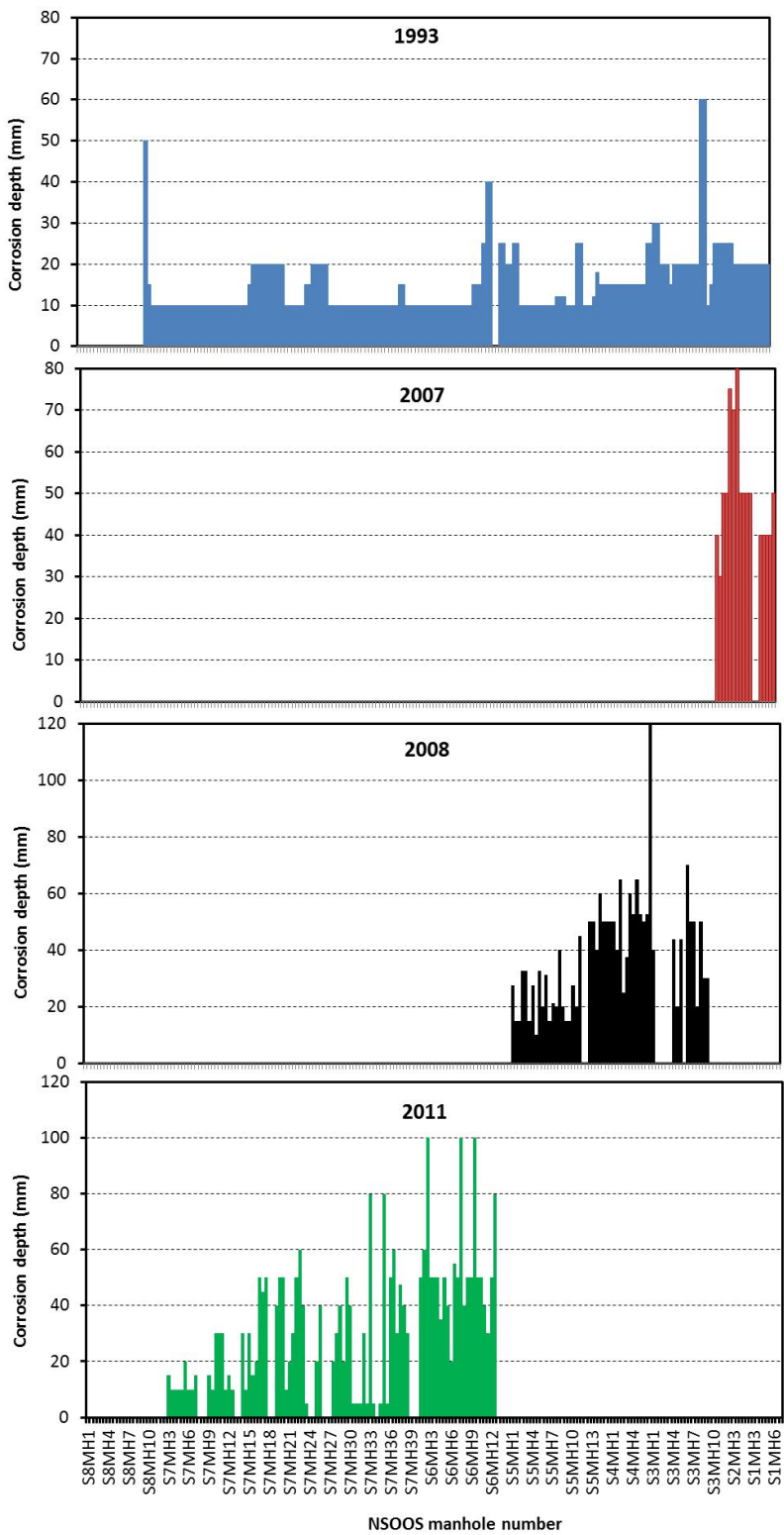


Figure 16. Corrosion losses observed along the NSOOS line.

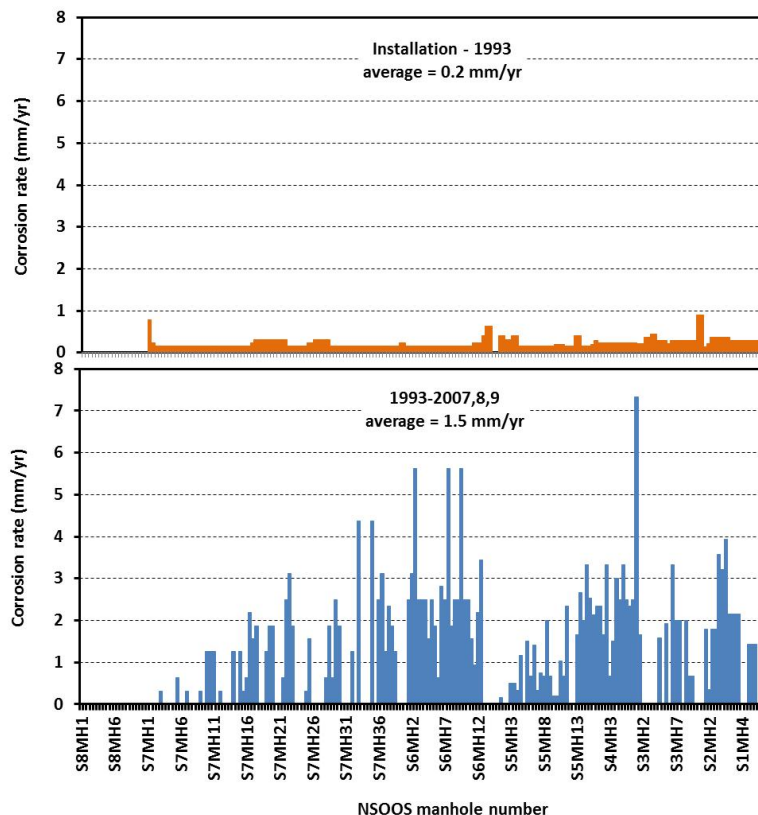


Figure 17. Calculated corrosion rates for the NSOOS line.

3.2.1.3 Sydney Water environmental data

Directly observed data.

Literature, field and laboratory work undertaken in this project have all pointed to three main parameters drivers for the corrosion process: H₂S concentration, temperature and humidity. For the corrosion data to have any meaning it is necessary to be able to match the observed losses with at least the H₂S gas concentration (however H₂S, temperature and humidity data is preferred). Unfortunately there is a limited pool of environmental data to draw upon. Since the year 2000 a number of 'long term monitoring' stations (LTM)s have been set up which enable some estimate of H₂S levels to be made (see Figure 18 for locations and Table 5 for operating details). Odour control units (OCUs) have also recently been put in place which are accompanied by H₂S monitoring. OCU and LTM data are restricted to H₂S and in most cases gas temperature data. No humidity data is recorded throughout the system (with the exception of humidity data recorded as part of the SP1B field work – see Section 5). Environmental data of any type prior to the current round of logging is extremely rare.

Environmental data was generally logged at 5 minute intervals. For the purposes of this study the environmental raw data was collated and averaged on a daily, monthly and yearly basis. 90 and 95 percentile values were also calculated in a similar fashion (table and graphs of data are listed in Appendix XII to Appendix XIV).

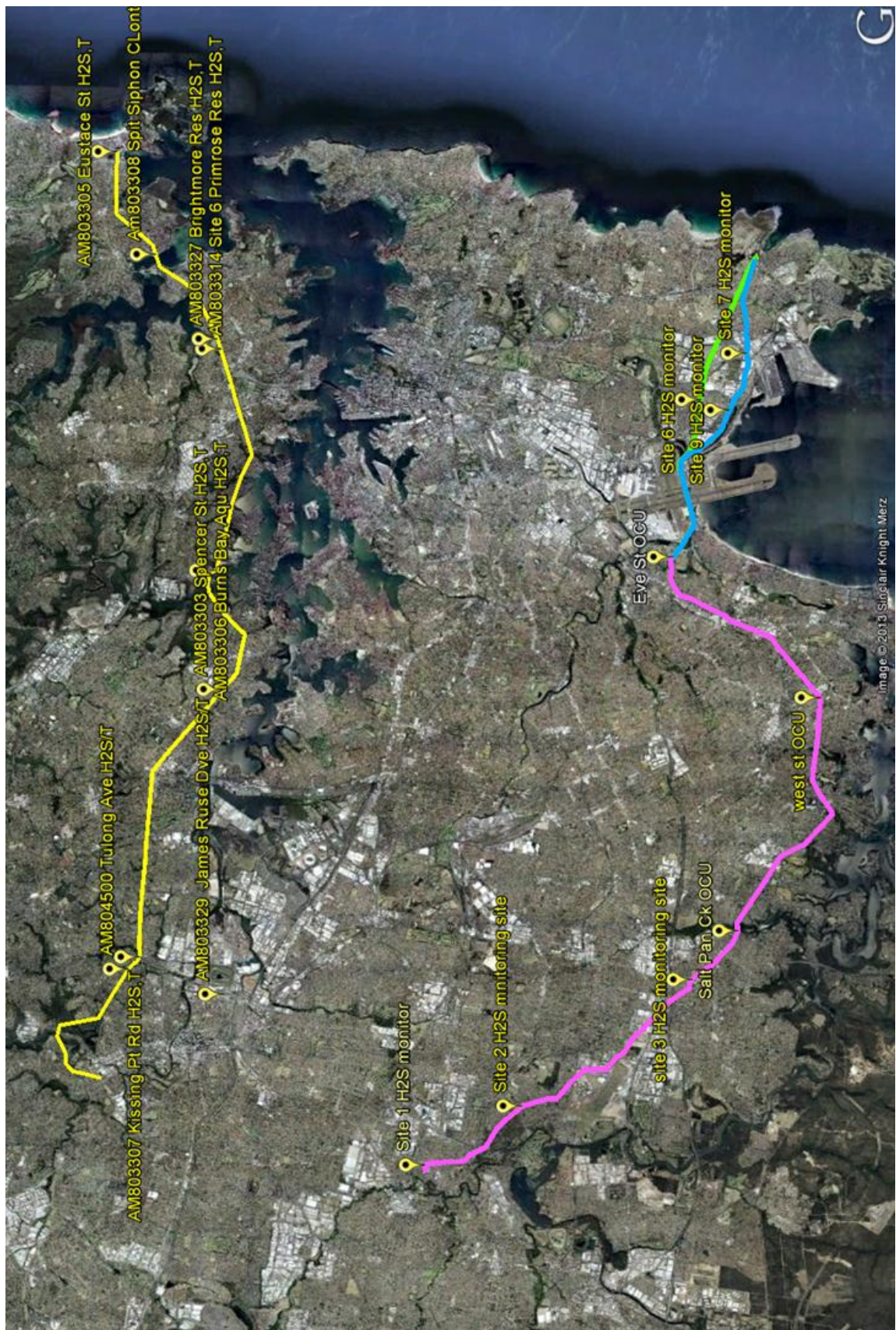


Figure 18. Locations of long term H₂S monitoring sites on the NSWOS (yellow), NGRS (pink) and SWSOOS (green and blue) lines in Sydney.

Simulated data.

While there is a large pool of corrosion data available from the traverse surveys the corresponding amount of environmental data is spatially relatively sparse (for example see Figure 19). Thus while it is possible to correlate corrosion behaviour with H₂S concentration at a few select sites there remains a large number of corrosion observations for which we do not know the underlying environmental conditions that is driving the corrosion observed at this point. (For example what is the H₂S concentration at manhole 11 in section 3 of the NGRS (S3MH11)). To enable the incorporation of these points into the model formulation/calibration a SEWEX simulation run was undertaken to predict the H₂S concentration down the length of the NGRS, SWSOOS and NSOOS sewers. Predictions were made for a baseline period (before dosing (nominally <2003) and after dosing (nominally after 2003)).

Table 5. Location and operating details of Sydney Water monitoring stations.

Sewer Line	Monitoring site	Location	Variables measured	Record of measurements
NGRS	Site 1 LTM	Hercules St, Carramar	Gas phase H ₂ S, T	28/3/2000-31/3/2000 29/6/2004-6/12/2004 6/1/2005-present
NGRS	Site 2 LTM	Caroline Cres., Georges Hall	Gas phase H ₂ S, T	29/6/2004-6/12/2004 6/1/2005-28/8/2008
NGRS	Site 3 LTM	Cahors Rd, Padstow	Gas phase H ₂ S, T	29/6/2004-6/12/2004 6/1/2005-12/8/2008 1/1/2010-present
NGRS	Salt Pan OCU	Salt Pan Ck	Gas phase H ₂ S (inlet/outlet), T	18/11/2004-30/9/2008
NGRS	West St OCU	West St, Hurstville	Gas phase H ₂ S (inlet/outlet), T	18/11/2004-30/9/2008
NGRS, SWSOOS1,2	Eve St OCU	Eve St merging Chamber	Gas phase H ₂ S (inlet), T	22/7/2004-30/9/2008
SWSOOS1	Site 6 LTM	Cnr Swinbourne St and Wilson St, East Botany	Gas phase H ₂ S, T	29/6/2004-31/12/2009
SWSOOS2	Site 7 LTM	Beauchamp Rd, Matraville	Gas phase H ₂ S, T	15/8/2005-18/1/2006
SWSOOS2	Site 9 LTM	Waratah Rd, Botany	Gas phase H ₂ S, T	16/1/2006-present
NSOOS	Site 2 LTM	Tulong Ave, Oatlands	Gas phase H ₂ S, T	1/2/2008-present
NSOOS	Site 3 LTM	Kissing Pt Rd, Oatlands	Gas phase H ₂ S, T	13/2/2007-present
NSOOS	Site 4 LTM	Spencer St, Putney	Gas phase H ₂ S, T	6/6/2008-present
NSOOS	Site 5 LTM	Burns Bay Aqueduct	Gas phase H ₂ S, T	7/11/2007-present
NSOOS	Site 6 LTM	Primrose Pk, Cremorne	Gas phase H ₂ S, T	6/5/2009-present
NSOOS	Site 7 LTM	Brightmore Reserve, Cremorne	Gas phase H ₂ S, T	13/2/2007-present
NSOOS	Site 8 LTM	Spit Syphon, Clontarf	Gas phase H ₂ S, T	13/2/2007-present
NSOOS	Site 9 LTM	Eustace Rd, Manly	Gas phase H ₂ S, T	26/2/2007-present

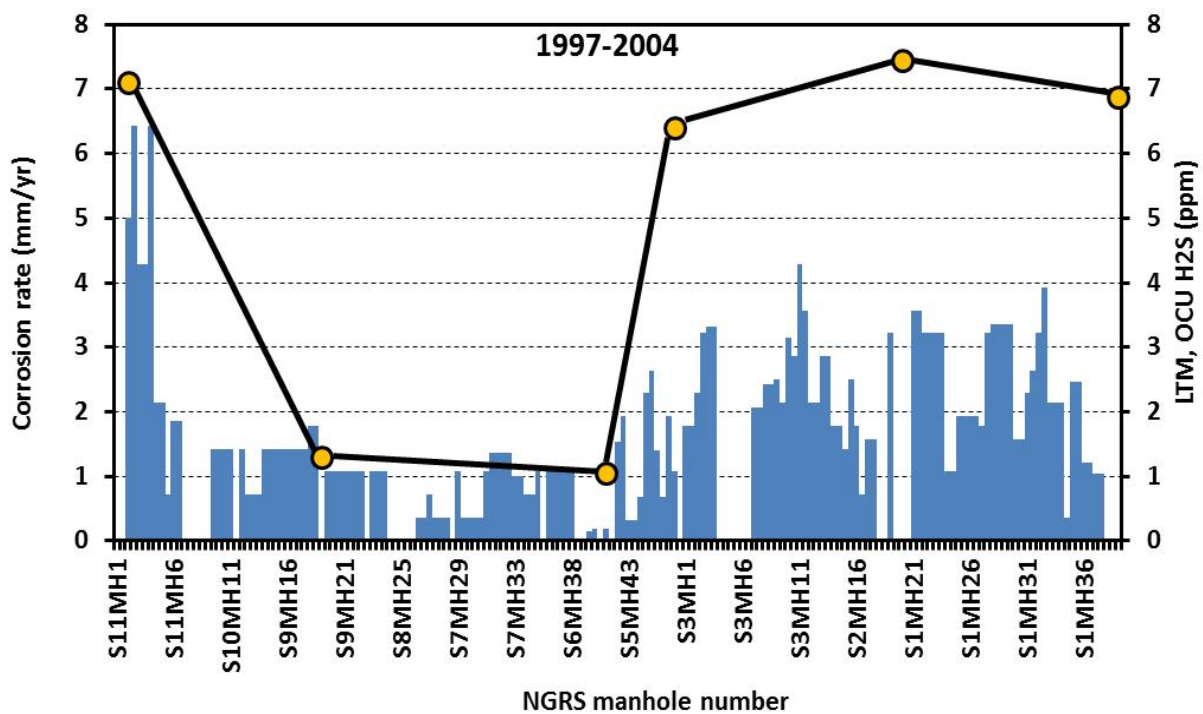


Figure 19. Observed H₂S data and NGRS corrosion rates calculated for the period 1997-2004.

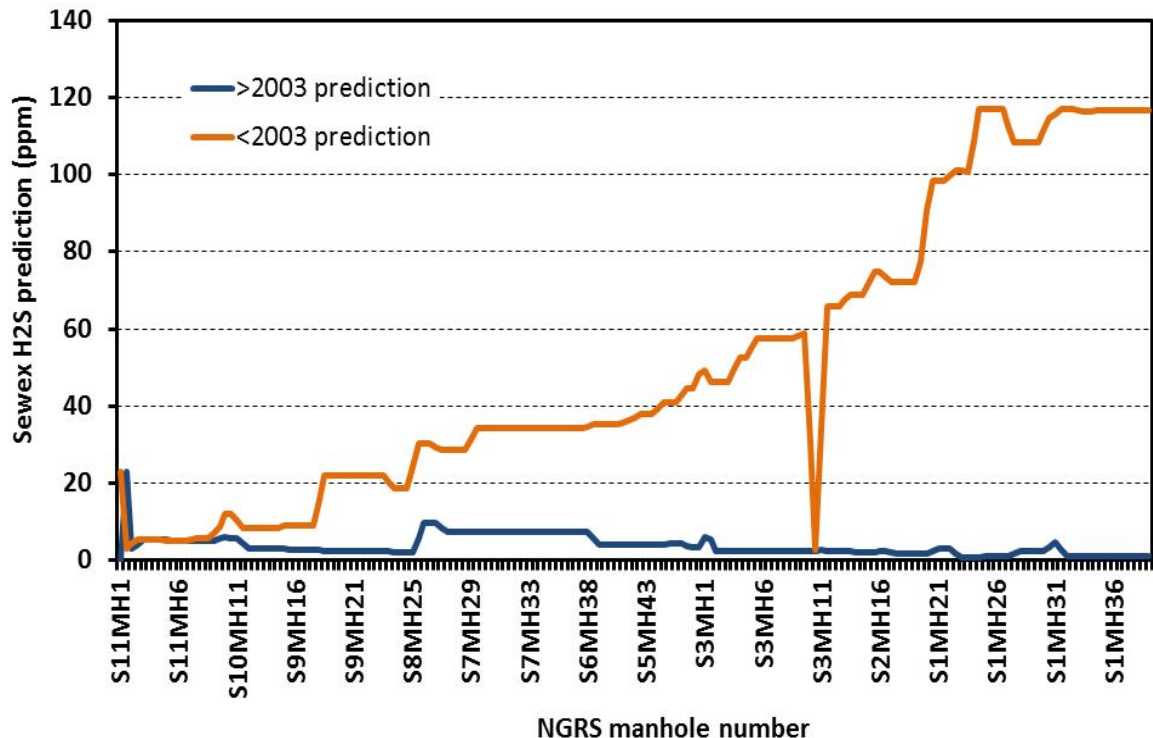


Figure 20. SEWEX predictions of NGRS H₂S concentrations down the length of the sewer.

The predicted H₂S profile for the NGRS system is shown in Figure 20. It is clear in this case (as with the other sewer lines) that the pre- and post- 2003 predictions differ significantly particularly in the downstream portions of the sewer line. To correlate the H₂S conditions at a given site with reported corrosion losses it was sometime necessary to calculate a time based average H₂S level from the two H₂S predictions provided by SEWEX. For example corrosion rates for the period 1997 to 2004 are available for the NGRS system. To estimate the average H₂S levels over this time period weighted average H₂S concentrations were calculated. In this study it is assumed that the rate of corrosion is related to the square root of the H₂S concentration (see Section 6.5.1) consequently when it was necessary to calculate an average H₂S level across a time period the following weighted average of the square roots of the pre- and post- 2003 H₂S predictions were employed:

$$\text{average } H_2S_{t=t_1 \text{ to } t_2} = \left(\frac{\left(\sqrt{H_2S_{t<2003}} \times (2003 - t_1) + \sqrt{H_2S_{t>2003}} \times (t_2 - 2003) \right)}{(t_2 - t_1)} \right)^2 \quad (6)$$

It should be remembered that the SEWEX simulation of the H₂S level represents only an approximation of the actual H₂S conditions. To gain an idea of the accuracy of the SEWEX simulation (>2003) predictions for several Sydney Water LTM and OCU sites were compared to observed values at these sites over time (only post 2003 data considered). As can be seen in Figure 21 SEWEX predictions are reasonable for a number of the monitoring sites however there exists some significant differences (both over and under prediction) between the predicted and observed values at a number of sites. This discrepancy should be kept in mind in future discussion of the correlation between observed corrosion behaviour and (predicted) H₂S conditions.

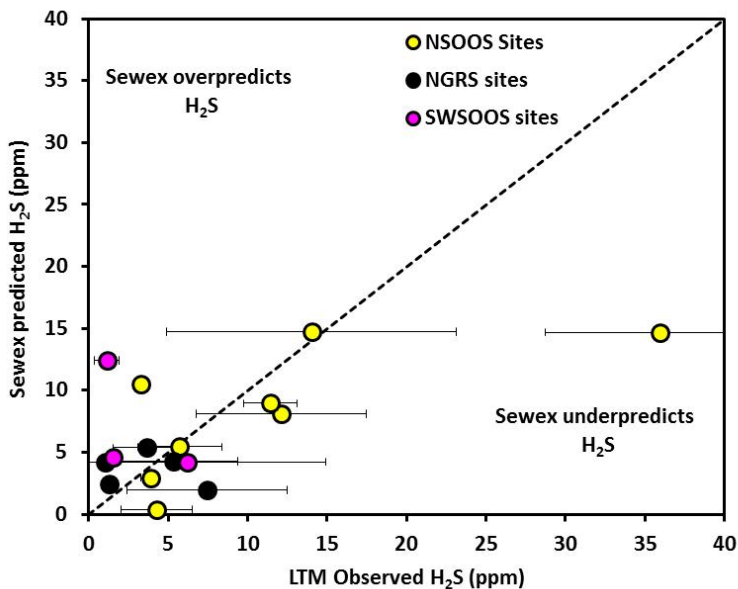


Figure 21. Comparison between predicted and average observed H₂S concentrations at a number of Sydney monitoring sites. Horizontal error bars represent 1 standard deviation of annual averages observed at each monitoring site.

3.2.2 Melbourne Water Historical data

3.2.2.1 Introduction

Data sourced from Melbourne Water consists of some laboratory work undertaken in the 1980's, a small amount of field data measured in the 1960s and a series of erosion pin measurements conducted in the period 1998-2008. Again accompanying environmental data is limited.

3.2.2.2 Corrosion Loss Observations

Melbourne Water laboratory trials

In the early 1980's a laboratory study was undertaken by the Melbourne Water Board's Central Laboratory [51]. In this study a number of concrete mortar "biscuits" were exposed to varying levels of H₂S and moisture. Six chambers each containing 40 biscuits were exposed to air saturated with ammonia, carbon dioxide and H₂S. The temperature of the biscuits were controlled to levels above (dry) or below the air dewpoint (wet). It was reported that when the samples were continually wet corrosion increased rapidly between 3 and 5 ppm H₂S. A cycle of 12 hours dry followed by 12 hours wet did not decrease the corrosion rate however cycles with longer dry periods (3 wet weeks followed by 1 dry week or 2 wet weeks followed by 2 dry weeks) did significantly impede the corrosion process (see Figure 22).

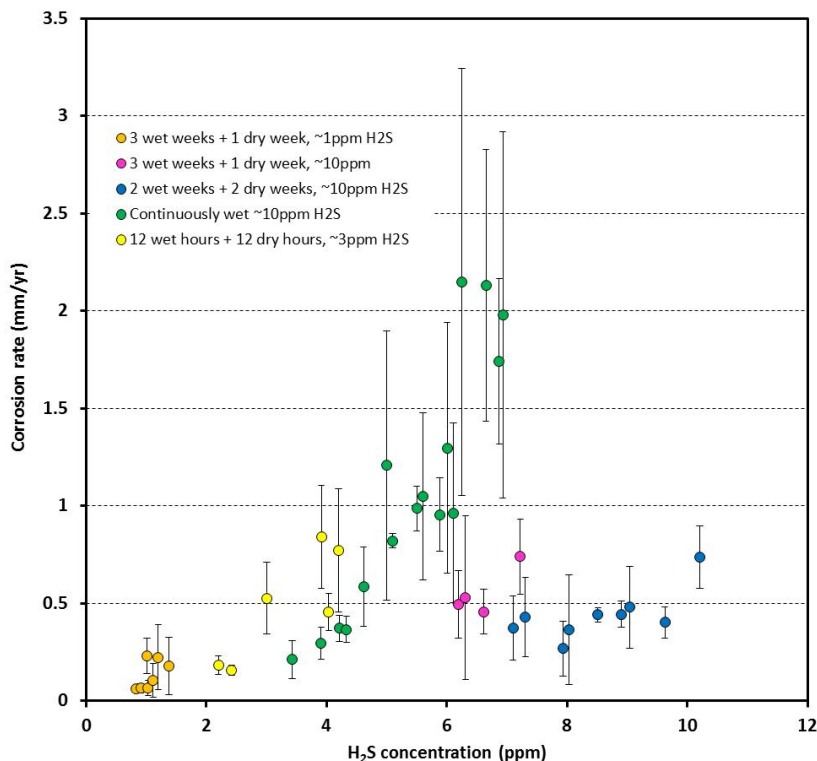


Figure 22. Results of the Melbourne Water laboratory trials (modified from a figure appearing in [51]).

Melbourne field data from the 1960's.

A small amount of field corrosion data measured in the mid 1960's by C.D. Parker is also reported in [51] – and is reproduced in SI units in Table 6. It would appear that the corrosion rates calculated in Table 6 have been determined by one off corrosion loss measurements and not a sequence of measurements such as reported in the Sydney traverse surveys. Consequently the data given is of limited use as it is widely agreed that corrosion rates vary over the lifetime of the pipe and therefore corrosion rates cannot be accurately determined from a single corrosion loss measurement. H₂S levels are reported as typically between 15 to 30 ppm H₂S for the sites in question.

Table 6.Corrosion losses determined from cross-section measurements of the Western Trunk Sewer line (Melbourne) [51].

Melbourne WTS Location	Observed corrosion losses and calculated rates		
	Corrosion depth (mm)	Exposure Period (yrs)	Corrosion Rate (mm/yr)
Werribee Section			
Point 1	76.2	40	1.91
Point 2	117.6	40	2.94
Point 3	127.0	40	3.18
Point 4	120.7	40	3.02
Point 5	95.3	40	2.38
		average=	2.7
Railway Section			
Point 1	64.0	33	1.94
Point 2	117.3	33	3.56
Point 3	57.2	33	1.73
Point 4	31.8	11	2.89
Point 5	31.8	11	2.89
Point 6	35.1	11	3.19
		average=	2.8
Brooklyn Section			
Point 1	50.8	40	1.27
Point 2	63.5	35	1.81
Point 3	101.6	37	2.75
Point 4	95.3	40	2.38
Point 5	54.9	40	1.37
		average=	1.9

Melbourne corrosion pin measurements.

In 1997-1998 Melbourne Water installed a number of stainless steel erosion pins into the walls at a number of sites in both the south eastern trunk sewer (SETS) and the Western Trunk sewer (WTS) systems (site locations are shown in Figure 23). The pins were positioned so that the head of the pins was initially flush with the sewer wall. Over the next 10 years the distance

between the top of the pins and the sewer surface was determined periodically to determine the rate of recession of the sewer wall.

Details of the locations, monitoring period and raw data are listed in Appendix XV to Appendix XVIII. The corrosion rates determined for each location are plotted in Figures 24 and 25.

The calculated SETS corrosion rates were remarkably consistent across the six sites tested with an overall average of $0.23+/- 0.05\text{mm/yr}$. Corrosion rates calculated for the six WTS sites showed more variation with an overall average of $1.56+/- 1.0\text{mm/yr}$. The significant difference between the SETS and WTS corrosion rates is in line with the more aggressive conditions present in the WTS sewer (see discussion in Section 5.4.1).

3.2.2.3 Melbourne water environmental data

The environment data available for the Melbourne sewer system is limited to that obtained during the SP1B field trials (discussed in the Section 5 of this report) and a limited survey of WTS locations conducted in the early months of 2013. Modelling of H₂S levels throughout much of the WTS line has also been conducted.

Directly observed environmental data.

Recording of H₂S and gas phase temperatures has been conducted at a number of sites along the Western Trunk Sewer between the 23rd of January and 13th February 2013. Data was recorded every 5 minutes over this period. As the overall data pool was small only the average values for the whole monitoring period were determined along with the 90 and 95 percentile values (a summary of the data is set out in Appendix XIX). Some data has also been collected for manhole 11 in the South eastern Trunk sewer (the field corrosion site) – this data is reported in Section 5 of this report.

In addition to the observed data a simulation run was conducted to predict H₂S levels along a majority of the WTS line. One set of predictions were made assuming current (as of April 2013) operating conditions and wastewater characteristics matching the analysis of field samples taken in January 2013. A further set of predictions were made assuming the same operating conditions coupled with waste water characteristics akin to that observed in dry years. The predicted H₂S values for the WTS are shown in Figure 26.

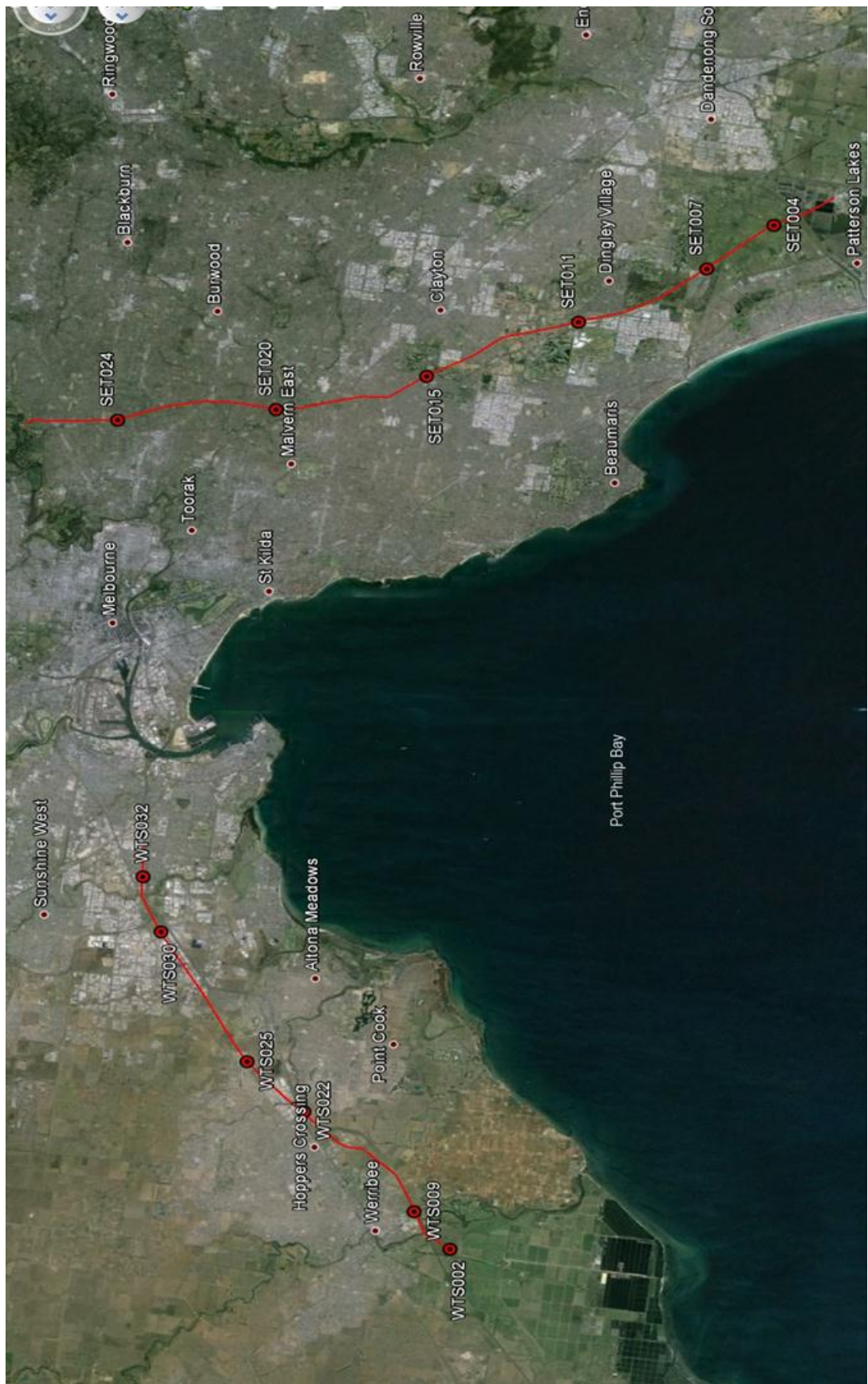


Figure 23. Locations of corrosion pin sites in the Melbourne area.

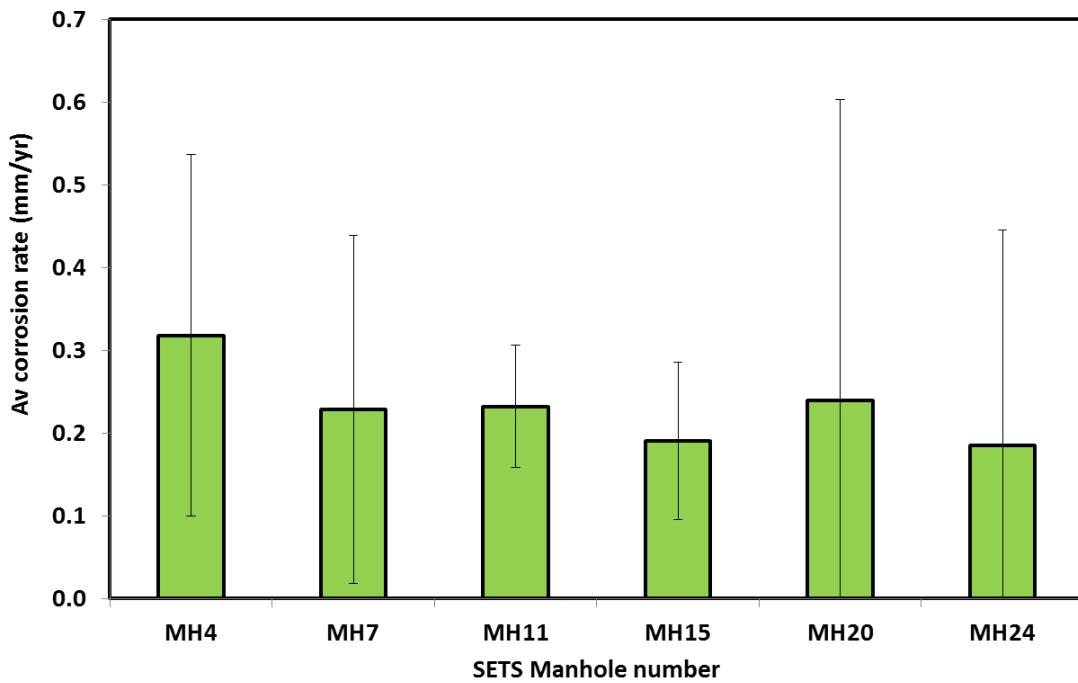


Figure 24. Average rates of corrosion calculated from erosion pin data collected at Melbourne SETS sites.

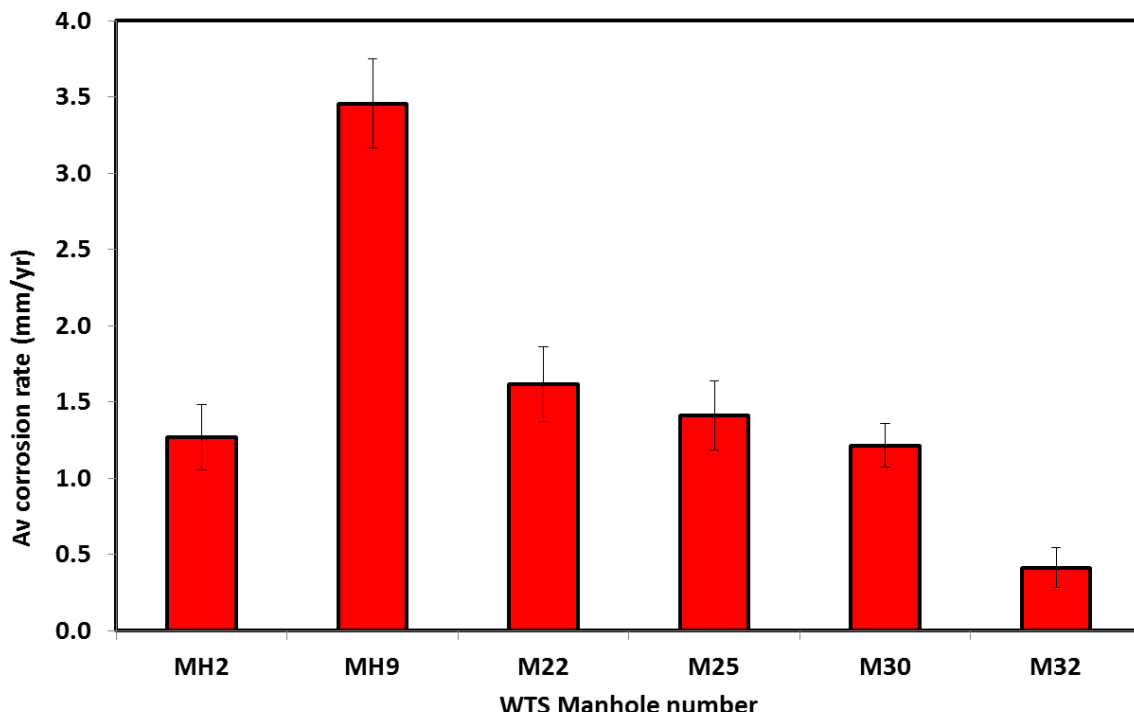


Figure 25. Average rates of corrosion calculated from erosion pin data collected at Melbourne WTS sites.

Simulated H₂S profile data for WTS

Ideally the predictions made using the waste water characteristics determined in January 2013 (the green line in Figure 26) should match the observed H₂S levels (yellow circles in Figure 26) and for a number of locations the agreement is good however at several sites (particularly for manholes 15 and above) the agreement is less satisfactory. Consequently this simulated data also has to be treated with some caution.

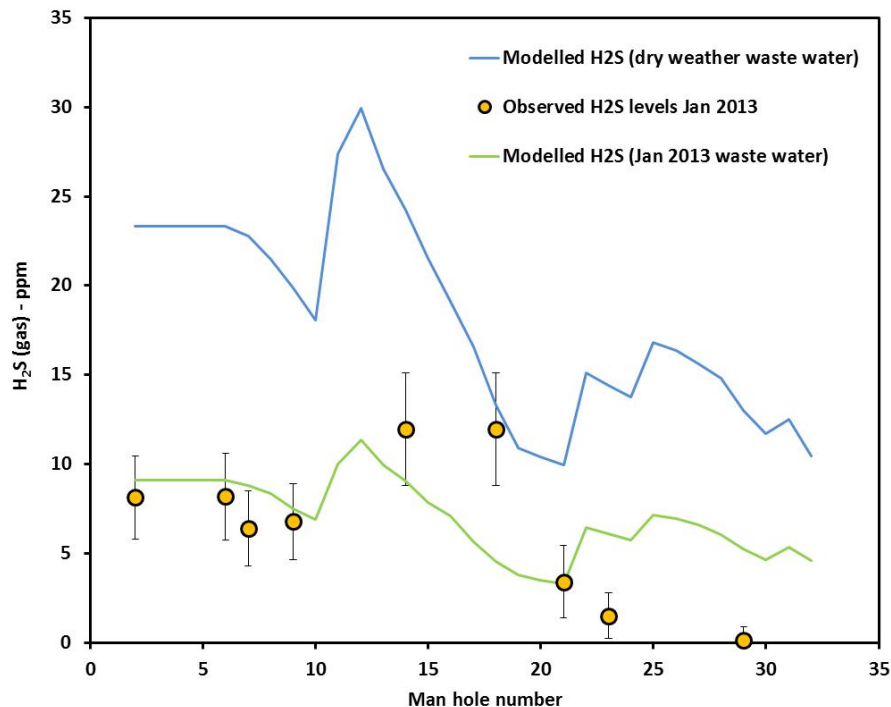


Figure 26. Observed and predicted H₂S levels in the Melbourne WTS sewer line.

3.3 Data in Scientific Literature

Surprisingly the data available in the scientific literature was quite limited. Most academic studies of sewer pipe corrosion were limited to laboratory scale studies conducted under idealised conditions. Little appreciation was made of the fact that the corrosion process evolves over time so that single loss measurements were often erroneously used to calculate corrosion rates. Environmental data accompanying the experiments was normally limited to H₂S gas concentrations and (possibly) temperature. Humidities were rarely reported.

A detailed survey of the scientific literature produced little data. The details of the data found are listed in Table 7.

Table 7. Summary of corrosion data available in the scientific literature.

Corrosion rate (mm/yr)		H ₂ S (ppm)		Relative Humidity (%)		Temperature (°C)		Source
Average	SD	Average	SD	Average	SD	Average	SD	
3.0		10		94%	3%			[52]
0.2		1		94%	3%			
0.1		0.1		94%	3%			
12.5		50						[53]
4.8	1.80	30	20					[24]
0.3	0.25	0.5	0.5					[54]
0.6	0.13	2	1					
1.0	0.25	5.5	2.5					
1.3		8						
0.4	0.38	0.5	0.5					
1.0	0.25	2	1					
1.7	0.38	5.5	2.5					
2.0		8						
4.5	0.20	202.5	197			20	10	[55]
1.4		202.5	197			20	10	
32.0		202.5	197			27.5	2.5	
5.7		202.5	197			20	8	
7.6		162.5	137.5			21	9	
6.1		400				20.5	8.5	

3.4 Summary of Activity 1 outcomes

- Corrosion data was successfully gathered from industry records supplied by Sydney and Melbourne Water.
- The loss data was obtained principally from a series of traverse reports conducted on the NGRS, NSOOS and SWSOOS sewer lines in Sydney and from corrosion pin measurements carried out in the WTS and SETS systems in Melbourne.
- Environmental data was relatively scarce and where possible H₂S levels were determined from simulations.
- The surveyed industry data suggests that lining of large sections of a sewer line may reduce the overall H₂S sink, and thereby increase H₂S levels in the sewer increasing corrosion of the remaining unlined sections of pipe.
- Only a small pool of data was available in the scientific literature.

4 Activity 2: Concrete characterisation

4.1 Introduction

Concrete samples employed in the field trials were sourced from two sources; newly manufactured reinforced concrete sewer pipe (“new coupons”) and sewer covers that had seen 70 years of service (“old coupons”). As part of the Sp1B sub-project a program of laboratory work was undertaken to evaluate a number of concrete characteristics that have an important bearing on the manner in which the samples will respond to acid attack once placed in the sewer during the Sp1B field trials.

The rate of concrete sewer pipe corrosion is in part determined by the rate of acid production within the sewer (whether by chemical or biological processes) and partly by the inherent nature of the concrete itself. Acid production is dictated principally by sewer gas properties (H_2S concentration in the gas phase, temperature and humidity) however concrete moisture content which is an important factor in determining biological activity is dictated not only by sewer humidity levels but also the size distribution of the concrete pore network (see Section 6.5.3 for discussion of this issue).

Other concrete traits that impact on the rate of corrosion include the concrete mineralogy (including the concentration of alkali components), the fraction of concrete that is cement binder and aggregate and the acid neutralisation capacity (a measure of how much acid it requires to change the pH of a given mass of concrete).

To fully quantify the relationship between the losses observed in the field trials and the sewer conditions it is necessary that these properties be evaluated for both the new and old coupon concretes. Consequently a laboratory program was undertaken to measure the above factors. This work entailed:

- x-ray fluorescence and x-ray diffraction analysis of the new and old coupon concrete
- pore size distribution analysis using mercury porosimetry
- determination of concrete density and aggregate fraction and
- determination of the Acid Neutralisation Capacity (ANC) curve for new and old coupon concrete exposed to sulphuric and several carboxylic acids.

4.2 Objectives

The overall objectives of the laboratory work discussed below are to determine:

- The pore size distribution of new and old coupon concrete.
- The mineralogical composition of new and old coupon concrete, as well as the corrosion product generated on the concrete surface during the corrosion process.

- The consumption of acid needed to produce the reductions in concrete pH observed during the Sp1B field trials.

4.3 Concrete characterisation methodologies

4.3.1 Mineralogical and pore size distribution

XRD and XRF analysis was also performed to build up a picture of the concrete mineralogy. Representative samples were cut from unexposed new and old coupons and dried at 105°C overnight before being ground down to <70µm in a motorised agate grinding mill. XRF analysis was then performed on 40mm pressed powder tablets (PVA binder) in a Spectro X'Lab 2000 polarised AED-XRF. A Philips X'Pert MPD diffractometer operating at 40kV, 40 mA with a step size of 0.008° (θ) was employed to determine the XRD spectra for the powdered samples.

The pore size distribution (PSD) was determined for $\sim 1\text{cm}^3$ samples of new and old coupon concrete material cut from the centre of unexposed coupons and dried overnight at 105°C. The samples were placed in a mercury porosimeter (Micrometrics Autopore IV 9500) and the PSD of each sample was determined for pore radii down to $\sim 0.01\mu\text{m}$.

4.3.2 Concrete aggregate content and density determination

In the concretes tested in this study it was assumed that the aggregate material was inert (i.e. no carbonate based aggregate was present). As the acid is thus restricted to attacking the cement binder it is important to know what fraction of the concrete as a whole is composed of aggregate and binder. For the purposes of this study aggregate is defined as stone/gravel material that will not pass through a 2.36mm sieve. The aggregate content was determined for samples of new and old coupon concrete via the following procedure:

- i. Several 2 cm thick cross-sections of new and old coupons (mass $\sim 500\text{g}$) were cut using a diamond saw (no water cooling).
- ii. The coupon cross sections were then dried (105°C oven overnight), weighed and the average density of each section determined using the Archimedes principle.
- iii. Each section was then broken up into smaller sections using a mallet and mortar and pestle.
- iv. To dissolve the cement binder the fragments were then placed in 500ml glass beakers to which were added approximately 200ml of distilled water and 200ml of 32wt% (approximately 10M) HCl.
- v. The beakers were sealed then left for 3 days before the acid was rinsed away and replaced with fresh acid and water. The samples were then left to stand for a further 2 days.

- vi. The acid was again rinsed away and the fragments washed over a 2.36mm sieve to remove any small particles.
- vii. The remaining fragments were then dried (105°C overnight) then weighed to determine the weight fraction of the >2.36mm aggregate.
- viii. The average density of the >2.36 mm aggregate was also determined using the Archimedes principle.

4.3.3 Acid neutralisation capacity (ANC) curves determination

To generate the ANC curves known amounts of nominal 0.4M acid solutions were contacted with a given mass of powder produced from the grinding of old and new coupon concrete. An acid strength of 0.4M was chosen to enable a suitable ratio of acid to concrete to be contacted. Also the pH of the acid solutions used fell roughly into the range of surface pH values observed on pipe walls suffering advanced corrosion (pH values ~ 1 to 2).

Three acids were utilised: sulphuric, oxalic and citric acids. Sulphuric acid was of most interest as it is the generation of sulphuric acid by SOB present in the sewer that is largely responsible for the loss of concrete observed during the active stages of the corrosion of sewer pipe. Citric and oxalic acids were also chosen to represent carboxylic acids produced by neutrophilic bacteria that are dominant in the pH range 9<pH<4. While not directly responsible for corrosion losses the action of these acids is important in bringing about acidification of the pipe surface that ultimately leads to eventual colonisation of the pipe surface by acidophilic bacteria and ultimately more aggressive corrosion.

(a) Acid preparation

- I. A nominal 0.4M stock solution of Sulphuric was prepared by dilution of a known weight of 98% H₂SO₄ with distilled de-ionized water.
- II. A nominal 0.4M solution of Oxalic acid solution was prepared by dissolving a known weight of anhydrous oxalic acid (Fluka >97%) in distilled de-ionized water.
- III. A nominal 0.4M solution of Citric acid solution was prepared by dissolving a known weight of citric acid monohydrate (BDH >99.7%) in distilled de-ionized water.
- IV. Solution concentrations were double checked after the trial had been completed by direct pH measurement. With knowledge of the pKa values for the acids it was then possible to calculate the solution strength. In all cases no appreciable change in the concentration of the stock solutions was observed over the course of the trial.

(b) Concrete sample preparation.

- I. Two sources of concrete were prepared by cutting approximately 100g of concrete from the centre of a new and old coupon using a diamond saw (no water cooling).
- II. Each block of concrete was then broken into smaller sections and disaggregated to free up any aggregate pieces that were larger than 2.36 mm – these were set aside.
- III. The remaining material (i.e. <2.36 mm) was then crushed in a motorised mortar and pestle until it passed through a 0.5mm sieve.
- IV. All material was then air dried at 40°C for 1 day to ensure samples were dry.

- V. Nominal 1g samples of the dried crushed powder was then placed in a tared plastic vial – the mass of the concrete material added was determined to +/- 0.0001g
- VI. Varying quantities of acid solution ranging from 0 to ~10g were then added to each vial and the solution made up to 10ml with distilled deionised water. The mass of each addition was determined on a balance to +/- 0.0001g .
- VII. The ratio of moles H+:kg concrete examined ranged from 0 to ~7 moles/kg.
- VIII. Each vial was capped and shaken vigorously before being placed on a shaker table.
- IX. The pH of each vial's contents were determined weekly using a standard pH probe until such a time as the pH reached a steady state (<0.1 units change per week).

The above procedure was also employed to determine the ANC of samples of the pre-existing corrosion layer present on the old coupons.

Some of the relevant properties of the three solutions used are listed in Table 8 below.

Table 8. Properties of the three acids used in the ANC experiments.

Acid	Sulphuric acid	Oxalic	Citric
Formula	H_2SO_4	 $C_2O_4H_2$	 $C_6H_8O_7$
pKa1 (25°C)	<0	1.25	3.13
pKa2 (25°C)	1.92	4.27	4.76
pKa3 (25°C)			6.4
pH of stock solution	0.5	0.9	1.7
Concentration	0.37	0.40	0.40

4.4 Concrete characterisation results

4.4.1 Mineralogical analysis

4.4.1.1 XRF and XRD analysis

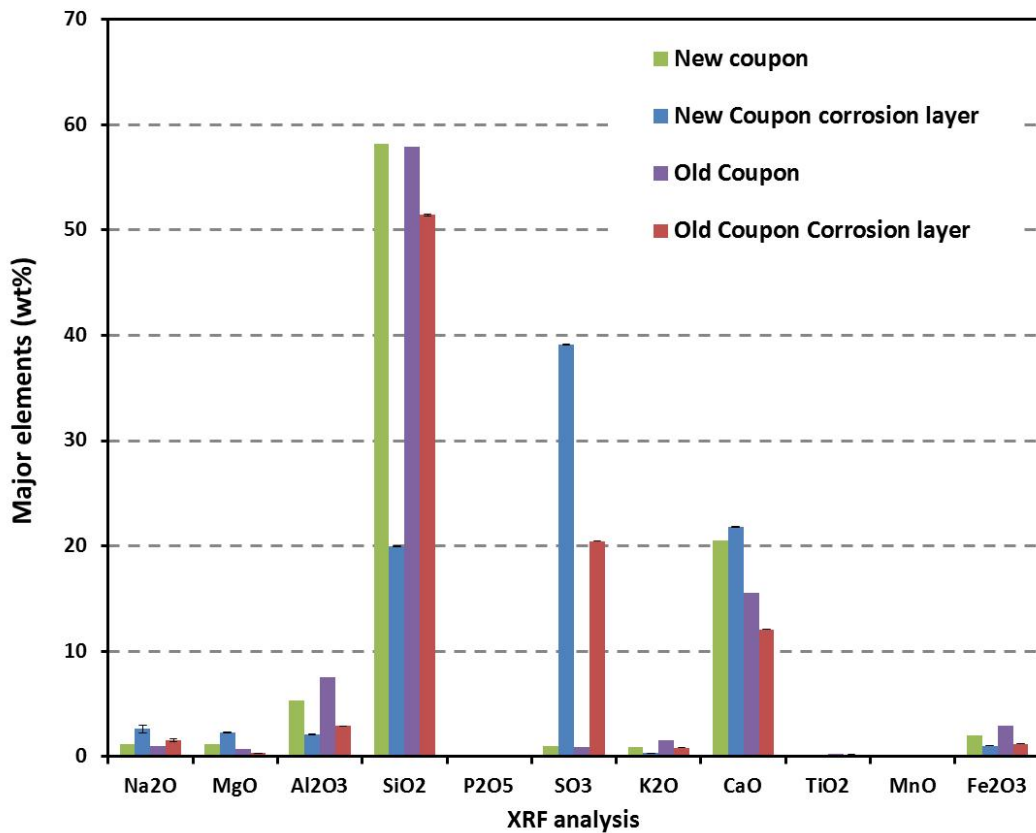


Figure 27. XRF analysis of new and old coupon concrete and the corresponding corrosion product.

The results of the major element XRF analysis of the old and new coupon concrete and corrosion products are shown in Figure 27. Inspection of the data reveals the following:

- The elemental compositions of the new and old coupon material were similar with the major point of difference being the lower levels of calcium in the old coupon material. This indicates either:
 - (a) Ca has been leached from the original concrete during its previous 70 years of service in the Sydney sewers or
 - (b) Ca levels were significantly lower in the original concrete mix used to make the sewer covers from which the old coupons were cut.
- Sulphur levels were significantly higher in the corrosion products of both the new and old coupons than in the parent material. This is consistent with the formation of

oxidised S compounds (elemental S, thiosulphates and sulphates) on the concrete surface as the concrete corrodes.

- Aluminium levels were significantly lower in both of the corroded products compared to the parent material. This may indicate the breakdown of calcium aluminates within the concrete and subsequent leaching of Al from the matrix.

XRD analyses of the new and old coupon material (Figures 28 and 29) both show a predominance of quartz in all samples as expected. XRD of the new coupon concrete also revealed significant levels of portlandite (calcium hydroxide) which is absent in the corroded new coupon material. No portlandite is present either in the old coupon concrete or old coupon corrosion product however there are significant amounts of calcite and vaterite (both forms of calcium carbonate) indicating that the original portlandite content of the old coupon concrete had been fully carbonated over the course of its previous exposure to the sewer environment.

XRD spectra of the old and new coupon corrosion product reveals a similar mineralogical composition dominated by gypsum suggesting that the corrosion of the new coupon material proceeds, at least in part, via the conversion of $\text{Ca}(\text{OH})_2$ to CaSO_4 while in the old coupon corrosion involves the conversion of CaCO_3 to CaSO_4 .

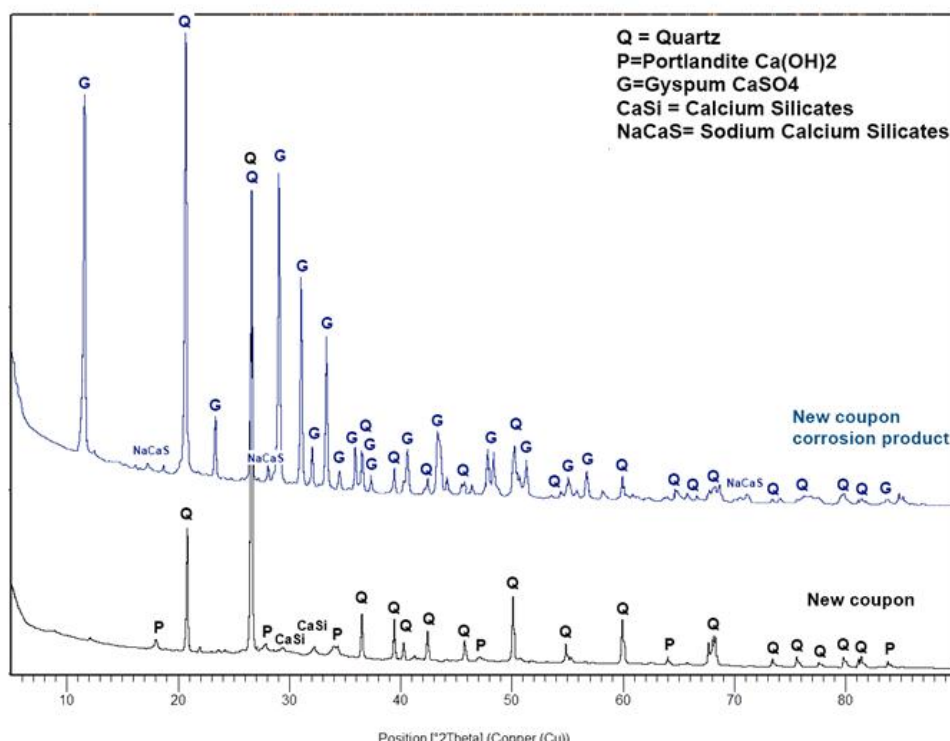


Figure 28. XRD spectra of new coupon concrete and new coupon corrosion product.

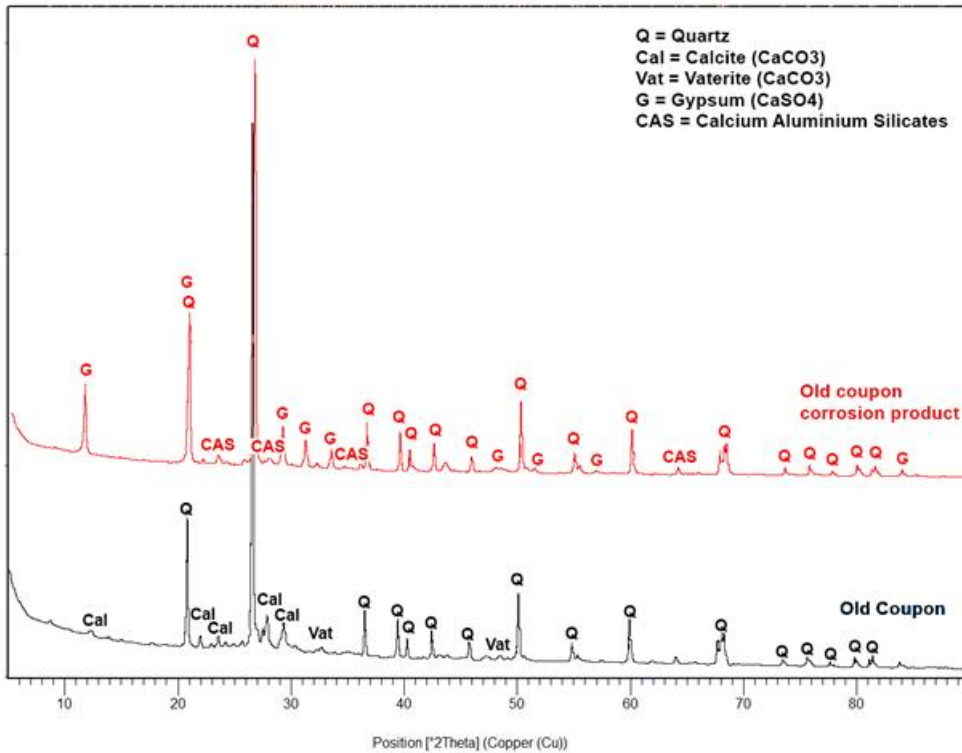


Figure 29. XRD spectra of old coupon concrete and old coupon corrosion product.

4.4.2 Pore size distribution (PSD)

The pore size distributions obtained for the new and old coupon concretes are shown in Figure 30. What is immediately clear is that the PSD of the new and old concrete coupons differ significantly. Firstly the old coupon concrete is significantly more porous than the new coupon concrete ($\sim 2.5\times$). The pores within the old coupon concrete are generally broader as well with a significant population of pores of $\sim 500\mu\text{m}$ diameter and $\sim 1\mu\text{m}$ diameter whereas the new coupon concrete has a high fraction of its pores are of diameters of approximately $0.05\text{-}0.1\mu\text{m}$ and $\sim 100\mu\text{m}$.

The differences observed may be a result of the manner in which the two concretes were originally prepared (the old coupon was cast as slabs and the new concrete was spun cast) or possibly, as suggested by Islander [25], that the pores of the old concrete have been widened as a result of the leaching of minerals (such as the portlandite mentioned above) that occurred during the old coupon source material's previous service in the sewer system.

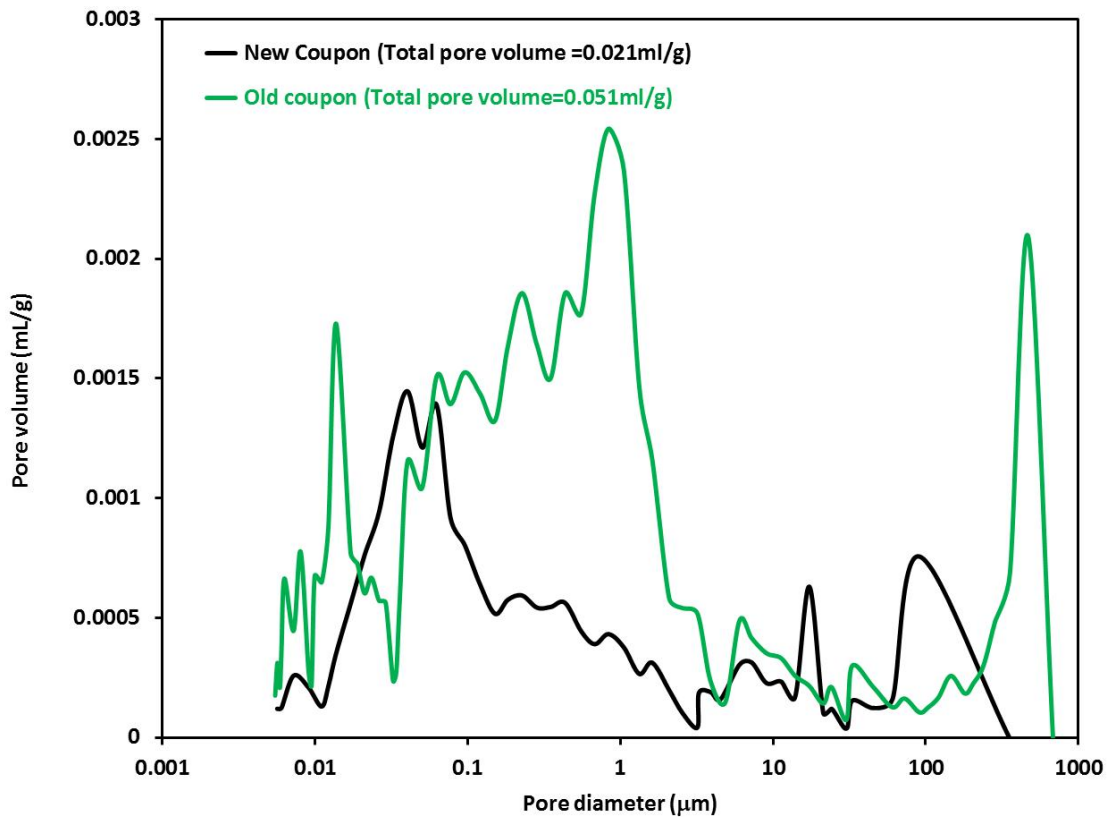


Figure 30. Pore size distribution of pores within new and old coupon concrete.

4.4.3 Aggregate content and density results

Concrete densities and aggregate content determined for new and old coupon concrete are listed in Table 9. The new coupon concrete was approximately 10% denser than the old coupon material however the mass fractions of aggregate in both concretes were (~50 wt%). Average aggregate densities were also similar and in both concretes the parent concrete was less dense than the aggregate.

Table 9. Concrete density and weight fraction of large aggregate.

Sample	Concrete density (g/cc)	>2.36mm aggregate density (g/cc)	>2.36mm aggregate fraction (wt%)
New coupon	2.43	2.54	49.9%
Old coupon	2.26	2.50	50.4%

4.4.4 Acid neutralisation capacity results

Each ANC experiment revealed the end point pH achieved when acid and concrete (minus the aggregate) of a specific weight ratio were brought into contact. Using the density and aggregate fraction information listed above this data was then converted to the pH resulting from the application of a number of moles of H⁺/kg concrete. When all data was collected for a specific acid and concrete (for example sulphuric acid and new coupon concrete) a characteristic curve of pH versus acid addition could be generated much like a titration curve (for example see Figures 31 to 38.) All curves took the form normally associated with titration curves generated when strong bases are titrated against strong acids. However this may be misleading as the ANC curves shown below are the result of the interaction between an acid and concrete which is comprised of many base elements which all have characteristic zones of pH in which they are stable (see Table 10). Thus it is more likely that the curves shown below represent successive interaction between the acid and each of the base compounds in turn, starting with the more basic elements (Ca(OH)₂) and eventually working down to the components more stable at lower pH (hydrated alumina oxides etc.)

Table 10. Principle hydrated cement paste compounds and their stable pH (as listed in [56]).

Species	Stable pH
Calcium hydroxide	12.6
Ettringite	10.7
C-S-H	10.5
Ca Aluminates	<10.5
Aluminium hydroxides	4
Hydrated aluminium oxides	3
Ferric hydroxides	2
Silica gel residue	<2

Sulphuric acid.

Sulphuric acid, which is principally generated by acidophilic sulphur oxidising microbes (ASOM) is thought to be the primary acid involved in the microbial attack on concrete sewer pipe. Figure 31 shows the sulphuric ANC curves observed for ground new coupon, old coupon and corrosion layer material. The main features to note are:

(a) New coupon material.

- The pH of the new coupon material before the addition of any acid was 12.5 well above the starting surface pH of the field coupons used in the field and laboratory trials (pH=10.3).

This indicates that exposure to the atmosphere in the time between manufacture and placement of the coupons in the sewer (a period of ~12 months) had resulted in a significant drop in surface pH (most likely via carbonation reaction with atmospheric CO₂).

- A large amount of H^+ ions are necessary to lower the concrete pH from its starting value to $\text{pH}=10$ as it is necessary to neutralise the Calcium hydroxide, Ettringite, C-S-H and some calcium aluminates that are stable in this pH range (see Table 10).
- The transition to $\text{pH}=4$ however can be accomplished with little further addition of H^+ .
- Once the pH is driven below $\sim\text{pH}=4$ large quantities of H^+ are again required to further reduce the pH (due to the buffering action of Aluminium hydroxides, hydrated aluminium oxides, ferric hydroxides and silica gel residue, again see Table 10).
- There is no suggestion of any buffering action at $\text{pH}=4$.

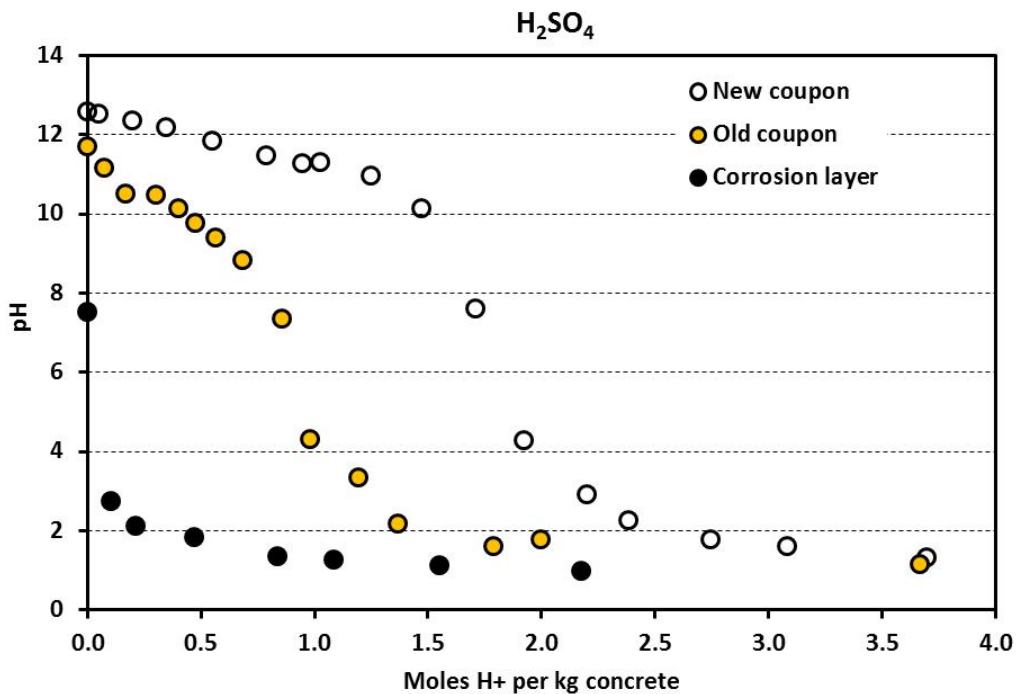


Figure 31. Acid neutralisation curves for concrete treatment with sulphuric acid.

(b) Old coupon material.

- The old coupon material demonstrates a significantly lower neutralisation capacity overall than the new coupon material.
- The initial pH for the old coupon material ($\text{pH}=11.6$) was significantly lower than that of the new coupon material suggesting that either the concrete originally had a lower alkalinity content or that the original alkalinity had been partially neutralised during the 7 decades in which the concrete source material for these coupons was in service.
- The starting pH of the old “bulk” coupon material ($\text{pH}=\sim 11.6$) was significantly higher than the initial surface pH (which was measured by wetting of the exposed surface (See 5.3.5) of the old coupons ($\text{pH}=\sim 8$) reflecting the difference between the bulk material that makes up the old coupon and the corrosion layer initially present on these samples used in the lab/field trials.

- The form of the neutralisation curve appears to correspond to that of the lower portion of the new coupon curve suggesting that it overlays the new coupon ANC curve if simply transposed to the right.
If this proves to be the case it would indicate that both new and old coupon concretes are following the same pH vs acid addition pathways and the old coupon concrete can be thought of as a “partially acidified” version of the new coupon concrete.
- Substantially less H⁺ is required to reduce the pH of the old coupon concrete from its starting pH down to a pH of 9 or 4 than is required for the new coupon concrete.
This has implications for the time it would take for old coupons installed in the sewer to reach conditions suitable for colonisation by neutrophilic or acidophilic bacteria which in turn has implications for the corrosion behaviour likely to be observed in the field trials.
- Interestingly however the additional acid required to move from pH=9 to pH=4 is similar to that required by new coupon concrete (~0.25 moles H⁺/kg concrete).
- Again there is no suggestion of a buffer at pH=4 while buffering is observed at pH=1.5. This buffering is likely to be due to the presence of Silica gel residue and possibly Ferric hydroxides that are stable at these low pH values (again see Table 10).

(c) Pre-existing corrosion product on old coupons.

- As expected the starting pH of the corrosion product (pH=~7.5) is close to that observed for the surface pH of the old coupons used in the field/lab trials (pH=~8) as this product covers the majority of the exposed surface of the old field coupons.
- The corrosion product showed very little neutralisation capacity with only small amounts of acid required to reach a steady state end point (pH~1.5).
- Even though the material is thought of as ‘spent’ it still acts to neutralise the acid to some extent (as the pH of the raw acid is ~0.5). This suggests that the corrosion layer still contains a substantial amount of material that reacts with the acid (the data in Table 10 suggest that this would be principally Silica compounds).
- The form of the neutralisation curve for the corrosion product appears similar to the right most portion of the new coupon neutralisation curve.

Interpretation of Sulphuric Acid ANC results

(a) Confluence of the new coupon, old coupon and pre-existing old coupon corrosion product curves.

The similar forms of the neutralisation curves shown in Figure 31 suggests that old coupon and corrosion product responses may represent partially acidified versions of the new coupon material. To see if this was the case the curves for the old coupon and corrosion product were shifted to right until the starting point of each curve fell onto the curve observed for the new coupon material (Figure 32). The remainder of the old and corrosion layer curves were then shifted over to the left by the same amount.

The results, (Figure 33), suggest that all forms of concrete used in this study follow the same basic neutralisation path when exposed to sulphuric acid. The old coupon bulk material and the old coupon corrosion product can be thought of as partially acidified versions off the new

coupon material, i.e. they are “further along in the corrosion process”. The coalescence of the curves also suggests that:

- Old coupon material behaves in the same manner as new coupon material that has already had 0.95 mol H⁺ /kg concrete added and
- Corrosion product present on the old coupons behaves in the same manner as new coupon material that has already had 2.1 mol H⁺/kg concrete added.

Calculation of Concrete Alkalinity

It is possible to calculate the equivalent alkalinity of the concrete from the data available in Figure 33. If it is assumed that reducing the pH of new coupon from the starting pH to pH=3 equates to fully corroding the concrete then the following calculations follow:

Moles H⁺ required to fully corrode the concrete = 2.09 moles/kg concrete

Moles OH⁻ neutralised during corrosion = 2.09 moles/kg concrete

Equivalent moles of Ca(OH)₂ neutralised = 2.09/2 = 1.05 moles Ca(OH)₂/kg concrete

The density of new coupon concrete (Table 9) is 2.43g/cc =2430 kg/m³

The concrete alkalinity = the equivalent Ca(OH)₂ content per m³ concrete

The alkalinity of new coupon concrete = 1.05×2430= 2550 moles Ca(OH)₂/m³ concrete

Organic acids.

While sulphuric acid generated by ASOM is considered to be the principle driver behind sewer pipe corrosion it is also recognised that carboxylic acids generated by neutrophilic bacteria and fungi that colonise the pipe wall at higher pH conditions also contribute to the corrosion process by driving down surface pH to values at which ASOM activity can commence. Citric and oxalic acids were chosen to represent organic acids likely to be secreted from some neutrophilic bacteria and fungi. The capacity curves for new and old concrete material treated with citric acid are shown in Figure 34 and with oxalic acid in Figure 35.

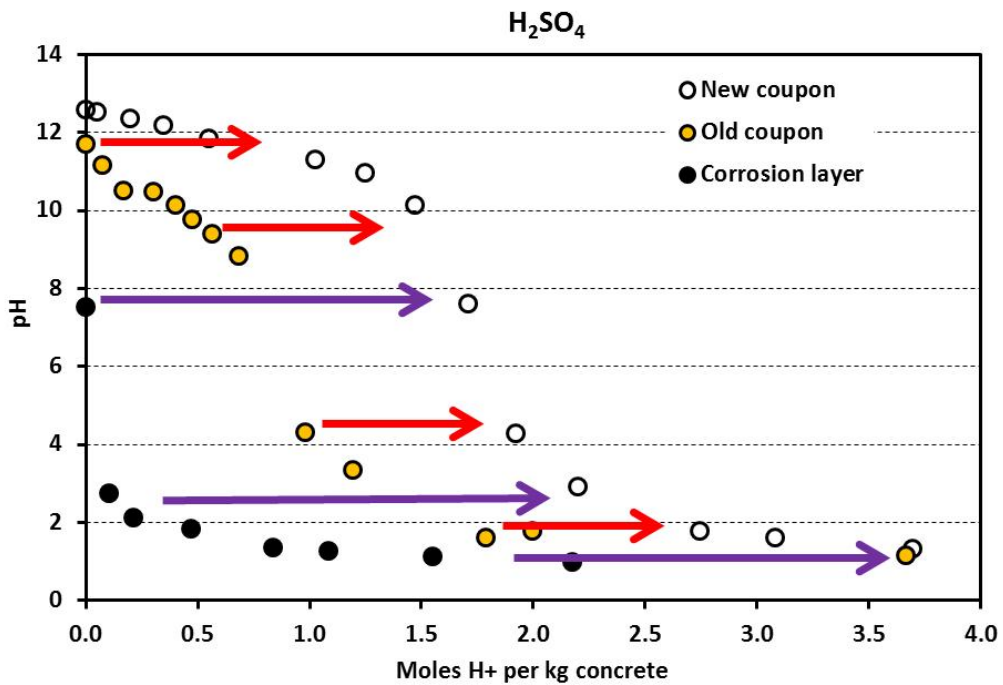


Figure 32. Transposing Sulphuric acid ANC curves to the right to check for confluence.

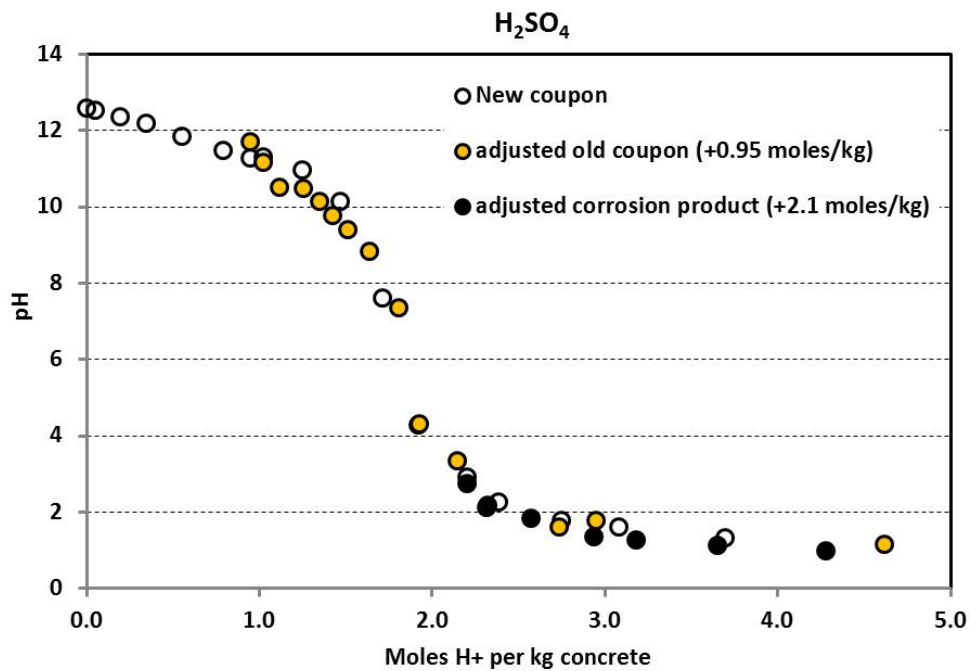


Figure 33. Confluence of Sulphuric acid ANC curves.

The main points of interest for the organic acid treatments were as follows:

- The acid neutralisation curves produced when the new coupon material was treated with the two organic acids were similar in form to the new coupon/sulphuric acid ANC curve with the exception that the end point pH was marginally higher for the citric acid treatment (reflecting the fact that the pH of the citric acid solution ($\text{pH}=1.7$) was higher than that of the oxalic and sulphuric acid solutions used in the study ($\text{pH}=0.9$ and $\text{pH}=0.5$ respectively)).
- It was evident that an amount of buffering occurred at $\text{pH}=7.5-8$ when the old coupon concrete was exposed to the organic acids (a feature not observed for the new coupon concrete) The reasons for the buffering are not clear (it was also not observed when the old coupon concrete was exposed to sulphuric acid) but as the phenomena is not seen in the new coupon material it may be linked to the interaction between carbonates present in the old coupon and the carboxylic acids.
- Again no buffering was seen at $\text{pH}=4$ but a level of buffering was observed at $\text{pH}=\sim 1.5$ for oxalic treated material (due to the presence of silica gel residue). This was not observed for citric acid treated material as the solution pH was >1.5 ($\text{pH}=1.8$)

Figures 36 and 37 show the adjusted neutralisation curves for new and old coupon concretes and the pre-existing corrosion product exposed to citric and oxalic acids on the assumption that the response of the new and old concrete as well as the corrosion product material fall on the same general response curve. Thus, as reported above for the case of sulphuric acid, it is possible to think of old coupon and old coupon corrosion product as partially acidified versions off the new coupon material when treated with carboxylic acids.

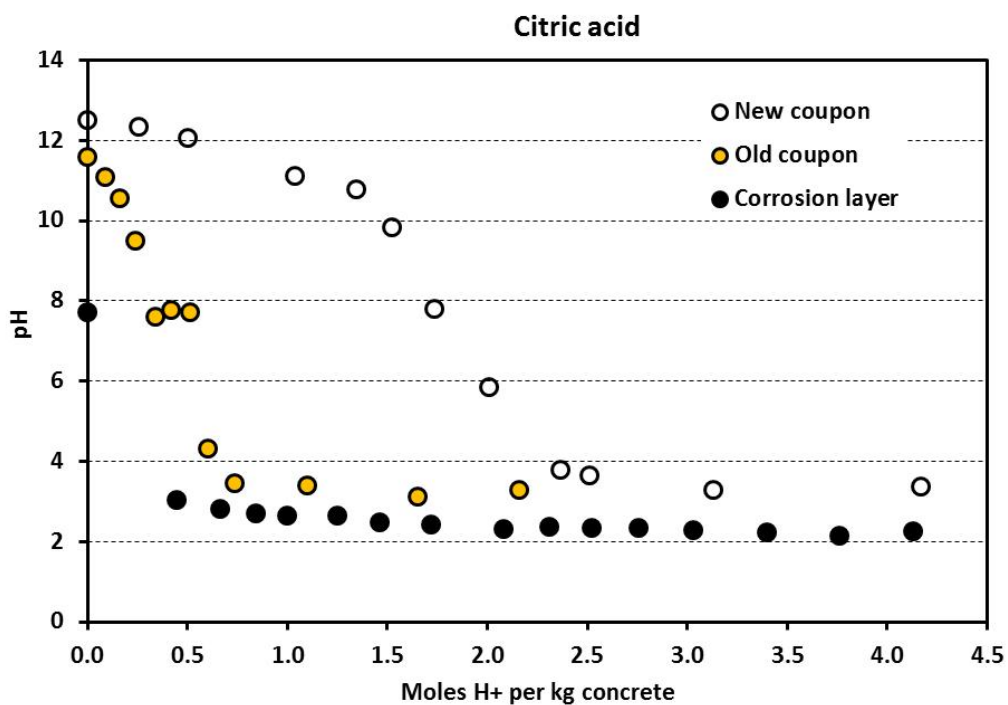


Figure 34. Citric acid ANC curves for new and old coupons and old coupon corrosion layer.

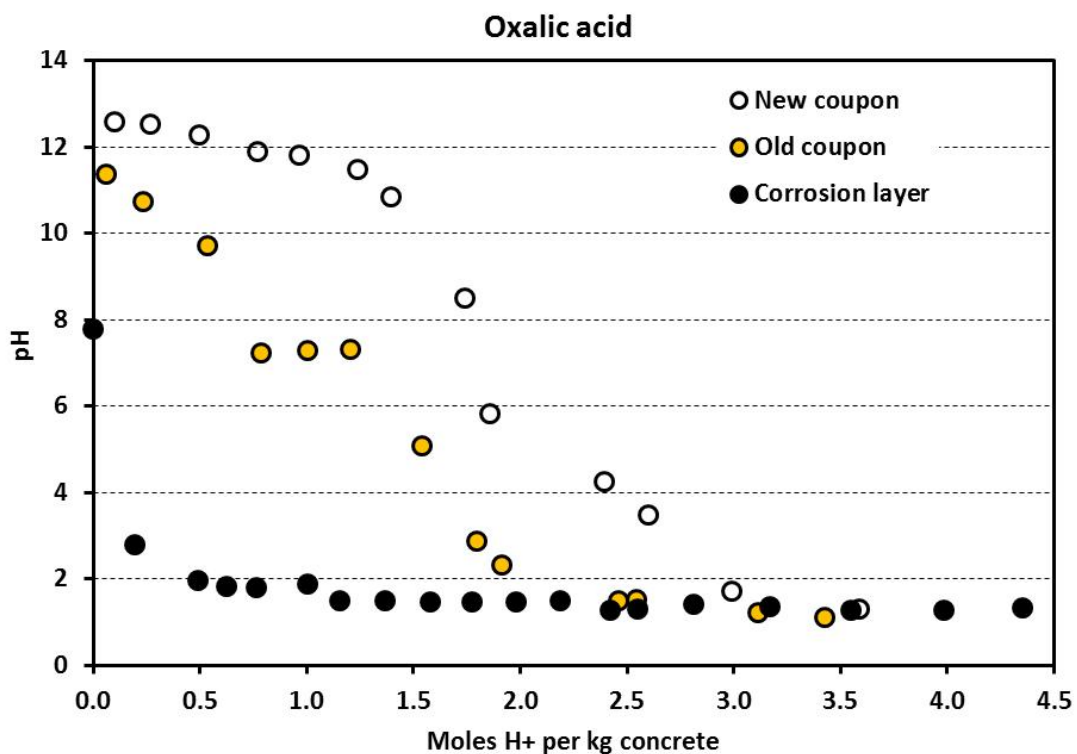


Figure 35. Oxalic acid ANC curves for new and old coupons and old coupon corrosion layer.

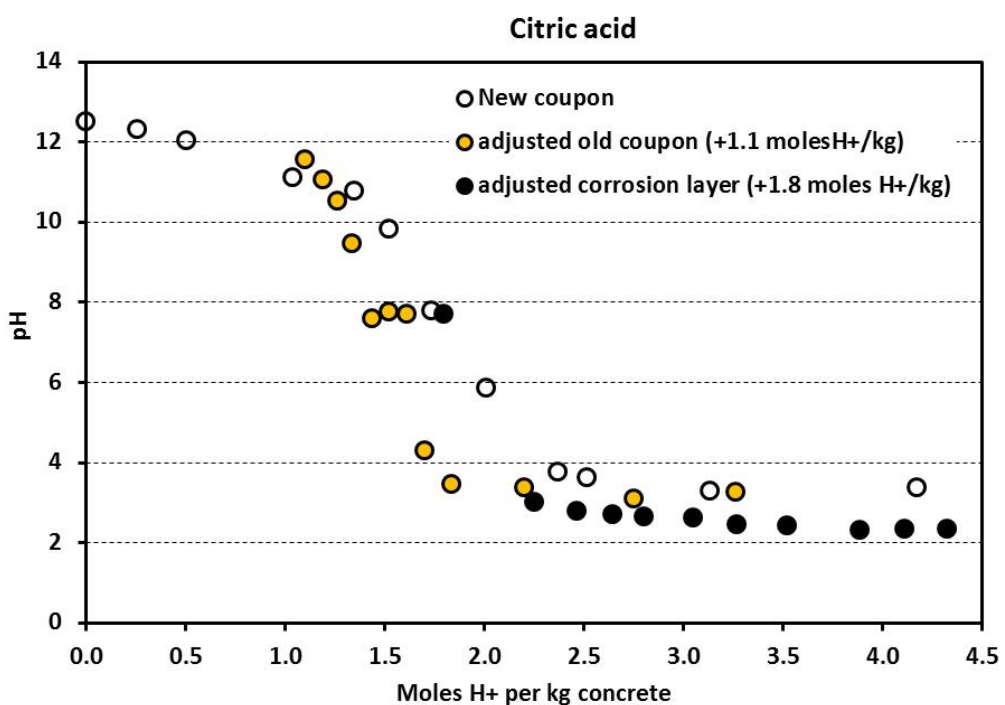


Figure 36. Adjusted citric acid ANC curves.

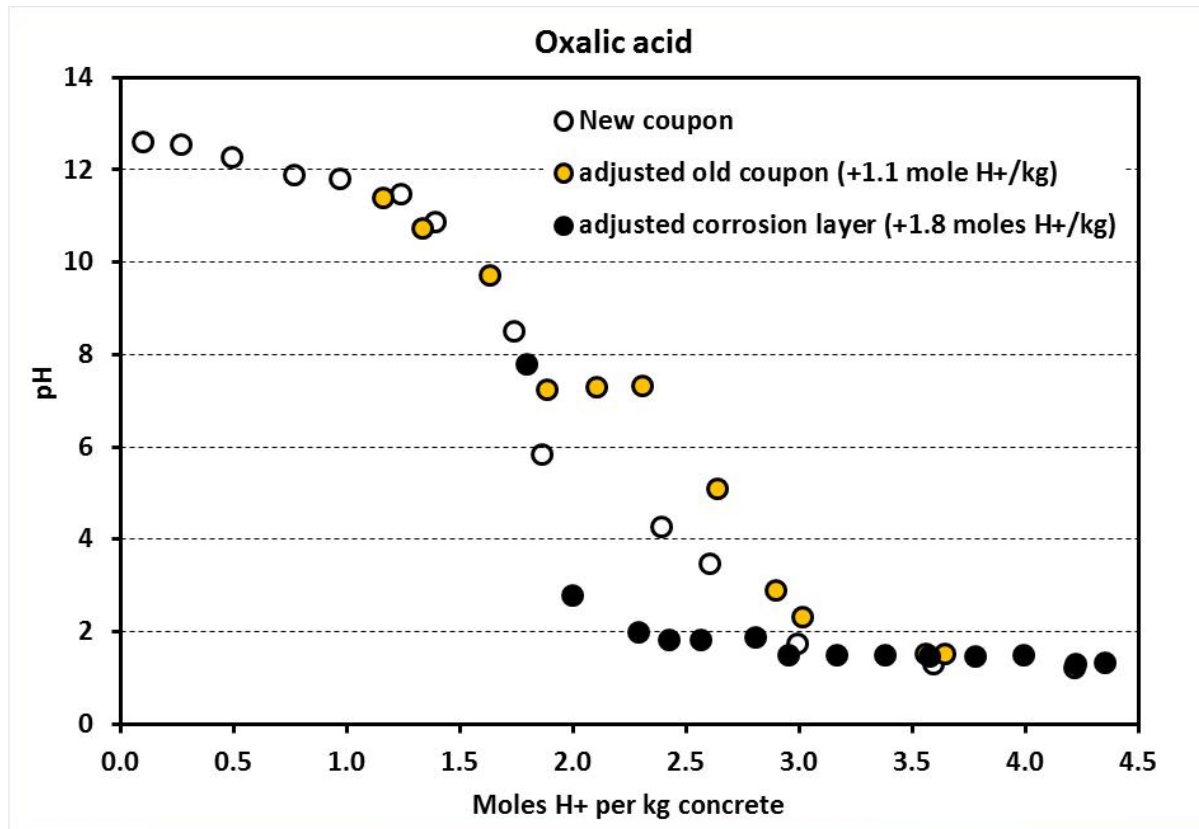


Figure 37. Adjusted oxalic acid ANC curves.

4.4.4.1 Comparing the ANC behaviour of Sulphuric and carboxylic acids

Figure 38 plots the adjusted ANC curves for sulphuric as well as the two carboxylic acids. While there are some minor differences (largely generated by the buffer behaviour exhibited by the old coupon material when exposed to the organic acids) Figure 38 shows the response of the concrete to all three acids is approximately the same.

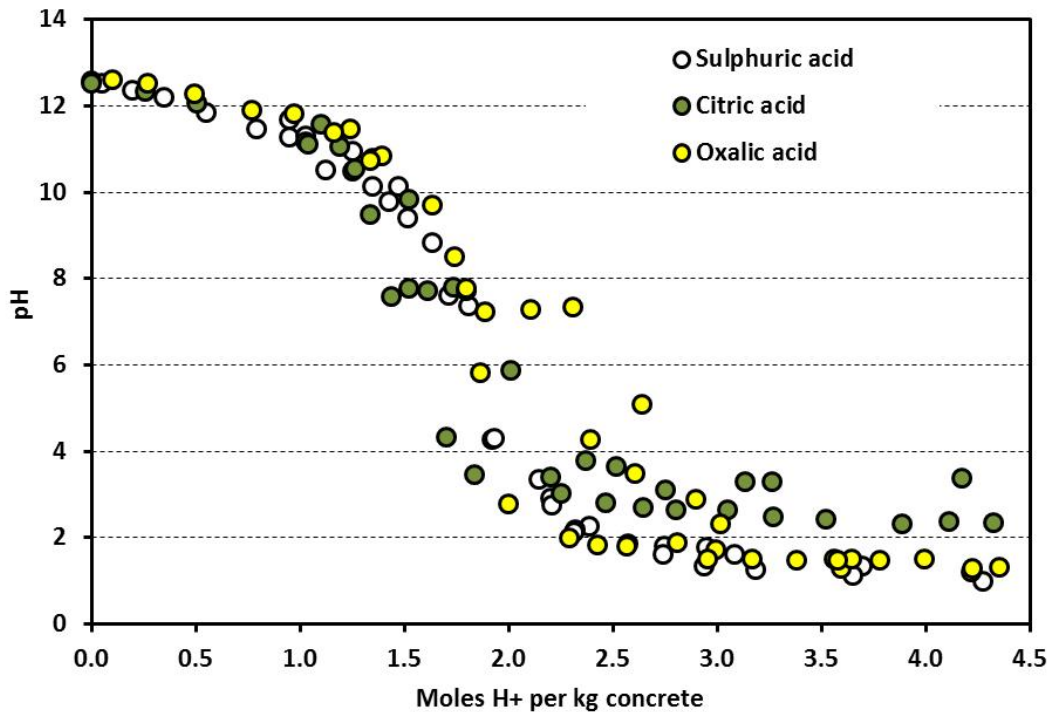


Figure 38. The generalised ANC curves for all three acid treatments.

Presence of natural buffers in the concrete material.

Early field pH survey results (Section 5.4.2.3) indicated that there may be a natural buffering point for the concrete/acid system operating at about pH=4 (for example see Figure 39). The ANC experiments however did not reveal any pH buffering at this pH however relatively stable pH regions were observed at $10 < \text{pH} < 12$ and $1.5 < \text{pH} < 2$ for most of the acids tested. Reference to Table 10 suggests that the neutralisation of calcium aluminates, C-S-H, and calcium hydroxide produce the relatively flat section of the ANC curve in the range $10 < \text{pH} < 12$ while the presence of silica gel residue stabilises the pH at $\text{pH} < 2$.

The “stable” surface pH=4 observed in the field samples therefore most likely represents an equilibrium values between the acidic corrosion layer ($\sim \text{pH}=2$) and the more alkaline wastewater aerosols that are constantly condensing on the outer surface of the corrosion material.

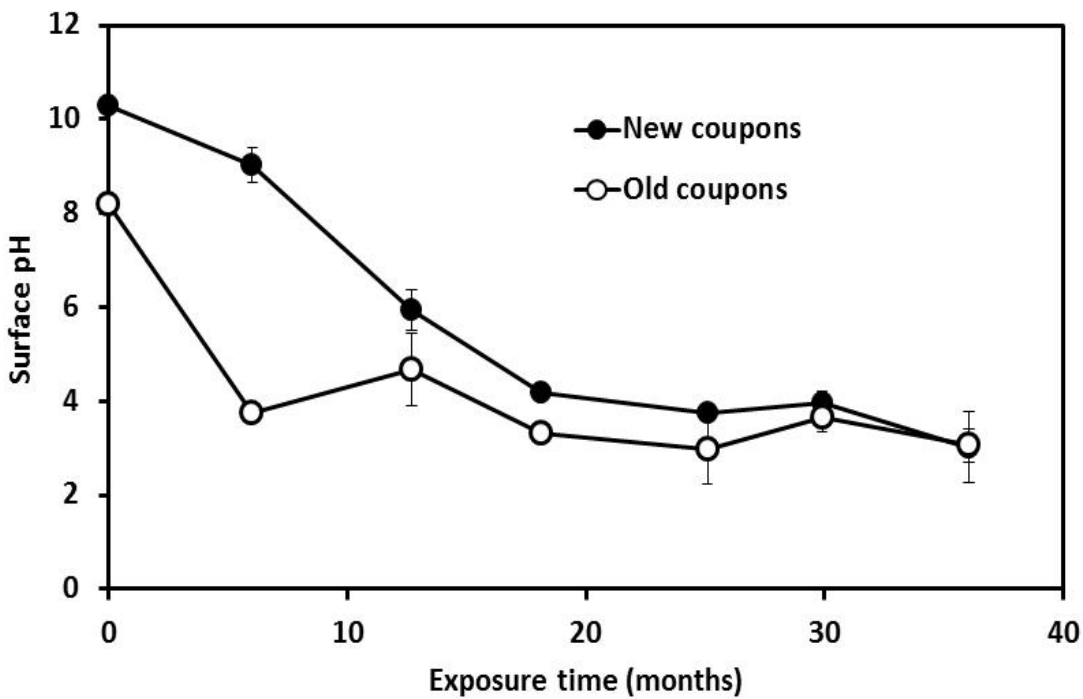


Figure 39. Trends in surface pH of Perth new field coupons over time.

4.5 Summary of Activity 2 outcomes

- An extensive program of concrete characterisation was undertaken to quantify concrete properties that impact on the corrosion behaviour of the concrete.
- Both new and old coupon concretes were characterised. Some properties of the corrosion products were also assessed.

Major findings were:

- Mineralogy/chemistry:
 - Elemental compositions of new and old coupon concretes were similar except that calcium levels in the old coupon concrete were lower.
 - Corrosion products were high in sulphur compounds but depleted of aluminium when compared to the parent concrete indicating the formation of gypsum and the possible leaching of aluminates during the corrosion process.
 - New coupon concretes were found to be high in Portlandite which was absent in the old coupon concrete. High levels of carbonate minerals in the old coupons suggest carbonation of the original portlandite content had taken place.
 - Corrosion products of old and new coupons contained gypsum.
- Density and aggregate fraction determination
 - Concrete densities: New coupon $\rho=2.43 \text{ g/cc}$; Old coupon $\rho=2.26 \text{ g/cc}$
 - Aggregate content: New coupon =49.9 wt%; Old coupon =50.4 wt%

- Pore size distribution
 - Pore size distributions for new and old coupon concrete were determined using mercury porosimetry.
 - Old coupon concrete was $2.5\times$ more porous than new coupon concrete.
 - Old coupon concrete pores were generally broader than new coupon pores.
 - Most new coupon concrete pore diameters fell in the ranges $0.05 < d < 0.1\mu\text{m}$ and $d = \sim 100\mu\text{m}$.
 - Most old coupon concrete pore diameters fell in the ranges $0.1 < d < 1\mu\text{m}$ and $d > 500\mu\text{m}$.
 - The differences in pore structure may be due to manufacturing methods or the consequence of the previous exposure to sewer conditions experienced by the old coupon concrete.
- Acid neutralisation capacity (ANC)
 - New and old coupon concrete and the corroded material pre-existing on the old coupons were exposed to various quantities of sulphuric, citric and oxalic acids to test their response to attack by acids generated by acidophilic and neutrophilic bacteria.
 - Curves relating how concrete pH changed upon the addition of acid were generated for all concrete/acid combinations.
 - All ANC curves were of the form normally associated with a strong acid/strong base titration. Despite this the curves are the result of the interaction between the acid and a number of basic minerals that reside in the cement binder which are stable at different pH ranges.
 - It was found that the curves generated for the different concrete materials could be superimposed for a single acid with a simple transposition to the right indicating that:
 - All concrete materials followed the same general response to acid attack
 - The old coupon concrete and the corrosion product could be thought of as "partially acidified" versions of the new coupon concrete
 - The generalised ANC curves for sulphuric acid and organic acids could also be superimposed with only small differences suggesting that the pH response of the concrete to each acid was essentially the same.
 - The curves will be employed later to help qualitative and quantitative analysis of the corrosion process.

5 Activity 3: Sp1B Field Corrosion Trials

5.1 Introduction

The field work component of the Sp1B sub-project was undertaken to study and quantify concrete corrosion occurring *in situ* in working Australian sewers under a range of environmental and operating conditions. This data was essential for the development of a corrosion model as, despite the number of laboratory studies that have focused on sewer pipe corrosion, there have been prior to this study no extensive organised field trials of concrete corrosion conducted in active sewers. The field work discussed below therefore afforded a unique opportunity to build up a qualitative and quantitative picture of the sewer pipe corrosion process and as such was an essential component of the model development.

5.2 Objectives

The objectives of the field trials were as follows:

- Observe the corrosion of reinforced concrete sewer pipe under a variety of realistic conditions.
- Determine how the corrosion process evolves over time under actual sewer conditions.
- Identify the link between surface pH decline, corrosion rate and various sewer environmental factors.
- Use the data obtained to assess the progress of the SP1A laboratory trials.
- Generate data that can be input into the corrosion model.

5.3 Methodology.

5.3.1 Field samples

Two different concretes were exposed in the sewer. The ‘new coupons’ were cut from newly manufactured 1.2m ID spun cast Class 2 flush joint standard reinforced concrete sewer pipe. The ‘old coupons’ were taken from reinforced concrete sewer covers that had been in service for 70 years and had corroded considerably leaving 80 to 100 mm remaining thickness. The old coupons retained a ~2 mm thick crystalline layer of corroded material generated during the earlier 70 years of exposure to the sewer environment.

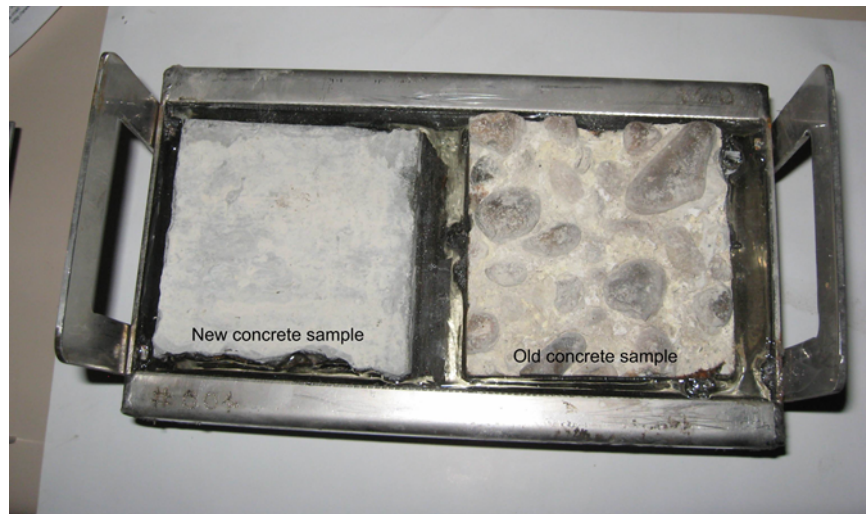


Figure 40. Field coupons mounted in the sample holders.

Aggregate in new concrete samples ranged in size from 10 to 15mm. Aggregate in the old coupons was significantly larger (typically 15mm but aggregate as large as 30mm was not uncommon).

The concrete source materials were cut to 100 mm (nominal) cubes. Care was taken to ensure the previously corroded face of the old coupons was left undisturbed during cutting and handling. After cutting all coupons were dried to constant weight at 60°C, cleaned and keyed in preparation for fixing into the sample holders. One old and one new coupon were embedded in resin (West System Kinetix R104 Epoxy) in specially designed 316 stainless steel holders (Figure 40). The inner pipe surface of the new coupons and the previously corroded surface of the old coupons were exposed above the resin. The exposed surfaces protruded approximately 10-20mm above the resin surface.

The sample holders were first trialled at a Sydney sewer site. Upon the successful completion of the Sydney trial the design of the coupon frames and a means for affixing them to the sewer roof/wall was finalised. The final design involved holder being bolted between pairs of 316 stainless steel angles which will in turn were bolted to the sewer wall or roof (Figure 42).

All coupon pairs were epoxied into the stainless steel sample holders each holder and individually numbered, (the sample frame was engraved and sample tags were buried in the epoxy) to ensure that an accurate comparison of before and after exposure condition could be determined for each individual sample. Prior to shipment to the field sites each coupon pair was photographed in preparation for photogrammetric assessment of the coupon thickness (see later discussion in Section 5.3.4).



Figure 41. Field samples awaiting photogrammetric imaging prior to despatch.

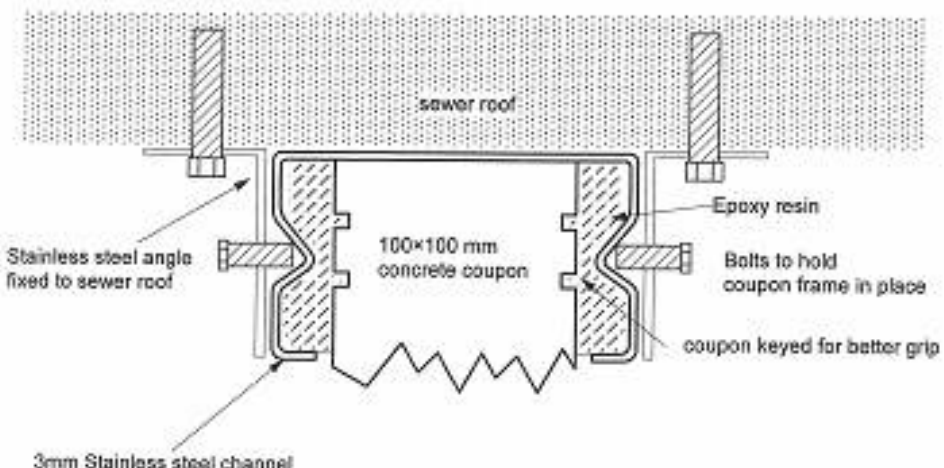


Figure 42. Schematic representation of the sample mounting frame.

5.3.2 Field sites.

After consultation with the project's industry partners it was decided to locate the field sites in three cities: Melbourne, Sydney and Perth. Some initial attempts to place samples in Brisbane sewers were eventually abandoned due to delays introduced by the restructuring of the water authority responsible for the Brisbane area.

The choice of 3 cities enabled the trials to be carried out over a range of temperature conditions with Melbourne as the coldest location followed by Sydney and Perth as the warmest location. Two sewer sites were chosen in each city representing a high and low H₂S site. At all sites the samples were mounted on the midline of the roof of the sewer. At one Sydney site samples were also mounted on the wall of the sewer just above the normal tidal range of the waste water stream. Field sites details are listed in Table 11. Field site locations are shown in Figures 43, 44 and 45.

The stainless steel sample holders were mounted in an inverted position along the midline of the sewer roof at each of the Melbourne field sites (Figure 46) and at the two Sydney sites (Figure 47). At the two Perth field sites, to avoid damage to the pipe lining, samples were mounted in an inverted position in specially designed racks manufactured by the Water Corporation that were fitted into manhole wells (Figure 48). Coupons at the Perth sites were mounted above the normal wastewater level. A set of samples was also mounted on the sewer wall just above the normal tidal zone of the waste water at one of the Sydney site (SWSOOS2 south trunk – see Figure 47 (right)). Installation dates for all sites are listed in Table 11.

Table 11. Sp1B field site details.

Site	Coupon Location	Size of sewer	Anticipated levels (ppm)	Position	# sample pairs	Samples installed
Sydney	South trunk of SWSOOS2	2.8m × 2m box section	High (>20)	Roof	24	21/9/2009
	South trunk of SWSOOS2	2.8m × 2m box section	High (>20)	Wall	24	21/9/2009
	North trunk of SWSOOS2	2.8m × 2m box section	Low (<20)	Roof	24	21/9/2009
Melbourne	Western Trunk Sewer	4m circular	High (10-30)	Roof	24	16/2/2010
	South eastern Trunk Sewer	3.5m circular	Low (1-10)	Roof	24	4/2/2010
Perth	Perth MS		Low (~80)	Manhole	24	6/5/2010
	Bibra Lake		High (>200)	Manhole	24	11/6/2010



Figure 43. Location of the Sydney field sites (SWSOOS2 near Hayden Place).



Figure 44. Locations of the Melbourne field sites.

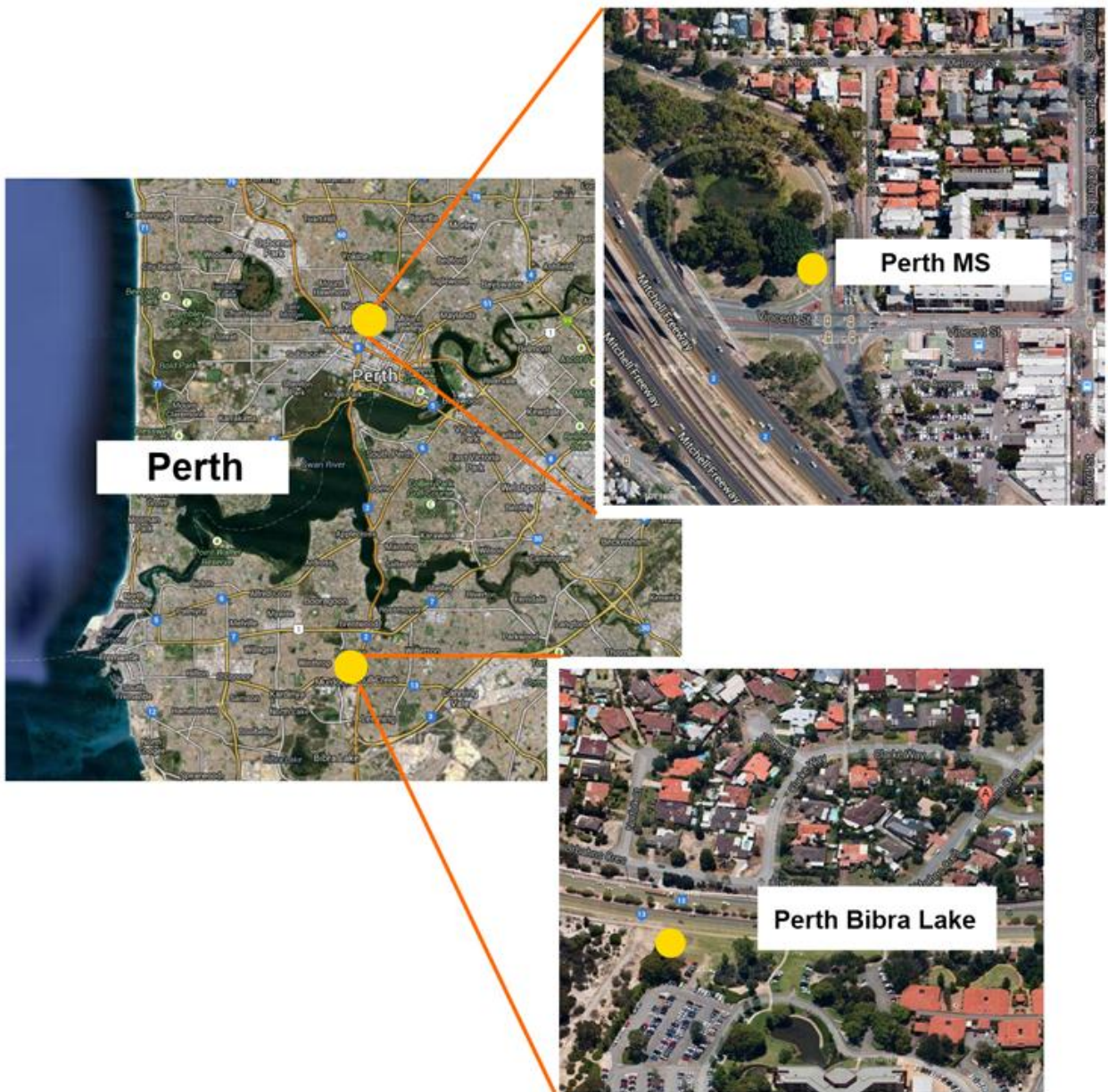


Figure 45. Locations of the Perth field sites.



Figure 46. Sp1B coupons mounted along the sewer roof at the Melbourne SETS (left) and WTS (right) field site.



Figure 47. Sp1B field samples at the Sydney field sites. Left: roof mounted samples in the SWSOOS2 north trunk; Right: roof and wall mounted samples in SWSOOS2 south trunk.



Figure 48. Sp1B field samples installed on racks in manhole wells at Perth MS (left) and Perth Bibra Lake (right).

5.3.3 Recovery of field samples

Field sample recovery took place approximately every 6 months in the early stages of the trial and yearly in the later stages however it was acknowledged at the commencement of the trial that this schedule was subject to variation depending on (a) the rate of corrosion observed at each site and (b) operational considerations. The retrieval times and corresponding exposure periods are listed in Table 12.

Unfortunately the field trials at the three Sydney locations had to be abandoned after 3 years of exposure due to the accidental coating of the samples with a magnesium hydroxide gel (sulfalok).

Table 12. Retrieval dates and exposure times for the Sp1B field samples.

Site	Date of recovery	Exposure time (months)	Site	Date of recovery	Exposure time (months)
Melbourne SETS	21/9/2010	7.5	Melbourne WTS	20/9/2010	7.1
	21/2/2011	12.6		22/2/2011	12.2
	16/8/2011	18.4		17/8/2011	18
	4/2/2012	24.4		16/2/2012	24
	7/9/2012	31.1		6/12/2012	33.7
	17/5/2013	39.4		25/5/2013	39
Perth MS	6/12/2010	7.2	Perth Bibra Lake	6/12/2010	6
	28/6/2011	13.9		28/6/2011	12.7
	6/12/2011	19.3		6/12/2011	18.1
	3/7/2012	26.3		4/7/2012	25.1
	4/12/2012	31		5/12/2012	29.9
	12/6/2013	37.2		12/6/2013	36.1
Sydney SWSOOS2S	17/6/2010	8.9	Sydney SWSOOS2N	17/6/2010	8.9
	21/9/2010	12		21/9/2010	12
	20/9/2011	24		20/9/2011	24
	25/9/2012	36.2		25/9/2012	36.2

At each recovery 3 coupon pairs were retrieved from each site. Two coupon pairs were couriered to Newcastle University and one pair to the University of Queensland. Samples sent to the University of Newcastle were examined to determine:

- Depth of the corrosion product layer
- Surface pH
- Amount of sound concrete that has been corroded away and
- Changes in the surface mineralogy

The samples sent to the University of Queensland were examined to determine:

- Sulphur species present on surface

- Microbial characteristics

After examination at the University of Queensland the samples were then sent onto Newcastle University to determine the amount of sound concrete lost.

The following discussion details the methods used to determine the above listed coupon characteristics.

5.3.4 Photogrammetric evaluation of the amount of corrosion product formed and the amount of sound concrete lost

The development of a robust method of determining the amount of concrete corroded from the exposed surface of the coupon and the depth of the corrosion product layer was a high early priority for the Sp1B sub-project. The problem was complicated somewhat by the uneven nature of the exposed concrete surface (particularly that presented by the old coupon throughout the trial and new coupons after a significant amount of corrosion had taken place) which made calculation of an average coupon height difficult to determine. To overcome this difficulty a photogrammetric imaging process utilising multiple sets of stereo images of each coupon was employed to construct a 3D image of the surface of each coupon (see Figure 49).

Before installation in the sewer, each individually numbered pair of samples were placed in an imaging frame (Figure 50-A). A targeting template comprising 60 unique circular targets (Figure 50-D) was placed in position surrounding the two coupons on the upper rims of the sample container. Five images of the exposed surface of each coupon were recorded from the fixed camera positioning rings (Figure 50-B) using a 7.1 megapixel digital camera (focal length 5.99mm, aperture f/2.6). Subsequently, a photogrammetric imaging software package (PhotoModeler Scanner ®) was used to create a 3D cloud point representation of each exposed coupon surface from the series of photographic images. (The images were first corrected for lens distortion using algorithms generated during a camera specific calibration process). The circular targets contained in the target template (which are visible in each image) were then used by the software to: (1) determine the position and orientation of the camera in 3D space at the time each image was taken and (2) scale each image. The plane passing through the targeting template was the reference plane against which the height of the coupon surface was referenced. The information from the five images was then used to generate a unified 3D point cloud representation of the surface of each coupon. The (x,y) grid spacing used to generate the point cloud was set at a nominal 0.5 mm. This typically generated a cloud containing 100,000 to 200,000 points for each coupon surface. An average coupon surface height prior to exposure was then calculated relative to the targeting frame by averaging the z coordinate values.

Upon recovery of the coupons from the sewer the imaging process was repeated for coupons in the ‘as-recovered’ state i.e. complete with corroded material still present on the coupon surface. A pH survey (see Section 5.3.5) then followed immediately. After the pH survey, a high pressure water wash was used to remove the corrosion product and strip the coupons back to ‘sound concrete’ (‘stripped’ state) (Figure 51). A Karcher 6030MS high pressure water washer delivering water at 8 l/min with a minimum pressure of 20MPa was used. The nozzle was positioned 300 mm from the coupon surface. A 3 minute wash cycle was employed (testing

showed that high pressure water blasting for longer than 3 minutes did not remove further material). Testing of the washing procedure on new and old control coupons not placed in the sewer resulted in very minor amounts of material removed from new coupons (an average of 0.04mm, considered to represent removal of some surface scale). As expected, more material was removed from old concrete coupon control samples (an average 2.05mm of the existing corrosion layer). These 'blank' values were taken into account when calculating the corroded product layer depth and corrosion losses. Following the high pressure water washing a final set of images were taken of the stripped samples.



Figure 49. Photogrammetric apparatus. (a) Field samples with target frame; (b) Photography frame.

In each of the 3 image sets (original, as recovered, and stripped) the target template was used as a fixed reference plane against which the movement of the coupon surface was assessed (upwards as a corrosion product layer accumulates on the surface and down as concrete is corroded away). Particular care was taken to ensure that the targeting template was in the same position for each of the three image sets. To ensure this was the case particular care was taken to ensure that the stainless steel rim of the sample holder, on which the target set sits, was in a clean and undamaged condition (as it happened no corrosion of the 316 stainless steel rim was observed during the study). In addition, as a further guard against errors resulting from an incorrectly seated target frame, the imaging process was carried out in triplicate at each stage.

After each imaging the 3D surfaces were generated. From these an average surface height relative to the target reference plane was determined for each coupon, in the original, as-recovered and stripped states. The movement of the 3D surfaces relative to the fixed reference plane was then calculated. From this the depth of the corrosion layer and the amount of sound concrete corroded away was determined (Figure 52).

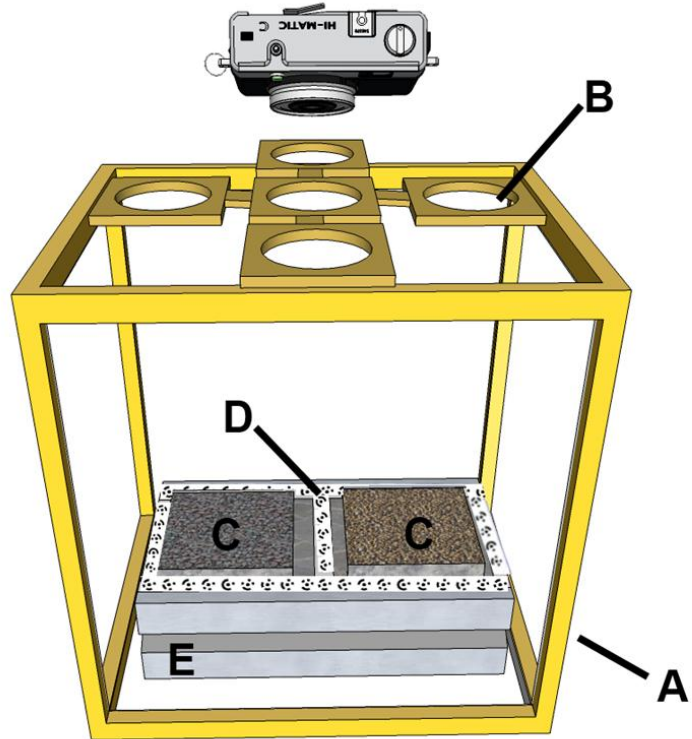


Figure 50. Setup used to generate photogrammetric 3D images of the coupon surface. A- Imaging frame; B- 5 fixed points of view for imaging; C- New and old coupon surfaces; D- Target frame; E- Coupon sample holder.

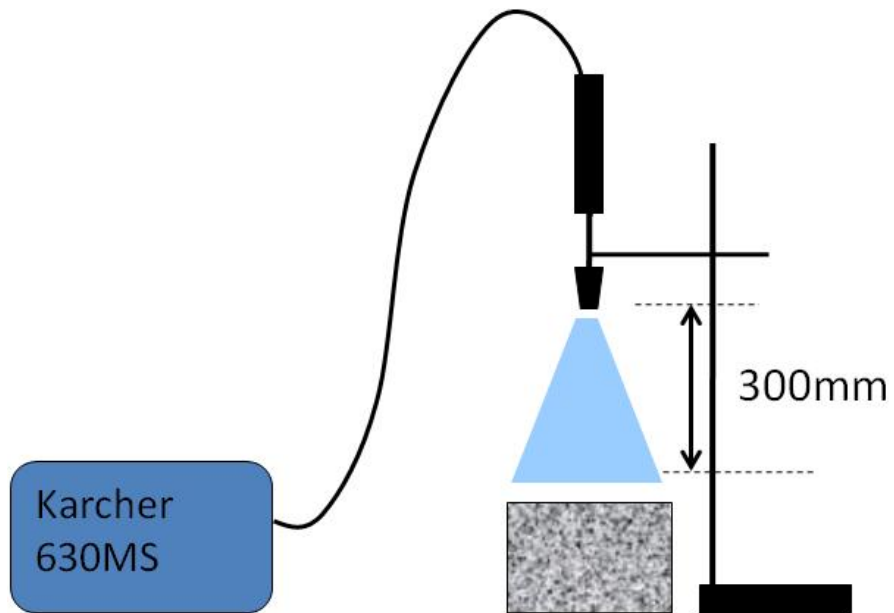


Figure 51. Setup used for high pressure water cleaning of Sp1B field coupons.

The sensitivity of the photogrammetric process was tested as follows. New and old coupons were placed in a small wooden box upon which a target template had been glued (Figure 53) and the average surface height determined as discussed above. A piece of thin cardboard was then placed under the wooden box. The coupons and target frame were re-photographed and the photogrammetry process used to calculate the new height of the coupon surface relative to the target plane. New pieces of cardboard were added and the process repeated until the coupons had been raised approximated 1mm. The change in surface height determined using the photogrammetric process was then compared to the change in height determined from digital vernier calliper measurements of the cardboard thickness. The results, (Figure 54), show a maximum deviation from the measured values of less than 0.1mm (typically less than 0.3mm) which was deemed satisfactory for the coupon measurement work.

Tests were also undertaken to determine the reproducibility of the photogrammetric procedure when measuring the thickness of the Sp1B coupons housed in the sample frames employed in the field trials. Repeated measurements of the field samples pointed to a standard deviation in average coupon thickness of 0.07mm for the new coupon samples and 0.15mm for the old coupon samples.

Using this approach to monitor coupon corrosion also conveyed other advantages over possible alternative techniques. The equipment needed is inexpensive (especially when compared to that needed for laser imaging), the process is generally faster and the photogrammetric techniques inherently involves a series of images which are more intuitive to interpret, provide a visual record of the surface and which can be reprocessed at later dates if the need arises.

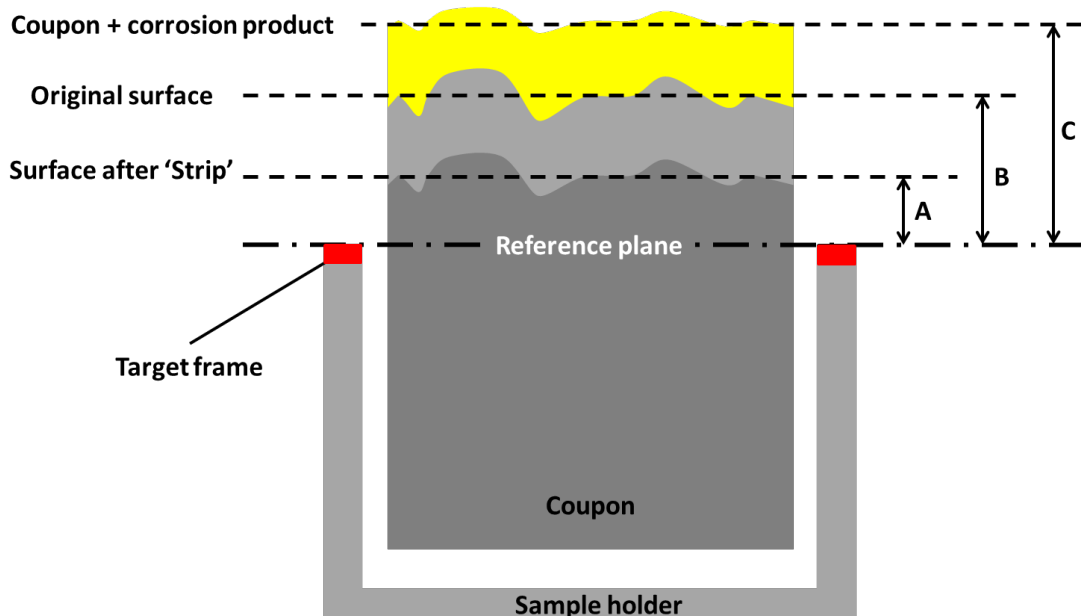


Figure 52. Determination of corrosion layer depth and concrete losses. Corrosion losses = B-A; Corrosion layer depth = C-A.

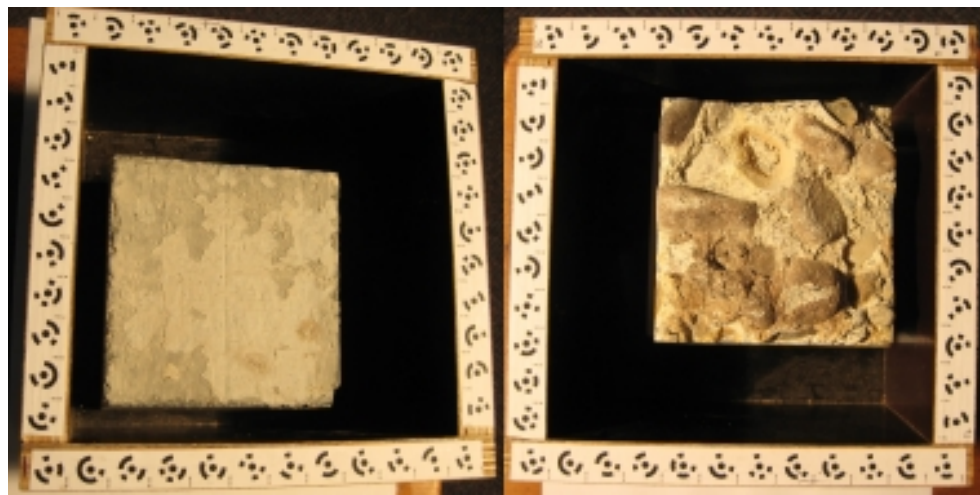


Figure 53. New (left) and old (right) coupons used in photogrammetric test.

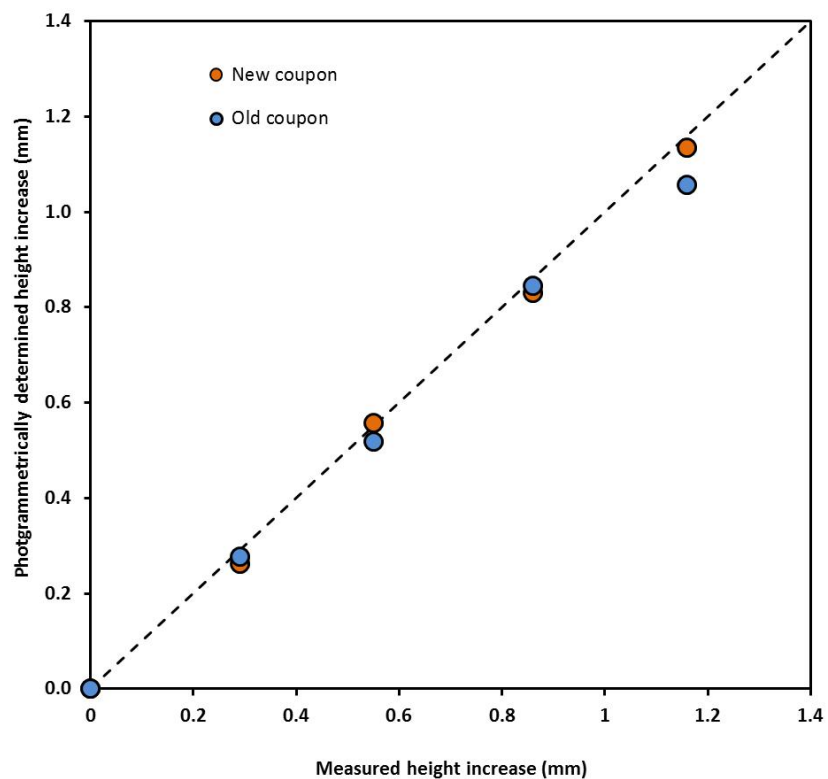


Figure 54. Sensitivity test results for the photogrammetric process. The dashed line represents perfect agreement between measured height increase as determined by digital vernier and heights predicted from the photogrammetry process.

5.3.5 pH survey of samples

An important aspect of the concrete corrosion process in a sewer environment is the lowering of surface pH as surface alkalinity is reduced through contact with acids generated either in the sewer. When first cast, concrete pipe has a surface pH of approximately 12-13 which is too high for microbial communities to form however over time the action of H₂S, CO₂ and other oxides dissolving into the condensate film lying on the concrete surface act to acidify the surface of the concrete, lowering its pH, and eventually creating an environment more conducive to microbial colonisation and activity. Once microbial populations increase the surface pH is further lowered and corrosion accelerates. The rate at which the pH changes in the initial (abiotic) and later (abiotic + biotic) phases is an important indicator to the progress of the corrosion process.

The pH of the surface of new and old concrete coupons was determined where possible at 9 equally spaced locations on the coupon surface using a flat-faced pH electrode (ExStik® 110 pH Meter – Figure 55). A bead of distilled water was first placed on the coupon surface under the head of the pH electrode and allowed to equilibrate for a minimum of 5 minutes before a reading was taken. The meter displays the pH to 2 decimal places. Before each measuring session a three point (pH=4, 7 and 10) calibration was carried out using appropriate buffer solutions.



Figure 55. Flat faced pH meter used in survey of coupon surface pH.

5.3.6 pH profiling

When attempting to calculate the amount of acid needed to bring about a given level of corrosion it is important to not only consider the acid needed to degrade the concrete that has been lost to corrosion (i.e. the “corrosion losses” measured in the field trials) but also any acid which has penetrated into the “sound concrete” ahead of the corrosion front. If the reaction between the acid and the concrete takes place so swiftly that the acid does not have a chance to penetrate into the concrete we observe a sharp well defined corrosion front with little or no lowering of the pH of the “sound concrete”. If however the reaction is slower acid has an opportunity to penetrate into the concrete before it is consumed and we observe a significant region within the sound concrete material which has a lowered pH (a “soft reaction front”). The depth of penetration therefore not only allows us to better calculate the quantities of acid needed to bring about a given corrosive state but also gives us a better insight into the relative rates of acid reaction and diffusion at the reaction front.

To determine the extent of acid penetration into the concrete matrix pH profiles were determined for recovered field coupons after various lengths of time in the sewer. Two techniques were employed to do so:

(a) pH profiling by drilling into the sectioned coupon (see Figure 56).

- I. A number of coupons were sectioned with a diamond saw. Care was taken to ensure that the cuts were made at 90° to the exposed surface.
- II. The newly exposed section faces of the coupon were sanded smooth with wet/dry paper. Once smooth they were dried then lightly brushed to ensure that no loose material was present.
- III. Surface samples (0-1mm depth) were then collected by drilling vertically into the exposed upper surface of the coupon using a 3.1mm masonry drill (no hammer action) down to a depth of 1mm. The ground material generated from the drilling was then carefully brushed into a pre-weighed plastic vial and weighed.
- IV. Sufficient distilled water was added to create a 1:20 dilution. The samples were then vigorously shaken and the pH determined using a flat faced pH probe.
- V. Subsurface (>1mm depth) samples were gathered by drilling horizontally into the coupon cross-section (i.e. parallel to the upper expose surface). Again the dust generated was carefully brushed into a pre-weighed plastic vial and sufficient distilled water added to produce a 1:20 dilution. Again the samples were vigorously shaken and the pH determined using a flat faced pH probe.
- VI. The pH of the excavated concrete dust was then correlated with the position of the drill holes relative to the exposed surface of the coupon. The position of each drill hole was determined by image analysis of microphotographs of the drilled cross section.

(b) pH profiling using universal indicator (see Figure 57)

- I. Coupons were sectioned and sanded.
- II. A number of coupon cross sections were also treated with universal indicator and the sections were then photographed under a low power microscope. A scale was also included in the image.
- III. The subsequent colour variation was compared to standard charts (Figure 58) which was then used to determine the depth of acid penetration.

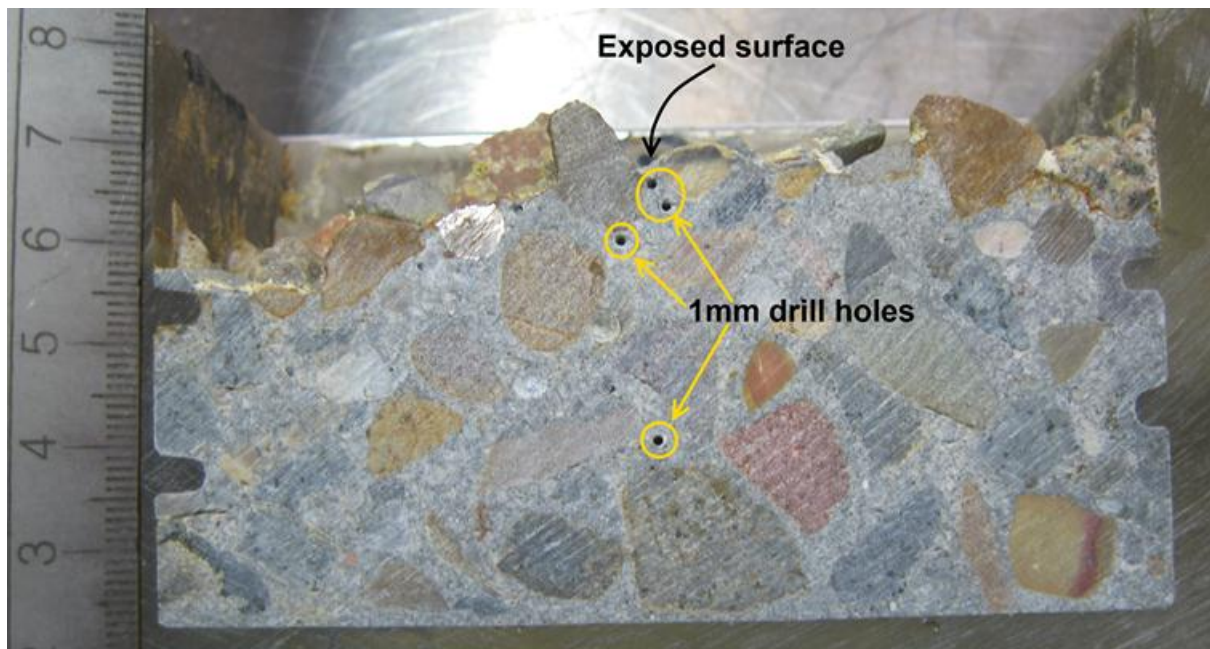


Figure 56. A cross section of a new coupon that has been drilled to obtain pH profile information.

5.3.7 Collection of Environmental data for the three field sites

Collection of the environmental data for the three field sites allows the corrosion behaviour observed at the three sites to be correlated with sewer conditions enabling a phenomenological model to be developed. During the initial stages of the project a monitoring plan was agreed upon with the project's industry partners to obtain the following data at the various field sites:

- Air temperature
- Humidity
- H₂S levels

Environmental monitoring was carried out for a minimum of a 2 week period during each of the four seasons of the year to enable both the diurnal and seasonal trends in these parameters to be determined. In addition to enabling a better correlation between "cause" and "effect" to be determined, the collection of the environmental data permitted a more meaningful

comparison between the corrosion behaviour observed in the laboratory trials (SP1A) and field trials to be conducted. The schedule of returned environmental data is shown in Appendix XX.

The collection of humidity data throughout the trial was problematic as sensors corroded quickly in the H₂S environment. Consequently the characterisation of the sewer humidity was somewhat sketchy. The implications of this are discussed more fully in Section 6 of this report.

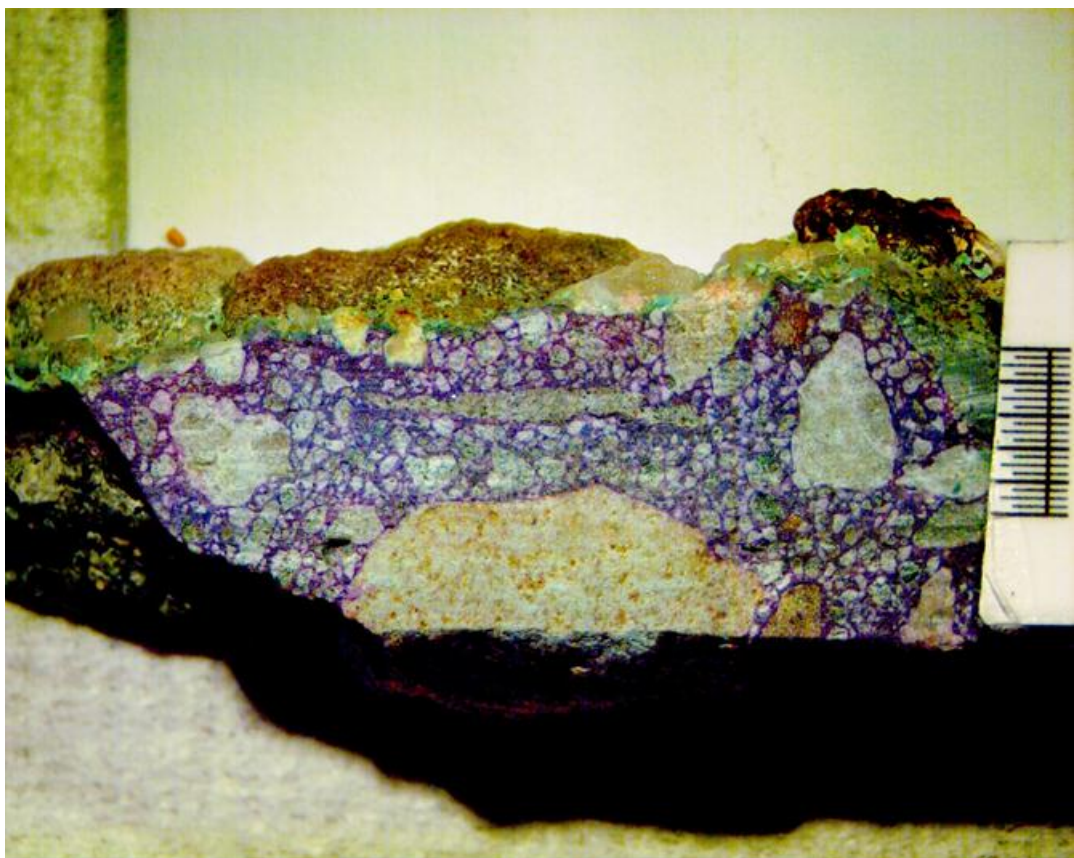


Figure 57. An example of pH profile determined with universal indicator.



Figure 58. Universal Indicator scale (numbers shown are pH values).

5.4 Field study results

The following section reports the observations made during the Sp1B field study. The following will be discussed:

- Environmental conditions
- Coupon surface pH and pH profile trends
- Coupon Losses
- Corrosion layer development

This will then be followed by a discussion of the picture of the corrosion process that has emerged from the data.

5.4.1 Environmental observations

5.4.1.1 General overall observations

Table 13 lists the values for H₂S, relative humidity and gas phase temperature averaged over the study period at each of the field sites. Average H₂S concentrations ranged widely from 1.5ppm at Melbourne SETS up to in excess of 400ppm at Perth Bibra Lake however only Bibra Lake and Perth MS had H₂S concentrations in excess of 6ppm. By way of contrast average sewer gas temperatures fell into a limited range from an average 19.7°C at Melbourne SETS to a high of 27°C at Perth Bibra Lake. Average relative humidities range from a low of ~90% at Bibra Lake to 99-100% at the two Melbourne sites. It should be noted however that obtaining relative humidity data in the sewers proved to be extremely problematic as the H₂S tended to corrode out the sensors quite rapidly. Consequently there was an extremely limited amount of humidity data collected, especially for the two Melbourne field sites and therefore there is a correspondingly low level of confidence in these figures.

5.4.1.2 Diurnal variations in H₂S, RH and temperature

In addition to obtaining overall environmental averages the high resolution data collected allowed a picture of the diurnal and seasonal trends in these factors to emerge. Figures 59 and 60 show typical diurnal cycles for H₂S, temperature and humidity at the Perth MS and Melbourne field sites respectively. At all sites H₂S generally started off relatively high after midnight but decreased until a minimum level in the cycle was achieved at 8 to 10am. Levels increased thereafter so that by ~10pm levels were at or near the peak for the day.

Both temperature and humidity were generally fairly stable on a daily timescale with humidity varying by less than 1% and temperatures varying by 0.1-0.2°C.

Table 13. Environmental data averaged over the study period.

Site	Averages over the study period					
	H ₂ S (ppm)	90%ci	Air temperature (C)	90%ci	Relative Humidity (%)	90%ci
Sydney SWSOOS2N	2.7	0.1	21.6	0.2	94.3	0.7
Sydney SWSOOS2S	2.2	0.1	21.3	0.2	94.4	0.8
Melbourne SETS	1.5	0.1	19.7	0.2	100	1.0
Melbourne WTS	6.0	0.4	20.7	0.2	100	1.0
Perth MS	125.3	13.8	25.8	0.2	96.5	0.6
Perth Bibra	422.1	19.9	27.0	0.6	90.0	1.0

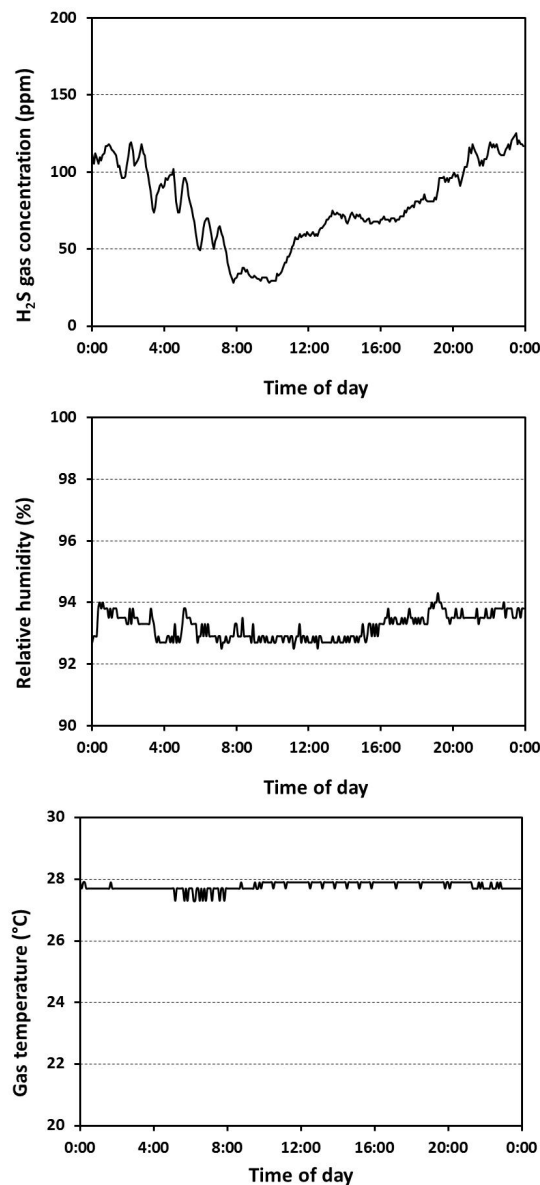


Figure 59. Typical diurnal cycling of H₂S (upper), humidity (middle) and sewer gas temperature (lower) recorded at the Perth MS field site (23rd march 2012).

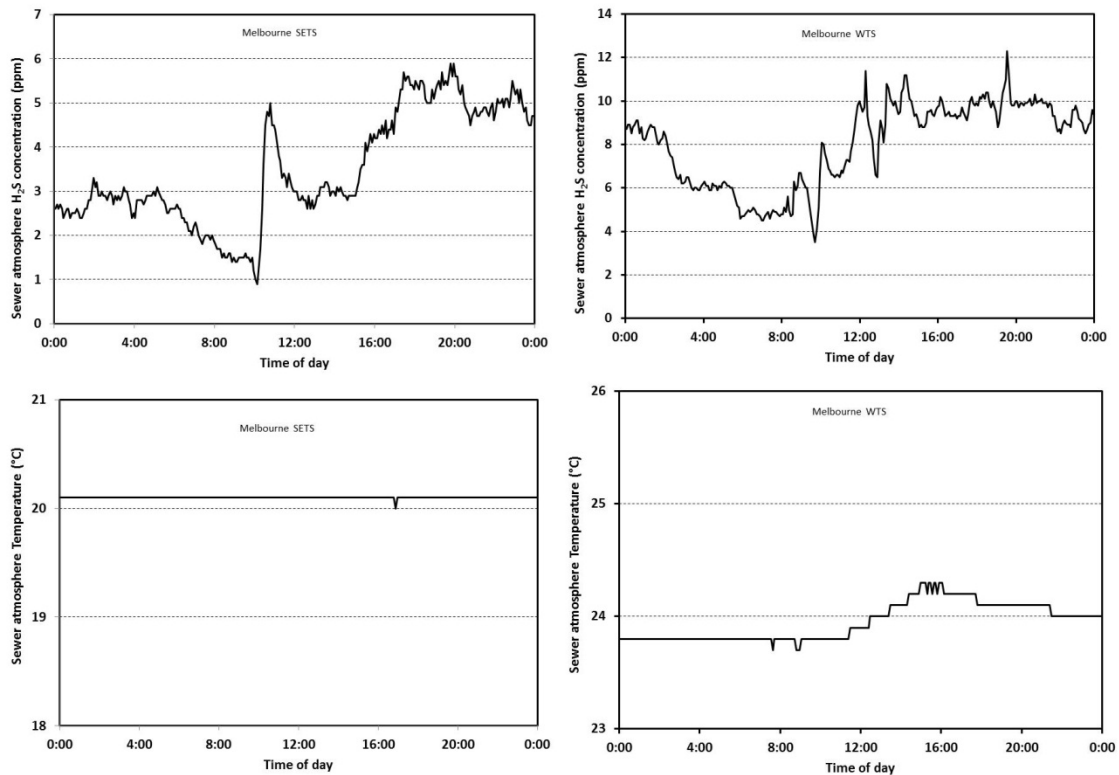


Figure 60. Typical diurnal cycling of H₂S (upper) and sewer gas temperature (lower) recorded on the 24th January 2012 for the Melbourne SETS field site (left) and Melbourne WTS site (right).

5.4.1.3 Seasonal variations in H₂S, RH and temperature

Figures 61, 62 and 63 show the seasonal variations in H₂S, temperature and humidity observed at the Melbourne, Sydney and Perth Field sites respectively. (Note there was not enough humidity data obtained at the Melbourne sites to enable a seasonal trend to be determined)

Generally speaking there wasn't a strong seasonal trend observed in either H₂S or relative humidity. At the Melbourne and Perth sites the H₂S levels in summer and autumn tended to be higher than spring and winter but this trend was not apparent at the Sydney sites. Humidity did not follow any distinctive seasonal trend at any site. As expected the sewer gas temperatures in summer and autumn tended to be higher than winter and for the most part spring. Temperature differences between winter averages and summer averages were as little as ~3-4°C at Perth MS but as high as 10-12°C at Perth Bibra Lake. Differences at the remainder of the sites fell between these two values.

Over the course of the study period some (weak) longer term trends in the sewer environment were noted at some sites. These include the following:

- Increasing temperature at the Melbourne WTS site.
- Increasing H₂S at the Perth MS site

- Decreasing humidity at the Perth MS site
- Increasing humidity at the Perth Bibra Lake site
- Increasing temperatures at the Perth Bibra Lake site

Despite these changes however the overall average conditions at each of the sites remained fairly constant over the study period. In Table 14 for example, which lists the average environmental conditions over the exposure periods for coupons retrieved at each of the field sites it is clear that the overall averages over the entire exposure period were relatively stable.

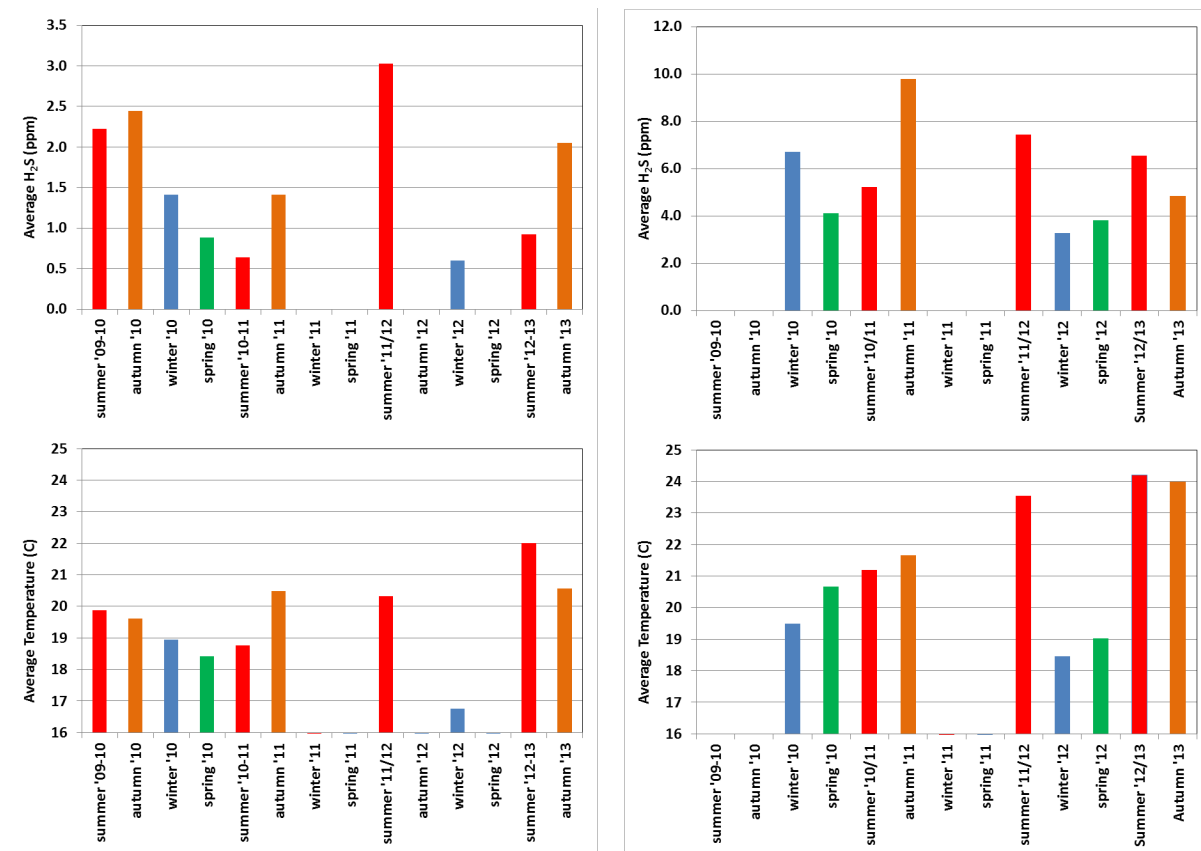


Figure 61. Seasonal variation in H_2S and sewer gas temperature at the Melbourne SETS (Left) and WTS field sites (right). (Red=summer, Orange=autumn, blue=winter and green=spring).

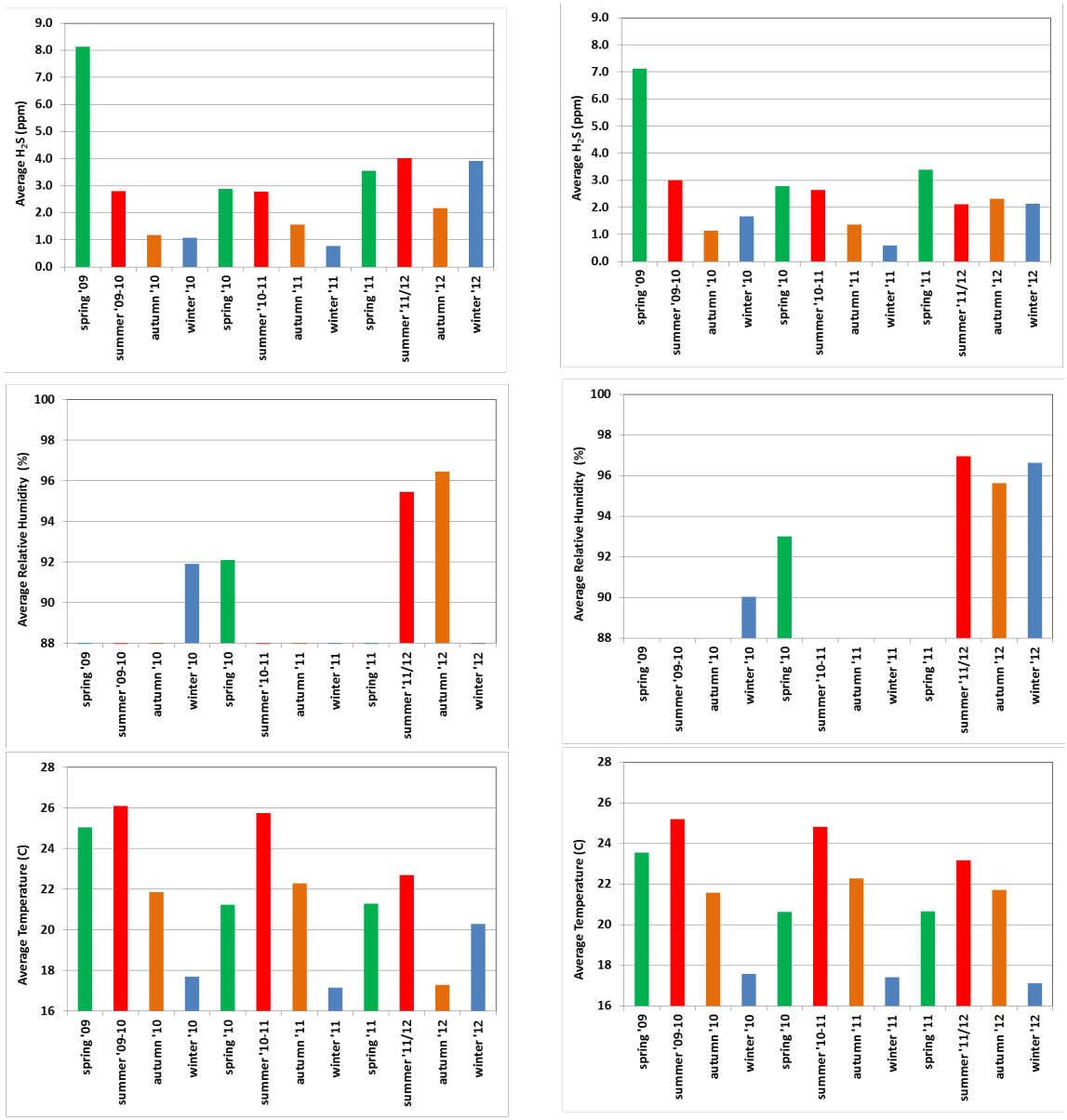


Figure 62. Seasonal variation in H₂S, relative humidity and sewer gas temperature at the Sydney North SWSOOS2 (left) and SWSOOS2 South field sites (right) (red=summer, Orange=autumn, blue=winter and green=spring).

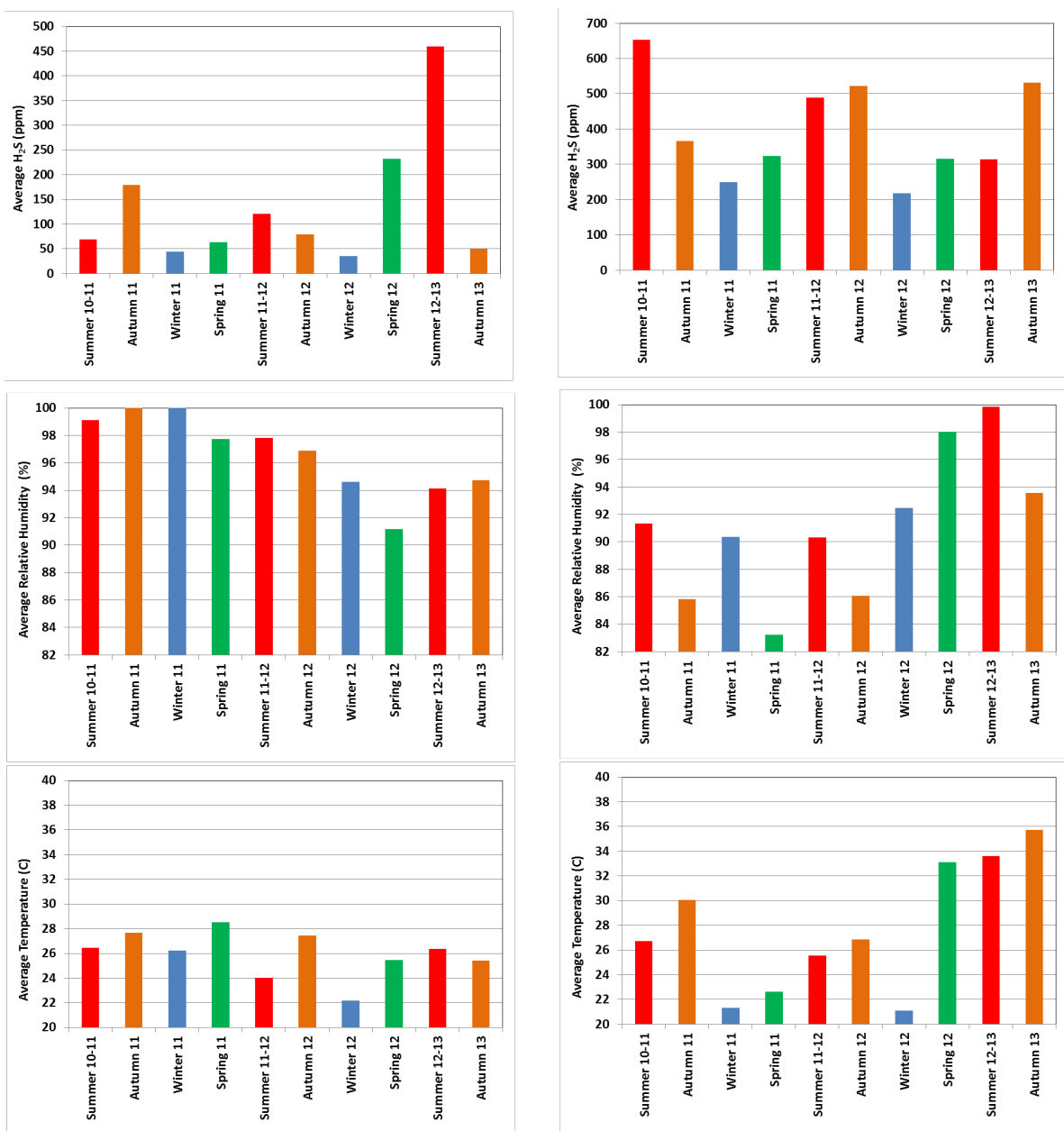


Figure 63. Seasonal variation in H₂S, relative humidity and sewer gas temperature at the Perth MS (left) and Bibra Lake field sites (right) (red=summer, Orange=autumn, blue=winter and green=spring).

Table 14. Environmental conditions averaged for the exposure period of retrieved coupons.

Data averaged from coupon installation to retrieval.								
Site	sample #	exposure	av H2S (ppm)	90%ci	av air T (C)	90%ci	av RH* (%)	90%ci
Sydney SWSOOS2N	1	9 months	2.8	0.3	24.1	0.3		
	2	12 months	2.4	0.3	22.2	0.3	91.9	0.7
	3	24 months	2.2	0.1	21.9	0.2	92.0	1.3
	4	36 months	2.7	0.1	21.6	0.2	94.3	0.7
Sydney SWSOOS2S	1	9 months	2.8	0.6	23.4	0.3		
	2	12 months	2.6	0.4	22.0	0.3	90.0	1.3
	3	24 months	2.1	0.2	21.6	0.2	90.9	1.4
	4	36 months	2.5	0.2	20.7	0.2	96.4	0.6
Melbourne SETS	1	7.5 months	1.9	0.2	19.5	0.1	100.0	1.0
	2	12.6 months	1.6	0.2	19.2	0.1	100.0	1.0
	3	18.4 months	1.6	0.2	19.6	0.1	100.0	1.0
	4	24.4 months	1.7	0.2	19.7	0.1	100.0	1.0
	5	31.1 months	1.6	0.1	19.2	0.2	100.0	1.0
	6	39.4 months	1.5	0.1	19.7	0.2	100.0	1.0
Melbourne WTS	1	7.1 months	7.2	0.5	19.8	0.2	100.0	1.0
	2	12.2 months	6.2	0.6	20.2	0.2	100.0	1.0
	3	18 months	7.8	0.6	20.8	0.2	100.0	1.0
	4	24 months	7.7	0.5	21.3	0.2	100.0	1.0
	5	33.7 months	6.0	0.4	20.3	0.2	100.0	1.0
	6	39 months	6.0	0.4	20.7	0.2	100.0	1.0
Perth MS	1	7.1 months	68.5	3.0	26.5	0.1	99.1	0.6
	2	13.9 months	105.3	14.5	26.9	0.2	99.4	0.4
	3	19.3 months	80.7	9.5	27.0	0.2	99.6	0.3
	4	26.3 months	84.3	7.0	26.6	0.2	98.6	0.4
	5	31.4 months	120.6	12.5	25.8	0.2	96.9	0.7
	6	37.8 months	81.1	6.8	26.3	0.3	98.4	0.4
Perth Bibra Lake	1	5.9 months	652.7	41.2	26.7	0.2	91.3	1.3
	2	12.7 months	546.2	51.6	28.0	0.5	89.3	1.1
	3	18.1 months	408.0	36.3	24.8	0.7	88.1	1.5
	4	25.1 months	442.8	27.5	25.3	0.5	87.9	1.0
	5	30.3 months	404.2	22.3	26.5	0.6	90.3	0.9
	6	36.6 months	422.1	19.9	27.0	0.6	90.0	1.0

- Note:** RH averages for Melbourne sites estimated from small number pool of data.

5.4.2 Analysis of recovered coupons

5.4.2.1 General appearance and surface features of the recovered coupons

Figures 65 to 71 show a pictorial summary of how the exposed surface of both new and old coupons changed in appearance over time.

The overall progression was fundamentally the same at each site however the timing of the surface evolution was dependent on the environmental conditions present at each individual site. For example at the aggressive Perth MS site new coupons transitioned from a smooth consolidated surface through to a surface covered with a pale, pasty (cottage cheese) consistency in 14-19 months. By this stage the surfaces of the old and new coupons at this site were virtually indistinguishable (Figure 65). By way of contrast the breakdown of the new coupon surface at the benign Melbourne SETS site (Figure 67) was considerably slower so that at the end of the study period (after 39 months exposure) while there had been noticeable changes in the surface of the new coupons the development of the corrosion layer was noticeably less developed than that present on the (pre-corroded) old coupons.

The first signs of corrosion on the new coupon surface took the form of a thin layer of corrosion material consisting of small (~0.1- 0.2mm) transparent hexagonal crystals or a more amorphous film (Figure 72). Inspection of the amorphous film and crystalline material under an SEM/EDS revealed that the film/crystals were principally composed of gypsum (CaSO_4).

As the pH of the surface dropped below 9 additional biological features were also observed on the surface of the new and old coupons. Observed biological growths took three main forms which may or may not be related. First observable growths took the appearance of small black nodules (Figure 73). Inspection of the black nodules under SEM did not shed much light on their nature. The markings were easily identified as small raised roughly hemispherical protrusions ~10 μm wide on the coupon surface however in the majority of cases the surface texture was identical to the surrounding coupon material. EDS spectral analysis of the protrusions, (see spectra in Figure 74), indicated that they were identical in composition to the surrounding (concrete) material indicating that either: (a) their chemical makeup was similar to the surrounding concrete or (b) the nodules were principally organic and therefore transparent to the EDS. (The SEM used is not directly capable of identifying elements with atomic weights less than sodium. The presence of organic material (i.e. carbon) is generally inferred by the fraction of "noise" generated at the low energy end of the spectra – the first peak at the zero keV mark on the EDS spectra).

Also present in the early stages of corrosion were colonies presenting clusters of pale green growths (Figure 75 to 77). Inspection of these growths under a low power microscope revealed that they collections of pale green hyphae (bacterial or possibly fungal) centred on mounds of white powdery material. Initially the clusters were quite isolated (Figure 75) however over time more continuous mats of the hyphae were observed particularly at more aggressive sites (e.g. Figure 76). SEM/EDS analysis of the material present within the "mounds" (Figure 77) showed that they were mainly comprised of silicon (quite different in

composition from nearby surface material). Further magnification of the hyphae themselves revealed the presence of numerous nodular strings. EDS analyses of these nodules were inconclusive again suggesting that the fine nodules may be organic.

As corrosion advanced the black nodules and green hyphae were generally replaced by dark ropey structures on the coupon surface. (Figures 78 to 80). Inspection of the black "webbing" revealed its braided rope-like nature (Figure 81) suggesting that it was comprised of thick braids of hyphae. Numerous prism shaped nodules were observed in amongst the braided hyphae. EDS analysis of the nodules suggested that were primarily elemental sulphur suggesting that the fungal or bacterial communities responsible for the hyphae were reducing H₂S (and possibly other sulphur sources) to elemental sulphur.

The corrosion layer itself was generally quite porous containing numerous pits, tunnels into the corrosion product and even into the sound concrete proper (see for example Figure 82). As corrosion advanced and the depth of the corrosion product layer increased numerous cracks throughout the corrosion product layer were observed. This was particularly the case in and around exposed aggregate (Figure 83) where the expansion of the corrosion product had lifted the corrosion layer away from the edges of the aggregate material.

Interestingly there were also numerous instances where pieces of exposed aggregate had been severely fractured by the corrosion process despite still being embedded in the sound concrete material (Figure 84).

Visual inspection of the corroded coupons retrieved from each field site indicated the following order of "corrosiveness". This hierarchy was confirmed by a comparison of the rates of change in surface pH and amounts of material lost at each site.



Figure 64. Ranking of Sp1B field site corrosion activity based on visual inspection of samples.



Figure 65. Development of coupon surface appearance over time at the Perth MS field site.



Figure 66. Development of coupon surface appearance over time at the Perth Bibra field site.



Figure 67. Development of coupon surface appearance over time at the Melbourne SETS field site.



Figure 68. Development of coupon surface appearance over time at the Melbourne WTS field site.



Figure 69. Development of coupon surface appearance over time at the Sydney SWSOOS2 North (roof) field site.



Figure 70. Development of coupon surface appearance over time at the Sydney SWSOOS2 South (roof) field site.



Figure 71. Development of coupon surface appearance over time at the Sydney SWSOOS2 South (wall) field site.

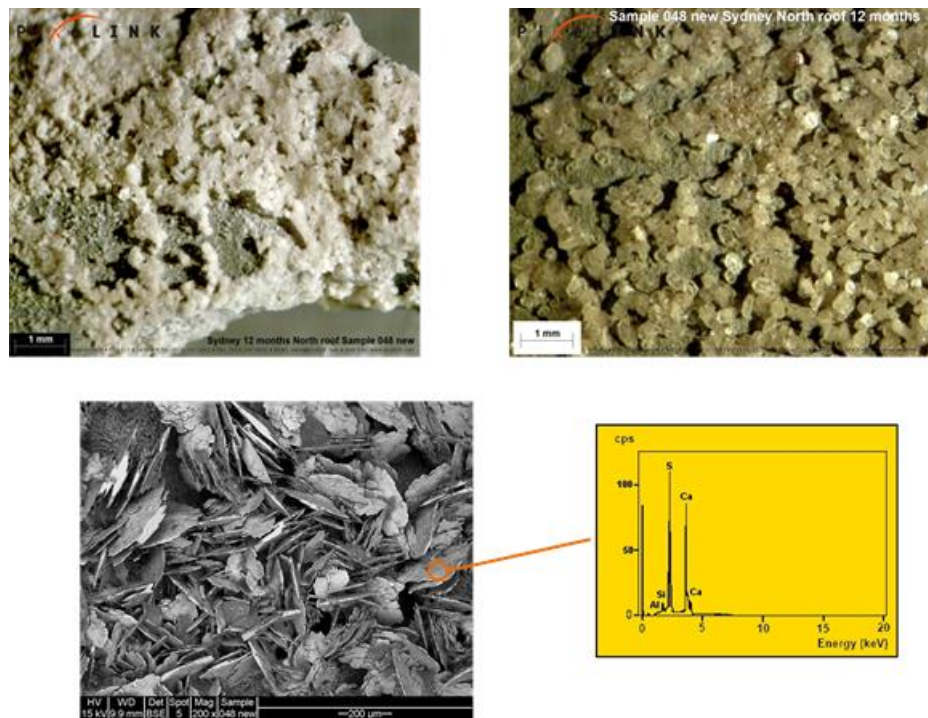


Figure 72. Gypsum crystals formed on the surface of a new coupon exposed for 12 months at Sydney SWSOOS2 North field site. Bottom photo shows crystals under SEM along with EDS spectra of crystalline material showing it is gypsum.

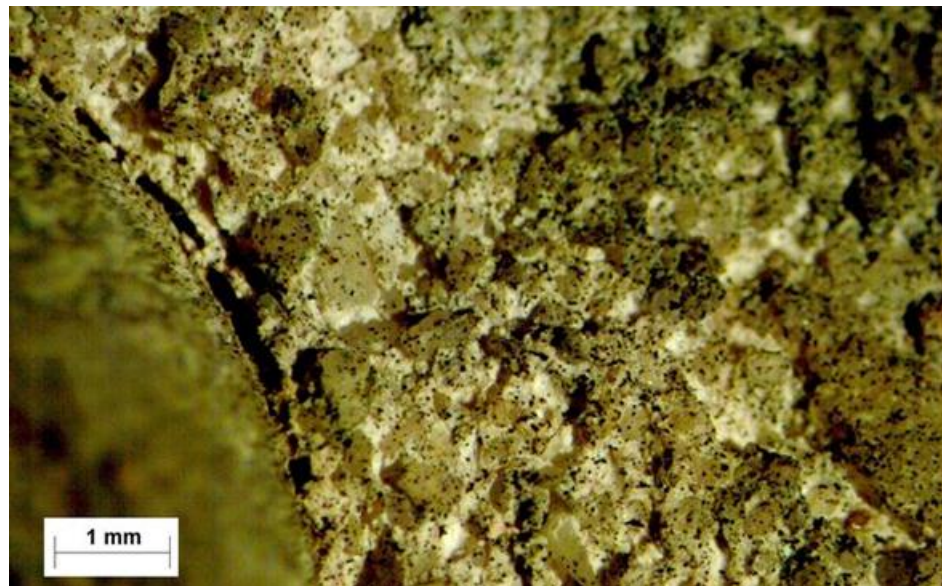


Figure 73. Black nodules (bacterial or algal colonies) observed on surface of an old coupon exposed at Sydney SWSOOS2 South roof site for 12 months.

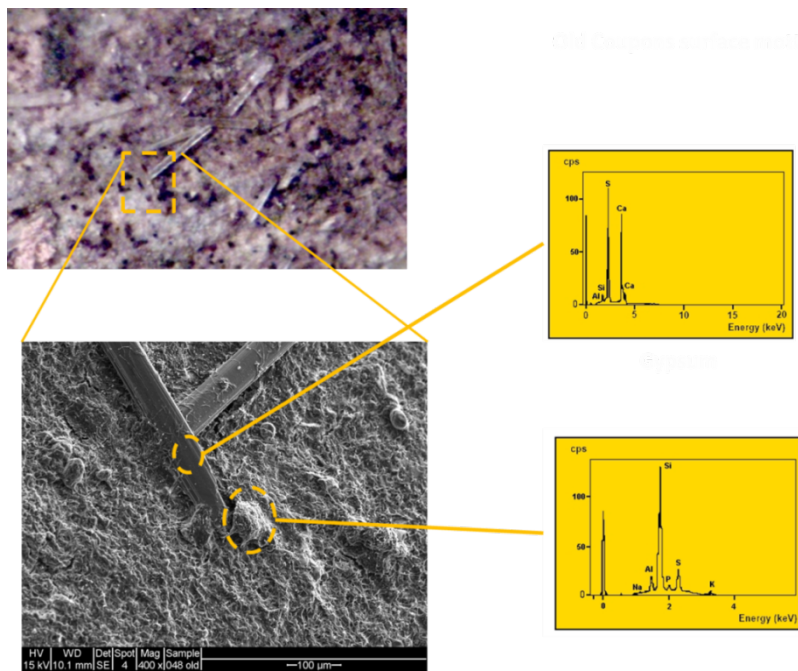


Figure 74. SEM and optical microphotograph of crystals and black nodules on the surface of old coupon (Sydney SWSOOS2 North roof, 12 months). EDS analysis of the surface crystals indicate that they are most likely Gypsum. EDS analysis of the black nodules indicated that they were principally composed of organic material.

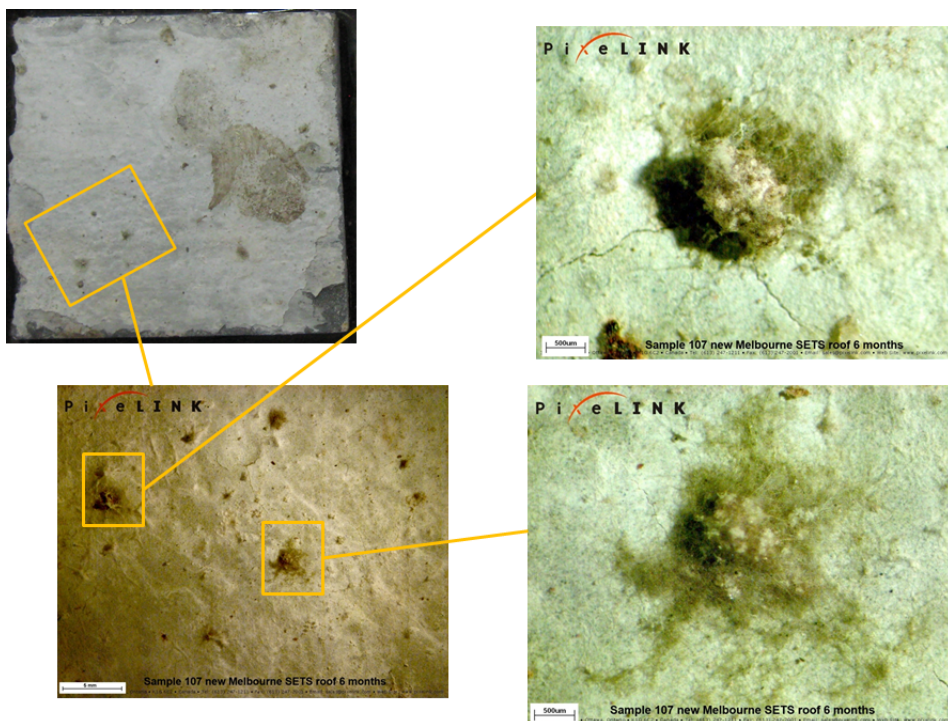


Figure 75. Fungal growth present on the exposed surface of a new coupon exposed for 12 months at the Melbourne SETS site.

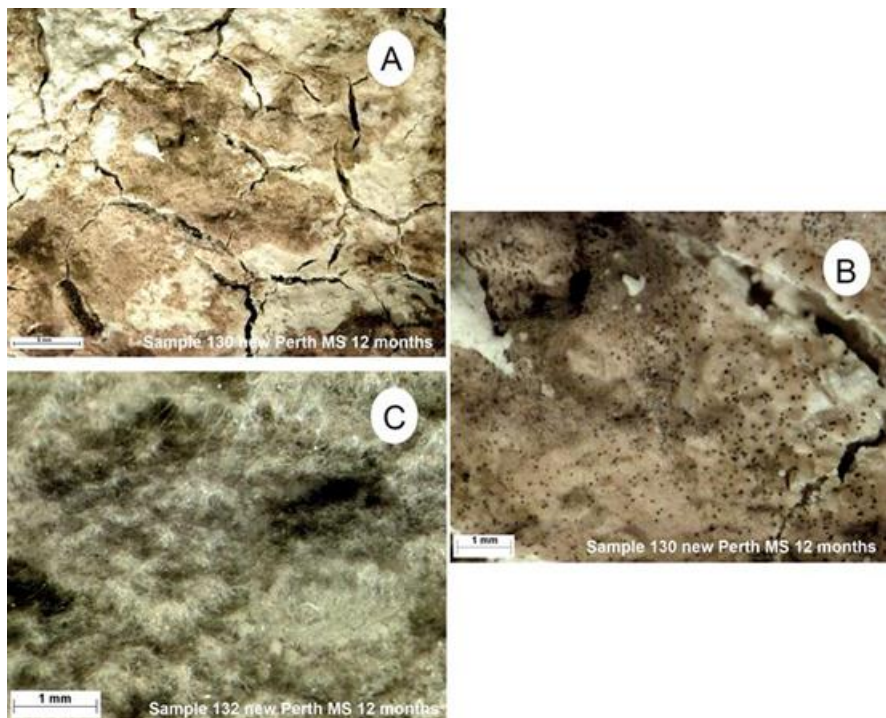


Figure 76. Microphotographs of the surfaces of new coupons exposed at Perth MS for 12 months showing evidence of: (a) extensive cracking of the corrosion layer; (b) the presence of numerous bacterial/algal colonies on the exposed surface of the corrosion layer and (c) mats of pale green hyphae on the coupons surface.

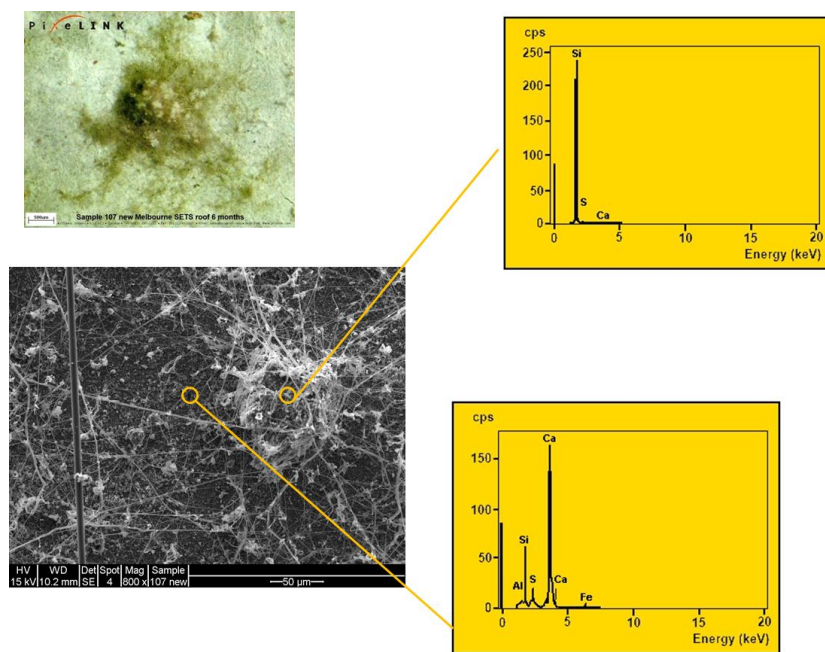


Figure 77. SEM and optical microphotographs of hyphae present on surface of new coupon (Melbourne SETS, 6 months). EDS spectra of specific locations is also shown.

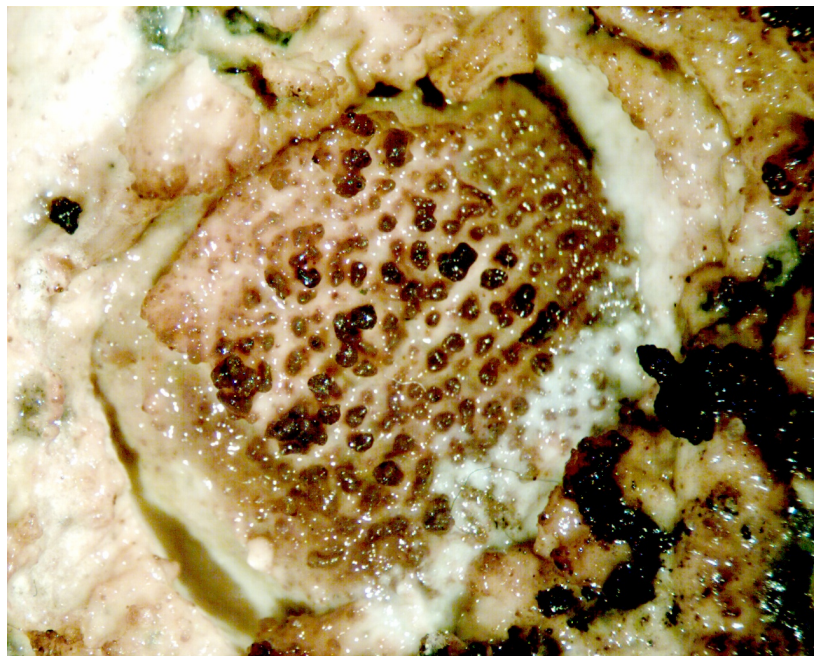


Figure 78. Dark algal/bacterial colonies formed on the surface of an old coupon exposed at the Melbourne WTS site for 39 months.



Figure 79. More intense black spotting observed on a new coupon after 36 months exposure at the Melbourne SETS field site.

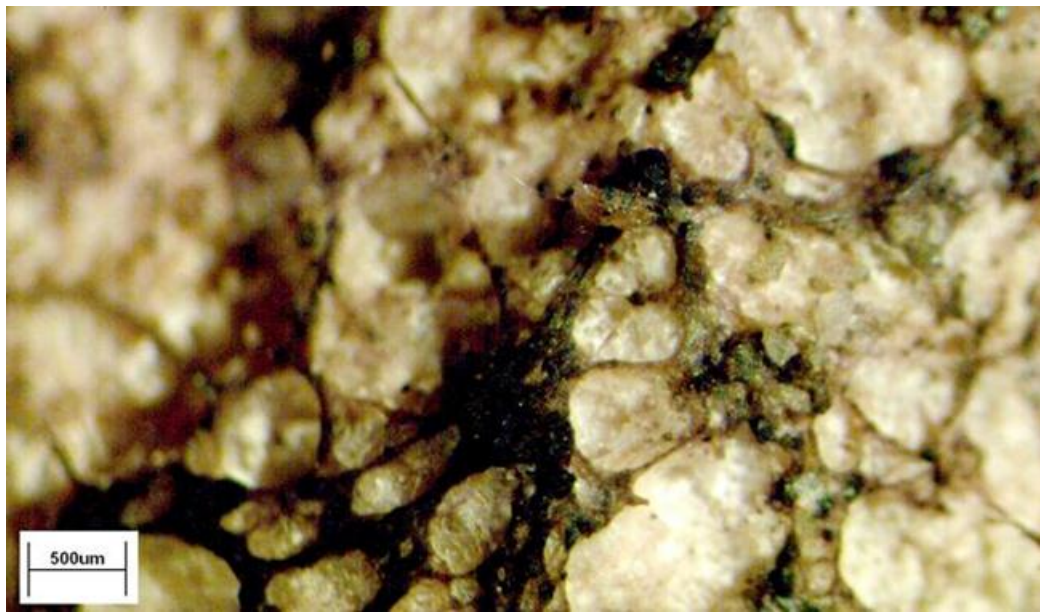


Figure 80. Thick, dark hyphae webbing observed on the surface of an old coupon exposed at Melbourne WTS site for 6 months.

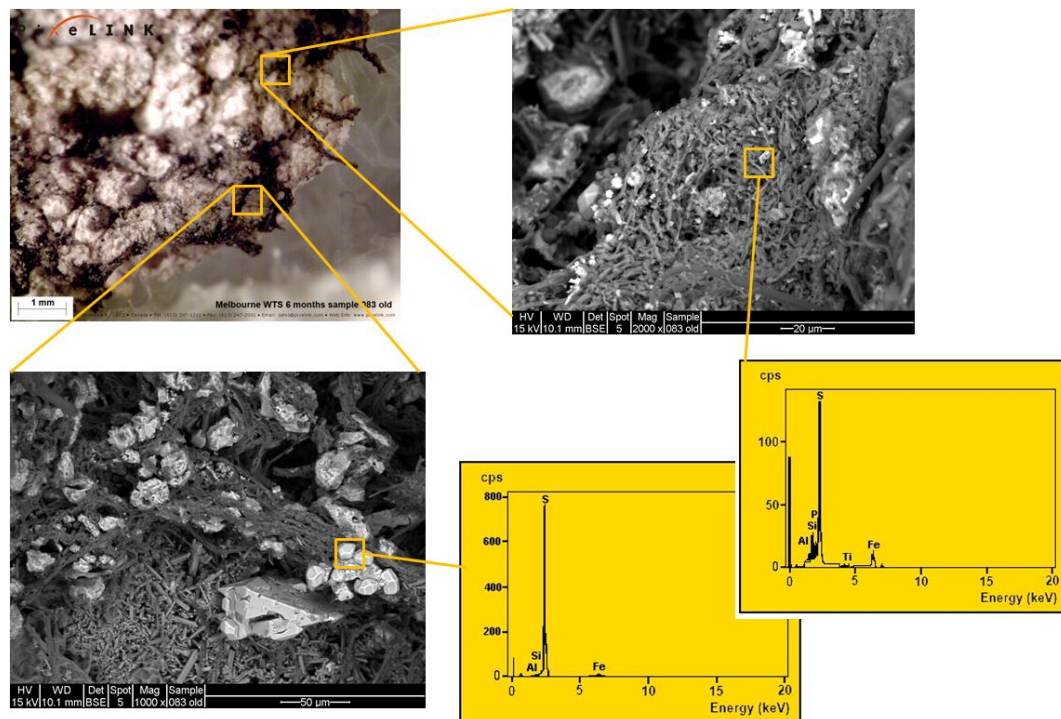


Figure 81. SEM and optical microphotographs of hyphae on surface of old coupon exposed at Melbourne WTS field site for 6 months. EDS spectra of specific locations is also included indicating the presence of pure S nodules.



Figure 82. Tunnels formed into sound concrete structure observed in an old coupon exposed at Sydney SWSOOS2 South wall field site.



Figure 83. An example of cracking in the corrosion layer that forms around a piece of aggregate as the corrosion product swells (old coupon Perth MS field, 38 months).



Figure 84. An example of the fracturing of the aggregate. (old coupon, Perth MS field, 38 months).

5.4.2.2 Corrosion Losses

Corrosion loss data collected over the study period for new and old coupons are listed in Table 25 to Table 30 in Appendix XXI and Appendix XXII. The loss of concrete over time for new and old coupons are plotted in Figures 85 through to Figure 90. Once again the loss trends observed for new coupons were assumed to mirror the corrosion behaviour at the beginning of the pipes life while losses observed on the old coupons demonstrated the corrosion behaviour of the pipe in later years when corrosion is well established.

Unfortunately as alluded to earlier the field trials at the three Sydney sites was curtailed before significant corrosion losses were observed in coupons exposed at those sites. Consequently the following discussion focuses on the four remaining field sites (two in Perth and two in Sydney).

New coupon corrosion losses

New coupon losses at all sites are plotted in Figure 85 and at individual sites in Figures 86 and 87. At the commencement of the trial there was a period for all new coupons during which no corrosion losses were observed. During this initial 'incubation' period corrosion activity in the form of a lowering of the surface pH was taking place (see 5.4.2.3) however no measurable amounts of concrete were being removed. The duration of the initial incubation period varied between sites falling between 8 to 24 months (see Table 15) with shorter times observed at more aggressive sites and generally longer times at more benign sites.

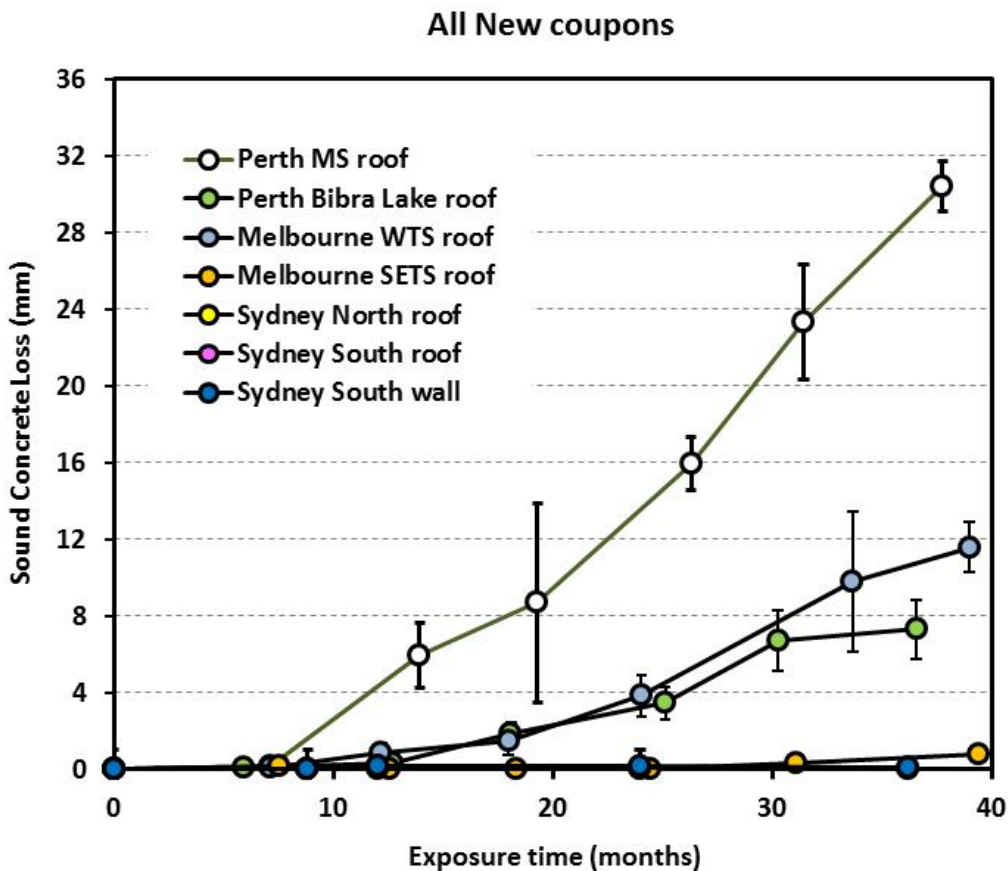


Figure 85. Loss of sound concrete from new coupons over time at all field sites.

At more aggressive sites the transition between the incubation phase and the corrosion phase was well defined and abrupt while at less aggressive sites the transition appeared to be less well defined. This however may have been due to the sample to sample variability which produced a range of measured corrosion loss observed at each site for each recovery period. This variability is accounted for by the vertical error bars shown on individual data points in Figures 85 to 87 which show the standard deviation of the losses recorded for the three samples retrieved from any one location at each retrieval time.

At the four field sites remaining at the end of the study period (the two Perth and two Melbourne sites) once corrosion commenced losses increased linearly over time, i.e. all new coupons experienced a constant rate of corrosion (see Figures 86 and 87).

Table 15 lists the length of the incubation period (time to the onset of corrosion losses) and Table 16 lists the subsequent corrosion rate experienced by the new coupons at the Perth and Melbourne field sites. The corrosion rate was determined at each site as the slope of the line of best fit to the loss data against time once corrosion has commenced (see Figures 86 and 87). The linear regression was a good fit to the data in all cases ($r^2 > 0.95$). The 90% confidence interval of the linear regression slope was also calculated and used to characterise the likely range of the corrosion rate (also listed in Table 15).

A wide range of corrosion rates were observed from over 1mm/year at the Perth MS site to as low as 0.6mm/year at the Melbourne SETS site. Interestingly the ranking of the field sites in terms of corrosion rates matches the ranking obtained when surface pH change and visual appearance is considered (see Figure 64). The time to first corrosion however does not totally correlate with the stated order of aggressiveness (Perth Bibra and Melbourne WTS swap positions).

One of the more surprising outcomes of the field study was the (relatively) low rate of corrosion activity observed at the Perth Bibra Lake site. Despite having the highest H₂S concentrations of all of the field sites corrosion activity ranked behind both Perth MS and Melbourne WTS sites where H₂S levels were significantly lower. Examination of the environmental data available for the site suggests that it however is considerably "drier" than the other 3 field sites (humidities between ~85-90% for a large part of the trial period). This anomaly suggests that humidity may play an important role in determining the rate at which corrosion progresses. This effect will be discussed in more detail in Section 6.5.3.

Table 15. Duration of the "incubation period" (the time elapsed before the onset of corrosion losses) for new coupons at the Perth and Melbourne field sites.

Site	Time to start of corrosion (months)
Perth MS	9
Perth Bibra lake	12
Melbourne WTS	15
Melbourne SETS	24

Table 16. The rate of corrosion experienced by new and old coupons (pH<6). (The 90% confidence interval of the slope of the regressed line through the loss data is used to characterise the corrosion rate uncertainty).

Site	New coupon		Old coupon	
	Rate of corrosion (mm/yr)	+/- 90% ci	Rate of corrosion (mm/yr)	+/- 90% ci
Perth MS	11.8	1.6	10.5	0.5
Melbourne WTS	6.1	1.2	6.5	0.6
Perth Bibra lake	3.7	0.7	5.0	0.9
Melbourne SETS	0.6	0.2	1.1	0.5

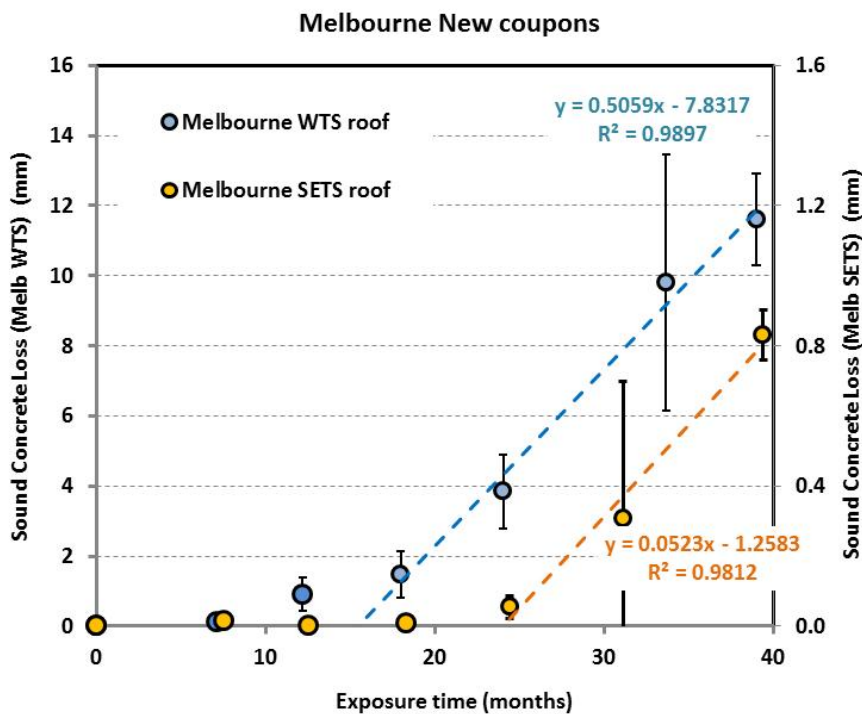


Figure 86. Loss of sound concrete from new coupons installed at the two Melbourne field sites.
Dashed lines are a linear regression of corrosion losses versus time once corrosion has commenced.

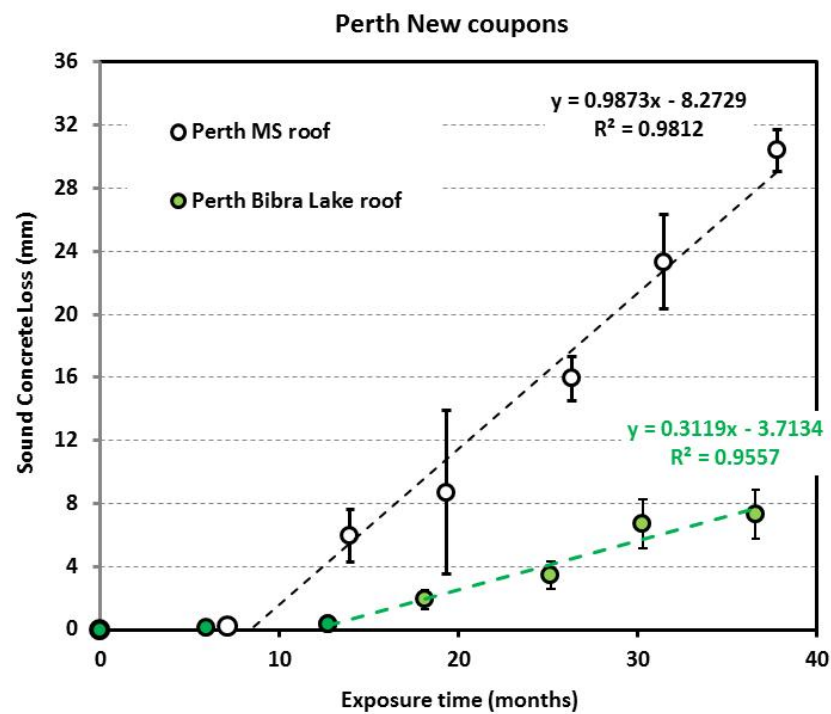


Figure 87. Loss of sound concrete from new coupons installed at the two Perth field sites.
Dashed lines are a linear regression of corrosion losses versus time once corrosion has commenced.

Old coupon corrosion losses

Old coupon losses at all sites are illustrated in Figure 88 and at individual sites in Figures 89 and 90. In contrast the behaviour observed for new coupons, old coupon corrosion losses commenced almost immediately upon their installation in the sewers. This was not unexpected as the initial surface pH of the old coupons was already lowered (to approximately pH=8) as a result of the prior history of exposure to sewer conditions experienced by these coupons. As a result old coupon surface pH rapidly reached the critical value (pH=6) and as the surface was already quite porous conditions for biologically induced corrosion were rapidly established and losses were quickly incurred.

There was a greater level of sample to sample variability in losses incurred by the old coupons compared to the new coupons at the same location/time. This was a result of the larger aggregate to be found in the old coupon concrete. The spalling (or not) of individual pieces of aggregate thus had a larger impact on the average losses calculated from the photogrammetric method resulting in a larger variance in the loss data between individual samples. Once again the sample to sample variability is illustrated in Figures 88 to 90 by the data error bars which represent the standard deviation of the losses of the three samples retrieved at any one time/location. The averaging of corrosion losses experienced by triplicate samples however tended to overcome this variability issue somewhat.

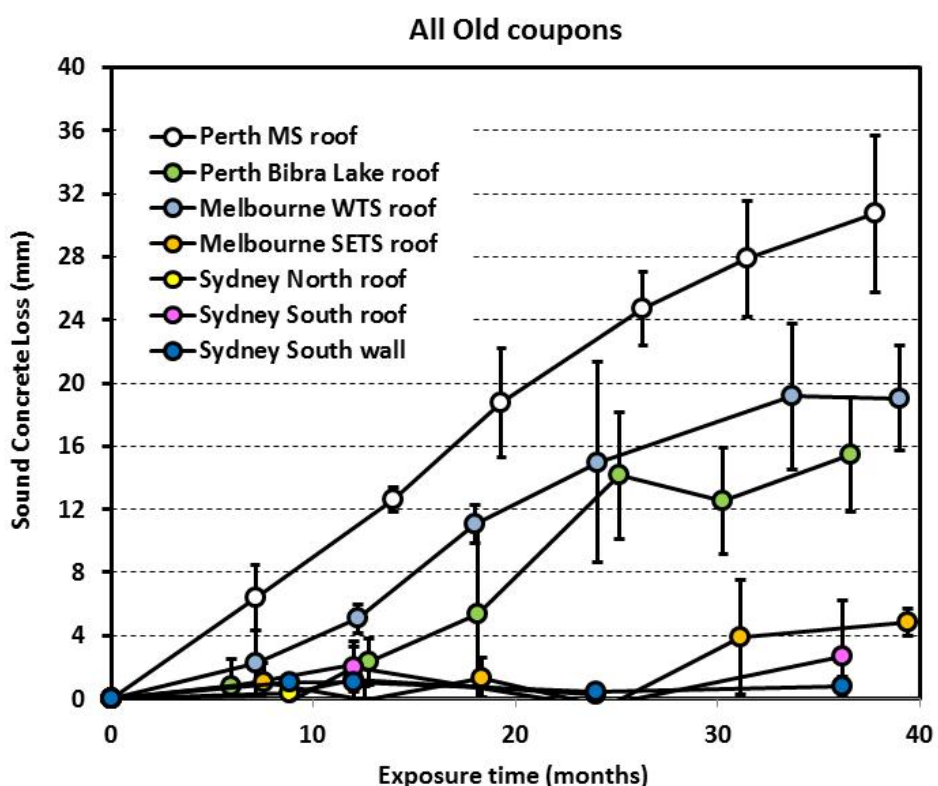


Figure 88. Loss of old coupon sound concrete over time at all field sites.

The corrosion rates were again determined by linear regression of the loss data against time however all data was considered and the intercept was forced through the origin. Again the 90% confidence interval of the regressed slope was used to characterise the possible variation in the calculated corrosion rate. Despite the greater sample to sample variability it is clear that the rate of concrete loss was once again close to linear with respect to time at all sites indicating that the corrosion rate is constant over time for these samples. It should be noted however that the r^2 values for the lines of best fit, while fair, were lower than that observed for the new coupon data (ranging from $r^2=0.54$ to 0.98). In part this is likely due to the aforementioned sample to sample variability particularly for data recorded at the Melbourne SETS site where sample to sample variability was similar in magnitude to the corrosion losses experienced by the coupons.

The corrosion rates calculated for the old coupons covered much the same range as those recorded for the new coupons once corrosion commenced. In fact the corrosion rates for old and new coupons corresponded well (the range of calculated rates overlapped at all sites – see Table 16 and Figure 91). This indicates that at all sites we are seeing an overlap between the corrosion behaviour of the new and old coupons allowing us to obtain a good picture of the whole corrosion cycle of the concrete pipe. Once again the corrosion activity at Perth Bibra Lake appeared to be suppressed by low humidities.

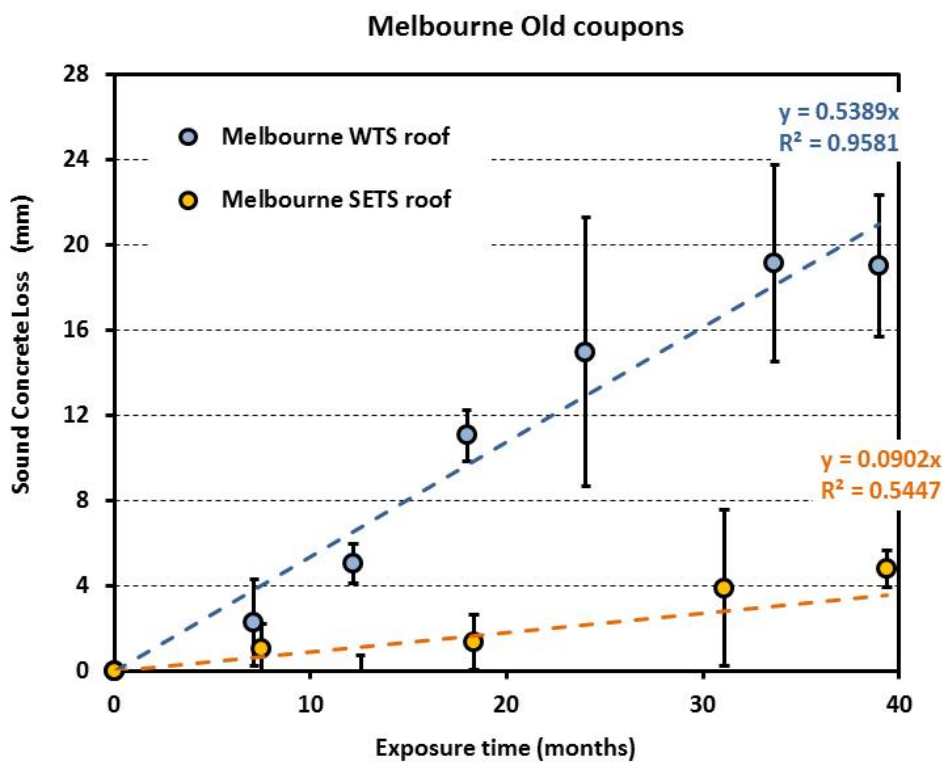


Figure 89. Loss of sound concrete from old coupons installed at the two Melbourne field sites.

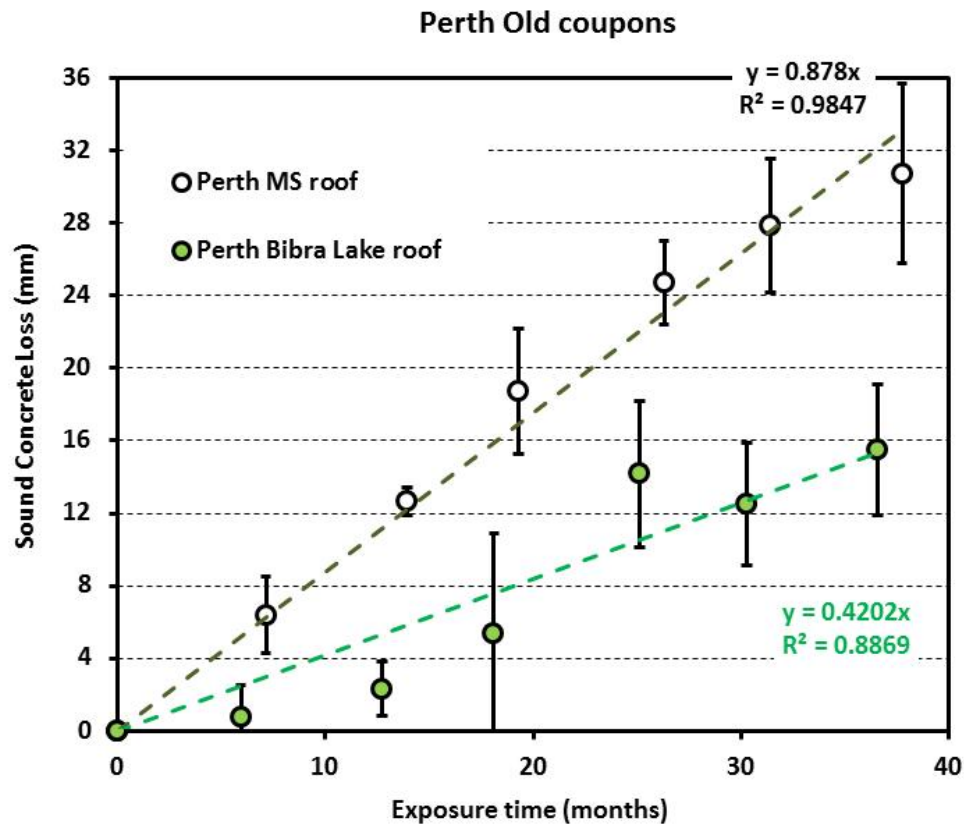


Figure 90. Loss of sound concrete from old coupons installed at the two Perth field sites.

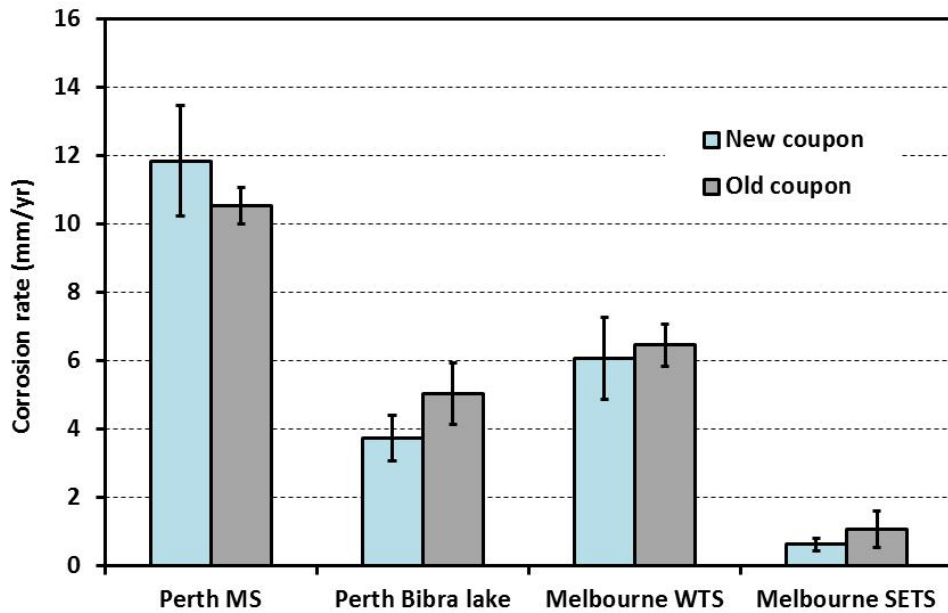


Figure 91. A comparison of new and old coupon corrosion rates.

5.4.2.3 Surface pH trends over time

New coupon surface pH trends

Average surface pH values were determined for new and old coupons recovered at each site by averaging the coupon surface pH average of the 3 samples recovered. The surface pH averages for new coupons are listed in Tables 25 to 27 in Appendix XXI and plotted in Figure 92. In studying the corrosion behaviour of the new coupons we are seeking to understand the corrosion process during the initial stages of the sewer pipes service life. New coupon surface pH declined at all sites over time and generally the rate of decrease in pH correlated with the aggressiveness of the field site. Initial acidification of the coupon surface from the initial pH of 10.3 was relatively rapid but tended to slow as the pH approached pH=4. The lowest new coupon surface pH observed was pH=2.3 recorded after 39 months exposure at Perth MS. The surface pH of the control samples by way of comparison were relatively stable, experiencing only small declines over the study period (pH drop of ~0.3 (new coupons) and 0.7 (old coupons)).

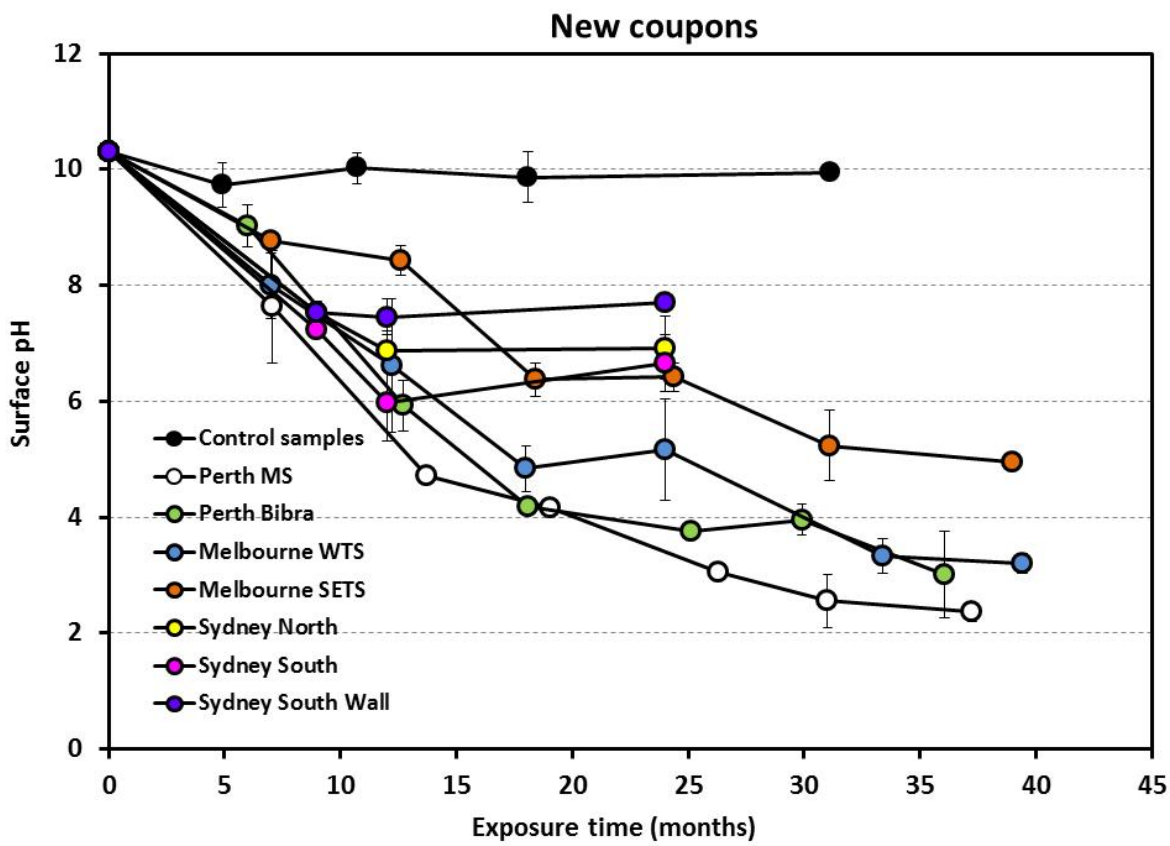


Figure 92. Surface pH of Sp1B new coupons. pH error bars calculated from standard deviation of measurements for the 3 three coupons retrieved at each site at each retrieval time.

In modelling the corrosion process a number of pH values are thought of as being significant. [25] for example proposed a three stage model of the corrosion process (Figure 1). In stage 1 of the process during which the surface pH is >9 , abiotic processes only take place as the pipe is too alkaline to support bacterial populations. These abiotic processes, involving attack of the cement matrix by inorganic acids formed when CO_2 and H_2S dissolve into the concrete pore water, act to reduce the surface pH from initial values to $\text{pH}=9$. When the surface falls below $\text{pH}=9$ neutrophilic bacteria populate the pipe surface producing (largely organic) acids which act to further lower the surface pH. Once the pH falls below $\text{pH}=4$ neutrophilic bacteria are replaced/supplemented by acidophilic bacteria which produce sulphuric acid from the oxidation of H_2S and other sulphur species. The acids produced during this last stage of the corrosion process are largely thought responsible for the loss of concrete material. Loss data collected in this study (see 5.4.2.2) suggests that in terms of material loss the picture is somewhat different. Field data at all four field sites show that irrespective of the aggressiveness of the location corrosion losses begin when the surface pH falls to ~ 6 at which point losses increase linearly over time (as per Figure 93)

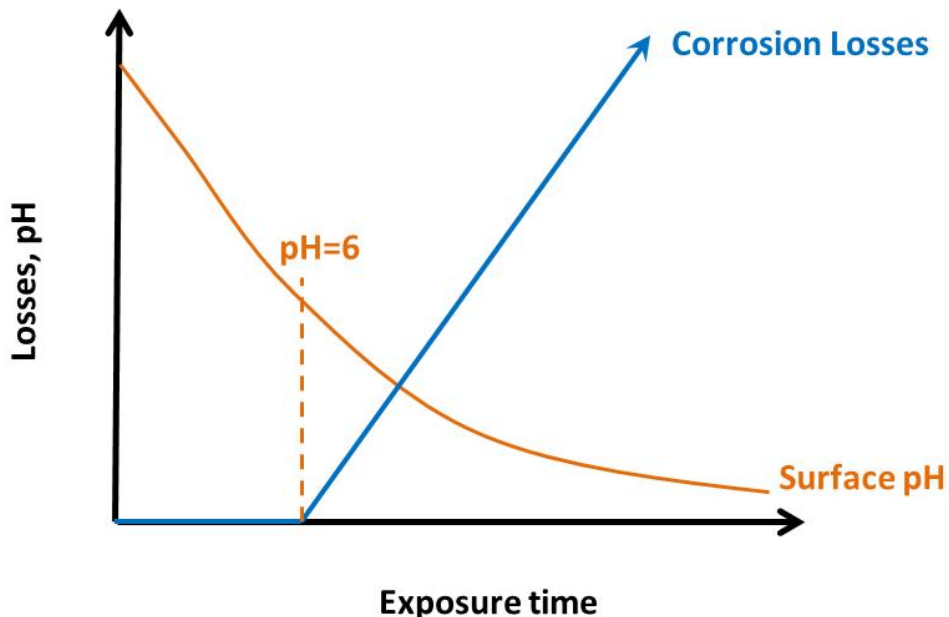


Figure 93. Schematic of relationship between corrosion losses and surface pH.

Table 17 lists the duration of the different stages as experienced by the new coupons at each of the field sites. It is clear that at even the most benign site the initial abiotic stage of the corrosion process is not long lived lasting a maximum of 7 months. Stage 2 ($9 > \text{pH} > 4$) lasts longer at the sites examined in this study but is still limited to a maximum of approximately 3 years and can be as short as 15 months at aggressive sites. Similarly the time to the onset of corrosion losses (found to occur at $\text{pH}=6$) was less than 2 years at all sites. The implications of this will be discussed further in the Section 6 of this report.

Table 17. Duration of the different corrosion stages experienced by the new coupons at different sites.

Site	Islander model		Sp1B model
	Stage 1 duration pH=10.3->9 (months)	Stage 2 duration pH=9->4 (months)	time to reach pH=6 pH=10.3->6 (months)
Perth Bibra	4	15	12.7
Perth MS	3	17	10
Melbourne WTS	4	26	14
Melbourne SETS	7	36	23
Sydney (South)*	3.8		
Sydney (North)*	5		

* - trial at Sydney sites did not progress to pH=6

The rate of decline in pH for new coupons during the abiotic stage of the corrosion process ($\text{pH}>9$) was found to vary between ~ 0.005 and 0.015 pH units per day (green data in Figure 94). Once $\text{pH}=9$ was reached however the rate of change in pH was observed to slow at all sites (blue points Figure 94) except at Perth MS where stage 1 and 2 surface acidification rates were approximately the same. After the pH fell to 4 the rate of acidification decreased further (purple points in Figure 94) to approximately 0.003 pH units per day at all sites. The rate of change in pH was found to be only a weak function of the field site gas phase H_2S concentration. At low H_2S concentration ($<10\text{ppm}$) increasing H_2S does accelerate the acidification process at all stages however above this H_2S concentration the effect is less pronounced. Laboratory studies examining the effect of H_2S concentration on the acidification of Portland cement samples [26], see red points in Figure 94) suggests a linear correlation between the rate of change in pH and the log of H_2S concentration. While some of the field data falls nicely on the projected relationship proposed by Roberts et al. it is clear that at the more aggressive sites the rate of acidification is not as pronounced as that observed in the study of Roberts et al. under similar H_2S conditions . This would seem to suggest that under real sewer conditions other factors in addition to the H_2S concentration (such as humidity) play an important role in determining the rate of acidification of the concrete surface.

In terms of the corrosion loss model being proposed in this study we are more interested in know how the duration of the initial “incubation” period, (the period prior to corrosion losses beginning, when $\text{pH}>6$), is affected by environmental factors such as H_2S concentration. Figure 95 plots the observed incubation time as a function of H_2S . The overall trend is, as expected, that as H_2S is increased the incubation time decreases. The data for Bibra Lake (right most point) does not quite fit this trend again indicating that the lower humidity present at this site depresses corrosion activity.

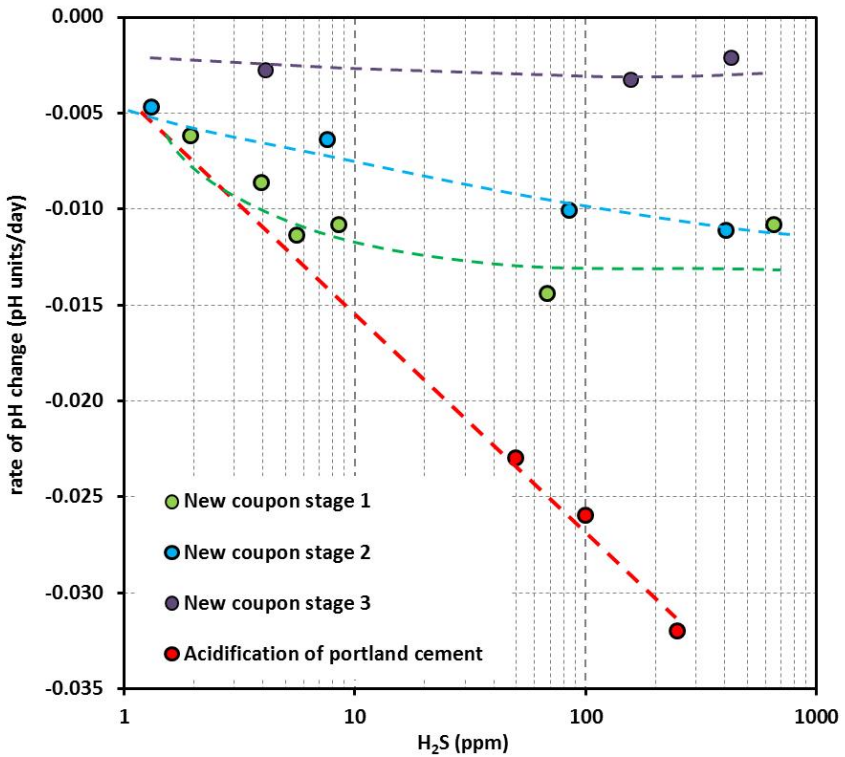


Figure 94. Rate of change in new coupon surface pH as a function of gas phase H₂S concentration (log scale). Additional data for Portland cement shown in red [26].

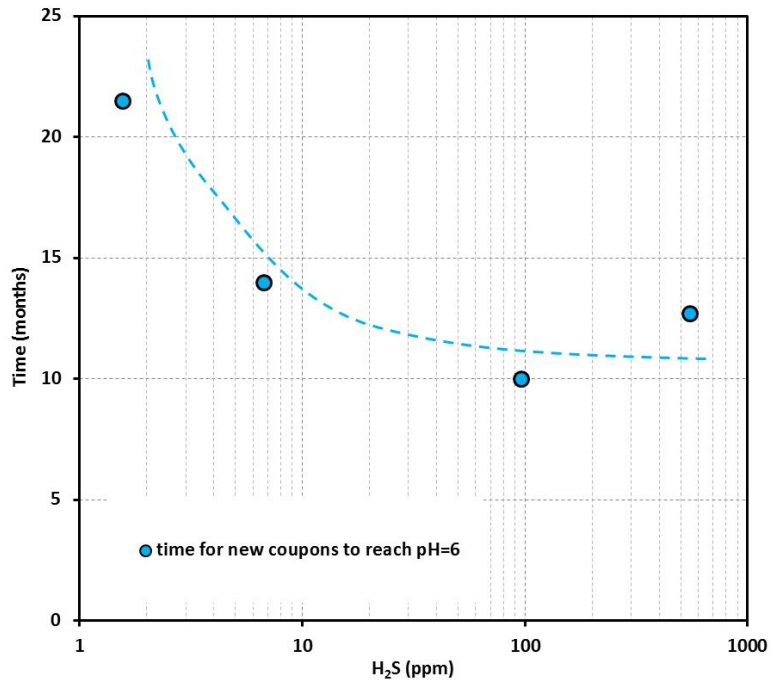


Figure 95. Time for new coupons to reach a surface pH=6 as a function of H₂S concentrations in the gas phase.

Old coupon surface pH trends

The surface pH averages for old coupons are listed in Tables 28 to 30 in Appendix XXII and plotted in Figure 96.

The corrosion behaviour of the old coupons lends an insight into the corrosion process during the latter stages of the sewer pipes service life when corrosion is well advanced. In contrast to the behaviour observed for new coupons the surface of old coupons were very rapidly acidified from the starting pH of pH=8.1 to pH values of 4 and below (Figure 96). However once the surface pH reached pH=4 acidification of the surface slowed somewhat. Rates of acidification during the neutrophilic stage of the corrosion process ($9 < \text{pH} < 4$) ranged from ~ 0.01 to 0.025 pH units per day (blue points in Figure 97) but again slowed appreciably when the surface pH dropped below 4 at which point the rate of acidification was ~ 0.002 pH units per day at all sites – a figure similar to that experienced by new coupons at the same stage of corrosion. The rate of acidification when $9 > \text{pH} > 4$ was found to increase as H_2S increased however as observed for new coupons the acceleration effect was primarily observed at lower H_2S values.

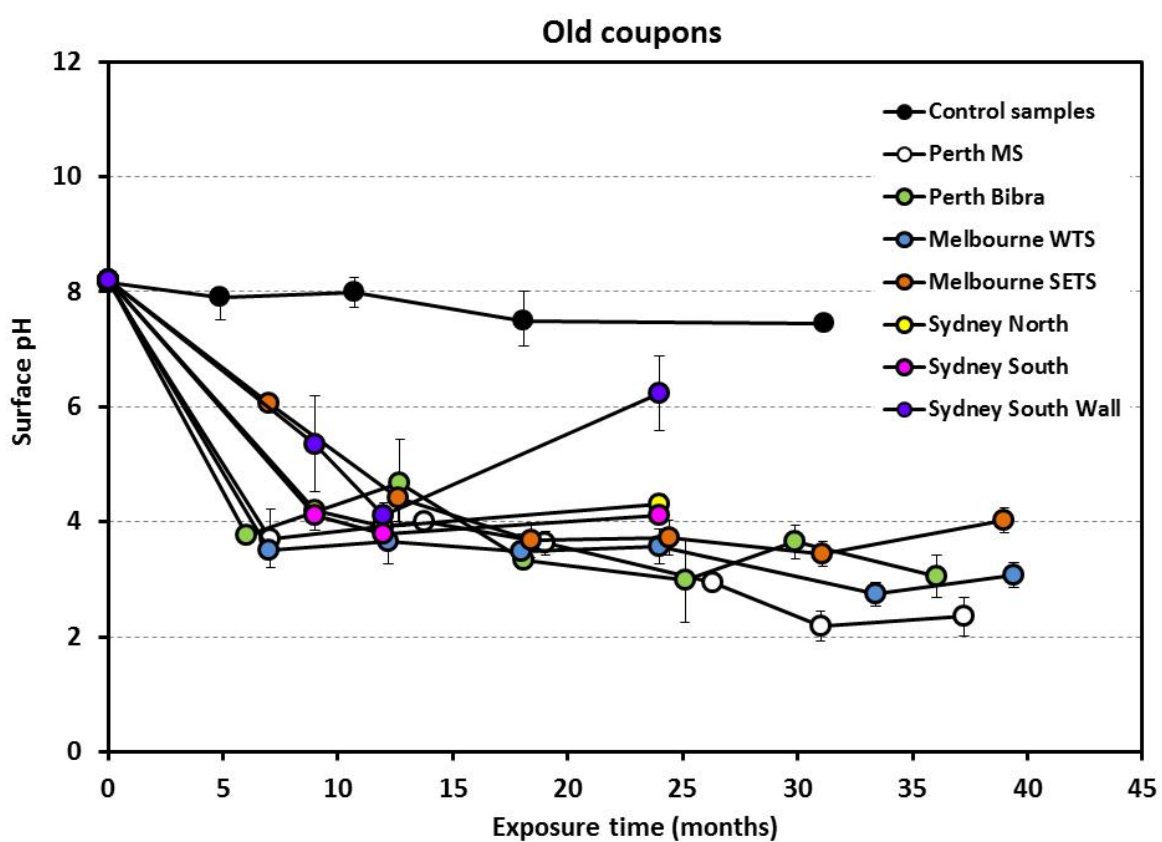


Figure 96. Surface pH of Sp1B old coupons. pH error bars show standard deviation of measurements for the three coupons retrieved at each location at each retrieval.

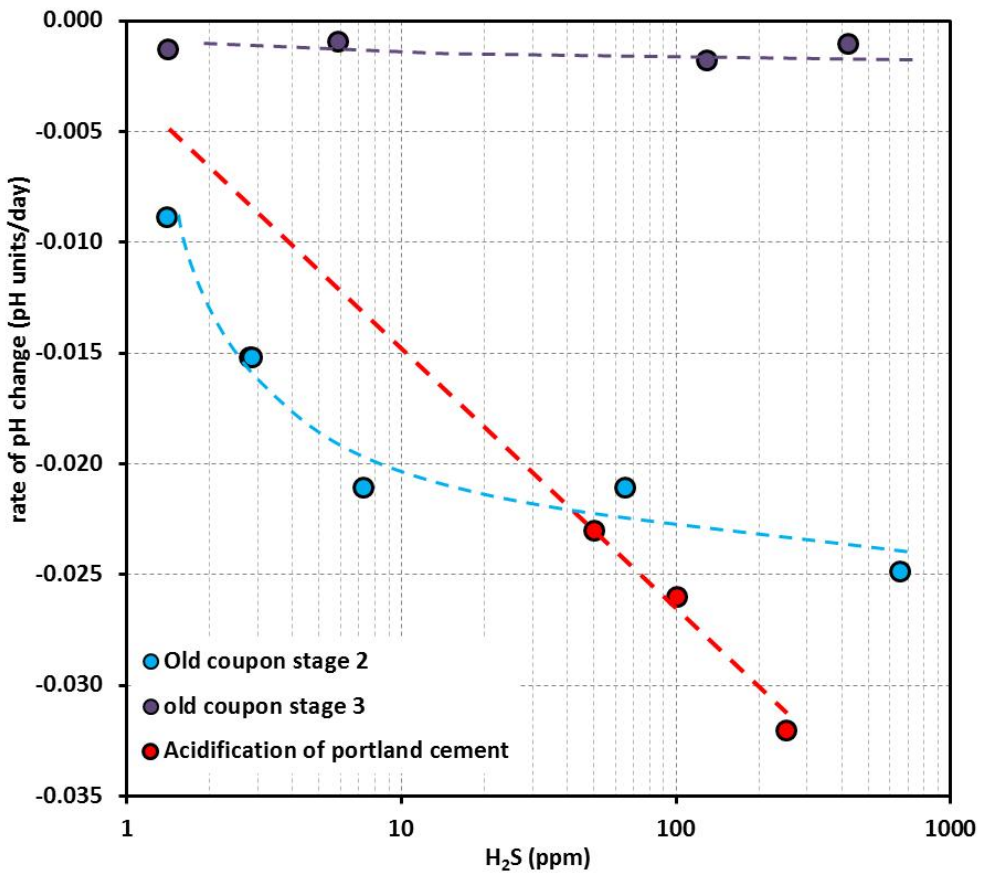


Figure 97. Rate of change in old coupon surface pH as a function of gas phase H_2S concentration (log scale). Additional data obtained by [26] is also shown in red.

5.4.2.4 pH profiling results

The ANC work detailed above provides us with information about the amount of acid needed to change the pH of the concrete on a mass per mass basis. To accurately determine the amount of acid required to achieve changes in surface pH and incur loss of material it is necessary to know the mass of material lost and also extent of any changes in pH of the remaining sound concrete (see Figure 98). To gain an understanding of the depth of acid penetration into the sound concrete pH profiling assessments were carried out on recovered field coupons exposed for various periods of time in the field trials sewers. As already discussed pH profiling was carried out using both universal indicator testing and micro-drilling.

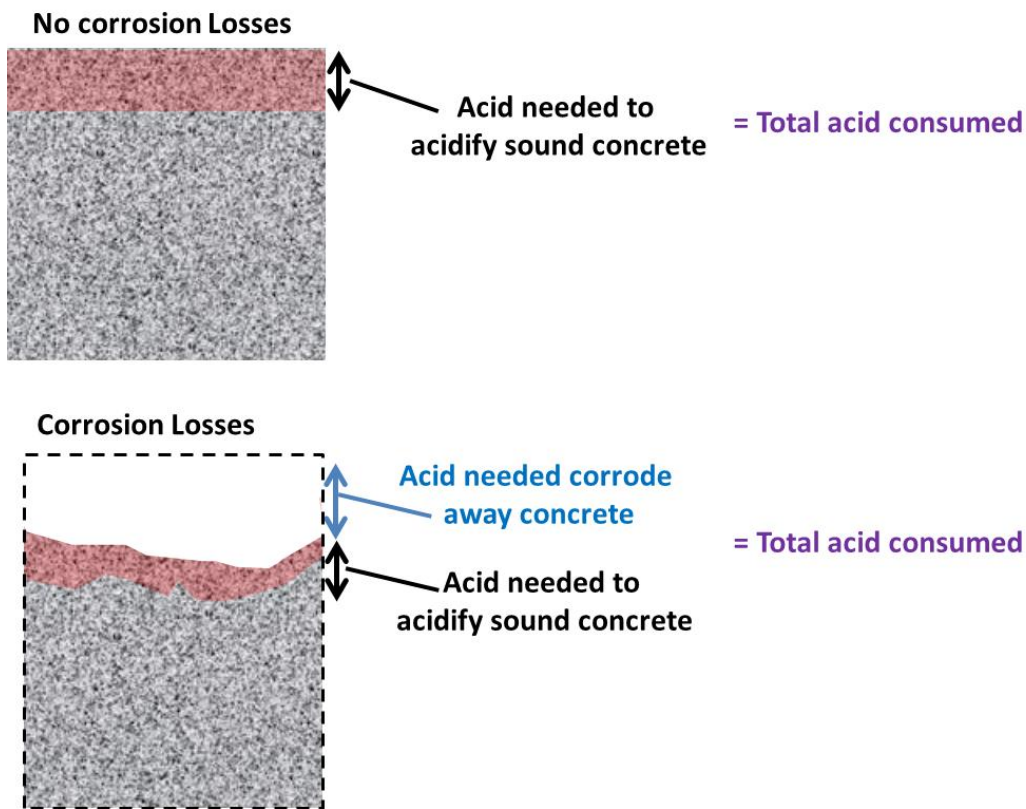


Figure 98. Calculations needed to assess the amount of acid needed to achieve a certain level of corrosion.

Universal indicator tests.

A typical outcome for the universal indicator test is illustrated in Figure 99. Universal indicator staining of all coupons tested indicated that the acid penetration into the concrete was minimal (generally less than 0.5mm) and that the acid effected region had a pH of approximately pH=9. The boundary between the acid affected region and the original unaffected concrete (purple region in Figure 99) was generally quite well defined indicating a sharp reaction front.

The depth of the acid affected region was generally quite uniform across the coupon cross section. However there were occasional points at which it was apparent that a preferential pathway into the concrete was present allowing for the potential of future “pitting” of the coupon to take place (see Figure 100).

Drilling tests.

pH profiles obtained from micro drilling tests are plotted in Figures 101 to 104. In all cases the transition from the surface pH to the bulk pH value was achieved within 0.4mm of the surface. In some instances it was possible to compare the point of transition to pH=12 indicated by the universal indicator tests with the pH profile determined by drilling (see blue circle in some of the graphs). In all cases there was a good agreement between the depth to achieve pH=12 determined by the two methods.

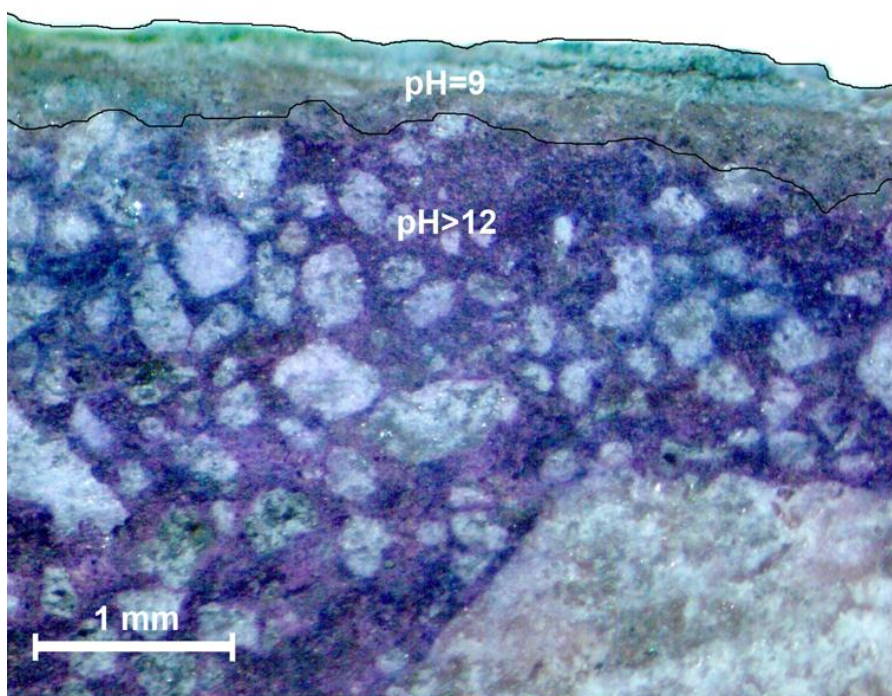


Figure 99. Typical universal indicator test outcome.

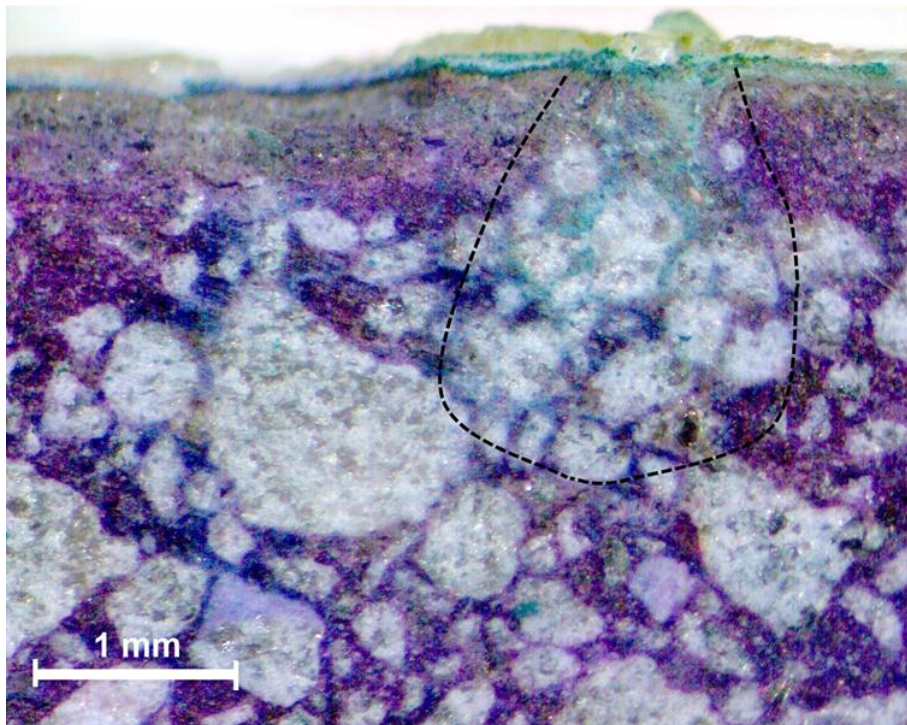


Figure 100. Universal indicator test revealing preferential acid penetration (inside dashed zone).

Table 18 lists the depth of acid penetration into the sound concrete for all of the samples examined (either by universal indicator or by drilling). The results do not indicate any particular trend except that the depth of acid penetration after exposure to sewer conditions is close to 0.3mm in all cases. For the purposes of future calculations therefore it will be assumed that acid penetration into sound concrete is 0.3mm irrespective of time or place of exposure.

The results of the indicator and drilling tests both indicate that the depth of acid penetration into the sound concrete is quite limited regardless of the length of exposure or the sewer conditions. This strongly indicates that once the acid has diffused through the corrosion layer to the reaction front (interface between the sound and corroded concrete) it is quickly consumed by the neutralisation reaction before it has a chance to diffuse very far into the concrete pore network thereby producing a sharp, well defined reaction front.

Table 18. Depth of acid penetration into the sound concrete of new coupons.

Sample	Penetration (mm)	variance (mm)
Unexposed new coupon	0.03	0.01
Melbourne SETS 6 months	0.36	0.12
Melbourne SETS 18 months	0.41	0.17
Melbourne SETS 36 months	0.3	0.05
Melbourne WTS 6 months	0.22	0.12
Melbourne WTS 18 months	0.23	0.13
Melbourne WTS 36 months	0.4	0.05
Perth MS 6 months	0.38	0.14
Perth MS 18 months	0.28	0.20
Perth MS 36 months	0.3	0.05
Perth Bibra Lake 6 months	0.34	0.12
Perth Bibra Lake 18 months	0.39	0.21
Perth Bibra Lake 36 months	0	0.05
Average =	0.3	0.1

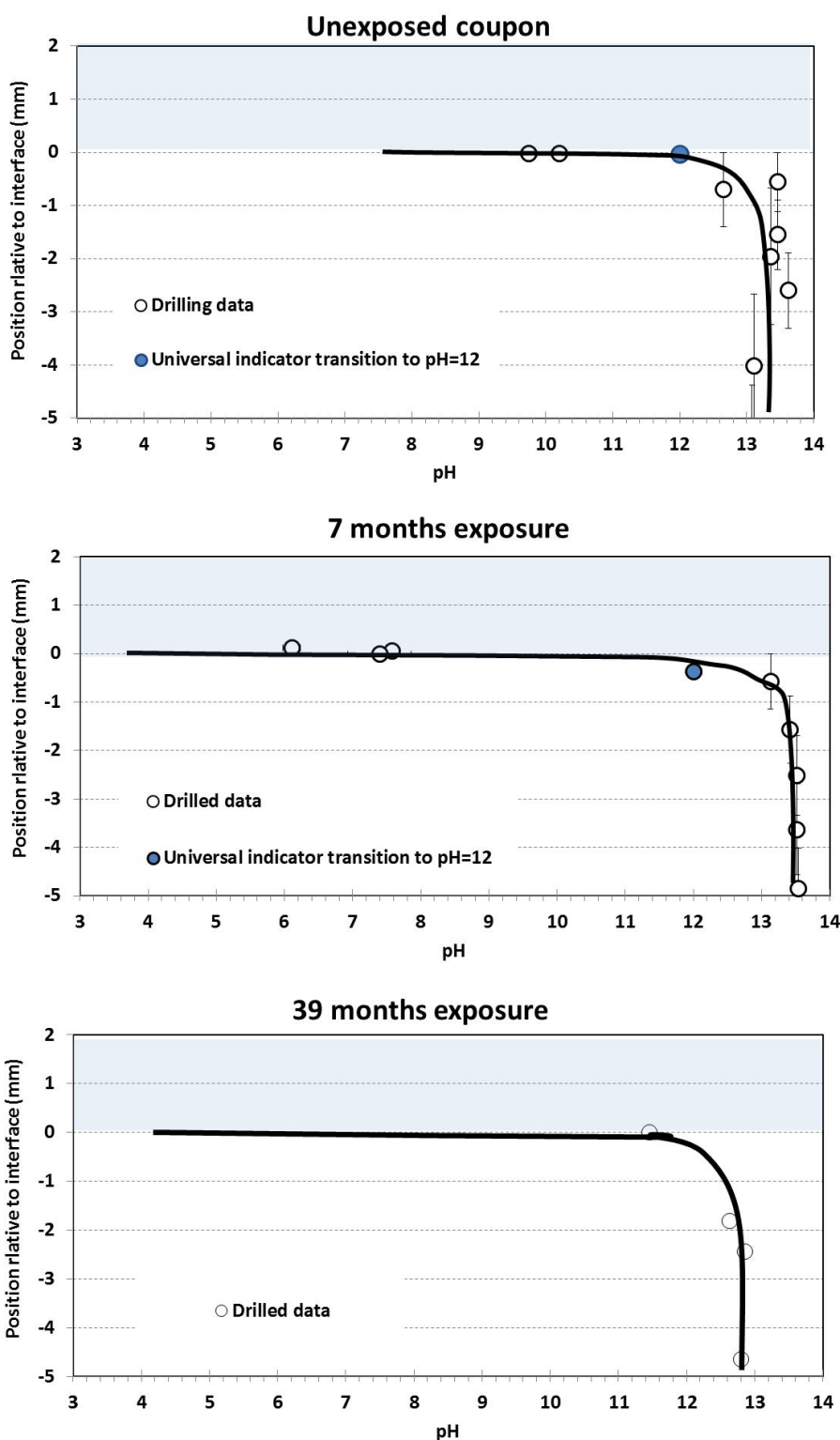


Figure 101. pH profiles for new coupons exposed at Melbourne SETS.

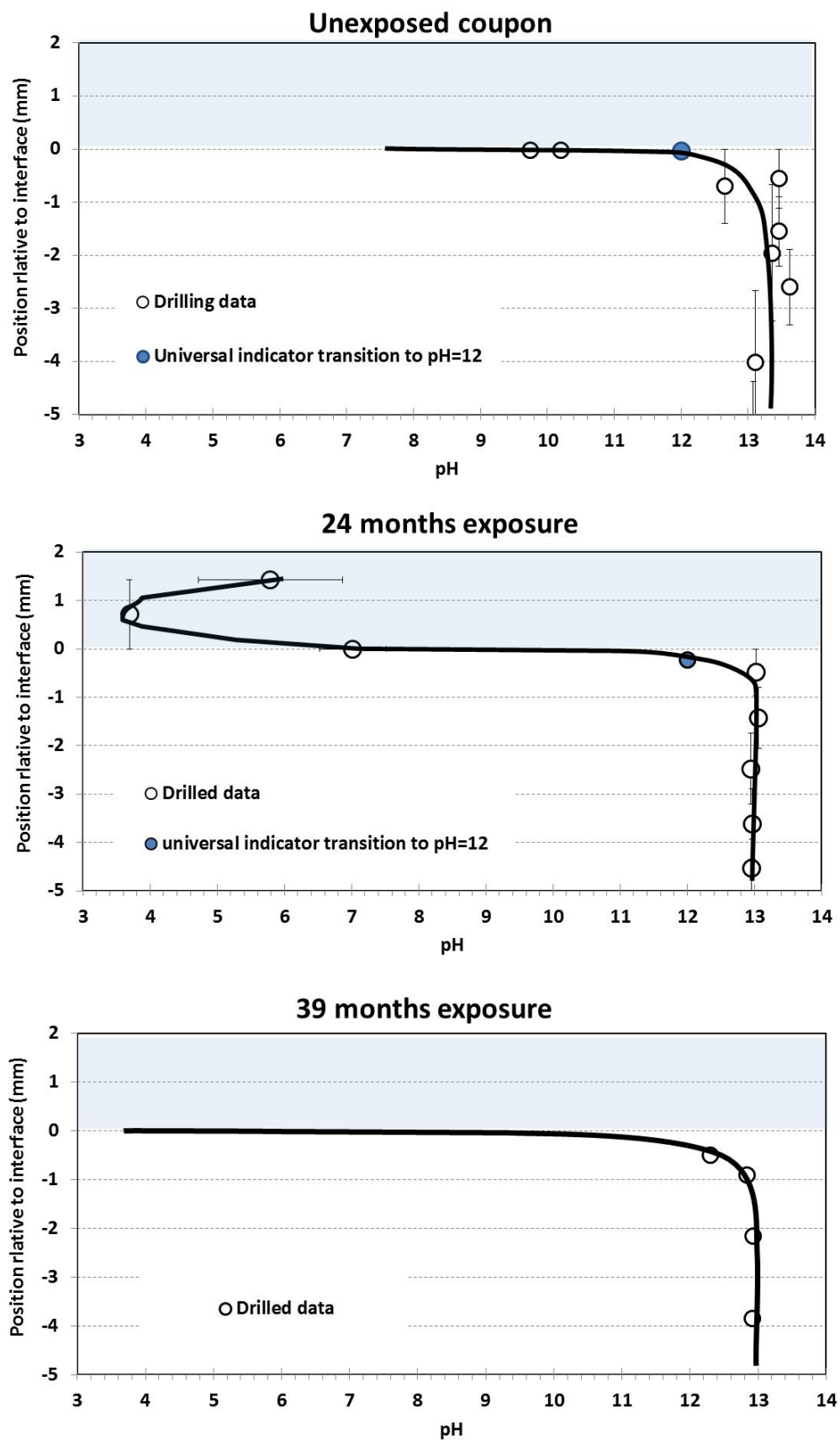


Figure 102. pH profiles determined for new coupons exposed at Melbourne WTS.

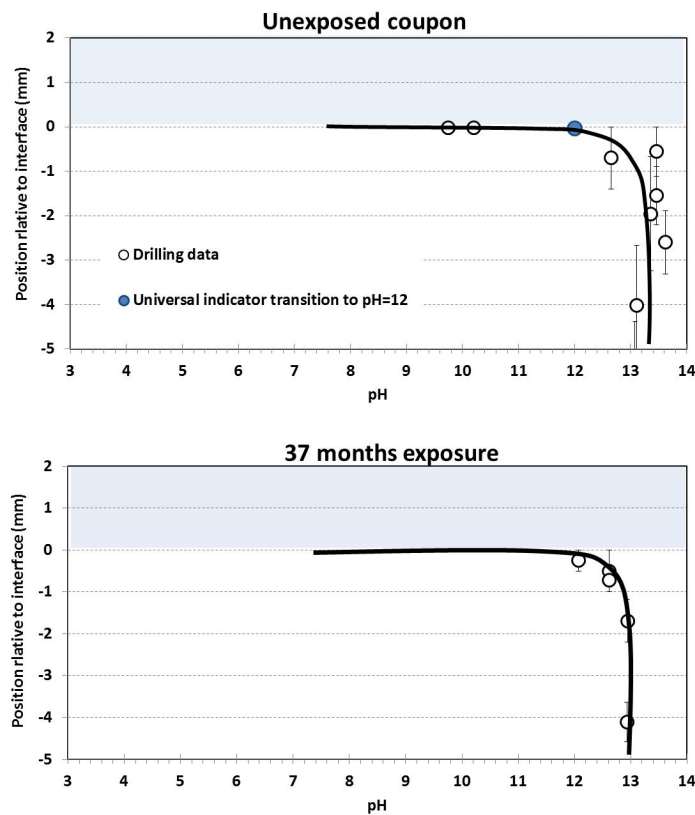


Figure 103. pH profiles for new coupons exposed at Perth MS.

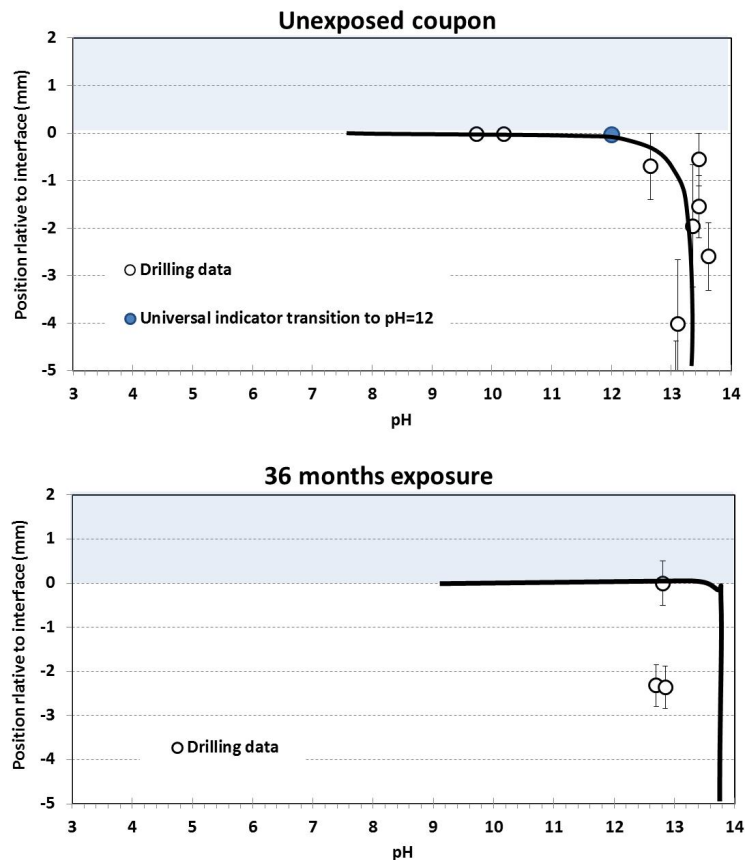


Figure 104. pH profiles of new coupons exposed at Perth Bibra Lake.

5.4.2.5 Corrosion product layer development

As the acidic species produced in the sewer environment react with the alkaline compounds of the concrete sewer pipe a layer of corrosion product consisting of sand particles, unreacted cement particles, gypsum, ettringite, and other sulphur bearing compounds forms on the concrete surface. The presence of the corrosion product changes the nature of the environment encountered by the bacteria and fungi. It can retain moisture, encouraging microbial growth and hence accelerate corrosion activity and/or possibly act as a physical barrier between the microbes and the concrete surface thereby slowing down the corrosion process.

The depth of the corrosion product layer is a function of the rate at which the corrosion product is formed (and its density) and the rate at which it is eroded away (either simply by spalling away or abraded by wastewater spray or the flow of the wastewater itself). The resultant depth of the corrosion layer is an important factor to be considered when modelling the corrosion process as the rate of diffusion of species such as O_2 , H_2S , nutrients, H_2O and H_2SO_4 across this layer may influence the rate at which the corrosion takes place.

Corrosion layer development on new coupons

The development of the new coupon corrosion product layer is illustrated in Figure 105 for samples recovered from all Sp1B field sites. The data indicates the average thickness for the three samples recovered at each time/location. The error bars shown represent the standard deviation of the three corrosion depth values. In general the depth of the corrosion layer increased a non-linear fashion over time at all sites. In fact data obtained from later retrievals indicated that the depth of the corrosion product might be nearing a maximum value (which would appear to be as high as 10mm at Perth MS).

Corrosion layer development on old coupons

Old coupon corrosion product layer depth trends over time are plotted in Figure 109 for all sites. Individual site trends are also shown in Figures 110 and 111. Again the average values for each time/location are plotted with the standard deviation of those measurements shown as the error bars. It should be noted that it was assumed that all old coupons had a corrosion layer of ~2 mm at the commencement of the trial (see Section 5.3.3).

Generally the sample to sample variability of the corrosion depths was higher than observed for the new coupons however a similar non linear but increasing trend similar to that experienced by the new coupons was evident for old coupons at all sites. Again it would appear that the corrosion layer depth may be trending towards a maximum value (as high as ~12mm at Perth MS).

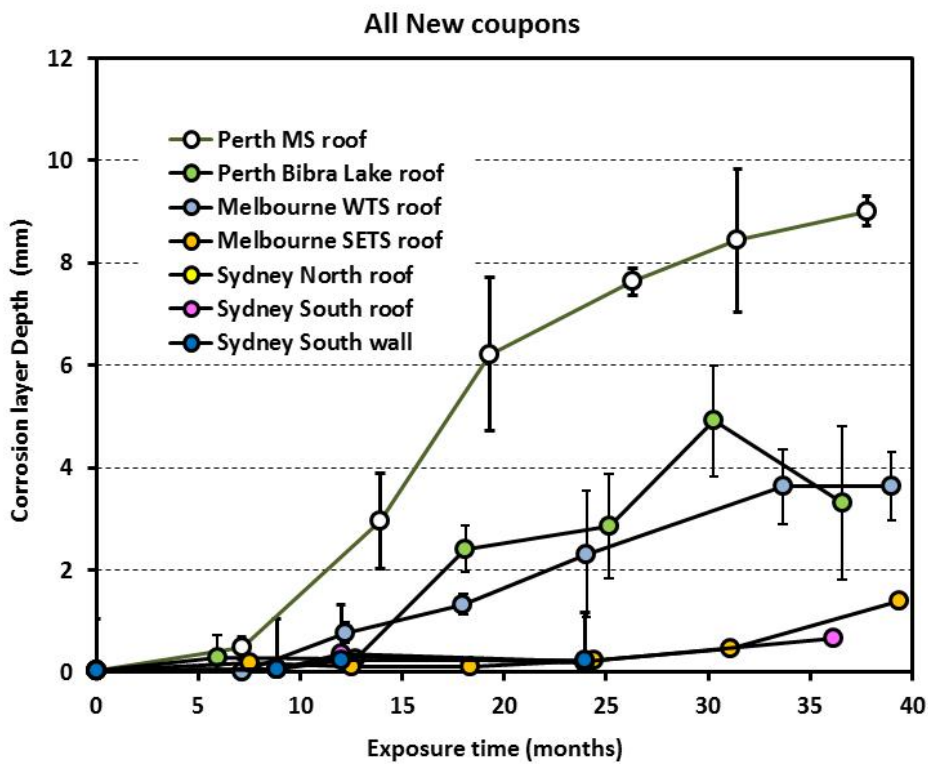


Figure 105. Generation of corrosion product layer on new coupons over time at all field sites.

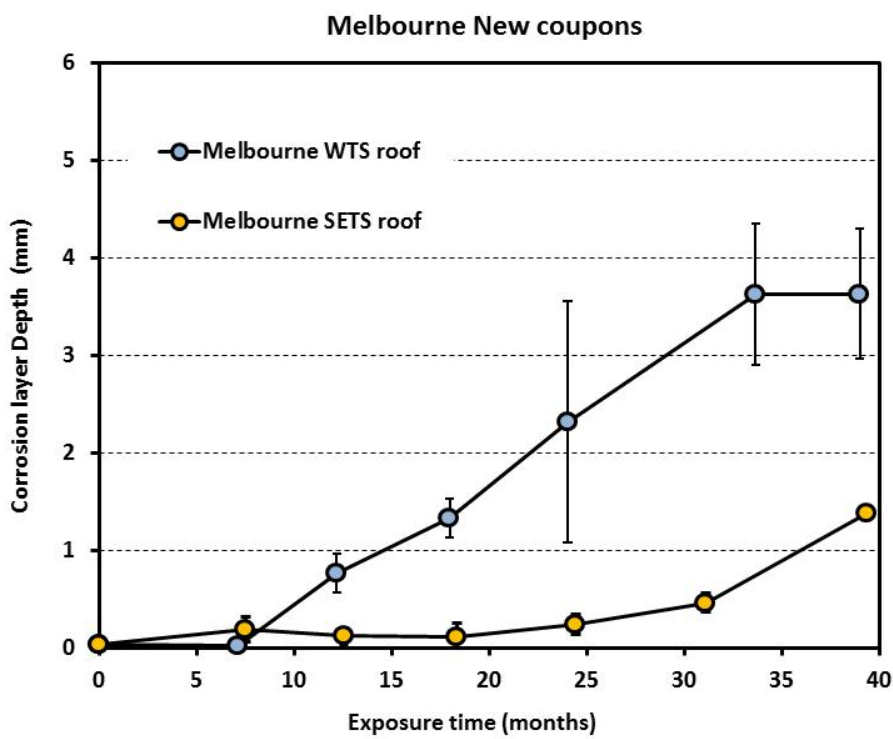


Figure 106. Generation of corrosion product layer on new coupons over time at the two Melbourne field sites.

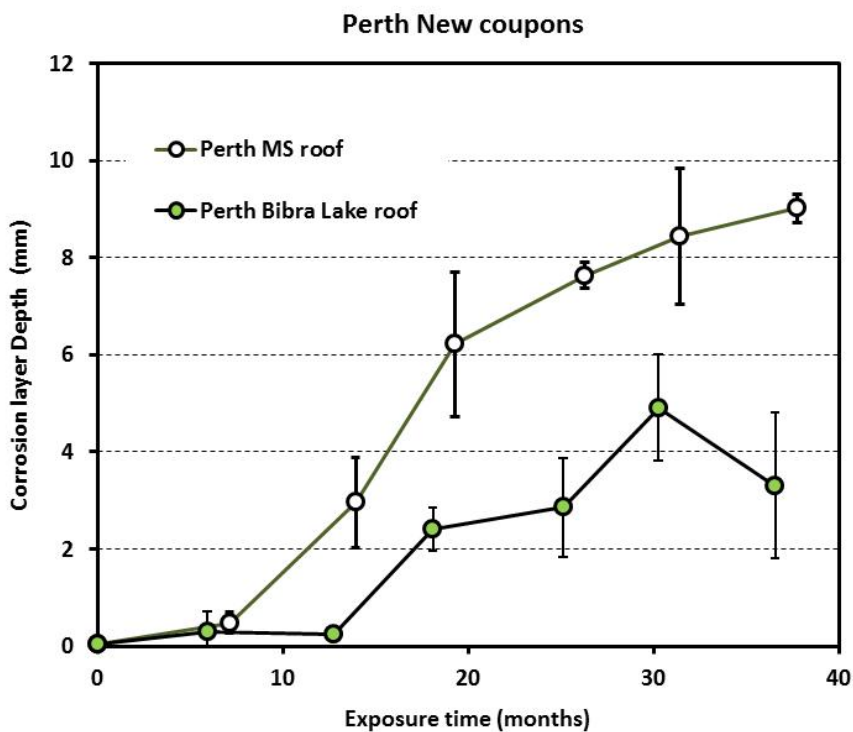


Figure 107. Generation of corrosion product layer over time on new coupons at the two Perth field sites.

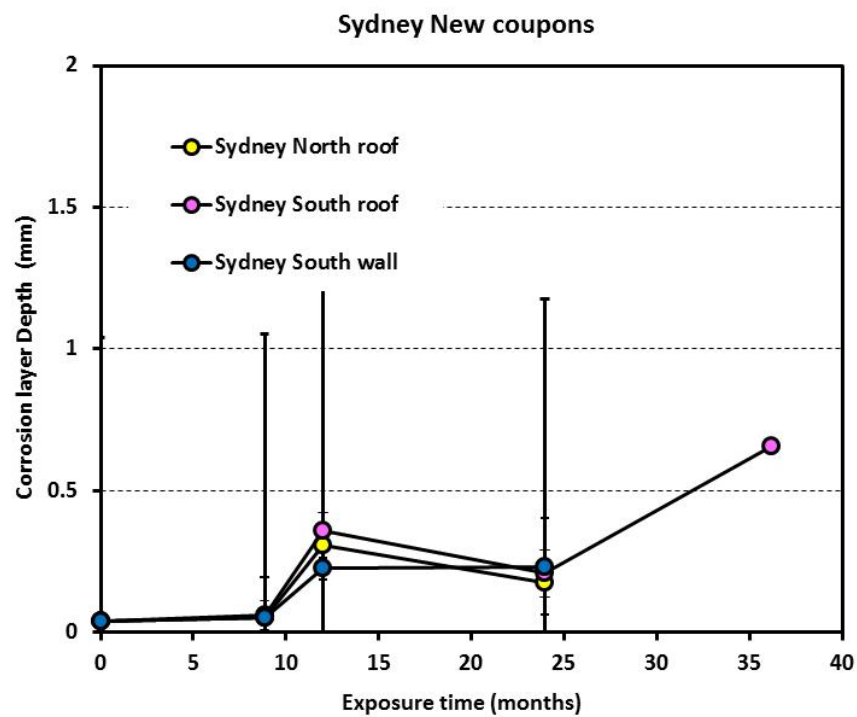


Figure 108. Generation of corrosion product layer on new coupons over time at the three Sydney field sites.

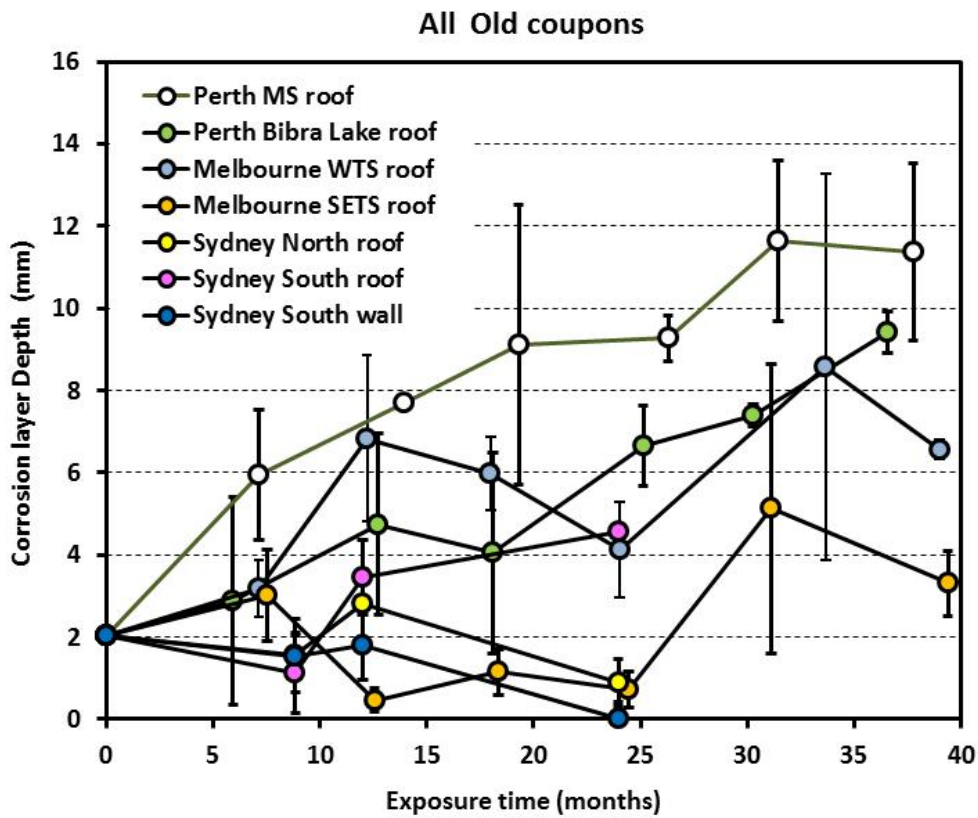


Figure 109. Generation of corrosion product layer on old coupons over time at all field sites.

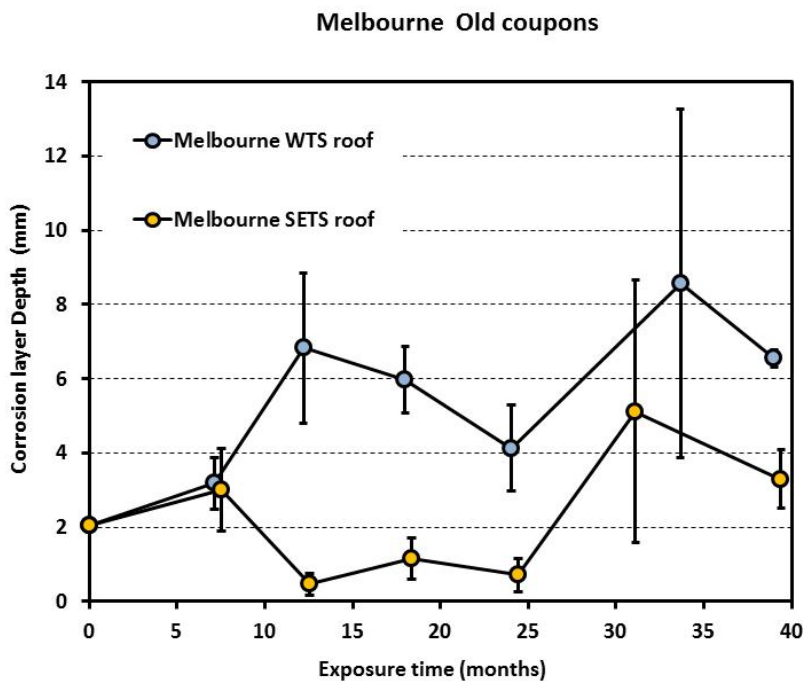


Figure 110. Generation of corrosion product layer on old coupons over time at the two Melbourne field sites.

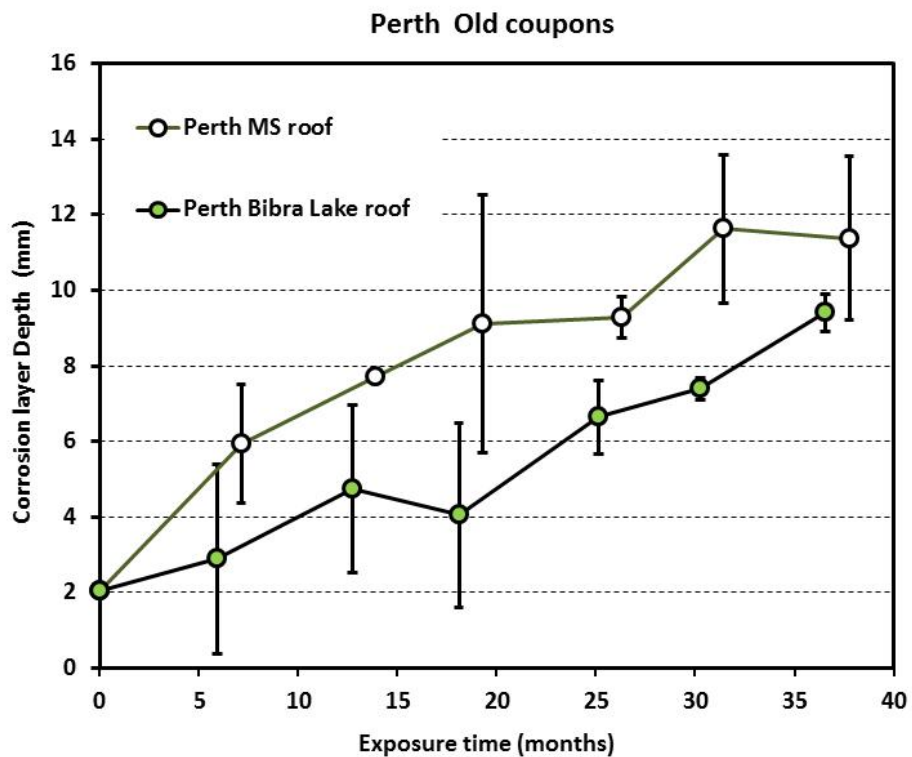


Figure 111. Generation of corrosion product layer over time on old coupons at the two Perth field sites.

5.4.3 Calculation of acid consumed during the corrosion of the field samples

The results discussed above have implications for the determination of the acid consumed during the course of the corrosion process. Following on from these findings acid consumption and H₂S oxidation calculations were performed based on the following assumptions (see Figure 112):

- The sulphuric acid/concrete ANC curve adequately represents the response of the concrete to all of the acids present in the sewer.
- It is assumed that at time=0 (when the coupons were installed in the sewer) all new coupons have a surface pH=10.3. This increases linearly with depth until at 0.3mm depth the pH is the same as the bulk concrete (pH=12.5).
- In the early stages of the coupon's life (prior to the corrosive removal of concrete) acid consumption is that required to lower the concrete pH to a depth of 0.3mm. In the acid affected layer it is assumed that the pH changes linearly from the recorded surface pH to a pH=9 at 0.3mm depth.
- After continued exposure when the coupon is experiencing mass loss (surface pH<6) it is assumed that the material removed from the coupon was reduced to a pH of 2 prior to its removal. Also the outer 0.3mm of the remaining sound concrete a layer has been reduced to a pH of 9. All other sound concrete is at its original pH.

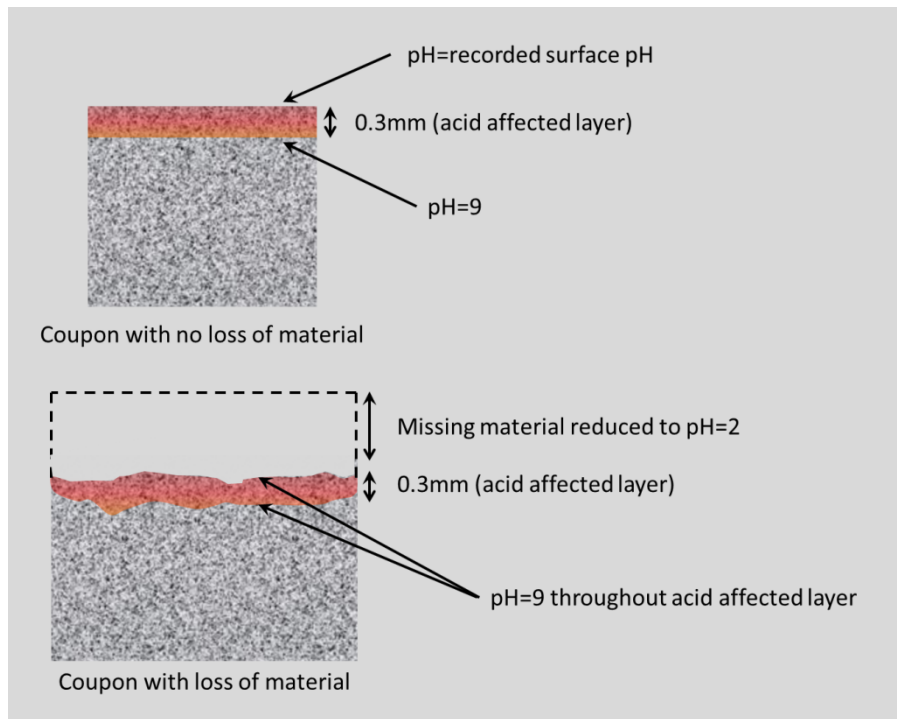


Figure 112. Assumptions used in calculating acid consumption.

The calculated consumption of acid for the new coupons at the Perth and Melbourne field sites over time is plotted in Figure 113. In calculating the total amount of acid consumed, the acid needed to acidify the thin (0.3mm) outer layer of sound concrete (yellow region) is generally insignificant compared to that consumed in the removed concrete (green region) except where:

- (1) the pH of the coupon surface is greater than pH=6 and
- (2) the corrosion rates are low (such as Melbourne SETS).

Only in those cases would the amount of acid needed to acidify the sound concrete need to be taken into account when calculating the total acid consumed. In all other cases this effect can be safely ignored and the acid consumed calculated solely from the amount of material lost.

It is also possible to calculate the subsequent rate of H₂S oxidation necessary to generate the acid consumption data shown in Figure 114. The trends in H₂S oxidation that follow from the data in Figure 114 are plotted for the four field sites in Figure 115. Not surprisingly they show minimal H₂S oxidation occurring during the early stages of the coupons exposure in the sewer. However once the pH of the concrete surface drops below pH=6 H₂S oxidation rates increase quickly as microbial activity increases before the rates of oxidation stabilise at a new, higher level.

The average H₂S oxidation rates for each site once corrosion is well advanced (pH<6) are listed in Table 19. The values are generally of the same order as that reported in laboratory studies

(e.g. an average 250 mgS-H₂S/m²/hr at 100 ppm H₂S [20] and ~180 mgS-H₂S/m²/hr reported at 100 ppm H₂S [57]). A plot of H₂S oxidation rates against average gas H₂S concentration observed at the four field sites reveals a log-linear relationship between the two factors if humidity is held ~ constant (i.e. at Perth MS, and the two Melbourne sites). At Perth Bibra Lake (the right most point in Figure 115) it is clear that lower humidity has impacted on the ability of the microbial population to oxidise H₂S.

Table 19. Average H₂S conversion at each site and average environmental conditions.

Site	mgS-H ₂ S/m ² /hr	av H ₂ S conc	T	RH
Melbourne SETS	8	0.6	19.2	97.2
Melbourne WTS	94	6	21.3	100
Perth MS	280	79	26.5	98
Perth Bibra Lake	85	404	25.9	85

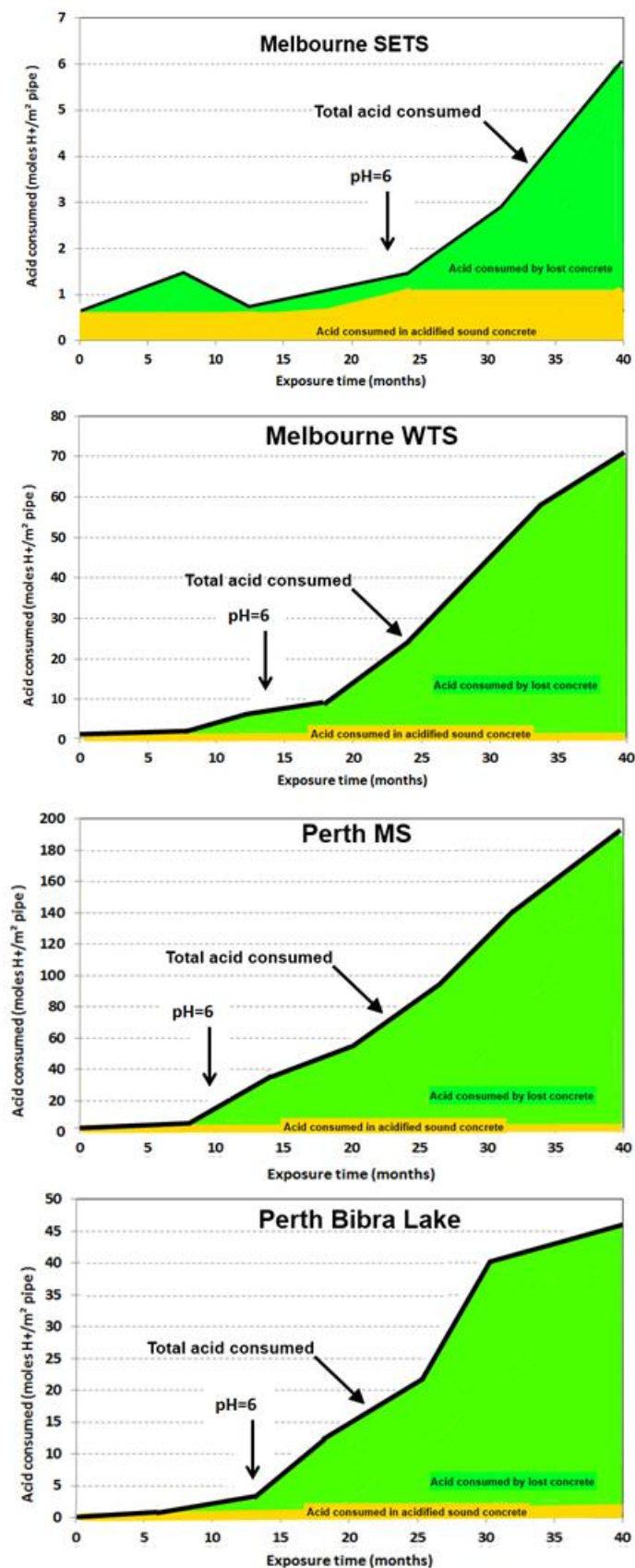


Figure 113. Acid consumed over time by the new coupons at the four field sites over time.

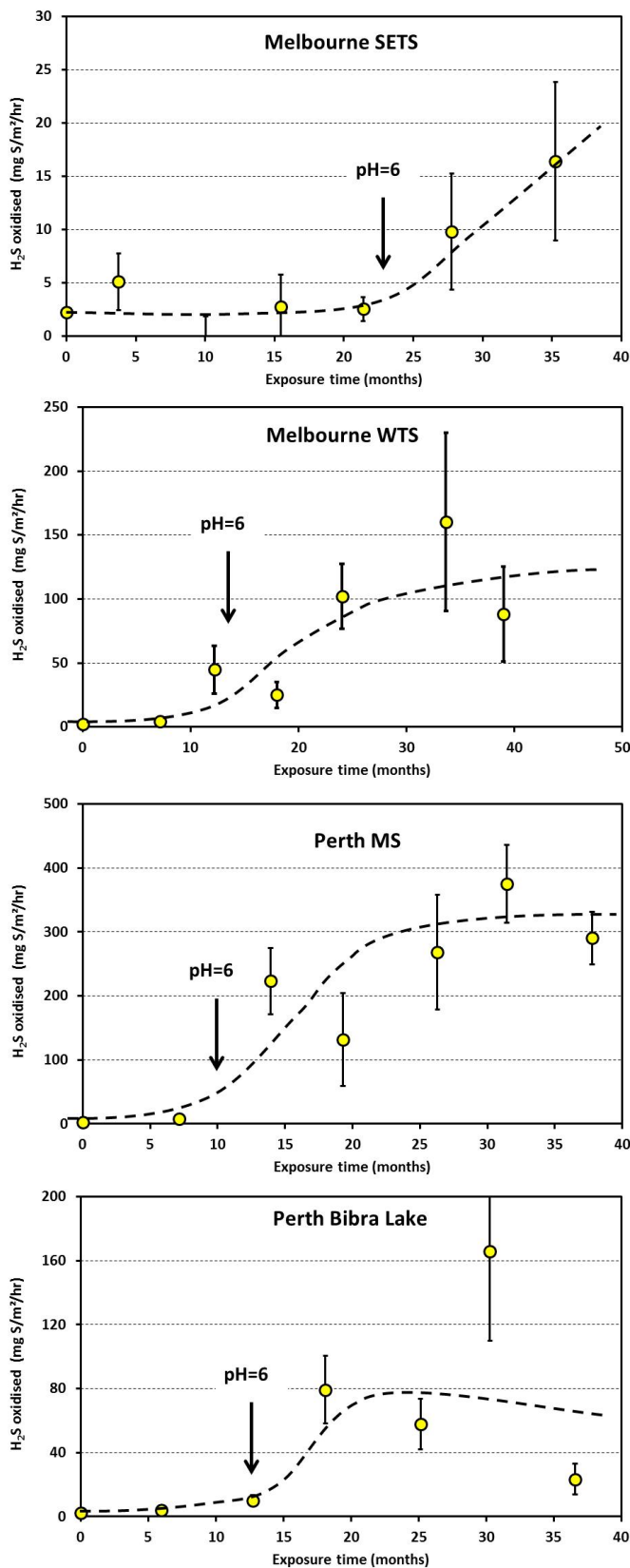


Figure 114. Trends in H₂S oxidation rates over time at the Melbourne and Perth field sites.

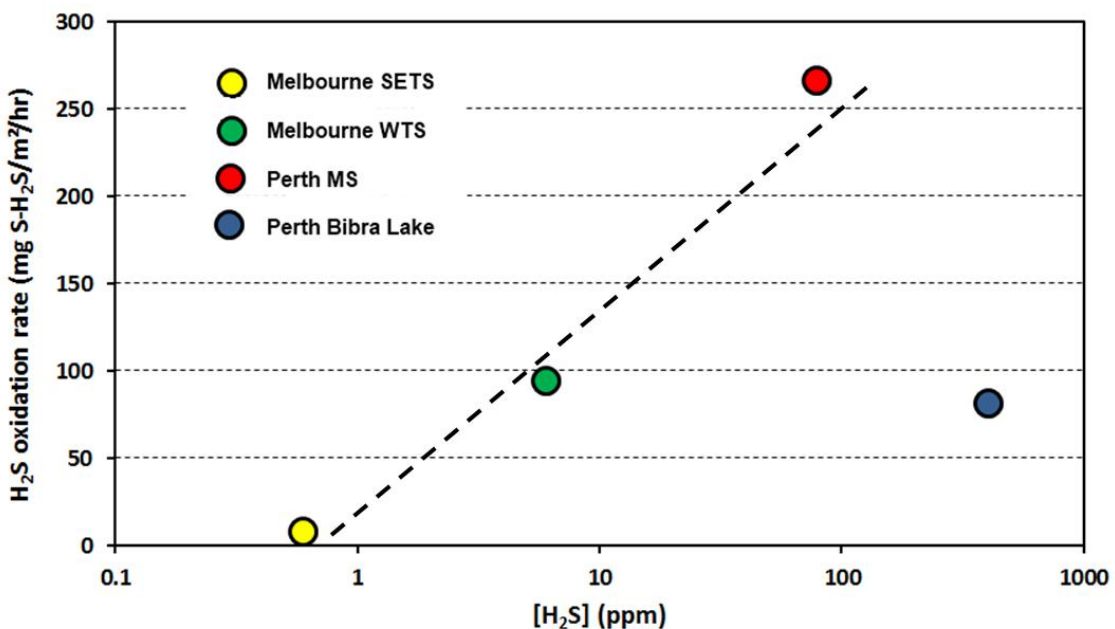


Figure 115. H₂S oxidation rate as a function of H₂S concentration in the gas phase.

5.5 Summary of Activity 3 outcomes

- For the first time a field trial of in-situ sewer pipe corrosion has been undertaken in working Australian sewers.
- The successful program of work was carried out in multiple active sewer sites in Sydney, Melbourne and Perth.
- Samples were recovered at 6 monthly to 1 yearly intervals and analysed at Newcastle University to determine changes in surface chemistry, the loss of concrete, corrosion layer characteristics as well as depth of acid penetration into the uncorroded material.
- Despite the premature end to the trials in Sydney, data obtained from the analysis of new and old corroding samples recovered from the Melbourne and Perth sewers enabled a detailed picture of the corrosion cycle to be built up for a wide range of sewer operating conditions.
- Environmental data (sewer gas temperature, humidity and sewer gas H₂S concentration) were also collected at the field sites to enable the corrosion cycle to be correlated against local sewer conditions.
- New and old coupon corrosion cycles appear to have overlapped at the more aggressive sites enabling a full picture of the corrosion cycle to be obtained.
- Main findings of the field trial program are:
 - Upon installation concrete pipe initially passed through a relatively quiescent stage (the “incubation period”) during which there is no noticeable loss of concrete.

- Surface pH declined rapidly during the initial stages of exposure however tended to level out once the pH of the surface reached pH=4.
- Hyphae and biological nodules (some associated with the production of elemental sulphur) were apparent on the coupon surface once the surface pH dropped below pH=9.
- The incubation period ends when the surface pH reaches 6 at which point corrosion losses commence.
- The length of the incubation period was dependent on the aggressiveness of the local environmental conditions but generally was only a matter of months.
- Once corrosion commences losses accumulated in a linear fashion over time at all field sites for both new and old coupons indicating that for a given set of environmental conditions the rate of corrosion is a constant.
- The rates of corrosion experienced by new and old coupons at any given site were very similar.
- There was however a wide range of corrosion rates experienced by coupons between sites.
- The rate of corrosion generally correlated well with H₂S concentration in the gas phase however the corrosion activity at Perth Bibra Lake ranked well behind Perth MS and Melbourne WTS despite the fact that H₂S levels were much higher at this site.
- The Bibra Lake anomaly points to the pivotal role that humidity may play in the corrosion process.
- pH profiling of a selection of recovered coupons indicated that acid penetration beyond the reaction front into the sound concrete was minimal (~0.3mm).
- The layer of corrosion product which formed on the surface was generally soft and porous. The prevalence of cracking, pitting and tunnelling through the corrosion product suggests that it would not provide a significant barrier to the transport of acid, moisture or nutrients.

6 Activity 4: Modelling the corrosion of concrete sewer pipe

6.1 Introduction

Sewer corrosion processes vary over time in a complex fashion. Conditions on the exposed pipe surface evolve as chemical (abiotic) and biotic processes alter the surface chemistry. In turn surface conditions help determine the nature and magnitude of corrosive activities taking place. This complexity was recognized in the three stage model of sewer pipe corrosion first proposed by Islander et al. [31] in which corrosion initially proceeds by chemical (abiotic) acidification of the pipe surface followed by microbial induced corrosion (MIC) driven by a succession of evolving microbial communities.

Unlike the majority of earlier work that simply assumed that the rate of deterioration of concrete in sewers proceeded at a constant rate over time, the approach adopted in this study starts with the premise that the instantaneous rate of corrosion will vary over time as a result of, for example, the build-up of corrosion products, microbial population dynamics and/or changes to the sewer pipe surface conditions (for example surface pH).

Any non-linearity in the corrosion function over time, such as that illustrated in Figure 116, presents a significant problem for the engineer trying to predict the remaining life of sewer pipes. If, as illustrated, a concrete pipe subject to a complex corrosion process is sampled at time t_a or t_b and the observed mass loss at those times is used to determine the mass loss (M_a , M_b) at a future time, t_c , there is the possibility of under or over prediction of the future mass loss if a constant corrosion rate is assumed. It is necessary, therefore, to develop a model of the corrosion process that incorporates any time varying complexity and consequently can estimate the instantaneous corrosion rate as a function of time over the course of the service life of the sewer.

The following sections of the report will discuss the overall physical picture of the corrosion process that has emerged during this study; the primary factors influencing the corrosion process as well as modelling of the corrosion process and the calculation tools that have been developed for the prediction of concrete sewer pipe service life.

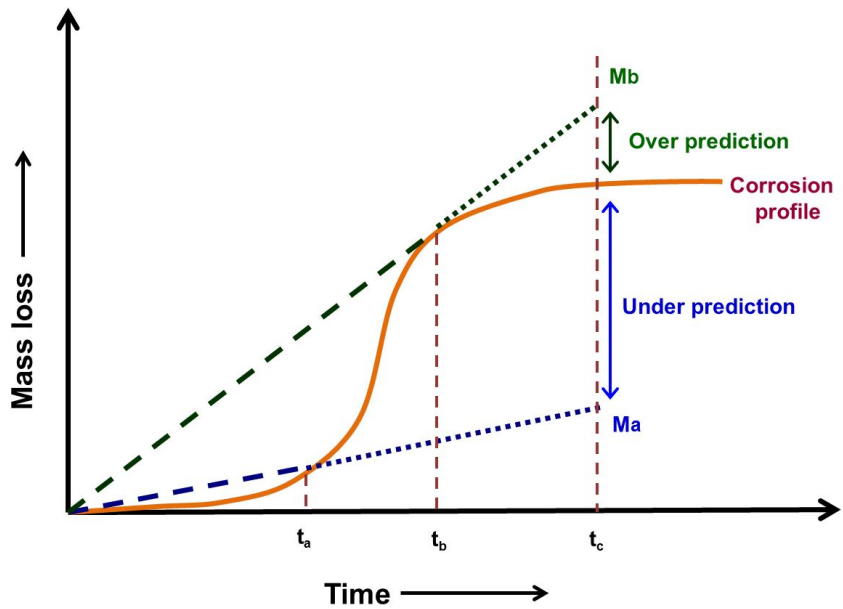


Figure 116. The instantaneous corrosion rate function.

6.2 Objectives

The aims of the modelling section of the Sp1B sub-project are to use industry/academic historical data and field and laboratory observations made during the course of this study to:

- i. Build a better understanding of how the corrosion of concrete sewer pipe evolves over the lifetime of the pipe
- ii. Identify primary factors controlling the corrosion of concrete sewer pipe
- iii. Develop a phenomenological model of the concrete sewer pipe corrosion process
- iv. Develop an application for predicting the service life of sewer pipes as a function of time and local environmental conditions within the pipe

6.3 A physical representation of the corrosion process

6.3.1 Timeline for the corrosion of concrete sewer pipe

6.3.1.1 The beginnings of the corrosion process

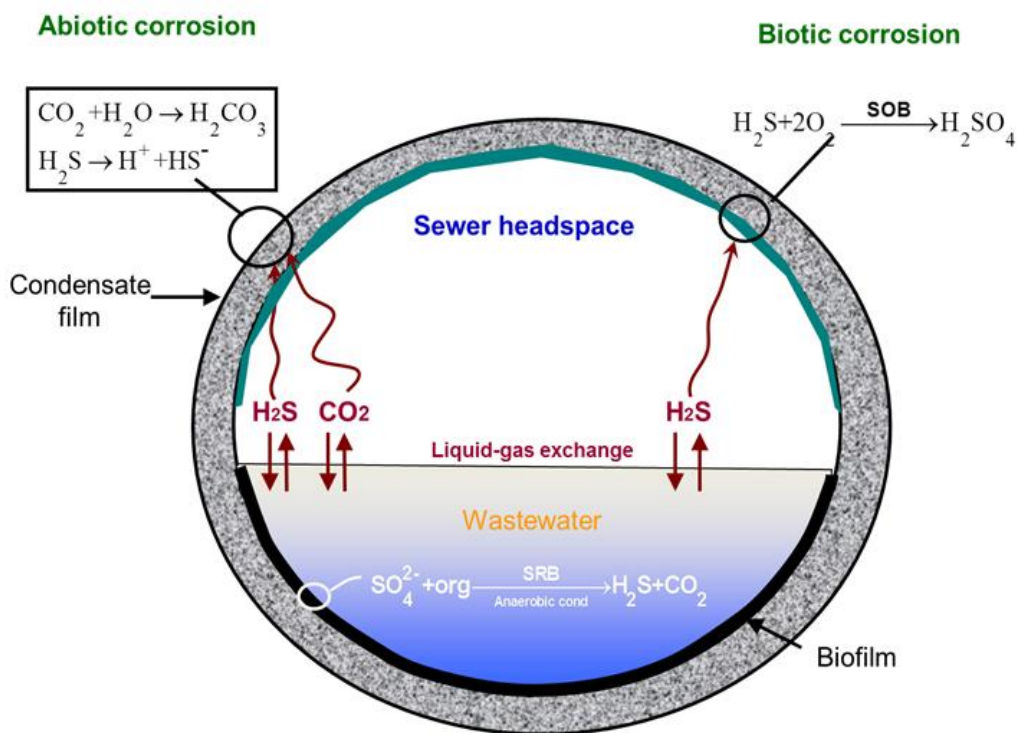


Figure 117. Diagram showing the sewer processes driving corrosion.

The sewer processes that drive concrete corrosion activity are illustrated in Figure 117. The corrosion cycle begins in the wastewater stream where colonies of anaerobic sulphate reducing bacteria (SRB) are active in biofilm layers that line the submerged sewer walls. In these films SRB reduce sulphates and oxidise biodegradable organic carbon and in doing so produce hydrogen sulphide and carbon dioxide (Eqn. (7)).



The hydrogen sulphide formed is transported through the biofilm into the wastewater stream where the molecular form of the sulphide co-exists in equilibrium with its dissociated ions, H^+ and HS^- . At normal domestic sewage pH, 25-35% of the dissolved sulphide exists as molecular H_2S . Carbon dioxide is also transported into the liquid phase where a portion is dissolved as carbonate and bicarbonate ions. At the liquid-gas interface some H_2S and CO_2 are volatilised into the sewer headspace. The gases diffuse through the headspace atmosphere and dissolve into moisture present in the concrete pore structure of the roof and walls of the sewer pipe.

What happens next is dictated by the age of the pipe and the conditions that exist on the pipe surface and in the sewer atmosphere. The following discussion will trace the corrosion process from the beginning of the pipe's service life through to its failure.

6.3.1.2 Abiotic corrosion: Pipe installation to $t_{pH=9}$

When a concrete sewer pipe is first manufactured the surface is very alkaline ($pH=12$ to 13). In the normal course of events it is reasonable to expect that the pipe will not be installed immediately and during the time between manufacture and installation it is likely that the surface pH will drop somewhat due to some level of surface carbonation resulting from its exposure to CO_2 in the atmosphere. (Such a drop in surface pH was observed on the Sp1B new coupons during the 12 months between pipe manufacture and installation of the coupons in the sewers). Never the less the high levels of alkalinity that remain will preclude any likelihood of microbial colonisation of the pipe surface until surface pH has dropped further.

Only the chemical (or abiotic) corrosion pathway is possible in the initial, alkaline surface environment. Under these conditions weak inorganic acids are formed from the H_2S and CO_2 that have dissolved into the concrete pore water as a portion of the H_2S re-dissociates to form HS^- and H^+ (Eqn. (8)) and dissolved CO_2 forms carbonic acid in its various forms (Eqn. (9)).



Elemental sulphur and thiosulphates are also known to be formed during this time by the abiotic oxidation of H_2S , [58]. While these species are not believed to take a direct part in the initial corrosion process they form a nutrient base for later biotic corrosion.

Newly manufactured concrete contains a suite of alkaline minerals within the cement binder (Figure 118). Corrosion of the concrete sewer pipe is initiated when these minerals are attacked by the weak acids thus formed from the dissolution of the H_2S and CO_2 . Acid attack of the cement binder destabilises each mineral in turn as the pH of the concrete falls below the stability limit for each (for example $Ca(OH)_2$ will begin to break down once the pH falls below ~ 12.5). Consequently in the initial months following installation the abiotically formed weak inorganic acids attack the more basic minerals present within the cement binder of the pipe surface ($Ca(OH)_2$, Ettringite and some Calcium-Silicate-Hydrates (C-S-H) (Figure 118).

ANC results obtained in this study, (for example see Figure 119), suggest that decreasing the sewer concrete pH in the early stages of the pipe's life requires a great deal of acid (see blue region in Figure 119). This is corroborated by XRD analysis of the new coupon concrete (see Section 4.4.1.1) which indicates that there are significant reserves of $Ca(OH)_2$, the most basic mineral, present in the newly manufactured concrete. pH profiling evidence however suggests that acid attack is most likely limited to a thin outer layer ($<0.5mm$) of concrete. As a result only a small mass of concrete is affected and therefore a relatively small amount of acid is required to deplete the available reserves of the more basic minerals and drop the surface pH. This explains observations made during the field coupon pH surveys that showed surface acidification is most

rapid during the early stages of the pipe's exposure to the sewer environment (see for example Figure 94).

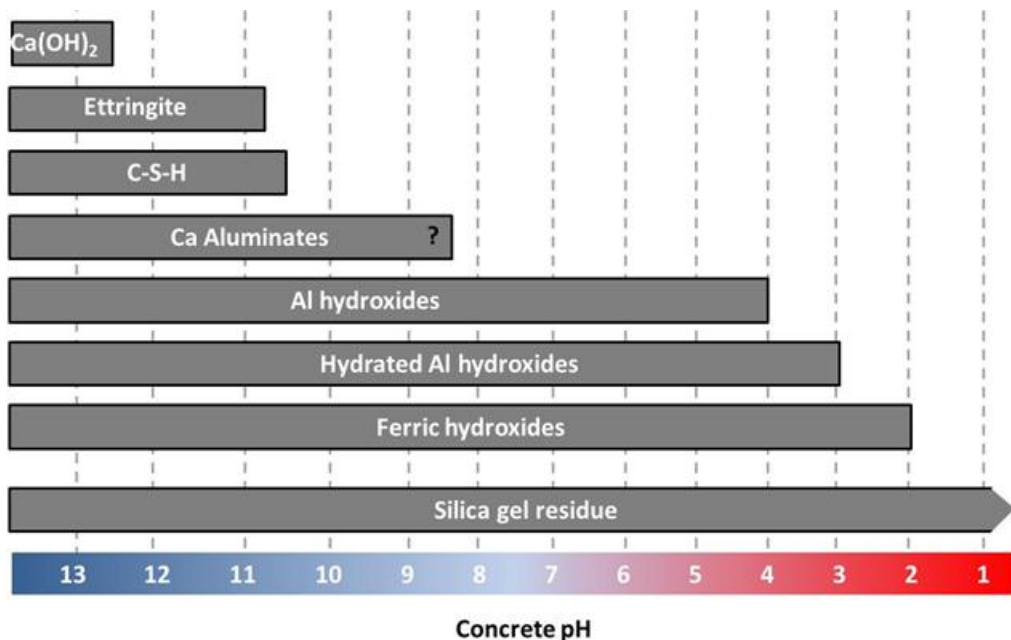


Figure 118. Principle hydrated cement compounds and their stable pH range (as listed in [56])

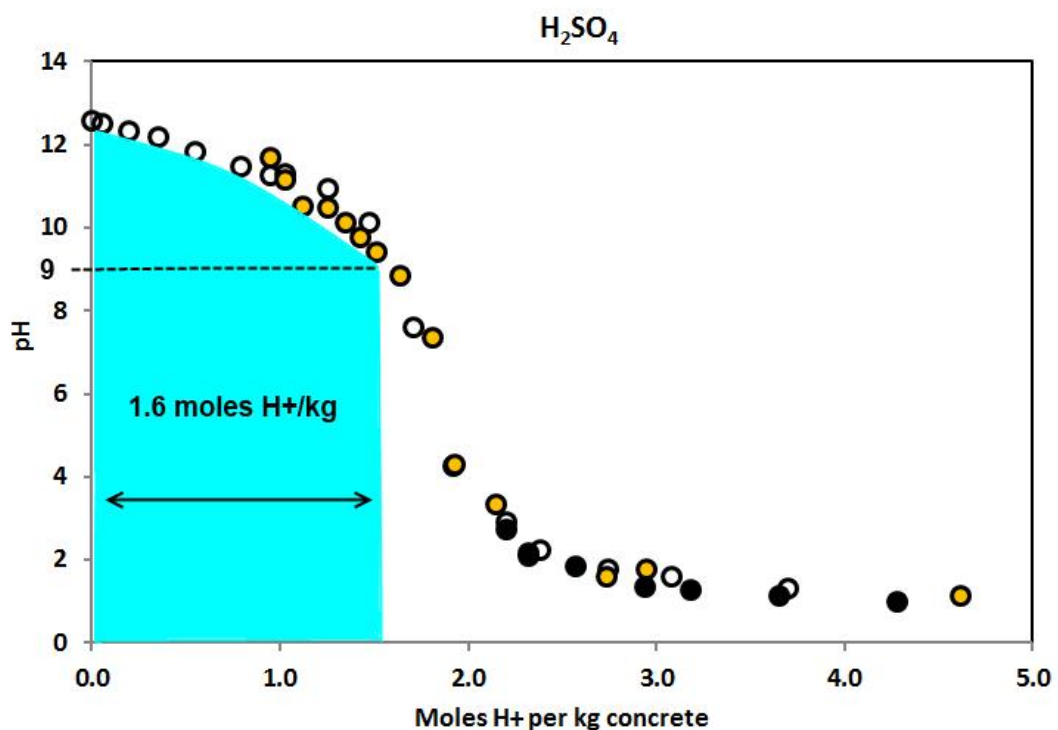


Figure 119. Quantities of sulphuric acid required to lower the pH of new coupons to pH=9.

Field work data suggests that the time it takes for a newly installed pipe to reach a surface pH of 9, ($t_{pH=9}$), is only a matter of months (the time varied between 3 to 7 months for our field samples). Thus when considered against the expected lifespan of the pipe the time spent in this stage of the corrosion cycle is minimal.

Never the less, despite the fact that no concrete is lost at this time, this stage of the process is important as the drop in surface pH that occurs sets the scene for the colonisation of the pipe surface by bacterial and fungal communities and the onset of more substantial corrosion activity.

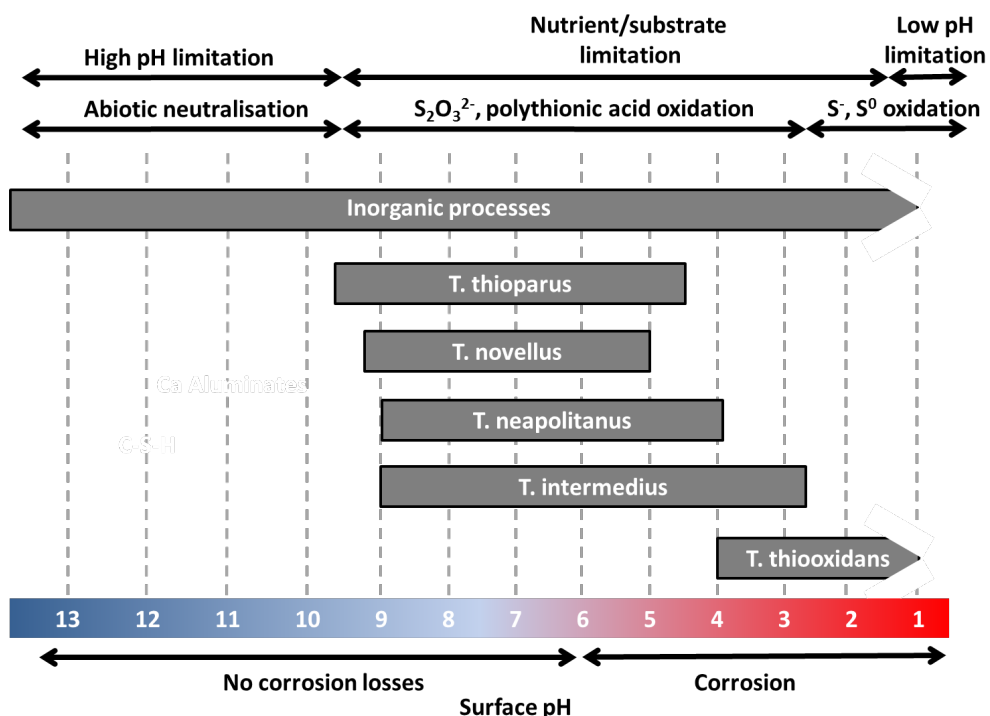


Figure 120. Succession of microbial species active on concrete in sewers [25, 26, 59].

6.3.1.3 First signs of life : $t_{pH=9}$ to $t_{pH=6}$

Once the pH of the concrete surface drops below 9 microbial and fungal colonisation of the pipe surface commences. The first signs of life on the field coupons appeared at this stage of the corrosion cycle manifesting themselves as small clusters of green hyphae and populations of small black nodules.

Previous studies have shown that as the surface pH continues to fall successive waves of different microbial communities will populate the pipe surface (Figure 120). Studies such as that conducted by Cayford [60] as a part of the SCORE project have revealed the large number of microbial species involved in this process of successive colonisation. While the function of many of these microbial species is currently unknown the occurrence and activity of the sulphur oxidising bacteria genus *Thiobacillus*, which are of primary interest in the corrosion of concrete sewer pipe, are better documented.

As the pH of the pipe surface falls below pH=9 for example *Thiobacillus thioparus* which oxidises sulphur and thiosulphate formed earlier are known to become active on the pipe surface. At these pH conditions the thiosulphate pathway for sulphur oxidation dominates and microbial activity is limited by S input and/or nutrient availability however as the pH decreases further the levels of sulphur (created by biotic and abiotic processes) and inorganic salts created by previous corrosion increase and bacterial species such as *T. neapolitanus* populations which are less inhibited by high salt levels flourish.

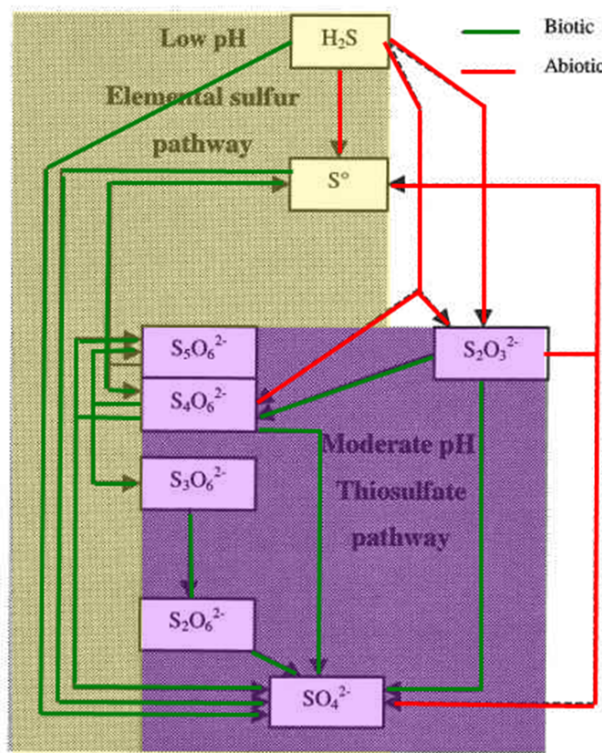


Figure 121. Sulphur species produced from oxidation of H_2S in a sewer environment (modified from a diagram presented in [58]).

During this period there is as yet still no significant loss of concrete from the pipe occurring however increased rates of sulphur oxidation and the production of polythionic and sulphuric acids from the neutrophilic bacteria described above (as well as carboxylic acids generated by other bacteria) are continuing to drive down the surface pH setting the stage for the appearance of more aggressive bacteria and the advent of significant corrosion losses.

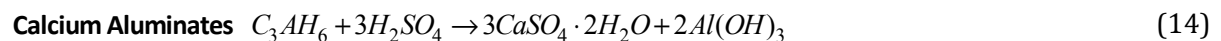
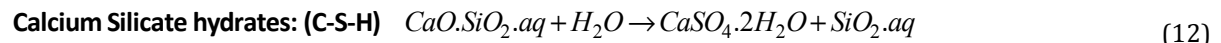
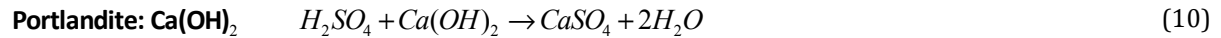
The total time spent by the Sp1B new coupons in the “incubation period” (the time taken for the surface to fall to $\text{pH}=6 = t_{\text{in}}$) ranged between 10 and 23 months (again depending on the aggressiveness of the local environment).

6.3.1.4 Initiation of corrosion losses: $t_{\text{pH}<6}$

As the surface pH continues to fall the biology present on the pipe surface evolves. In this study we observed the colonies of green hyphae replaced by mats of thicker, dark braided hyphae

interspersed with nuggets of pure sulphur covering the coupon surface. As the pH decreases below pH=6 sulphur oxidising bacteria such as *T. intermedius* and *T. novellus* in turn begin to dominate the pipe surface replacing bacteria such as *Thiobacillus thioparus*. *T. intermedius* and *T. novellus* are heterotrophs (are unable to fix carbon and must obtain it from other organic sources). *T. intermedius* grows best at pH=5.5 to 6.0 but can grow in more acidic conditions (down to pH=2-2.8). As the surface pH falls below 4 colonies of *T. thiooxidans* flourish. *T. thiooxidans* is an autotroph (an organism that produces complex organic compounds such as carbohydrates, fats, and proteins from simple substances present in its surroundings). Populations of *T. thiooxidans* act to directly oxidise sulphur present on the pipe surface to produce sulphuric acid which is largely responsible for the corrosion observed in the sewer.

Observations of corrosion behaviour of new coupons at all filed sites revealed that when the surface pH=6 loss of sound concrete commenced with cement binder at the pipe surface being replaced by a layer of soft pasty material composed primarily of gypsum. With the surface pH falling below 6 more of the basic cement minerals (the calcium aluminates) in the near surface region are now also becoming vulnerable to acid attack. The degradation of the cement binder takes the form of the following reactions [56, 61]:



The corrosion behaviour of old and new coupons indicates that once mass loss commences losses accumulate linearly over time (i.e. the rate of corrosion at each field site is constant). The corrosion rates however differs significantly from site to site.

As corrosion continues the depth of the corrosion product layer (soft pasty white gypsum) increases. Interestingly however the presence of the corrosion layer did not affect the corrosion process in either a positive or negative sense. This is most likely because the microbial communities are for the most part situated on the exposed surface of the corrosion product layer and the layer itself is quite porous. Consequently the corrosion layer is not likely to act as a barrier between the bacteria and its nutrient supply and also is not likely to significantly slow down the diffusion of acid produced by the bacteria to the reaction front (the interface between the sound concrete and the corrosion product layer).

6.3.1.5 Advanced corrosion: $t > t_{ph=6}$

Old field coupons which begun the Sp1B trials with much lower starting pH levels reached the final stage of the corrosion cycle very early on (before the first recovery of coupons were made). Over the course of the study they experienced rates of corosions that were also, (within error),

essentially constant over the entire study period. The rates of corrosion experienced by the old coupons were also very similar to the new coupons at the same site. As the behaviour of the old coupons reflects what is expected to occur during the latter stages of the pipe's service life the field study evidence therefore indicates that the linear corrosion behaviour observed once the pH falls below 6 is likely to remain unchanged until the pipe fails.

6.3.2 Time dependence of the corrosion rate function

The corrosion loss data returned from the Perth and Melbourne field sites (Figures 86, 87, 89 and 90) all point to the same general corrosion loss scenario: A period of little or no loss which lasts from installation until the surface pH reaches approximately pH=6 followed by losses that increase linearly over time for the remaining life of the sewer pipe. Put in terms of a corrosion rate function this corresponds to an initial period during which the corrosion rate is zero followed by a rapid increase to a higher, stable corrosion rate which remains constant for the remainder of the pipe's service life (see Figure 122).

In modelling this bilinear behaviour only two parameters need to be determined- the time to initiation of corrosion loss (t_{in} in Figure 122) and the rate of corrosion once corrosion commences (CR in Figure 122). Both of these parameters will be specific to each sewer site as they are a function of a number of local environmental factors. The relationships between these parameters and the local sewer environment will soon be discussed in detail (Section 6.5).

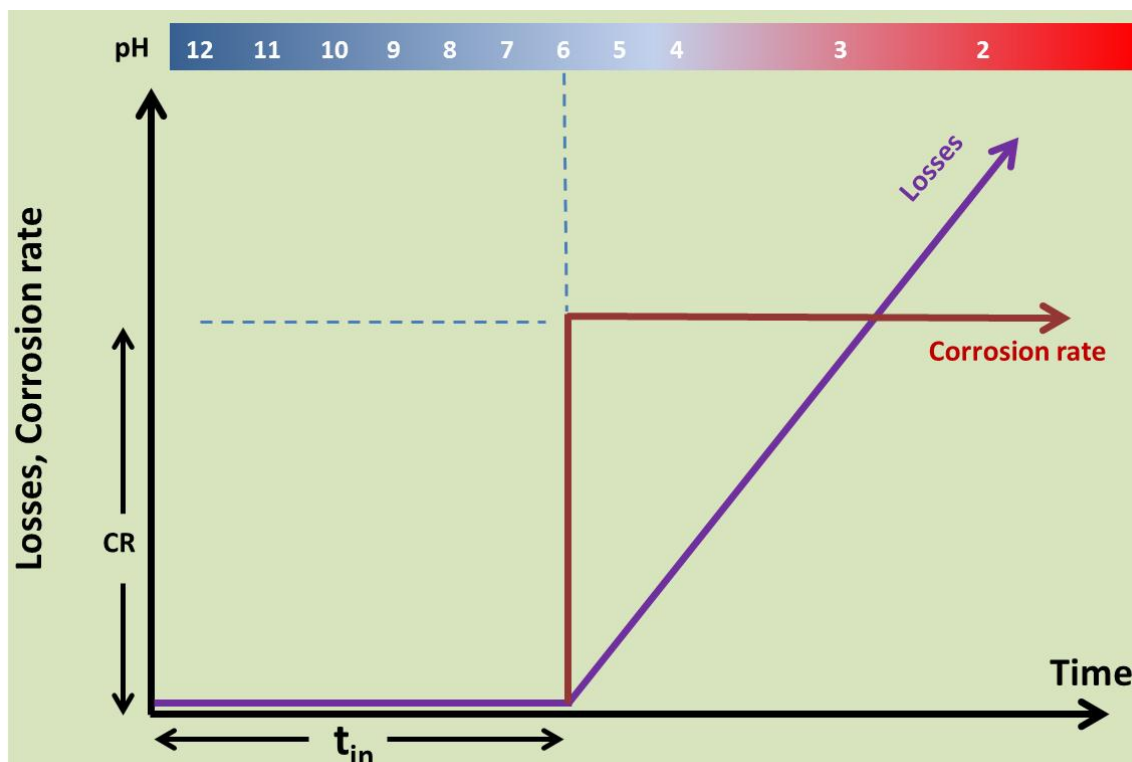


Figure 122. Bi-linear form of the sewer pipe corrosion process.

6.3.3 The spatial nature of the corrosion process

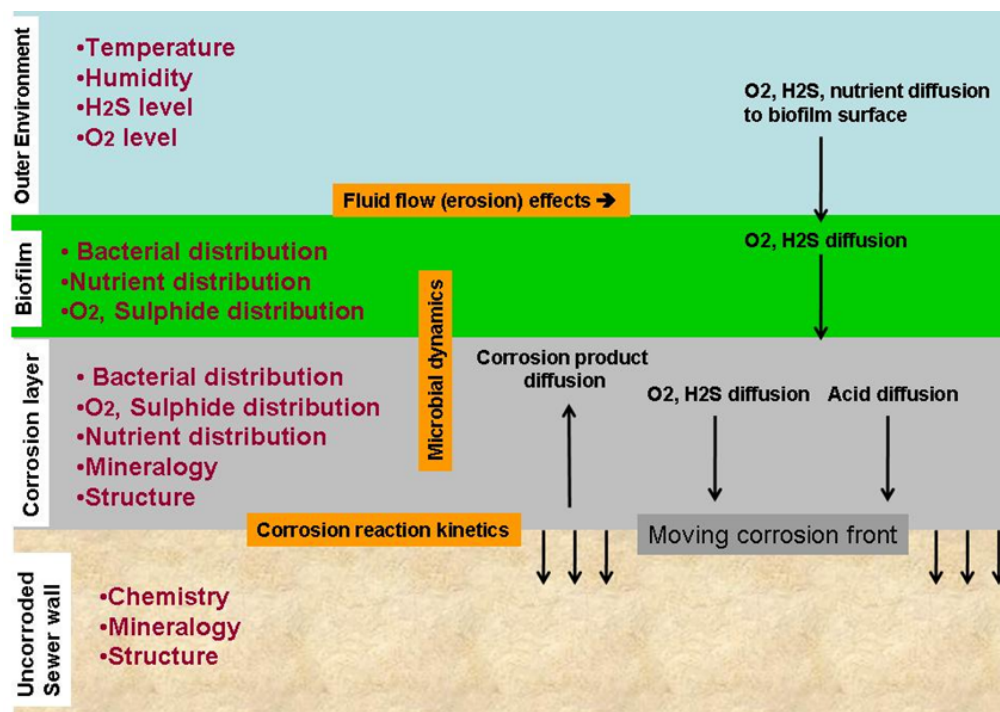


Figure 123. Overall picture of fluxes and reactions of corroding concrete.

The previous discussion illustrates the complex manner in which the corrosion process unfolds over time. For modelling purposes it is also important to consider the spatial nature of the corrosion process (its ‘geometry’). At any given time the rate of corrosion is dependent on the interplay between a number of physical processes taking place such as the transport of various nutrients, waste products and other chemicals and the rates at which species are consumed/generated by chemical reactions taking (Figure 123). Acids produced by the microbial colonies for example must diffuse down through the corrosion product layer before reaching the sound concrete interface and then if not immediately consumed by the neutralisation process will continue to diffuse into the concrete pore structure. The relative rates at which all of these processes occur will dictate the geometry of the corrosion process.

6.3.3.1 Impact of the corrosion product layer

There was much speculation at the beginning of the Sp1B sub-project as to whether the buildup of corrosion product on the exposed pipe surface would hinder or aid the corrosion of the concrete pipe. One school of thought suggested that the corrosion product layer would slow corrosion by acting as a physical barrier to the diffusion of acid and/or nutrients from the exposed surface to the corrosion layer/sound concrete interface however it was also suggested that corrosion may be accelerated as a deep, moist corrosion layer may act as a nurturing environment beneficial for bacterial growth.

Losses experienced by new and old coupons at the Perth and Melbourne field sites are plotted in conjunction with the corresponding growth in corrosion product layers in Figure 124. In all cases it is clear that the rate at which losses accumulated over time remained constant despite a significant increase in the depth of the corrosion product. This would suggest that the depth of the layer of corroded concrete has little effect on bacterial populations/activity and also its presence did not significantly slow down the diffusion of critical species (be it nutrients, oxygen, H₂S or acid) throughout the corroding region.

This was a surprising result. However it can, at least in part, be explained by findings in studies such as that conducted by Okabe [16] which indicate that microbial populations are largely concentrated at or near the exposed surface of well-established corrosion layers (Figure 125). This would suggest that the microbial population would not be significantly affected by the depth of the layer as they have a preference for an environment exposed to the sewer gas stream. In this position the corrosion layer cannot act as a barrier to nutrient, H₂S, oxygen supply to the bacterial colonies.

There is still the possibility however that the corrosion product layer may slow down corrosion by acting as a barrier to the transport down to the sound concrete interface of acid produced by bacteria on the exposed surface. However visual and low power microscopic inspection of the morphology of the corrosion layer (see for example Figure 126) reveals that the corrosion layer (which is primarily composed of gypsum and unreacted sand) features large fissures and tunnels particularly in and around exposed aggregate providing numerous pathways for acid to migrate unhindered to the sound concrete interface. In such circumstances the corrosion layer is unlikely to provide a significant barrier to the transport of acid and thus is unlikely to act as a physical barrier hindering the corrosion process.

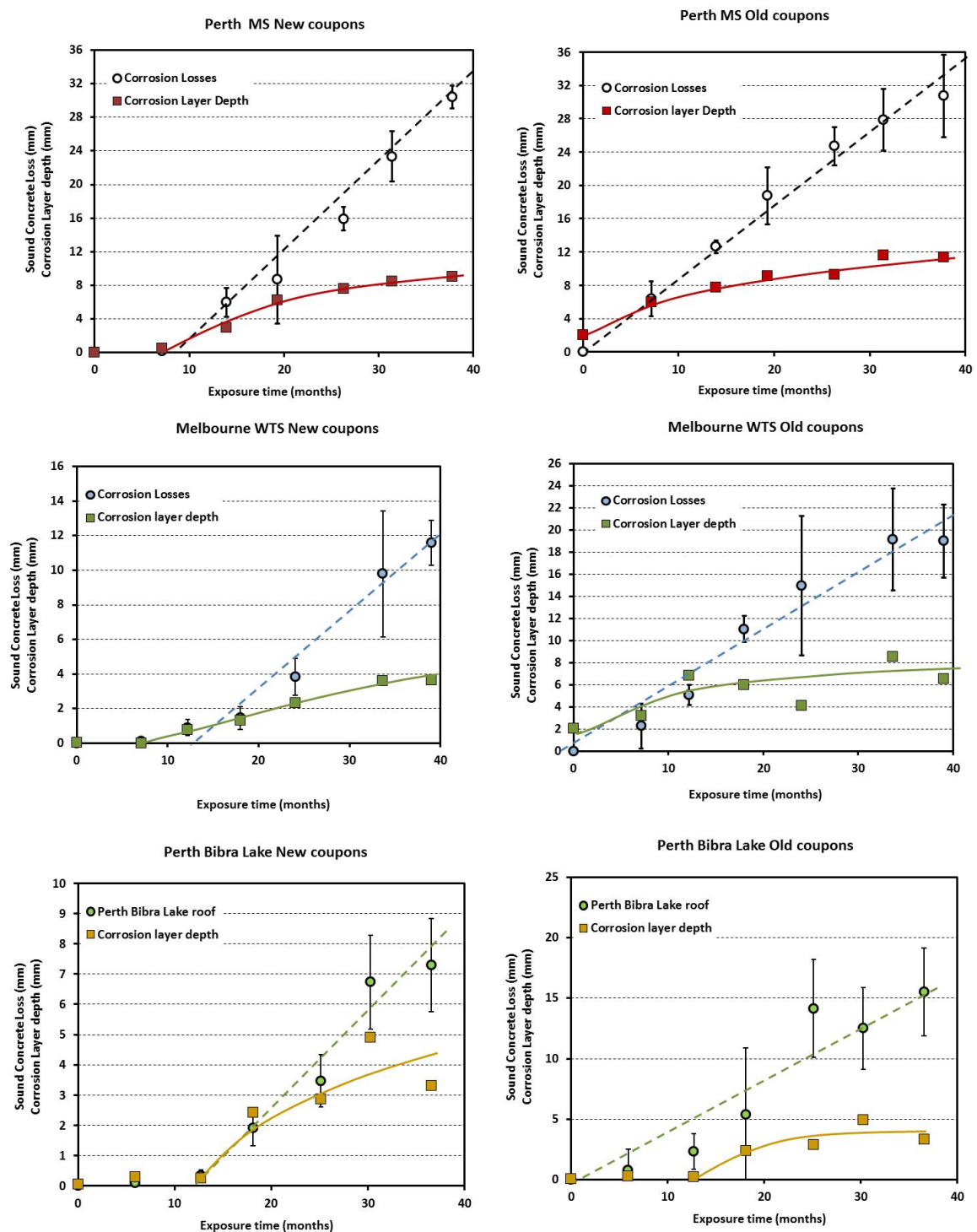


Figure 124. Growth of corrosion layer and corrosion losses observed for new and old coupons at the Perth and Melbourne field sites.

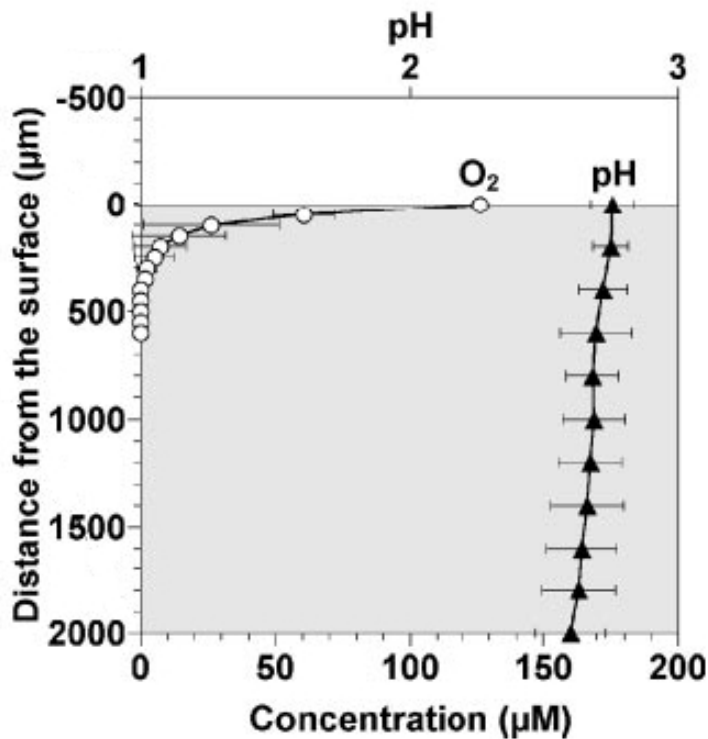


Figure 125. O_2 Concentration and pH profiles in the top 2mm of the heavily corroded gypsum layer that was exposed to a H_2S ($30+/- 20$ ppm) atmosphere for 1 year (reproduced from [16]).

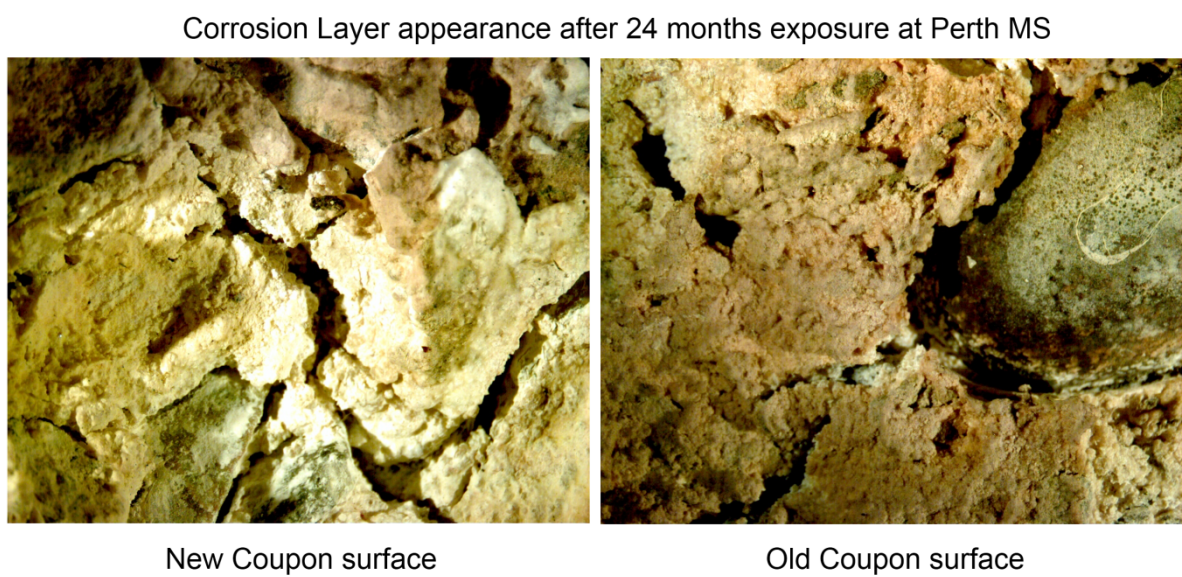


Figure 126. Morphology of corrosion layer on Perth MS coupons exposed for 24 months.

6.3.3.2 The reaction front

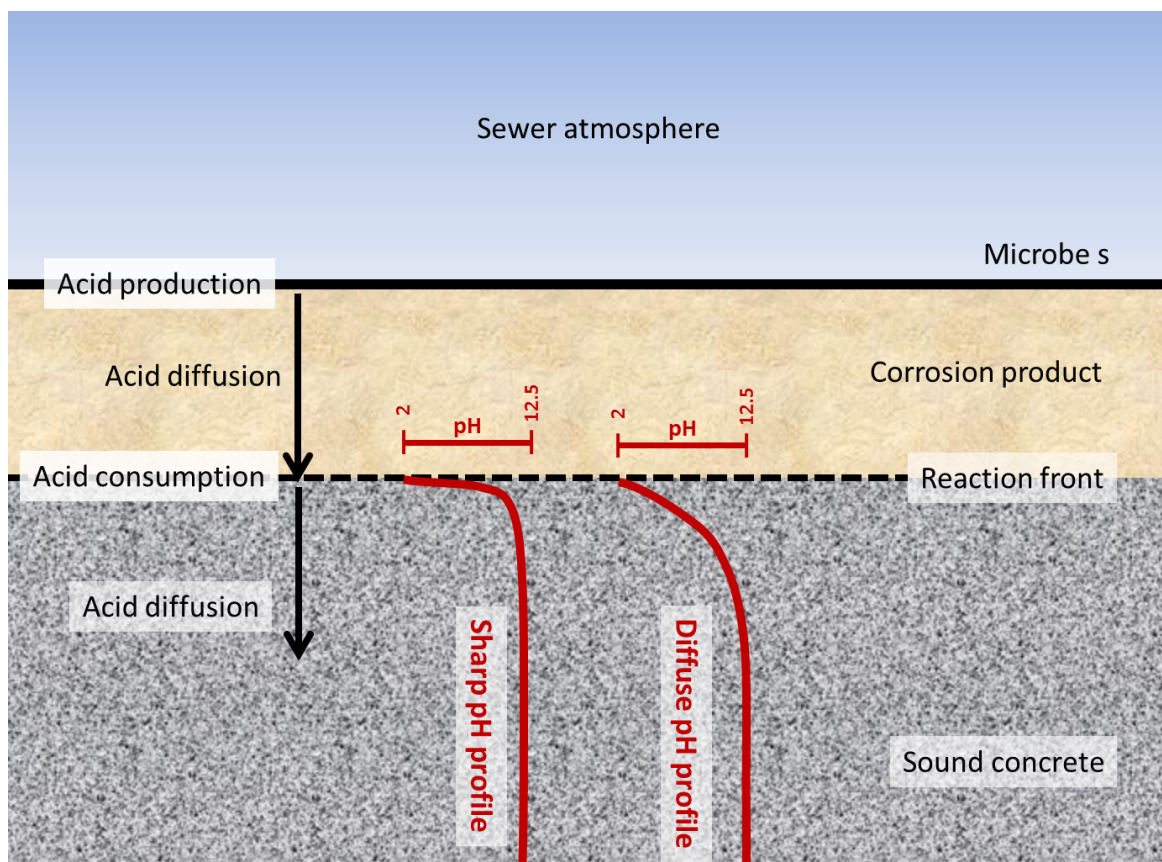


Figure 127. Possible reaction front profiles.

At the interface between the sound concrete and the corrosion layer (the “reaction front”) the corrosion of the sound concrete is impacted by the relative rates of the following processes:

- (a) acid diffusion through the corrosion product layer to the reaction front
- (b) acid consumption at the reaction front by reaction with the basic minerals in the cement binder and
- (c) acid diffusion away from the reaction front into the sound concrete matrix.

The porous nature of the corrosion product layer indicates that diffusion of acid to the reaction front is rapid and therefore not likely to limit the level of corrosion activity. If the rate of reaction between the incoming acid and the cement binder is significantly fast compared to the rate at which the acid can diffuse into the concrete then we would expect little acid penetration into the sound concrete producing a sharp profile and a well-defined reaction front (leftmost profile in Figure 127). If on the other hand the rate of diffusion into the concrete is faster than the rate of acid consumption we would expect greater penetration of the acid into the concrete before it is consumed producing a more diffuse, less well defined reaction front (right profile in Figure 127).

pH profiling work conducted within the Sp1B sub-project (Section 5.4.2.4) points to a sharp well defined reaction front with only minimal ($\sim 0.3\text{mm}$) penetration of acid into the sound concrete matrix. This indicates that after diffusing through the corrosion layer acid is consumed rapidly before it can diffuse to any great degree into the concrete structure.

6.3.3.3 Spatial framework for phenomenological model of sewer pipe corrosion

These findings suggest the following spatial framework for the phenomenological model of the corrosion process:

- The model will consist of three zones (or domains): a bulk gas phase, a corrosion product layer and underlying this a region of sound concrete.
- Acid production takes place only at the exposed surface of the corrosion product layer (the interface between the corrosion product and the bulk gas phase).
- Diffusion of the acid through the corrosion product layer will be rapid.
- Diffusion into the concrete will be relatively slow.

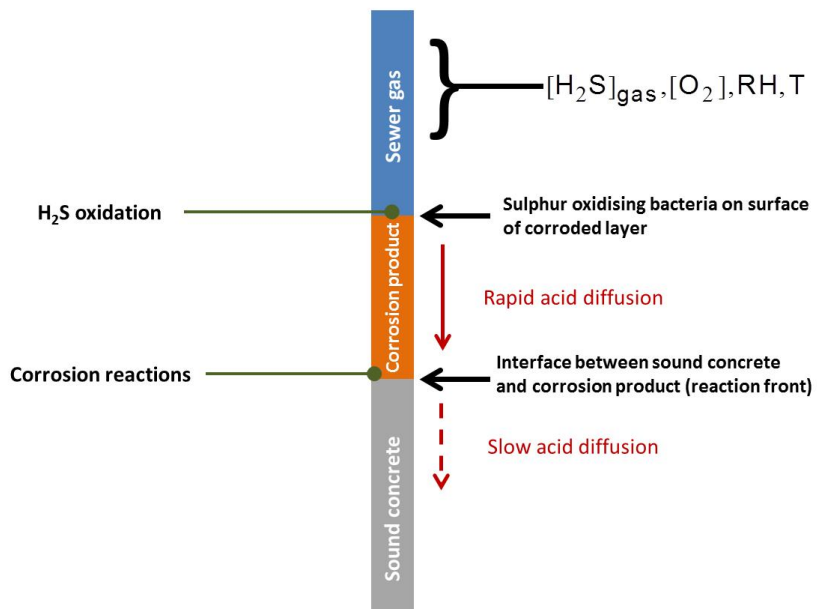


Figure 128. Physical arrangement used in 1D modelling of the corrosion process.

The criteria by which the model will be optimised will include:

- A sharp reaction profile is produced matching pH profiles observed in this study
- The profiles will remain sharp for the duration of the corrosion cycle
- The rate of loss is unaffected by the growth of the diffusion layer

In addition the model will need to reproduce rates of corrosion observed at the different field sites.

6.4 Phenomenological model of concrete sewer pipe corrosion

A one dimensional (1D) phenomenological model of sewer pipe corrosion was developed to explore the effects of diffusion and reaction kinetics on the overall reaction process and determine if any one process is likely to govern the overall corrosion behaviour (i.e. is the rate controlling step).

As has already been discussed the corrosion process is complex as it incorporates many factors that vary across time and space. The 1D model enables many of the complexities inherent in the process to be considered and the corrosion outcomes for a given set of factors in play to be examined. The aim of the phenomenological modelling work is to gain a better insight into the working of the corrosion cycle. This is achieved by comparing the predictions of the model operating under a range of different assumptions with corrosion behaviour (pH profiles, relationships between corrosion activity and time and environmental conditions) observed in the sp1B field and laboratory work.

6.4.1 Framework for the 1D model

A diagram of the physical layout of the 1D corrosion model is illustrated in Figure 129. The model is broken up into 3 regions: the sewer bulk gas phase (shown in blue), the corrosion product layer (orange) and the unaffected or sound concrete region (grey). Only movement and creation/consumption of the acidic species “ H^+ ” and the alkali species (collectively $Ca(OH)_2$, C-S-H, etc.) are considered in the model. The incubation period is not simulated in this model. The model starts with a completely uncorroded section of concrete at time=0 and as time progresses the formation of acid from the oxidation of H_2S on the exposed surface of the pipe ($t=0$), or the corrosion product layer ($t>0$), is simulated. The acid diffuses away from the exposed surface down through any corrosion layer present until it encounters sound concrete, (the reaction front), at which point the reaction between the acid and base minerals in the concrete takes place. As the alkalinity of the concrete is consumed the reaction front moves downward and is replaced by a porous corrosion product layer. By monitoring the position of the reaction front at any time relative to its initial position the model predicts the rate at which concrete is lost for a given set of environmental conditions.

The main features of the model are now listed working from the top of Figure 129 (the bulk gas phase) to the bottom (sound concrete phase).

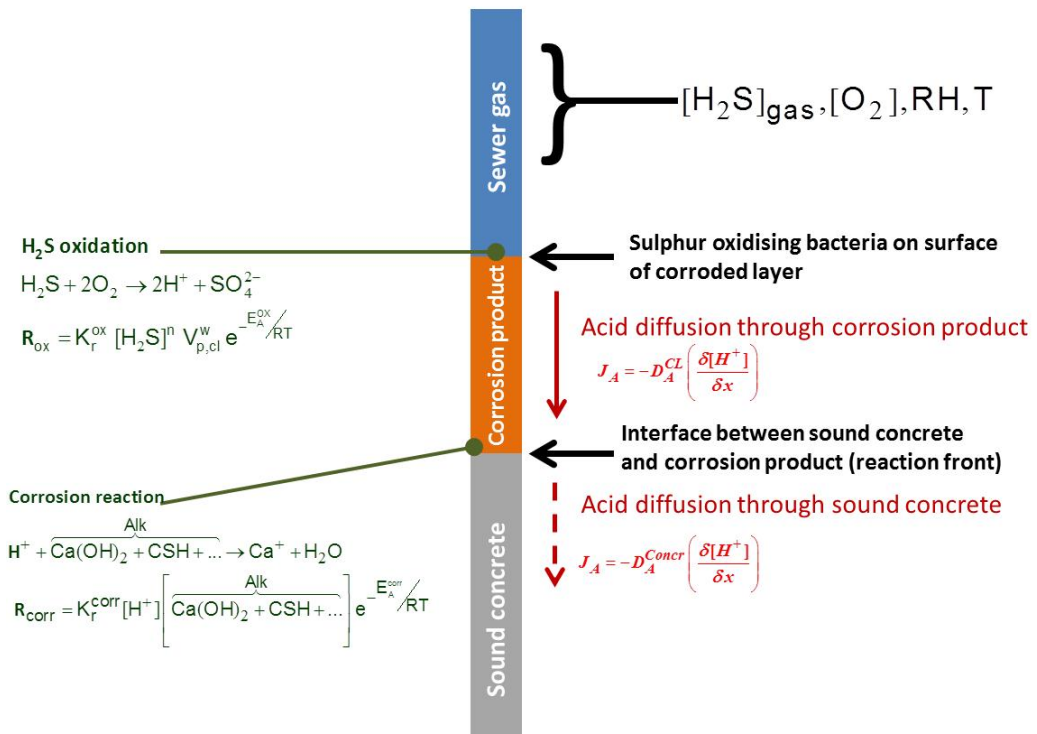


Figure 129. One dimensional model of sewer pipe corrosion.

6.4.1.1 Bulk gas phase

- The sewer gas phase is well mixed and consequently all of the characteristics of that phase (e.g. $[H_2S]$, T etc.) are uniform and unchanging over time.
- The characteristics of the bulk gas phase are represented by the time averaged environmental data observed over the Sp1B field trial study period (i.e. temperature, humidity and H_2S concentration shown in Table 13 were used as inputs into the model).

6.4.1.2 Exposed surface of corrosion product layer

- The bacteria that are responsible for the oxidation of H_2S to acid are all assumed to reside at the boundary between the corrosion product and the bulk gas phase
- H_2S from the bulk gas phase dissolves into the concrete pore water (at $t=0$) or corrosion product pore water ($t>0$) located at the exposed surface.
 - The H_2S concentration is determined by application of Henry's Law (i.e. the dissolved H_2S is assumed to be in equilibrium with the gas phase H_2S).
- The concentration of alkaline elements at the exposed surface is zero.

Acid production

- Acid production takes place only at the corrosion product layer/bulk gas phase interface. Acid is assumed to be produced via the simple oxidation of H₂S which has dissolved into the pore water at the interface:



- The oxidation kinetics are assumed to follow a power law relationship with respect to the bulk H₂S concentration as suggested by Vollertsen [20] in his 2008 study of the biological oxidation of H₂S in a pilot scale sewer. To his considerations we have added a factor to account for the effect of concrete moisture content and also a classical Arrhenius style temperature factor to produce the following general expression:

$$R_{ox} = K_r^{ox} \times [H_2S]^n \times V_{p,cl}^w \times e^{-\frac{E_a^{ox}}{RT_k}} \quad (17)$$

Where R_{ox} is the rate of oxidation reaction; K_r^{ox} is the characteristic rate constant; $V_{p,cl}^w$ is the volume fraction of pores filled with water; E_a^{ox} is the activation energy; R and T_k are the universal gas constant and sewer gas temperature (in Kelvin) respectively.

- Vollertsen's work [20] suggests that the rate of H₂S oxidation is proportional to [H₂S]^{0.45-0.75} and consequently n was set to a value of 0.5 in this model.
- The rate of H₂S oxidation was also assumed to be proportional to the moisture content of the corrosion layer, V_w^{CL} , which is a function of humidity and the PSD of the corrosion layer (see later discussion in Section 6.5.3). Eqn. (29) was used to determine the volume fraction of water filled pores from the given humidity level.
- A study conducted by Franzmann [62] which looked at the effect of temperature on the rates of bacterial oxidation of sulphur suggests activation energies lie in the range of 26 to 47 kJ/mol. For the purposes of this model E_a^{ox} was set at 30 kJ/mol.

6.4.1.3 Corrosion product layer

- Once formed the acid diffuses through the corrosion product layer until it encounters uncorroded concrete at the reaction front.
- The flux of the acid through the corrosion layer, $J_{cl}^{H^+}$, is proportional to the acid concentration gradient through the corrosion layer and a characteristic diffusion coefficient for the acid, $D_{cl}^{H^+}$, that is:

$$J_{cl}^{H^+} = -D_{cl}^{H^+} \left(\frac{\partial [H^+]}{\partial x} \right)_{cl} \quad (18)$$

Where $\left(\frac{\partial H^+}{\partial x} \right)_{cl}$ is the local acid concentration gradient within the corrosion layer.

- Visual inspection of the corrosion layer of recovered field samples revealed that it was quite porous and consequently it is assumed that the diffusion coefficient governing flux rates through the corrosion layer is likely to be significantly higher than that governing diffusion transport of the acid into the concrete. To accommodate this in the 1D model the following relationships are used to calculate the diffusion coefficients:

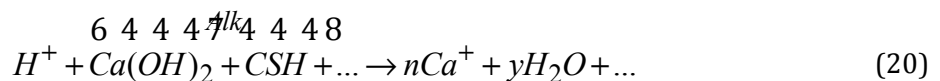
$$D_{cl}^{H^+} = D_c^{H^+} \times \left(10 - 9 \times \frac{[Ca(OH)_2 + CSH + \dots]_t}{[Ca(OH)_2 + CSH + \dots]_{t=0}} \right) \quad (19)$$

Where $D_{cl}^{H^+}$ and $D_c^{H^+}$ are the effective diffusion coefficients for acid through the corrosion product layer and sound concrete respectively.

- A factor $\left(10 - 9 \times \frac{[Ca(OH)_2 + CSH + \dots]_t}{[Ca(OH)_2 + CSH + \dots]_{t=0}} \right)$ is used to represent the increase in diffusion coefficient for acid expected as the concrete degrades (and the level of alkalinity decreases). If for example the alkaline elements within the corroded layer have been totally depleted ($[Ca(OH)_2 + CSH + \dots]_t / [Ca(OH)_2 + CSH + \dots]_{t=0} = 0$) the effective diffusion of acid through the corrosion layer is set at 10 times that through the concrete. If less material has been removed the diffusion coefficient fell to a value closer to that of H^+ in concrete.

6.4.1.4 Sound concrete

- The initial concentration of Alkali components in the sound concrete is set at 2550 gmol/m^3 (determined from the ANC study) and the concentration of H^+ is $3.2 \times 10^{-10} \text{ gmol/m}^3$ ($\text{pH}=12.5$).
- Once the acid reaches the sound concrete it reacts with the alkaline elements within the sound concrete ($Ca(OH)_2$, C-S-H etc.) via the following simplified reaction:



- The corrosion reaction rate is set proportional to the local concentrations of the alkaline components in the concrete and the local acid concentration, that is:

$$R_{corr} := K_r^{corr} \times \left[H^+ \right] \times \left[\frac{6 \ 4 \ 4 \ 4 \ 4 \ 4 \ 4 \ 8}{Ca(OH)_2 + CSH + \dots} \right] \times e^{-\frac{E_a^{corr}}{RT_k}} \quad (21)$$

Where R_{corr} is the rate of corrosion reaction; K_r^{corr} is the characteristic rate constant; E_a^{corr} is the activation energy of the corrosion reaction; R and T_k are the universal gas constant and sewer pipe wall temperature (in kelvin) respectively.

- The activation energy for the corrosion reaction, E_a^{corr} , was determined from data reported in [63] that the rate of concrete corrosion when attacked by sulphuric acid increases by approximately 25% when temperatures are increased from 25°C to 40°C. This would suggest that the activation energy is 8.9kJ/mol, the value used in this model.
- Any acid not immediately consumed in the reaction with the alkaline elements of the concrete can diffuse from the reaction front into the sound concrete. The transport of the acid, $J_c^{H^+}$, into the sound concrete is assumed to follow the classical diffusion form:

$$J_c^{H^+} = -D_c^{H^+} \left(\frac{\partial[H^+]}{\partial x} \right)_c \quad (22)$$

Where $D_c^{H^+}$ is the acid diffusion coefficient through concrete and $\left(\frac{\partial[H^+]}{\partial x} \right)_c$ is the acid concentration gradient in the sound concrete.

- The diffusion coefficient $D_c^{H^+}$ is calculated in the following manner:

$$D_c^{H^+} = \frac{1}{\tau} \left(D_{air}^{H^+} \times (1 - V_{p,c}^w) + D_w^{H^+} \times V_{p,c}^w \right) \quad (23)$$

Where $D_{air}^{H^+}$ is the diffusion coefficient for hydrogen ions in air (assumed =0); $D_w^{H^+}$ is the diffusion coefficient for H^+ ions in water ($=9.3 \times 10^{-9} \text{ m}^2/\text{s}$) and $V_{p,c}^w$ is the fraction of concrete pores filled with water (calculated from Eqn. (29))

- Acid that penetrates into the sound concrete continues to react with alkaline elements within the local volume of concrete.
- It is also assumed that the alkaline material within the concrete is immobile (no diffusion).

6.4.2 Operation of the 1D model

The two unknown parameters within the model, the reaction rate constants, K_r^{corr} and K_r^{ox} , were varied to obtain the optimum fit between the model predictions and the field observations. As a result of the inherent complexity of the model described above there are no analytical solutions, (the solution to the model cannot be represented by a single (or set of) equation(s)), and consequently the model was solved numerically using a finite element approach. This approach involves breaking up the problem domain (in this case the thickness of the concrete

coupon and corrosion product) into a series of smaller intervals and finding approximations for the problem solution for each of the smaller elements ('sub domains'). Time is also divided up into a series of smaller time elements for calculation purposes.

The mathematics to accomplish this are complex but software packages such as the COMSOL MULTIPHYSICS 3.5 Finite element software package used in this study are commercially available to handle the finite element calculations. All that is required from the user is a detailed description of the space over which the model is operating and details of the physical processes taking place (Figure 129).

Simulations were carried out over a 10 year period employing different values of K_r^{corr} and K_r^{ox} until simulation predictions best matched the corrosion behaviour observed at the Melbourne and Perth field sites. The aim was to best match model predictions with field observations of:

- The rate at which losses occur at the different field site conditions.
- How losses accumulated over time (note: the incubation period was not included in the model).
- The shape of the reaction front (a sharp, well defined reaction front as indicated by pH profiling measurements).

6.4.3 1D modelling results

To simulate the sharp reaction front indicated by the pH profiling survey it was necessary to set the rate constants, K_r^{corr} and K_r^{ox} to values that ensured the oxidation reaction was significantly slower than the corrosion reaction (i.e. R_{ox} in Eqn. (17) $\ll R_{corr}$ in Eqn. (21)). In other words the rate at which H₂S was oxidised at the exposed surface was the rate controlling step governing the entire corrosion process. In this scenario acid generated from biological activity at the exposed surface diffuses quickly to the sound concrete interface where it is rapidly consumed in the neutralisation reaction. As a consequence of the rapid consumption of the acid at the reaction front very little acid diffuses into the sound concrete structure resulting in very sharp pH profiles (the alkaline content of the bulk concrete is preserved right up to the reaction front itself - Figure 130).

Once it was established that the oxidation process was the rate limiting step, the value of K_{ox} in Eqn. (17) was optimised to align 1D model predictions of corrosion activity at the Melbourne and Perth sites with observed values. When K_{ox} was set to a value of 1.18 m³/mol.s the 1D model predictions of the rate of loss of sound material was a reasonable match to the observed values at each of the field sites with an average error of +/- 1.3 mm/yr.

The value of K_{corr} could not be fully optimised in this model as it was not a rate controlling step however at values below 10⁻⁵ m³/mol.s it was evident that the reaction front was not as well defined so it is assumed that the value of K_{corr} is somewhat higher than this value (increasing K_{corr} above this value does not alter the rate at which material is lost).

The model also successfully predicts that the rate at which sound concrete is corroded away increases linearly with time (for example see Figure 132) which is also in agreement with the field observations further strengthening the model credentials.

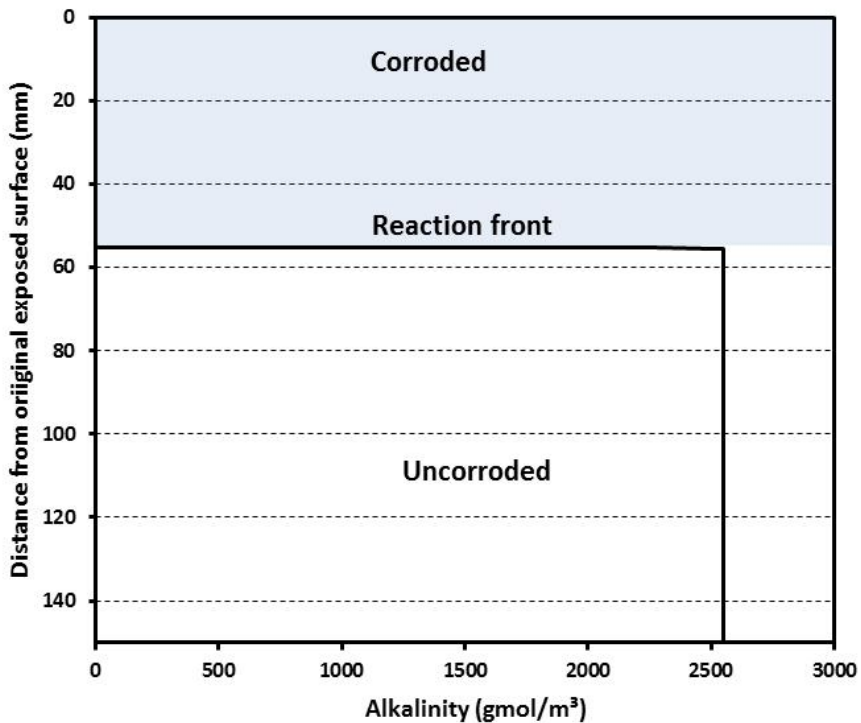


Figure 130. The shape of the reaction front predicted by the 1D model, (compare the sharpness of the front to the pH profiles shown in Figures 101 to 104).

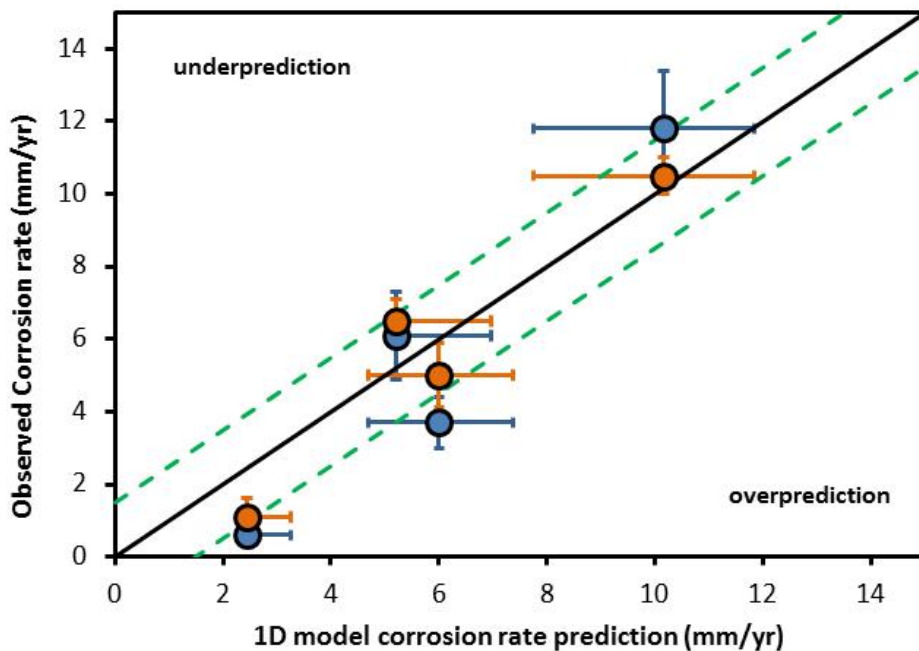


Figure 131. 1D model corrosion rate predictions compared to rates observed at the Melbourne and Perth field sites. Vertical error bars reflect the uncertainty in the measured rates of corrosion (90% confidence interval) and the horizontal error bars represent the range of predicted values (based on 90% ci of the environmental data).

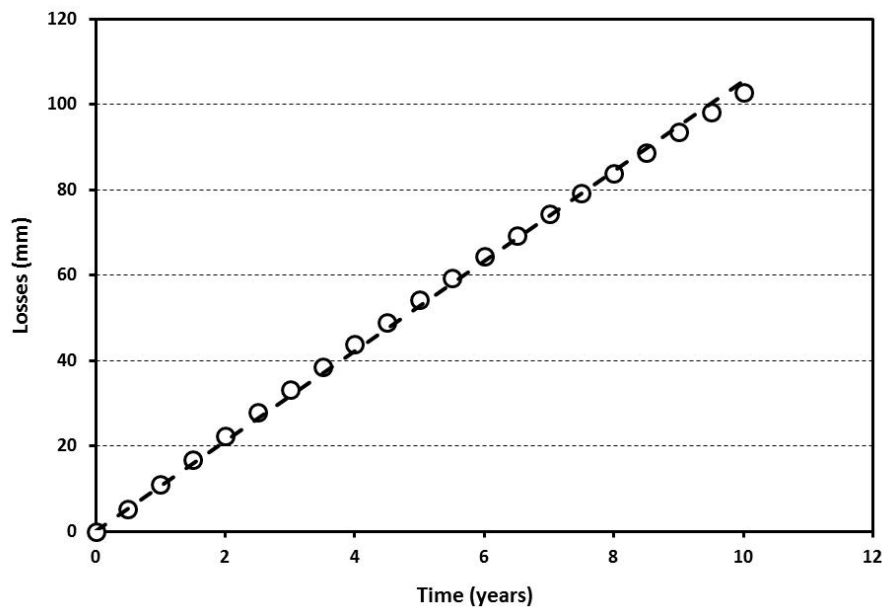


Figure 132. Accumulation of losses over time predicted by the 1D corrosion model for the Perth MS field site. (Dashed line shows a linear fit to the data)

6.5 Factors impacting the rate of corrosion

Once corrosion is established losses accumulate at a constant rate. The corrosion rate however differs from site to site as it is a function of the local environmental conditions. These factors and their impact will now be discussed in detail.

As the Sp1B field data was limited to 4 sites the impact of temperature, humidity and H₂S concentration on corrosion activity was difficult to fully determine. Consequently analysis of industry data, scientific literature, Sp1A laboratory data and theoretical considerations were also used to elicit possible impacts of these parameters.

6.5.1 Impact of H₂S concentration in the sewer headspace

6.5.1.1 Previous scientific studies

The results of the 1D modelling suggest that the rate at which acid is generated (H₂S is oxidised) by bacteria at the exposed pipe surface is the process determines the overall corrosion rate. As mentioned previously studies of the kinetics H₂S oxidation conducted in a pilot scale sewer in 2008 [20] showed that the rate of H₂S oxidation was proportional to $[H_2S]^{0.45-0.75}$. A study of the kinetics of biological sulphide oxidation in aqueous solutions [64] indicated that the oxidation

rate was proportional to $[H_2S]^{0.41}$. The results of these studies therefore suggest that if H_2S oxidation is the rate limiting reaction then the overall corrosion activity is likely to be proportional to approximately the square root of the H_2S concentration.

6.5.1.2 Industry data.

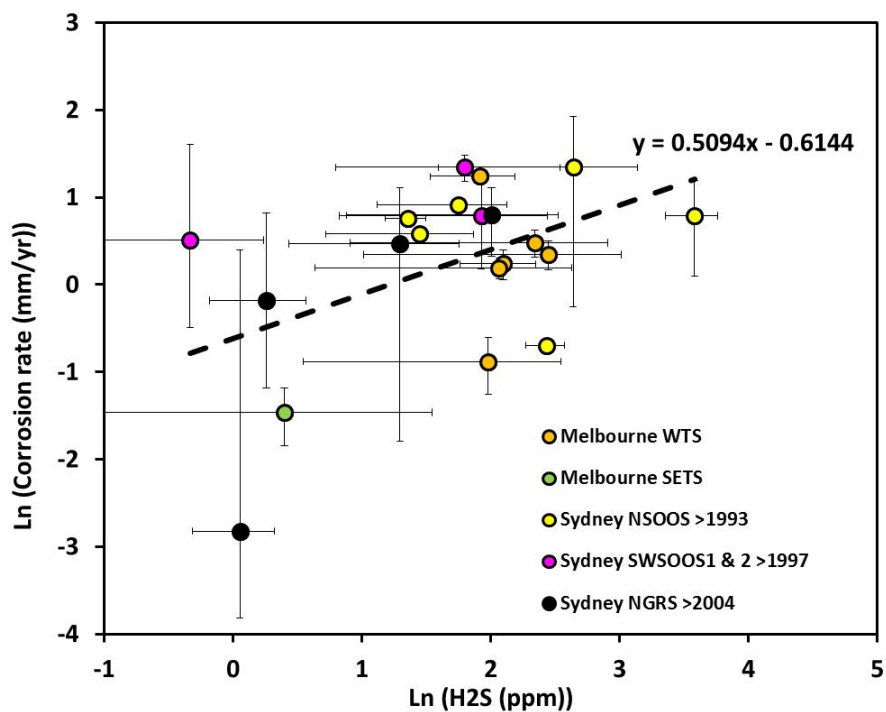


Figure 133. Plot of the natural log of the corrosion rate against the natural log of the observed H_2S level. The line of best fit indicates that the corrosion rate is proportional to $H_2S^{0.51}$.

Generally while there was a considerable pool of loss data available from the project's industry partners there was considerably less environmental data to complement the corrosion observations. One parameter however that is measured more than most is the concentration of H_2S in the sewer headspace (gas phase).

In correlating the observed rates of corrosion with H_2S levels however it should be remembered that other factors that influence the level of corrosion activity (humidity principal amongst them) are generally not available. Ideally to assess the impact of H_2S the humidity level should be constant and there is no guarantee that this was the case with the industry data gathered. Never the less as a first estimate it is assumed that the humidity conditions (as well as the sewer temperature) were relatively constant for the data pool available.

Figure 133 shows the natural log of the corrosion rate plotted against the natural log of the H_2S concentration for steady state corrosion data reported from traverse and erosion pin measurements conducted by Sydney and Melbourne Water. The H_2S data shown has been directly observed (no simulation data). If the power law relationship between rate of corrosion and the H_2S concentration is assumed, i.e. :

$$CR \propto ([H_2S]_{gas})^n \quad (24)$$

Where the value of n is determined by the slope of the line of best fit of the log-log plot.

While the data shows some scatter (possibly due to differing humidities and temperatures as discussed earlier) the line of best fit indicates that the rate of corrosion is proportional to the square root of the H₂S level, (slope of the log-log line of best fit was 0.51). In other words:

$$CR \propto ([H_2S]_{gas})^{0.5} \quad (25)$$

6.5.1.3 Sp1A laboratory data

The data generated from the Sp1A laboratory trials was to be used to determine the impact of temperature, humidity and H₂S concentration on corrosion losses (and subsequently corrosion rates) under controlled conditions. To be consistent with the field observations it was decided that only laboratory loss data obtained for coupons with a surface pH<6 would be examined in terms of corrosion loss characteristics. This ensured that the data was taken from coupons in the final stage of the corrosion cycle. Unfortunately the levels of corrosion observed in the SP1A trial were lower than observed in the field so that by the time of writing of this report only a limited number of new coupons could be considered for analysis (Figure 134). There were however a larger number of old coupons that fell into the pH<6 range (see Figure 135).

Unfortunately the level of scatter in the data precluded a direct determination of the relationship between H₂S and the rate of corrosion however the data were used to test the validity of Eqn. (25). The Sp1A data was analysed in the following manner:

- i. The surface pH data was examined to determine at which points in time the coupon surface pH fell below pH=6 at each of the conditions examined (see yellow shaded regions in Figure 134 and 135)
- ii. All data points where pH>6 were discarded.
- iii. Any data sets where less than 3 loss data points remained were discarded.
- iv. For each of the remaining data sets the loss data was plotted as a function of H₂S concentration (Figure 136 A). The rate of corrosion at set of each conditions was then determined from the slope of the line of best fit. The uncertainty in the corrosion rate was estimated from the 90% confidence interval of the slope of the line of best fit (Figure 136 B). The rate (and uncertainty) of the corrosion rate determined at a given temperature, relative humidity and coupon type was then plotted as a function of H₂S and Eqn. (25) superimposed to check on its validity (or otherwise), (Figure 136 C).

The results are plotted in Figures 137 and 138. The high level of scatter in the loss data is reflected in the large error bars in the calculated corrosion rates at each condition. Never the less the square root relationship proposed in Eqn. (25) is not refuted by the data and in some cases (see first two plots in Figure 137) provides a good fit to the data.

As a result of the analysis of the literature, industry data and SP1A data it appears likely that the rate of corrosion is proportional to the square root of the H₂S concentration in the sewer gas.

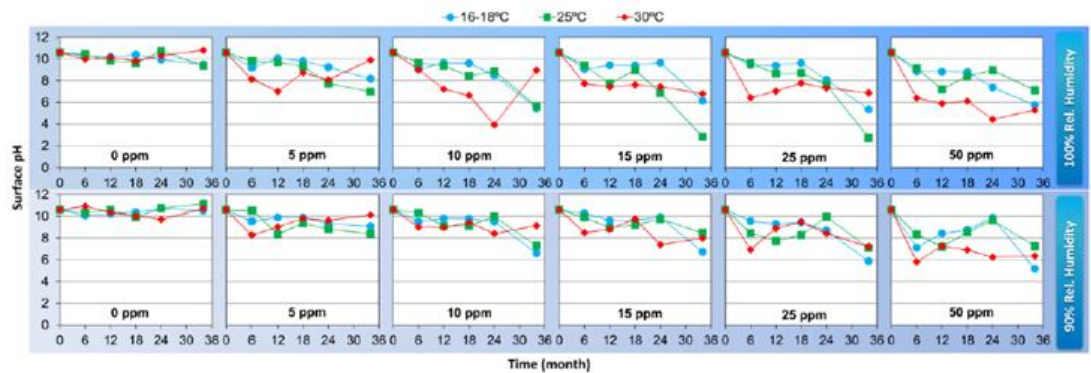


Figure 2-2. Surface pH of fresh concrete coupons exposed to the gas phase in H₂S chambers for 34 months.

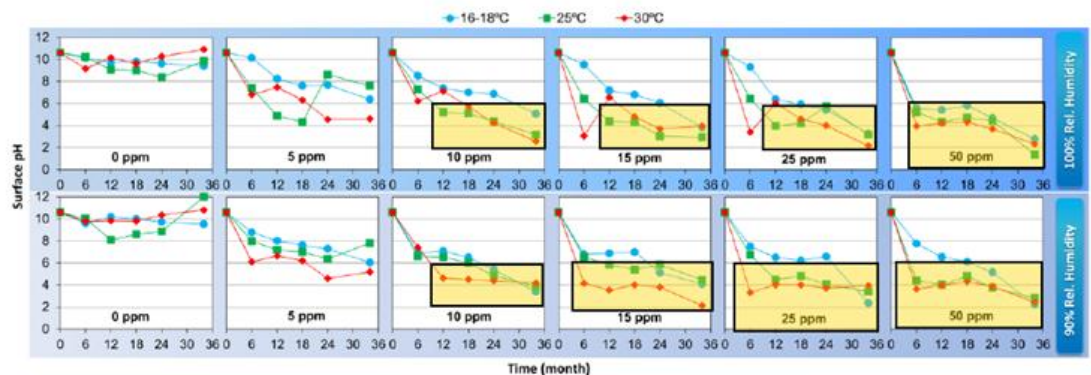


Figure 2-6. Surface pH of fresh concrete coupons partially submerged in sewage in H₂S chambers for 34 months.

Figure 134. Surface pH of SP1A new coupons (modified from figures in the SP1A 6 monthly report Feb 2013). Areas shaded yellow show coupons which have a surface pH<6.

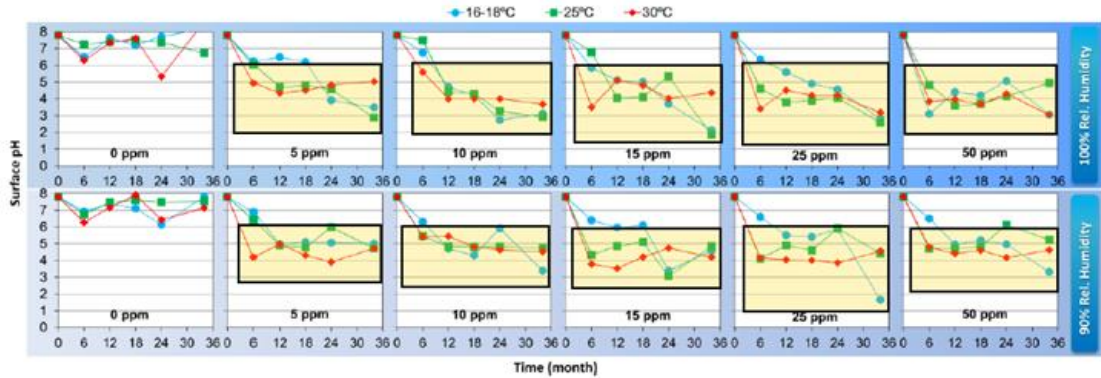


Figure 3-1. Surface pH of precorroded concrete coupons exposed to the gas phase in H₂S chambers for 25-26 months.

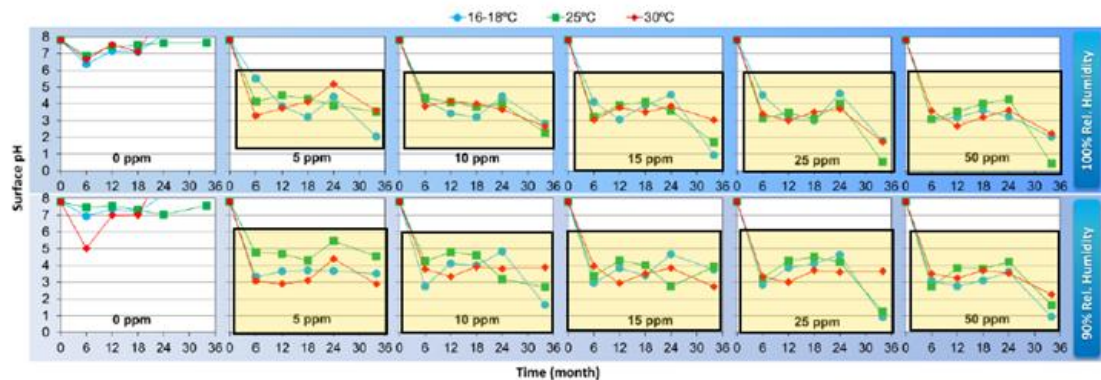


Figure 3-4. Surface pH of precorroded concrete coupons partially submerged in sewage in H₂S chambers for 25-26 months.

Figure 135. Surface pH of Sp1A old coupons (modified from Figures in the SP1A 6 monthly report Feb 2013). Areas shaded yellow show coupons which have a surface pH<6.

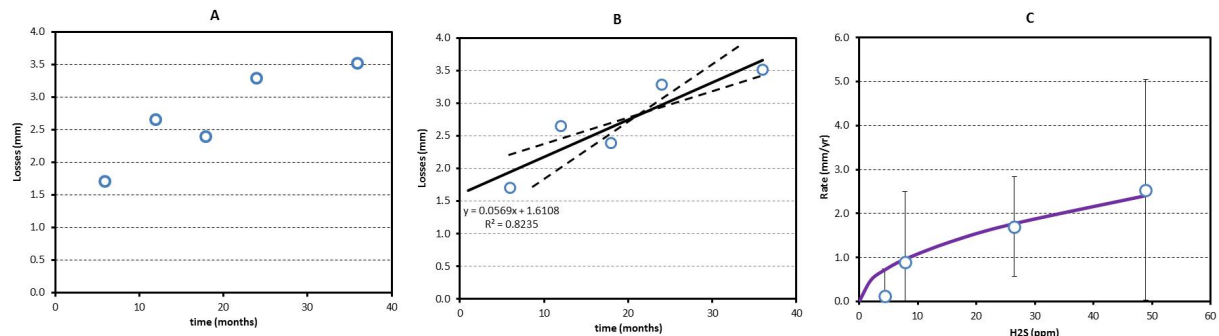


Figure 136. Process of analysing Sp1A laboratory data to verify Eqn. (25).

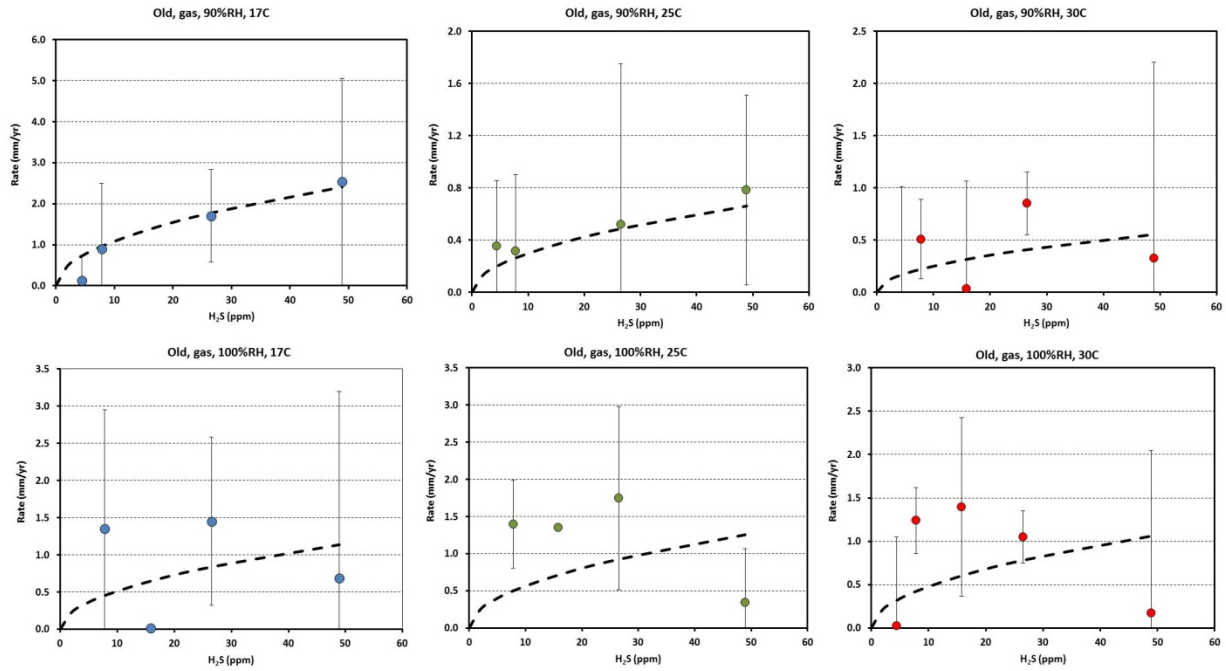


Figure 137. Comparison of Sp1A gas phase corrosion rate data and predictions of Eqn. (25).
The dashed curves are the lines of best using Eqn. (25).

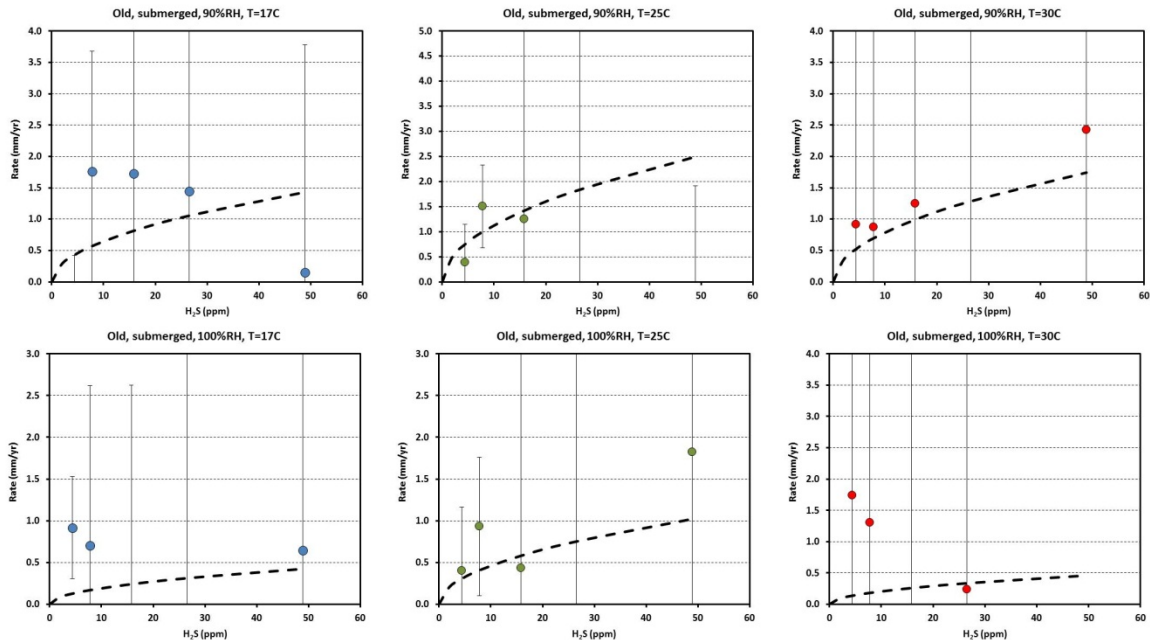


Figure 138. Comparison of Sp1A submerged corrosion rate data and predictions of Eqn. (25).
The dashed curves are the lines of best using Eqn. (25).

6.5.2 Impact of sewer gas temperature

6.5.2.1 Industry data

Average sewer gas temperatures do not vary widely between sewers particularly in Australia (for example see Table 13). Consequently an assessment of the impact of temperature on corrosion activity is difficult to carry out using the pool of industry data. Instead the relationship was estimated from previous scientific studies.

6.5.2.2 Previous scientific studies

Temperature can impact on the corrosion process through its effect on corrosion reaction rates (neutralisation, sulphur oxidation reactions), rates of diffusion (through the corrosion layer or into the concrete) as well as the impact of temperature on the populations, species mix and activity of microbial colonies. However as the 1D modelling indicated that H₂S oxidation was the rate controlling step in the corrosion process it was the impact of temperature on the oxidation reaction that was of most interest.

In general it is assumed that the relationship between temperature and the rates of biological and chemical processes takes the form of the Arrhenius relationship i.e.:

$$\text{Corrosion reaction rate} \propto e^{-E_a/RT_k} \quad (26)$$

Where E_a is the activation energy of the biological processes generating the acid ; R is the universal gas constant and T_k is the temperature (in Kelvin).

Studies of the impact of temperature on the acid generation behaviour of a number of bacteria including *T. thiooxidans* [62] suggests that the activation energy, E_a , for the oxidation of elemental sulphur lies between 26 to 50 kJ/mol. For the purposes of this study it was assumed that the overall activation energy is 30 kJ/mol that is:

$$CR \propto e^{(-30,000/(R \times (T+273)))} \quad (27)$$

Where T is the sewer gas temperature, (°C).

6.5.2.3 Sp1A data

Verification of Eqn. (27) was sought from the SP1A laboratory data. The pool of SP1A data was filtered as discussed above for the H₂S analysis. Analysis of the remaining SP1A data pool however was unproductive as the data presented a range of (conflicting) trends with temperature including many instances where corrosion rates appear to decline with increasing temperature which for this system is unlikely (Figure 139).

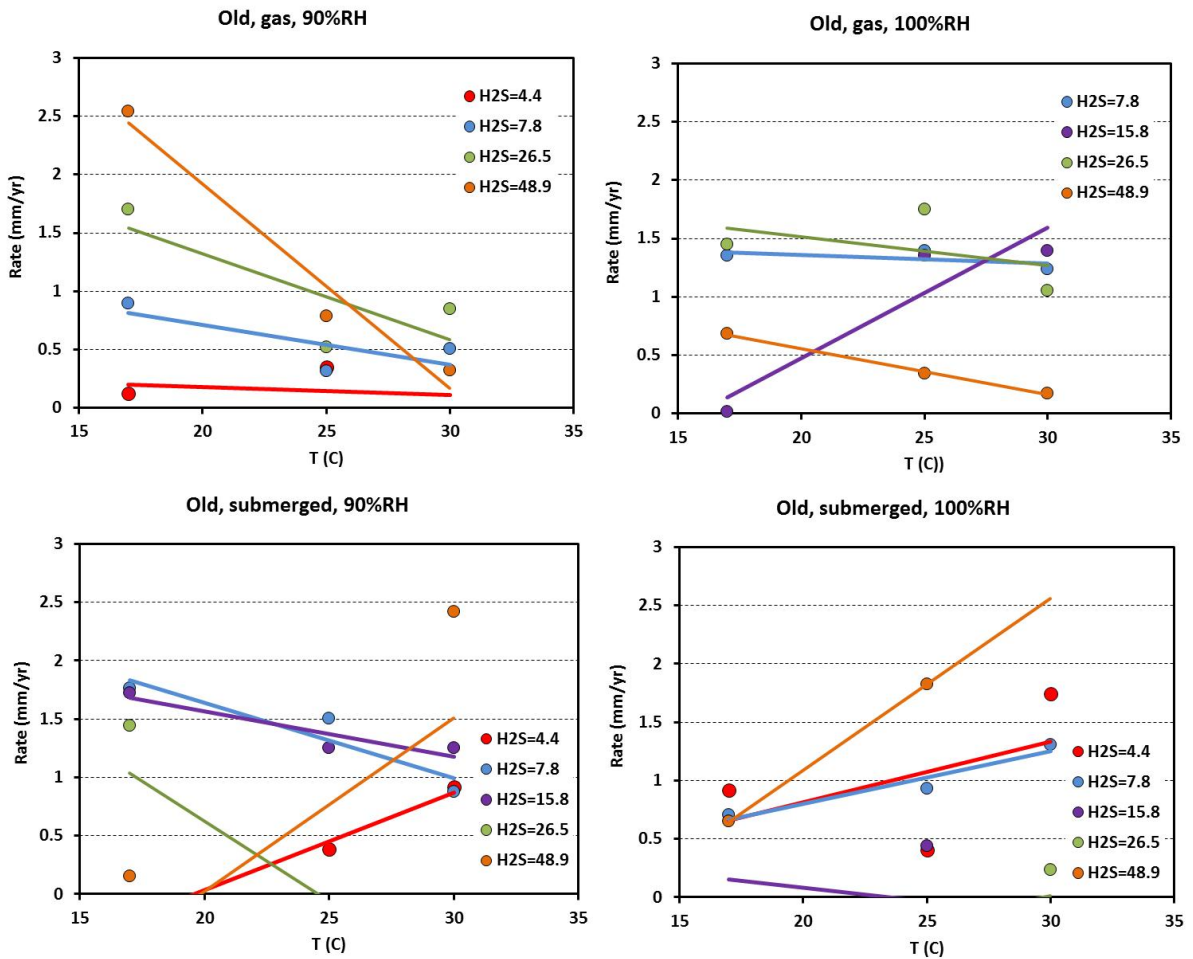


Figure 139. The impact of temperature change on Sp1A submerged old coupon corrosion rates. (Note: error bars have been removed for clarity).

The only data available therefore suggests that Eqn. (27) is a reasonable description of how sewer gas temperatures impact on the rate of corrosion and consequently the relationship was used in the modelling of the corrosion process.

6.5.3 Impact of humidity

The influence of humidity on the rate of sewer pipe corrosion is often over-looked; partly because it is difficult to measure in a sewer (the H_2S present corrodes the sensors very quickly). It is well recognised however that the bacteria that cause sewer pipe corrosion require a moist environment in which to grow and also that moisture facilitates the transfer of H_2S in the sewer atmosphere to the concrete pore structure.

A study conducted by Melbourne Water in 1986, [51], highlighted the link between the level of moisture in the sewer wall and the activity of acidophilic bacteria. In the 1986 study a section of sewer was subjected to forced ventilation resulting in the drying out of a

significant length of the sewer pipe wall (Figure 140). A microbiological survey of the wall was then conducted along with measurements of the wall moisture content. The results (see red and blue curves in Figure 140) show a clear correlation between moisture content and the population levels of *Thiobacillus* bacteria.

The importance of moisture was also highlighted by one of the more interesting field trial results. This involved the field site with the highest level of H₂S (Perth Bibra Lake). Despite having a H₂S level that was many times higher than that of any other site (an average 420ppm H₂S versus 125ppm for Perth MS for example) the resultant rate of corrosion observed was significantly lower. This surprising outcome was eventually explained by the low humidity at the Bibra Lake site (90% for Bibra Lake compared to >96% for Perth MS). Indeed average humidities in the first year or so of the trial were as low as 87% at Bibra Lake. This data along with the 1986 Melbourne Water study suggest that the corrosion process is quite sensitive to concrete moisture content which is driven in part by the sewer gas humidity.

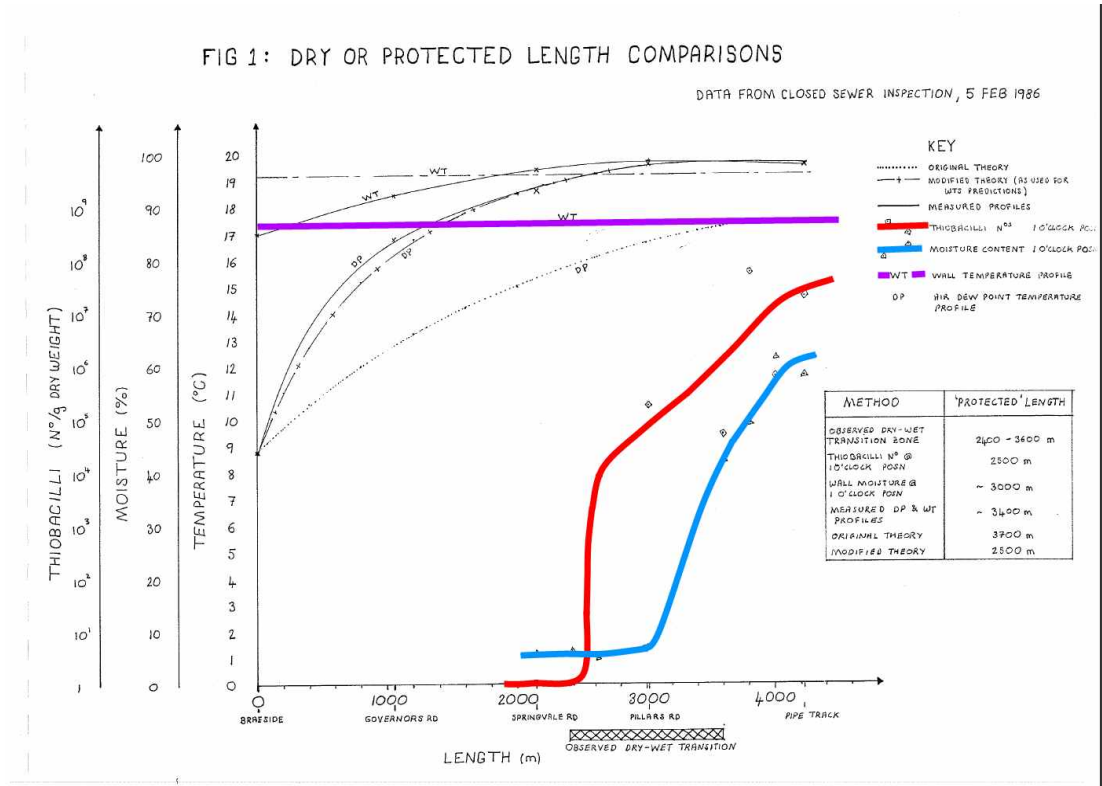


Figure 140. Results of a test of the effect of ventilation on acidophilic bacteria levels and sewer pipe wall moisture undertaken by Melbourne Water in 1986 [51].

6.5.3.1 Theoretical considerations

To model the impact of humidity it is first necessary to understand the link between humidity and the moisture content of the concrete. Concrete is a porous material containing a population of pores of differing diameters. As humidity rises within a sewer the concrete pores begin to fill with condensate. Importantly this happens below the condensation point.

(The condensation point coincides with the filling of all pores and the subsequent film that forms on the surface of the pipe). Figure 141 illustrates how the pore structure of the concrete is filled as relative humidity increases.

Small diameter pores are filled first and as humidity increases the larger pores are progressively filled until at 100% relative humidity all pores are filled. As humidity increases and pores fill with moisture the pore volume suitable for colonisation by microbial communities increases and hence corrosion activity would be expected to increase. The ionic nature of the corrosion reaction dictates that reactions take place in a liquid medium and as a result increased water filled pore volume also benefits the corrosion process.



Figure 141. Filling of the concrete pore structure as humidity increases.

The relationship between the moisture content and relative humidity is dictated by the distribution of pore size within the concrete (i.e. the pore size distribution or PSD). In this study the PSD was determined for new and old coupon concretes (see Section 4.4.2). The relationship between humidity and the fraction of available pore spaced filled with water can be estimated using the classic Kelvin equation:

$$\ln \frac{p}{p_0} = \frac{-2\gamma V_m}{rRT_k} \quad (28)$$

Where p is the water vapour pressure; p_0 is the water saturated vapour pressure; γ is the surface tension of water; V_m is the molar volume of water; r is the pore radius; R is the universal gas constant and T_k is the temperature in Kelvin.

This equation assumes that (1) the pores are cylindrical in shape and (2) there is no hysteresis effect incurred when humidities rise and fall. Both assumptions represent an idealisation of the real situation. Pores normally adopt a range of shapes (Figure 142) which in turn creates a hysteresis effect i.e. the relationship between humidity and concrete moisture content is different when the concrete is being wetted up to that when it is being dried out (see for example Figure 143). For example if pores have an "ink-bottle" shape moisture entering the pores enters relatively easily however when the pores are full of water and are drying out water molecules find it a lot more difficult to leave the pores hence moisture content is higher than expected when the concrete is moving through a drying phase.

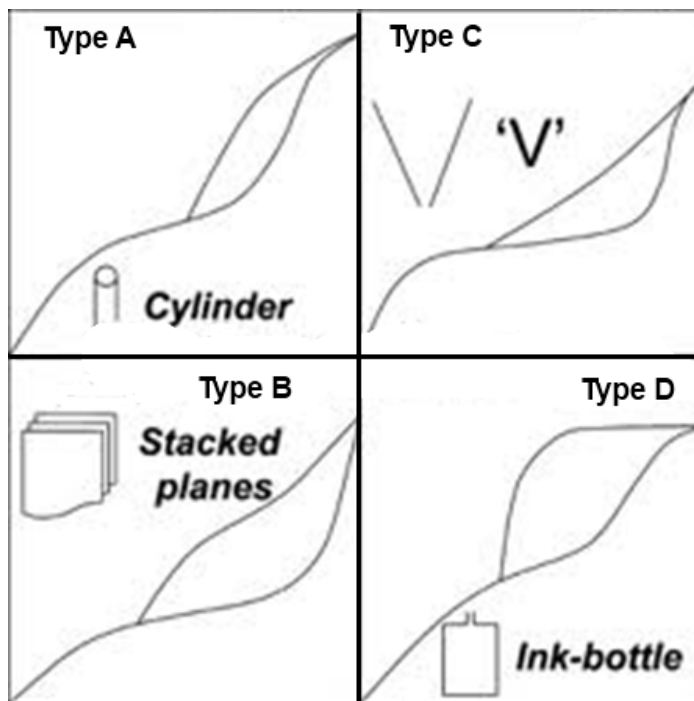


Figure 142. Pore shapes that can induce wetting/drying hysteresis.

In practice this means that as sewer humidity cycles between low and high humidities the average water content is higher than you would expect from Kelvin equation considerations alone and in some circumstances (if the deviation in humidity is small enough) there may not be any appreciable change in concrete water content and consequently we would expect the corrosion behaviour to be a lot less sensitive to changes in humidity. This effect however would be dependent on the pore structure of individual concrete pipes and also on the nature of the humidity cycle at any one location. For practical modelling purposes

therefore it is assumed that the Kelvin equation adequately describes the relationship between concrete moisture content and relative humidity. Given the importance of this factor in the corrosion process however a better understanding of this relationship (and the gathering of more data) should be a focus of future work.

Application of Eqn. (28) allows us to calculate the portion of the concrete pore network that is filled at a particular relative humidity (i.e. the moisture level as a function of humidity). Figure 144 for example illustrates how the new coupon concrete pore network is filled as humidity increases from 85 to 100% (the range of humidities observed in sewers in this study). The results show that at humidities of ~90% little of the pore network is filled and the concrete would appear quite "dry". As humidity increases the pores fill (smallest pores first) until as 100% humidity is approached the remaining pores fill rapidly. Concrete moisture content is therefore very sensitive to changes in humidity in the upper humidity level. Unfortunately this is the region in which humidity sensors are least sensitive making quantitative monitoring of this effect difficult. Figure 145 plots the volume fraction of pores filled with moisture as a function of humidity for new coupon concrete.

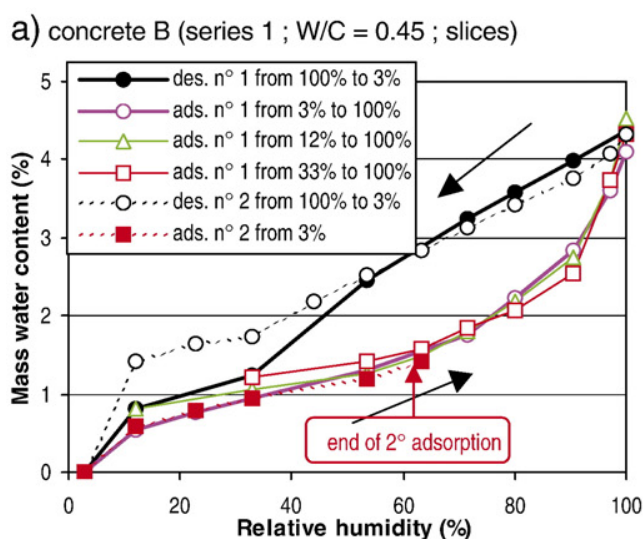


Figure 143. Water adsorption hysteresis for a typical concrete [65]

In this study the rate of corrosion is assumed to be directly proportional to the water filled pore volume and hence for a given pore size distribution is a rapidly increasing function of humidity (see data points in Figure 145). To describe the relationship between the water filled pore fraction, V_p^w , and humidity in a simpler manner for use in corrosion modelling a curve (the red curve in Figure 145) has been fitted to the Kelvin equation results for the new coupon pore size distribution. The following relationship was determined from the optimised curve fit:

$$CR \propto V_p^w = \frac{(1 - 0.01245 \times RH\%)}{(0.0955 \times RH\% - 9.8044)} \quad (29)$$

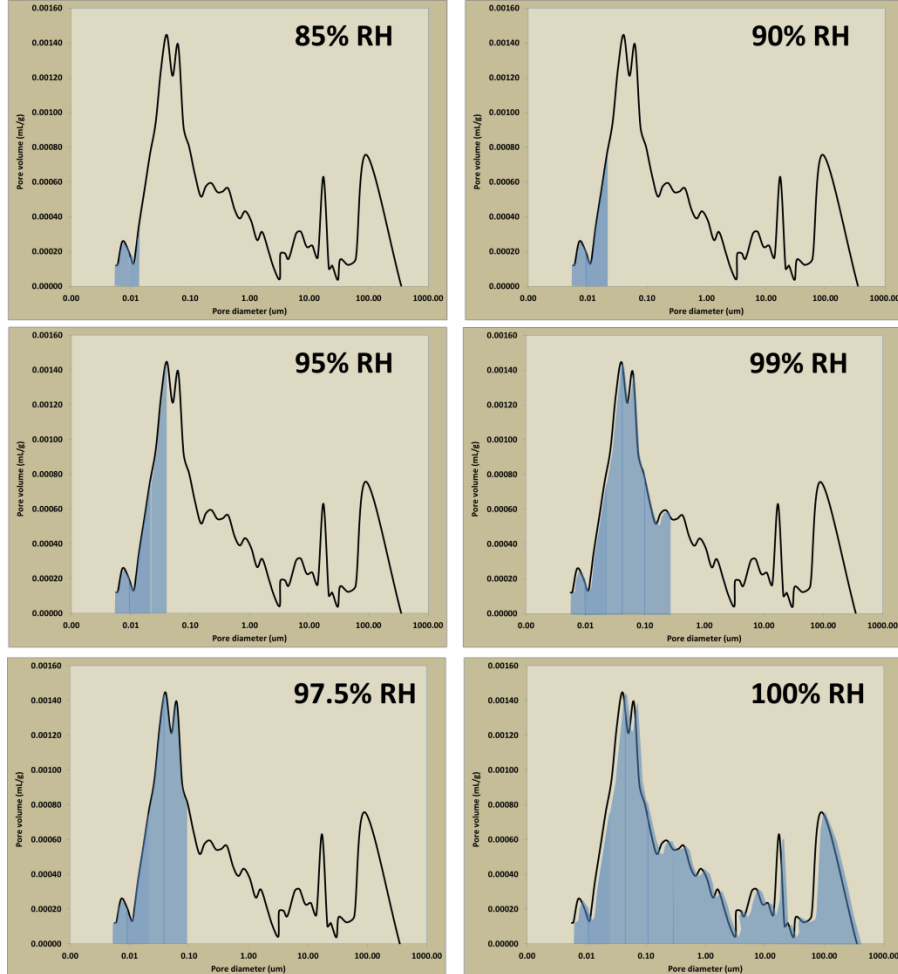


Figure 144. Progressive filling of the new coupon pore network as predicted by Eqn. (28).

6.5.3.2 Sp1A data

Sp1A laboratory work was undertaken at 90 and 100% humidities with the aim of discerning the impact of humidity on the rates of corrosion. While an effort was made to determine the ratio of corrosion rates observed at the two humidities from the previously described subset of the available Sp1A data the large amount of scatter in the data precluded any meaningful analysis of the data in regards to the impact of humidity.

As no data is available for verification (or refutation) of Eqn. (29) it will be assumed for the purposes of the current study that the relationship shown provides a reasonable description of how sewer gas humidities impact on the rate of corrosion and consequently the relationship will be used in the modelling of the process.

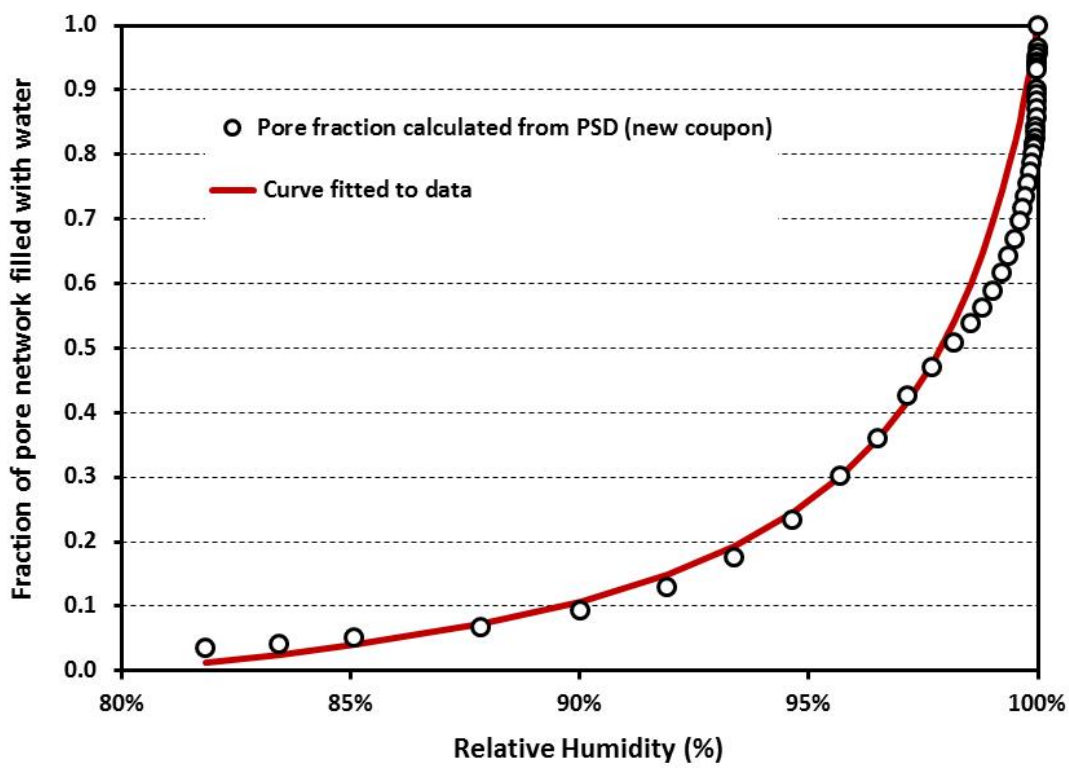


Figure 145. The volume fraction of water filled pores in new concrete coupon as a function of humidity. Fitted curve: $V= (1-0.01245\times RH\%)/(0.0959\times RH\%-9.805)$

6.5.4 Impact of sewer pipe wall temperature.

Anecdotally it has been suggested that whether the sewer pipe is exposed above ground or alternatively buried may have an impact on the rates of corrosion experienced within the pipe. This effect is most likely linked to the sewer wall pipe temperature and its subsequent effect on the moisture level in the concrete pipe pore network.

The sewer gas headspace is generally warm and humid (>85% humidity). Under such circumstances if the pipe wall is significantly cooler than the sewer gas atmosphere, moisture is more likely to condense within the concrete pore network. When formulating the impact of humidity on corrosion rate (as discussed above) it is inherently assumed that the pipe wall and sewer gas phases are at the same temperature. If the pipe is exposed externally to significantly different temperatures, (for instance an above ground pipe exposed to a sustained cold period during winter or a sustained hot period during summer), it is possible that the temperature of the internal surface of the exposed pipe may be slightly different to the gas phase temperature. This would change the relative humidity within the pore network which ultimately is what determines the level of moisture in the pore network, (Figure 146).

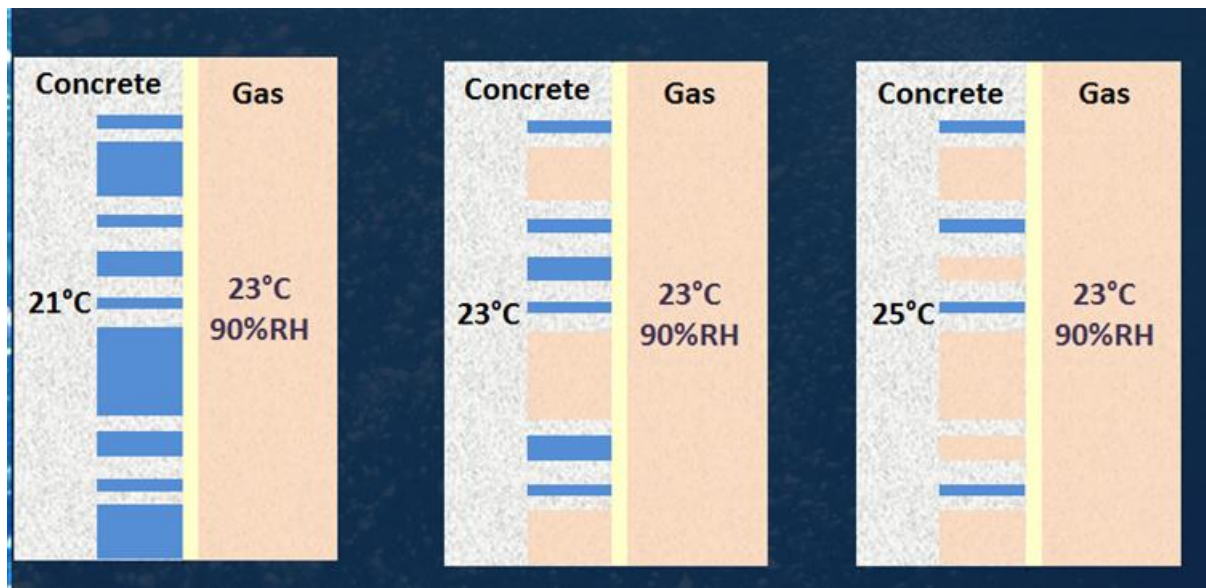


Figure 146. The impact of sewer pipe wall temperature on concrete moisture content.

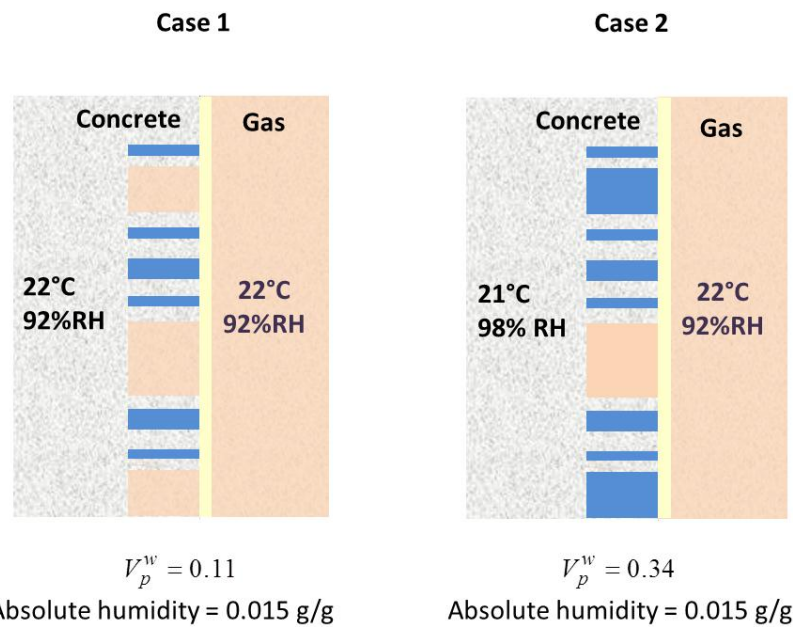


Figure 147. Calculation of the effect on moisture content of a 1°C temperature difference between the sewer wall and the sewer gas.

No pipe wall temperatures were measured during the course of the field study however it is strongly recommended that these measurements be undertaken in future studies. It is possible however using Eqn. (28) to estimate the impact of the wall temperature effect. This is accomplished by determining the fraction of the pore volume filled with water at a given humidity and temperature but varying wall temperatures (Figure 147). Initially the absolute humidity (g water vapour/g air) is calculated for a given set of conditions (e.g. 22°C, 92% humidity). It is then assumed that the absolute humidity remains the same

within the pore structure as the wall temperature changes (a simplification of the real situation as it implies perfect mixing of the bulk and pore space gas phases). The new relative humidity is then calculated within the pore structure and the new value for the fraction of pores that are water filled is then re-calculated from Eqn. (28).

If it is assumed that the rate of corrosion is proportional to the fraction of concrete pores filled with water calculations of the type outlined above can be used to build up an understanding of the effect of pipe wall temperature on the expected rate of corrosion for a range of temperatures, temperature differentials and humidities (for two examples see Figure 148).

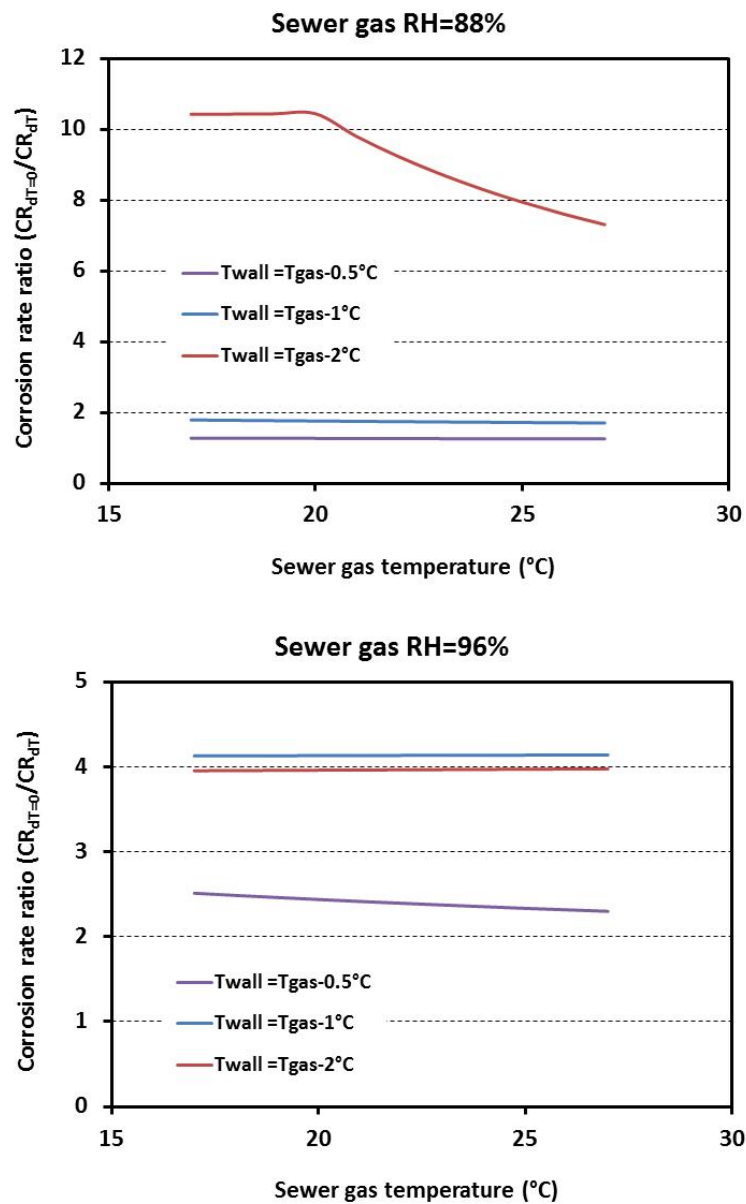


Figure 148. Plot of the effect of pipe wall temperature on expected corrosion rate as a function of sewer gas temperature. The data shows the expected change in corrosion rate if the sewer wall temperature deviates from the sewer gas phase temperature.

The modelling suggests that small differences in the temperature between the sewer pipe wall and the sewer gas phase can have a large impact on concrete moisture content and hence the expected rate of corrosion especially when conditions are driving the relative humidity in the pore structure close to 100%. The results however are complicated further by the fact that a change in temperature also alters the rates at which corrosion reactions take place. If we assume that the impact of temperature on corrosion activity is described by Eqn. (27) (with a value of $E_a = 30,000 \text{ J/mol}$) it is possible for the enhancement in corrosion brought about by increased pore moisture to be offset by the downturn in corrosion activity brought about by lower temperatures (for example note the similar rates of corrosion enhancement predicted for a pipe wall 1 and 2°C cooler than the gas temperature in Figure 148).

Again this is an area that requires further investigation.

6.5.5 Impact of position around the sewer circumference

Within the literature and the water industry there are conflicting views as to whether corrosion of sewers proceeds faster at the crown of the sewer or just above the waterline. To examine this issue coupons were placed in both locations at one of the Sydney field sites however as already mentioned the field trial at this site was terminated before this question could be adequately addressed.

It has been speculated that any differences in corrosion experienced at the crown and water line may be the result of moisture availability. The sewer wall immediately above the "tidal range" of the wastewater flow will tend to be, as a result of wave action and water level movement, fully saturated with moisture irrespective of the gas phase humidity. In sewer locations where the sewer gas humidity is low then we would expect, (following on from the previous discussion), that corrosion losses would be significantly greater near the waterline than experienced at the crown of the sewer. If however the humidity is high we would expect that the moisture content of the concrete at the crown of the sewer would be similar to that near the water line and consequently the rate of corrosion would be similar at the two locations. The difference in comparative behaviour between the two locations at high and low humidity sites may help explain why there is conflicting evidence on the effect of position on corrosion activity.

Again this is an issue worthy of further investigation.

6.6 Concrete sewer pipe service life estimation

6.6.1 Introduction

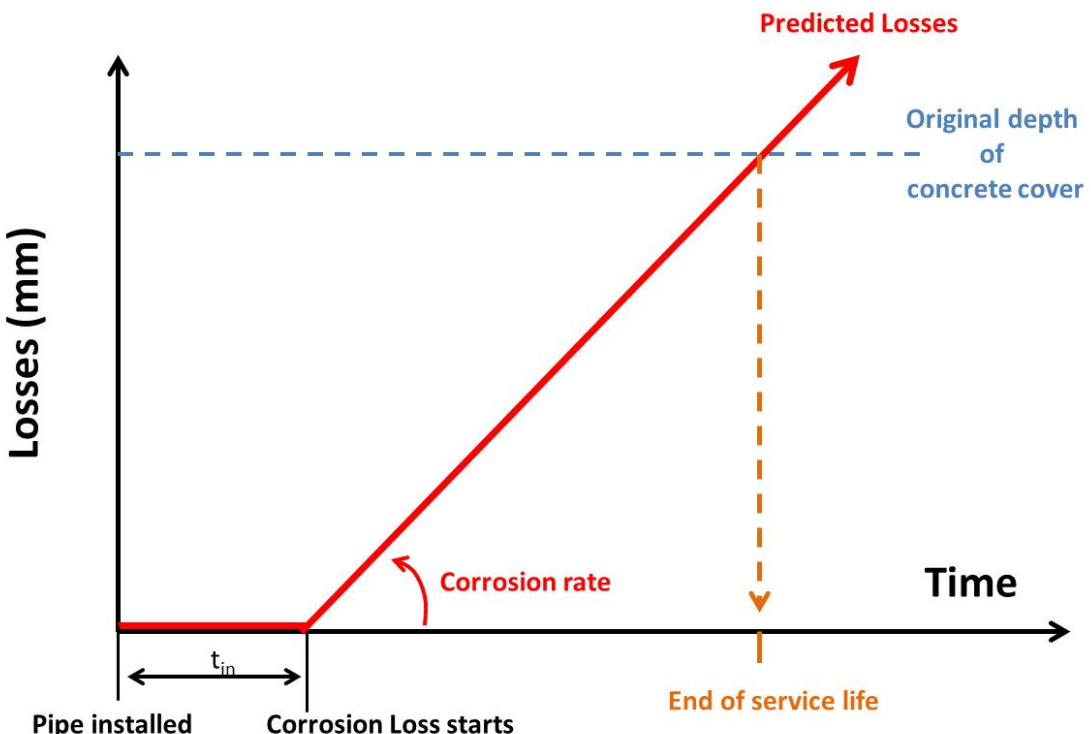


Figure 149. The method by which service life is determined.

To determine the service life of a concrete sewer pipe it is necessary to predict the instantaneous rate of corrosion over time and from this calculate the cumulative loss of concrete. When the cumulative loss of concrete exceeds the depth of concrete covering the pipe reinforcement, (the “concrete cover”), the service life of the pipe has come to an end. (It is assumed that once the metal reinforcement of the pipe is exposed structural failure of the sewer pipe is imminent).

The previous discussion of the corrosion timeline (Section 6.3.1) concluded that the corrosion loss function is bi-linear (see Figure 122). The concrete service life is determined by comparing the cumulative corrosion loss predicted by the bi-linear function with the depth of concrete cover (Figure 149).

As the rate of corrosion is constant with respect to time ($t > t_{in}$) the cumulative loss of concrete can be calculated using the following expressions:

$$\begin{aligned}
 \text{Cumulative losses (mm)} &= 0 & t < t_{in}; \\
 \text{Cumulative losses (mm)} &= \int_{t=t_{in}}^t CR_{t>t_{in}} dt = CR \times (t - t_{in}) & t > t_{in}
 \end{aligned} \tag{30}$$

The service life is then determined from the following expression:

$$\text{Service Life (years)} = \frac{CD_{t=0}}{CR} + t_{in} \tag{31}$$

Where CR is the calculated corrosion rate ($t > t_{in}$) (mm/yr), $CD_{t=0}$ is the depth of concrete overlaying the metal reinforcement at the time of the pipe installation (mm) and t_{in} is the length of the incubation time (years).

The following discussion details how the two factors t_{in} and CR can be determined from a knowledge of the local sewer gas phase environmental parameters: temperature, humidity and H_2S concentration.

6.6.2 Time to initiation of corrosion losses (t_{in})

The Sp1B field data suggests that corrosion losses commence once the surface pH falls below pH=6. The time taken for the surface of the new coupons to reach pH=6, (the incubation time or ' t_{in} '), varied from site to site but fell into the range of 10 to 23 months (see Table 20). Compared to the likely lifespan of the sewer pipe this does not constitute a significant length of time and consequently can usually be ignored when calculating the service lifespan of a sewer pipe. The impact of the initiation or incubation period, t_{in} , would however be more significant if corrosion predictions for a limited period of a pipe's service life are required (for the next decade for example). In these circumstances it would be of benefit to be able to estimate the value of t_{in} for a given site from the available environmental data.

Table 20. Corrosion initiation times for each Sp1B field site.

Site	Time to reach pH=6 (months)	rate of change pH units/month	Average environmental conditions for that period		
			H_2S (ppm)	Temperature (C)	Humidity (%)
Perth MS	10	-0.13	95.60	26.83	99.39
Perth Bibra	12.7	-0.10	546.20	27.96	89.30
Melb. WTS	14	-0.09	6.67	20.33	100.00
Melb. SETS	23	-0.06	1.55	19.61	100.00

6.6.2.1 Impact of H₂S concentration in the sewer gas on t_{in}

Above pH=6 it is assumed that there is little biological activity on the sewer pipe surface hence corrosion results from the action of inorganic acids formed when CO₂ and H₂S dissolves into the pore water and when the latter is oxidised abiotically.

As we have little information available on the levels of CO₂ in the sewer we will limit our considerations to the influence of H₂S. Once dissolved in the pore water the HS⁻ ion formed can undergo a series of chemical (i.e. abiotic) oxidation reactions to form a variety of oxidized acidic sulphur species [66]:



A study of the chemical oxidation kinetics of the above reactions in wastewater at pH=8 and T=20°C [66] reported the following relationship between the H₂S oxidation rate and the H₂S and dissolved oxygen concentrations:

$$r_{H_2S}^{oxidation} = -\frac{d(S(-II)_T)}{dt} = k[S(-II)_T]^{0.8 \pm 0.1} [DO]^{0.2 \pm 0.1} \quad (36)$$

Where S(-II)_T is the total sulphide content (i.e. H₂S+HS⁻+S²⁻, g of S/m³) in the aqueous phase and k is the reaction rate constant. In the absence of any other data and assuming that the H₂S content in the liquid phase is proportional to the H₂S concentration in the gas phase (i.e. governed by Henry's law) we will assume that:

$$\text{rate of abiotic oxidation} \propto [H_2S]_{gas}^{0.8} \quad (37)$$

We would expect that the time to reach pH=6, t_{in}, is inversely proportional to the abiotic rate of corrosion therefore:

$$t_{in} \propto [H_2S]^{-0.8} \quad (38)$$

6.6.2.2 Impact of temperature on t_{in}

As was the case when we considered the effect of temperature on the biological oxidation of H₂S it is again assumed that the impact on temperature on abiotic oxidation of H₂S follows an Arrhenius relationship i.e.:

$$\text{rate of abiotic oxidation} \propto e^{-E_a/(RT_k)} \quad (39)$$

Where E_a is the activation energy for the abiotic oxidation reaction; R is the universal gas constant and T_k is the sewer gas temperature in Kelvin.

A study of the abiotic oxidation of H₂S in water (pH=8) conducted by Millero [67] found that the activation energy was 56 +/- 4 kJ/mol (slightly higher at 66 +/- 5 kJ/mol in seawater). Thus:

$$\text{rate of abiotic oxidation} \propto e^{-56,000/(RT_k)} \quad (40)$$

$$t_{in} \propto \frac{1}{e^{(-56,000/(8.314 \times (T+273.15)))}} = e^{(56,000/(8.314 \times (T+273.15)))} \quad (41)$$

6.6.2.3 Impact of humidity on t_{in} .

It is assumed that increasing pore moisture availability increases the rate of abiotic oxidation as the oxidation reactions take place in an aquatic environment. The relationships developed in Section 6.5.3 relating humidity to concrete moisture content therefore will be utilised again. Thus:

$$\text{rate of abiotic oxidation} \propto \frac{(1 - 0.01245 \times RH\%)}{(0.0955 \times RH\% - 9.8044)} \quad (42)$$

Therefore:

$$t_{in} \propto \frac{(0.0955 \times RH\% - 9.8044)}{(1 - 0.01245 \times RH\%)} \quad (43)$$

6.6.2.4 Correlation of predictions with observed values.

The following general expression for predicting t_{in} is formed when the above equations are combined:

$$t_{in}(\text{years}) = A \times [H_2S]^{-0.8} \times \frac{(0.0955 \times RH\% - 9.8044)}{(1 - 0.01245 \times RH\%)} \times e^{\frac{56000}{(8.314 \times (T+273))}} + B \quad (44)$$

Where A and B are constants optimised to provide the best fit to the values of t_{in} observed in the field study (Table 20) for the temperature, humidity and H₂S conditions averaged over the period from installation to the point in time at which the surface pH has fallen to 6 at each location. The observed values for t_{in} , are plotted against the values predicted by Eqn. (44) in Figure 150. The optimised values for the fitting constants A and B were found to be $A=1.24 \times 10^{-10}$ and $B=0.91$. When these values are employed Eqn. (44) predicted the observed initiation period values well for each site (+/- 0.1 years).

Thus final expression for predicting t_{in} therefore becomes:

$$t_{in}(\text{years}) = 1.24e - 10 \times [H_2S]^{-0.8} \times \frac{(0.0955 \times RH\% - 9.8044)}{(1 - 0.01245 \times RH\%)} \times e^{(56,000/(8.314 \times (T+273)))} + 0.91 \quad (45)$$

In the absence of temperature or humidity data t_{in} can be approximated by the following expression:

$$t_{in} (\text{years}) = 1.62 - 0.083 \times \ln[H_2S] \quad (46)$$

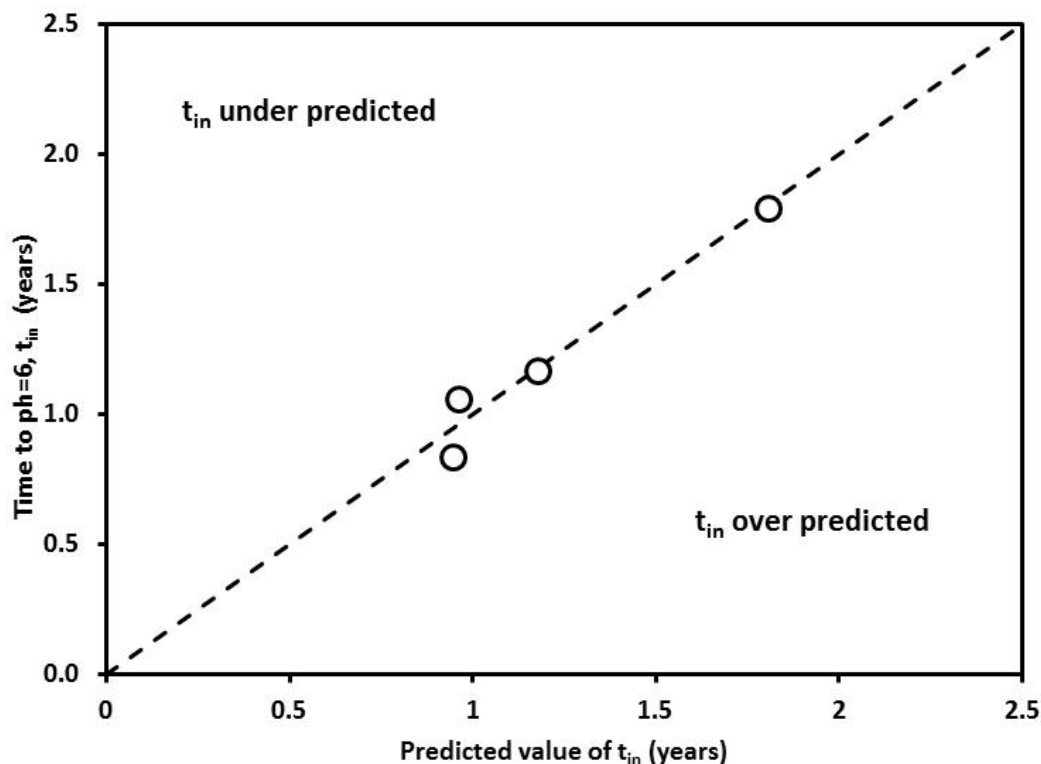


Figure 150. Predicted values of t_{in} predicted by Eqn. (44) using the average temperature, humidity and H_2S concentration for the period $\text{pH}>6$ at each site.

6.6.3 Calculation of the corrosion rate (CR).

The relationships between the rate of corrosion and sewer gas temperature, humidity and H_2S concentration discussed in Section 6.5 (Eqn. (25), (27) and (29)) can be combined to form the following expression for predicting the rate of corrosion once the surface pH drops below 6:

$$CR = A \times [H_2S]^{0.5} \times \frac{(1 - 0.01245 \times RH\%)}{(0.0955 \times RH\% - 9.8044)} \times e^{(-30,000/(8.314 \times (T+273.15)))} \quad (47)$$

Where CR is the rate of corrosion (mm/yr) experienced by the sewer pipe once the pipe surface pH drops below pH=6 (mm/yr), A is a scaling constant (to be determined by fitting predictions with observed values of the corrosion rate), $[H_2S]$ is the time averaged gas phase concentration of H₂S (ppm), RH% is the time averaged relative humidity of the sewer gas phase (%) and T is the time averaged sewer gas temperature (°C).

6.6.3.1 Calibration of the corrosion rate equation using the Sp1B field data

The scaling constant, A , in Eqn. (47), was determined by fitting the equation to the rates of corrosion calculated from the loss of concrete observed for the new and old field coupons in the field trials (see Figure 151). The optimised value of A in Eqn. (47) was determined to be 458,000. The vertical error bars shown on the field data points in Figure 151 represent the 90% confidence interval for the observed corrosion rates, (i.e. the 90% confidence intervals of the slopes of the line of best fit for the loss versus time data). The horizontal error bars represent the range of CR predictions when the 90% confidence intervals for the environmental parameters are taken into account. Data falling on the diagonal black line represents a perfect match between observed and predicted values of the corrosion rate. Eqn. (47) provides a reasonable fit to the data with all 8 predictions lying within +/-1.5mm/yr of the observed corrosion rates (see green dashed lines in Figure 151).

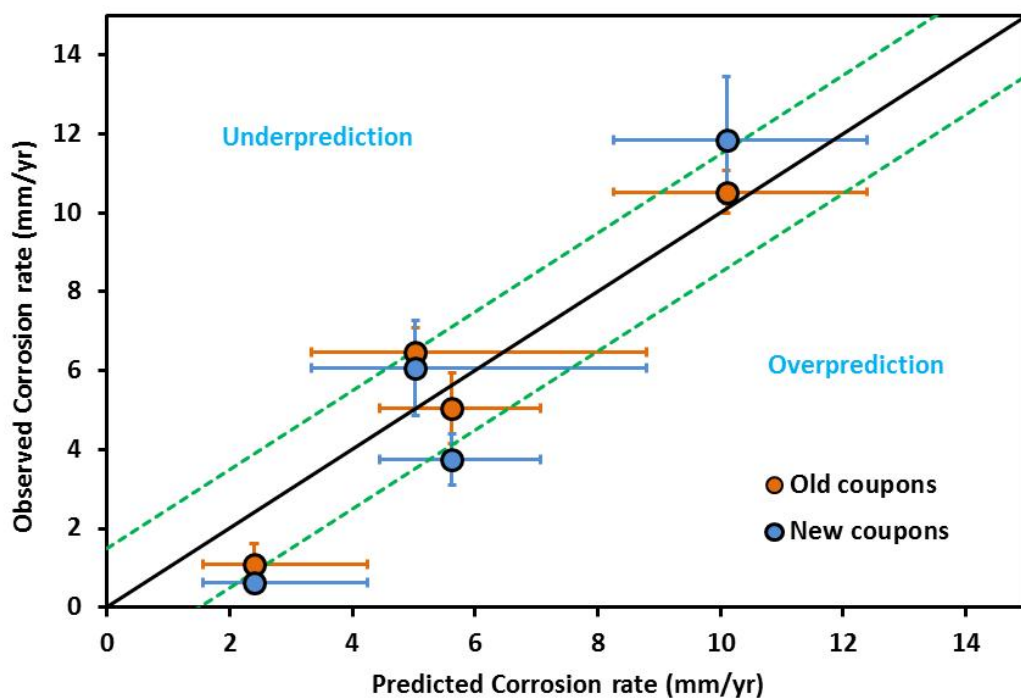


Figure 151. A comparison of observed corrosion rates for new and old coupons (surface pH<6) with rates predicted by Eqn. (47) ($A=458,000$).

The best fit model of the corrosion rate as a function of H₂S gas phase concentration, sewer gas temperature and humidity is therefore:

$$CR = 458,000 \times [H_2S]^{0.5} \times \frac{(1 - 0.01245 \times RH\%)}{(0.0955 \times RH\% - 9.8044)} \times e^{(-30,000/(8.314 \times (T+273)))} \quad (48)$$

It should be noted however that this model is calibrated with very little data (only 4 sets of environmental conditions). Thus it would be expected that as more data becomes available modifications to the above expression are possible.

6.6.3.2 Application of the corrosion rate function to the available literature and Industry historical data

In order to predict the rate of corrosion at a given sewer location Eqn. (48) requires a knowledge of the H₂S concentration in the gas phase, the sewer gas temperature and the humidity. While the concentration of H₂S is regularly measured in sewers, temperature is less often known and the humidity is rarely measured. In order to test the veracity of Eqn. (48) it is therefore necessary to make some assumptions as to the application of the model.

As a starting point a generalised corrosion chart was created which shows the range of corrosion rates predicted by Eqn. (48) plotted against the log of the H₂S concentration (Figure 152). The range of corrosion activity is mapped for an “average” sewer temperature of T=22°C between “dry” sewer conditions (estimated at 85% humidity from the environmental data gathered in the field studies) and a sewer with 100% relative humidity. The average temperature of T=22°C was chosen as it represented the median of sewer temperatures recorded during the Sp1B field trials. If Eqn. (48) is valid the great majority of corrosion rate data sourced from industry and the scientific literature should fall within the predicted envelope when plotted as a function of H₂S concentration.

Figure 153 shows the corrosion rate data obtained from the field studies and the scientific literature plotted as a function of H₂S concentration. The fact that the data falls neatly within the predicted envelope increases our confidence in Eqn. (48). Figure 154 shows the same plot however in this case the historical data supplied by the various industry bodies has also been included (this includes data where H₂S levels have been estimated by the Sewex sewer model). Again the great majority of the data falls within the predicted corrosion envelope adding further credence to the proposed relationship between corrosion rate and the three environmental parameters.

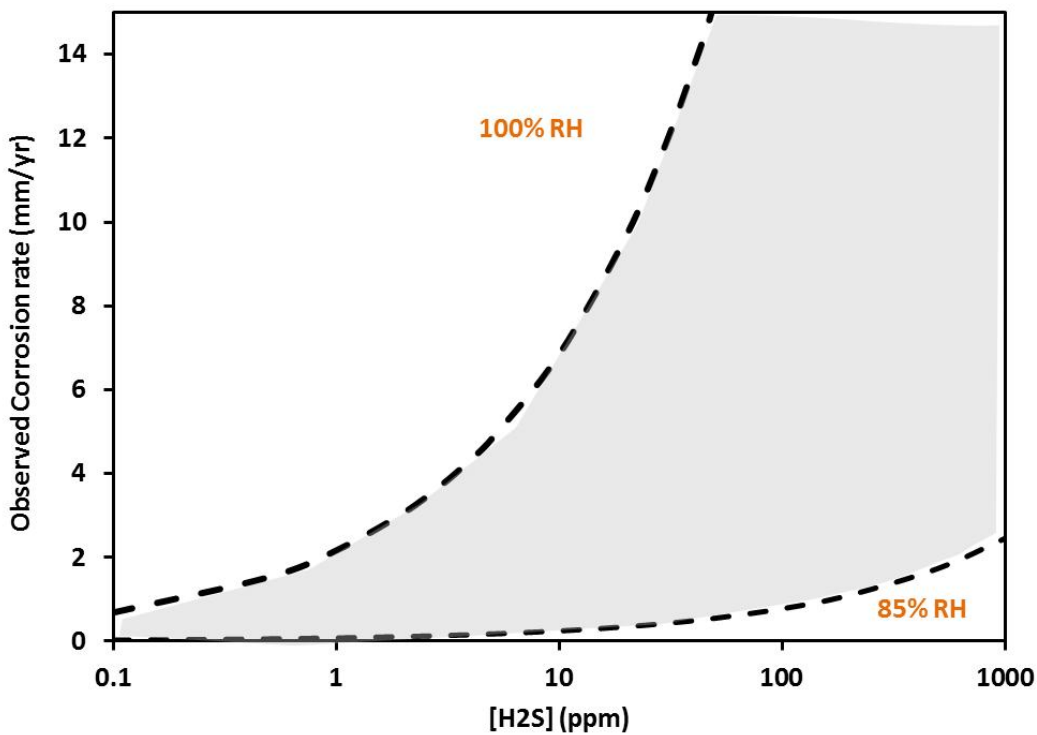


Figure 152. Corrosion envelope predicted by Eqn. (48) as a function of H_2S concentration (log scale) for the range of humidities observed in the Sp1B field study program. The sewer gas temperature is assumed to be at 22°C.

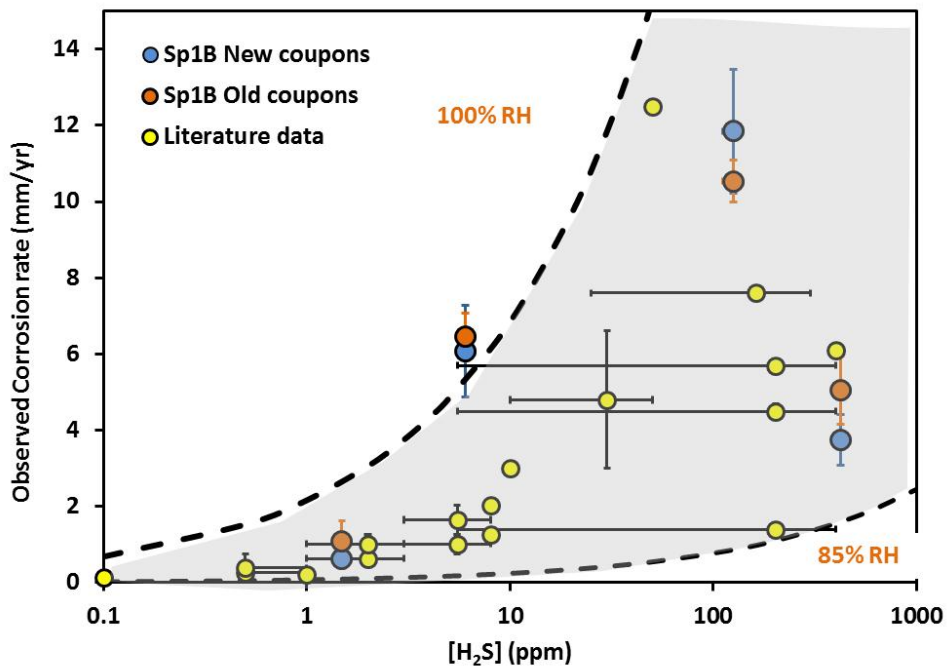


Figure 153. Sp1B field data corrosion rates and data reported in the scientific literature relative to the predicted corrosion envelope.

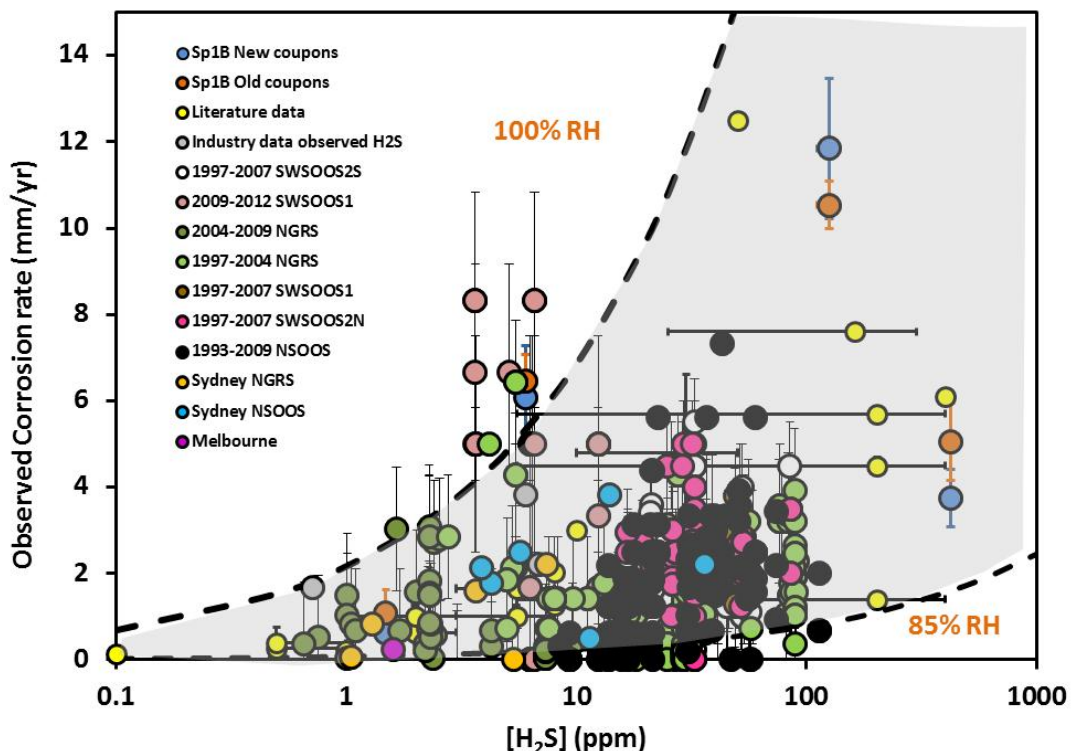


Figure 154. Location of all available corrosion rate data including Industry historical data relative to the predicted corrosion envelope.

The data presented in Figures 153 and 154 shows that Eqn. (48) satisfactorily predicts the range of corrosion behaviour likely to be observed at a given sewer location. In order to pinpoint the rate of corrosion however Eqn. (48) requires H₂S, temperature and humidity to be known and as already mentioned this is rarely the case. Inspection of Figure 154 however suggests that much of the data lies on or near the 95% relative humidity curve (purple curve in Figure 155). Consequently when humidity and temperature data are not available it is possible to provide a **first estimate** of the rate of corrosion by assuming that T=22°C and RH=95%. Substituting these values into Eqn. (48) reduces it to the following:

$$CR = 0.56 \times [H_2S]^{0.5} \quad (49)$$

Where again CR is the rate of corrosion (mm/yr) and [H₂S] is the time averaged concentration of H₂S in the sewer gas (ppm).

It should be stressed however that Eqn. (49) should only be used as a first estimate of corrosion and that the predicted corrosion rate may significantly underestimate the actual corrosion rate especially if the true sewer humidity is approaching 100%.

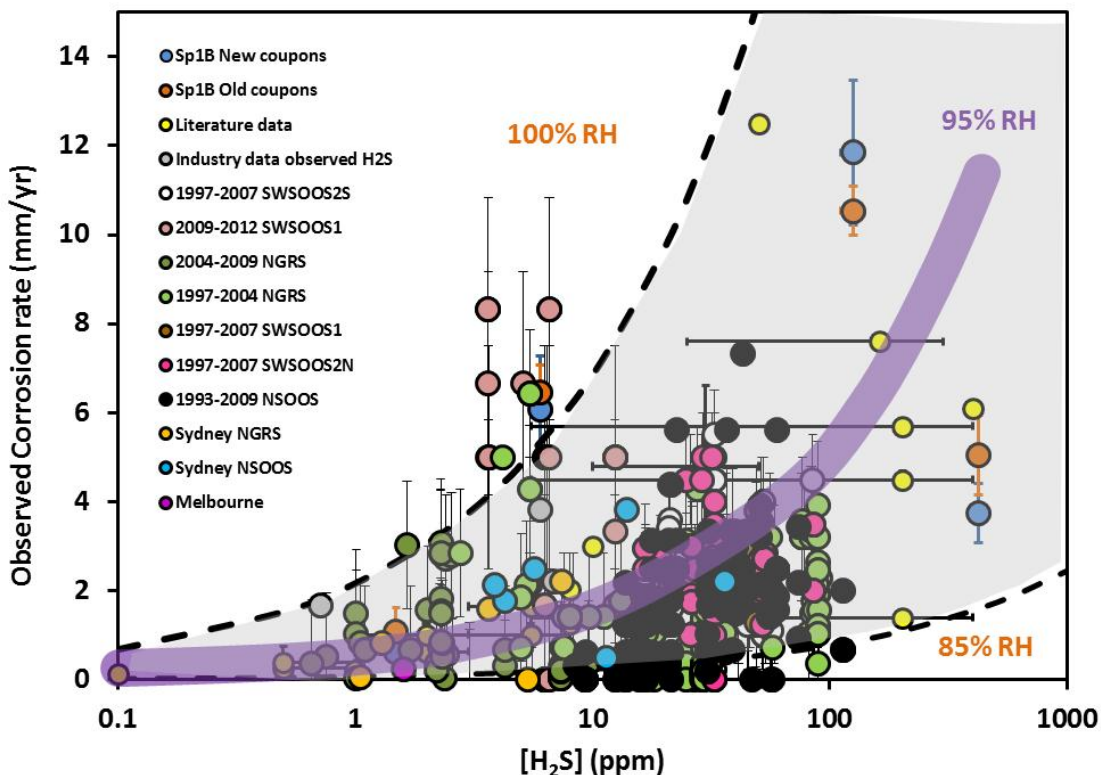


Figure 155. Superimposition of predicted corrosion rate (95% relative humidity) curve over the corrosion rate data.

6.6.4 An example calculation of the service life of a concrete sewer pipe

To summarise the above discussion, the service life of a concrete sewer pipe is determined via:

$$\text{Service Life (years)} = \frac{CD_{t=0}}{CR} + t_{in} \quad (50)$$

If temperature, humidity and H₂S concentration are known (or can be estimated) t_{in} can be estimated via:

$$t_{in} (\text{years}) = 1.24e - 10 \times [H_2S]^{-0.8} \times \frac{(0.0955 \times RH\% - 9.8044)}{(1 - 0.01245 \times RH\%)} \times e^{(56,000/(8.314 \times (T+273)))} + 0.91 \quad (51)$$

If only H₂S concentration in the gas phase is known t_{in} can be estimated via:

$$t_{in} (\text{years}) = 1.62 - 0.083 \times \ln[H_2S] \quad (52)$$

If temperature, humidity and H₂S concentration are known (or can be estimated) CR can be estimated via:

$$CR = 458,000 \times [H_2S]^{0.5} \times \frac{(1 - 0.01245 \times RH\%)}{(0.0955 \times RH\% - 9.8044)} \times e^{(-30,000 / (8.314 \times (T + 273)))} \quad (53)$$

if temperature, humidity and H₂S concentration are known (or can be estimated) or via the following if only H₂S concentration is known (or can be estimated):

$$CR = 0.56 \times [H_2S]^{0.5} \quad (54)$$

The level of uncertainty in the value of *CR* calculated is estimated to be 1.5mm/yr.

The procedure for calculating the service life of a concrete sewer pipe service is:

1. Estimate the average sewer gas temperature, humidity and H₂S concentration if possible.
2. Calculate *t_{in}* and *CR* using Eqn. (51) and (53) if all three environmental variables are known or Eqn. (52) and (54) if only H₂S levels are known
3. For a given level of concrete cover depth it is then possible to calculate the service life using Eqn. (50).

Example 1.

Concrete cover over reinforcement, *CD*, = 75 mm depth

Estimated average sewer gas temperature = 20°C

Estimated average sewer humidity = 100%

Estimated sewer gas H₂S concentration = 3 ppm

Apply the above equations:

t_{in} = 1.4 years (Eqn. (51))

CR = 3.4 mm/yr (Eqn. (53))

Therefore service life = 75/3.45 + 1.4 = 23.2 years

Example 2.

Concrete cover over reinforcement, *CD*, = 50 mm depth

Estimated average sewer gas temperature = unknown

Estimated average sewer humidity = unknown

Estimated sewer gas H₂S concentration = 5 ppm

Apply the above equations:

t_{in} = 1.5 years (Eqn. (52))

CR = 1.25 mm/yr (Eqn. (54))

Therefore service life = 50/1.25 + 1.5 = 41.5 years

An excel spread sheet has been prepared to carry out the calculation of losses and service life using Eqns. (51) and (53) for specified H₂S concentration, temperature, humidity, date of pipe installation and depth of concrete cover. If humidity and temperature are not known, Eqns. (52) and (54) are used instead to estimate the incubation period and the corrosion rate. The program returns the estimated time to first corrosion and an estimate of the service life of the pipe (Figure 156). A range of estimated end of service life dates is also provided that reflects the uncertainty in the calculation of CR. The spread sheet also generates plots of the predicted cumulative losses and concrete cover depth as a function of time (Figure 157).

	A	B	C	D	E	F	G	H	I	J	K	L
1												
2												
3												
4												
5												
6												
7												
8												
9												
10												
11												
12												
13												
14												
15												
16												
17												
18												
19												
20												
21												
22												
23												
24												
25												
26												
27												
28												
29												
30												
31												
32												
33												
34												
35												
36												
37												
38												
39												
40												
41												
42												

UON/SCORe

Service Life prediction

PIPE DETAILS

DATE OF PIPE INSTALLATION 2014 (year)

DEPTH OF CONCRETE COVER OVER REINFORCING 75 (mm)

ENVIRONMENTAL CONDITIONS

Average H₂S concentration in sewer gas 3 (ppm)

Average sewer gas temperature 20 (*C) leave blank if unknown (assumed to be 22°C)

Average sewer humidity 100 (%) leave blank if unknown (assumed to be 95%)

CALCULATIONS AND RESULTS

Estimated time to start of corrosion, t_a: 1.4 years

Rate of corrosion (CR) after 1.4 years (mm/yr): 3.45 mm/yr (range 1.9 to 4.9 mm/yr)

Total service life: 23.2 years (range 16.6 to 40 years)

Expected end date of pipe service life: 2037 (range 2031 to 2054)

Replot Data

Figure 156. Screen view of excel spread sheet used to predict concrete sewer pipe service life.

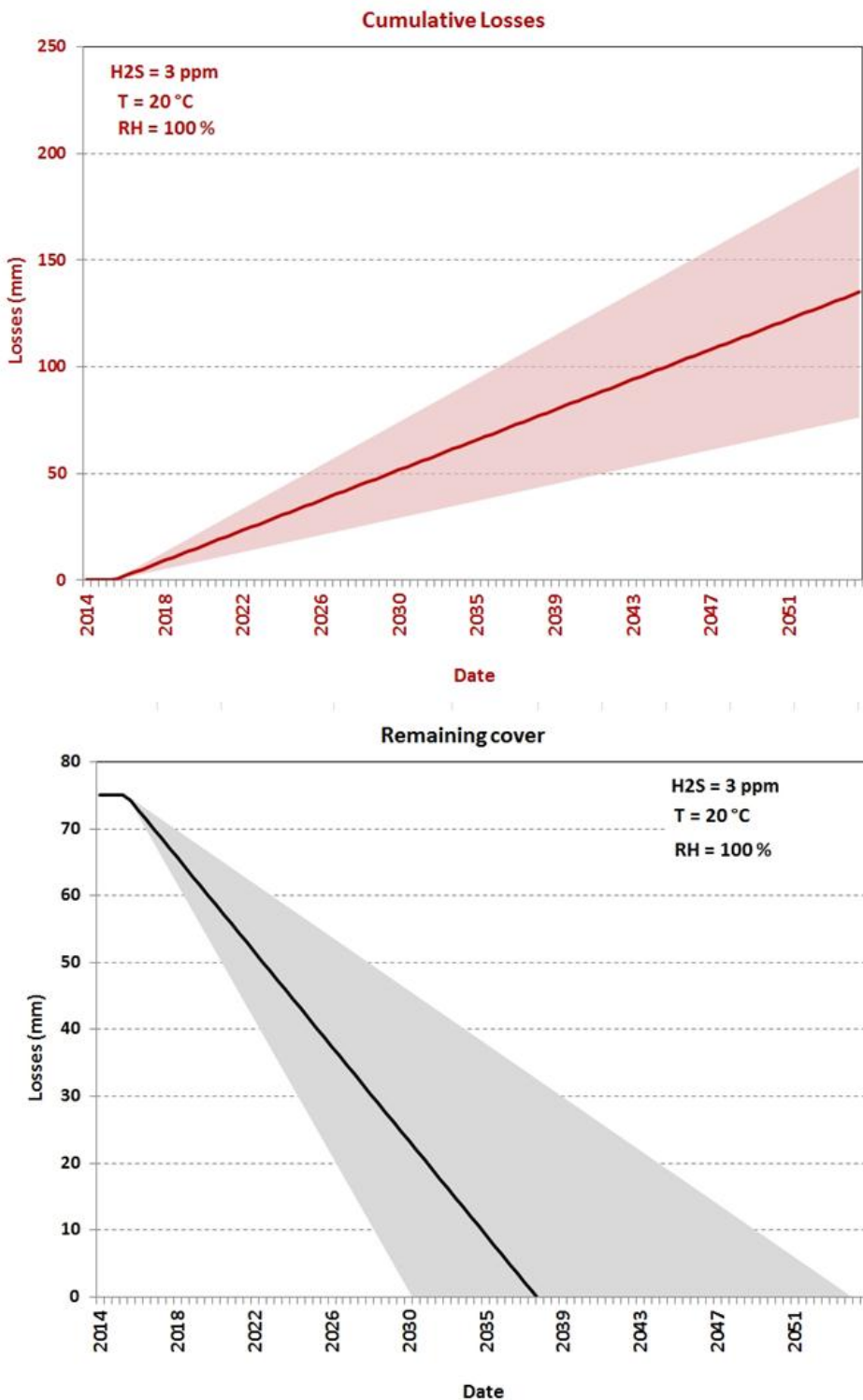


Figure 157. Plotted output from the sewer pipe service life prediction excel program. Solid lines represent predictions based on the average corrosion rate and the shaded region represents the range of predictions based on a possible error in the CR model of +/- 1.5mm/yr.

6.6.4.1 Assessing the range of conditions where corrosion rate is acceptable.

Eqns. (51) and (53) can also be manipulated to predict combinations of H₂S, temperature and humidity conditions that will produce satisfactory/unsatisfactory rates of corrosion. A series of excel spread sheets (for example see Figure 158) have been produced that will map out the region of temperature, humidity and H₂S concentration that will produce rates lower than a maximum corrosion rate specified by the user (Figures 159 to 161).

Thus for example if the H₂S concentration in the sewer gas is specified as 10ppm and the maximum desired rate of corrosion is 1mm/year the spread sheet returns a graph (Figure 159) showing the temperature/humidity region which will produce rates of corrosion less than 1mm/yr. Conditions conducive to corrosion rates less than that specified lie under the curve shown. Inspection of Figure 161 for example reveals that if a sewer is operating at 95% humidity and 20°C then a H₂S concentration of 3.7ppm or lower is necessary to produce corrosion rates less than 1mm/yr.

A copy of the excel program can be accessed through the SCORe project knowledge management system.

A	B	C	D	E	F
1					
2					
3					
4					
5					
6					
7					
8					
9					
10					
11					
12					
13					
14					
15	ENVIRONMENTAL CONDITIONS				
16					
17					
18	Sewer gas temperature	20	(°C)		
19	maximum allowed corrosion rate =	0.5	(mm/yr)		
20					
21					
22					
23					

Figure 158. Screen view of excel spread sheet for predicting combinations of temperature, humidity and H₂S concentration that will produce 'satisfactory' levels of corrosion.

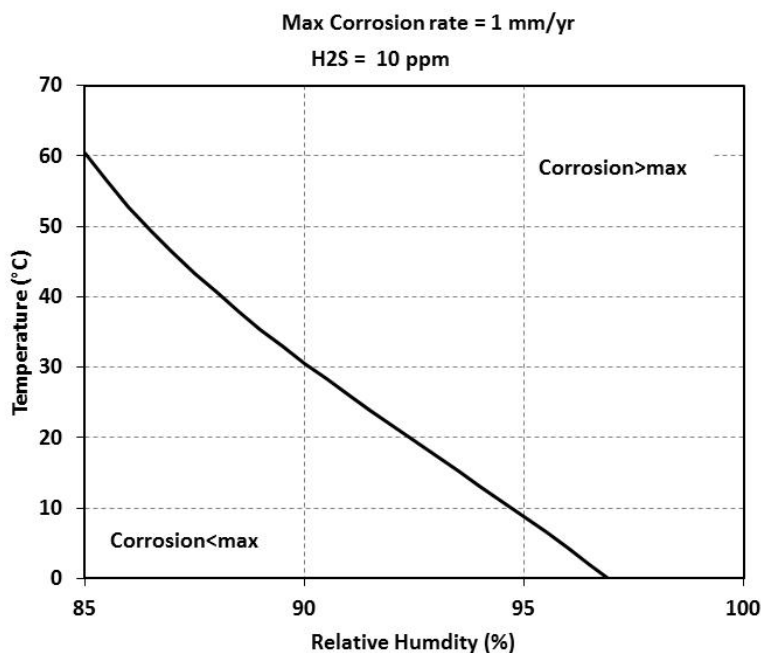


Figure 159. Excel spread sheet results showing the temperature/humidity region that will produce rates of corrosion of <1mm/year at H₂S levels of 10 ppm (desired corrosion behaviour applies at humidity/temperature conditions below the curve).

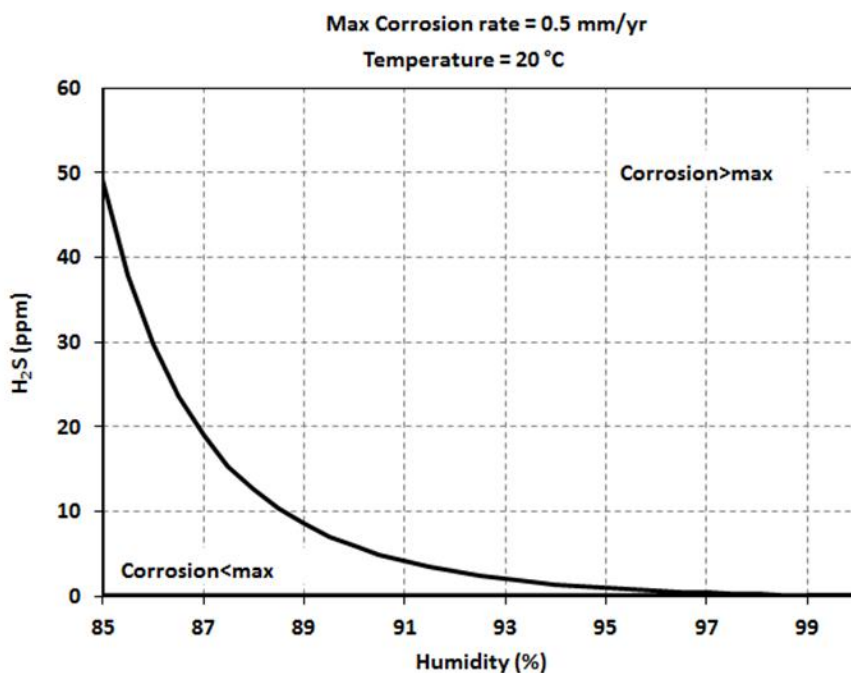


Figure 160. Excel spread sheet results showing the H₂S /humidity region that will produce rates of corrosion of <0.5 mm/year at 20°C (desired corrosion behaviour applies at humidity/H₂S conditions below the curve).

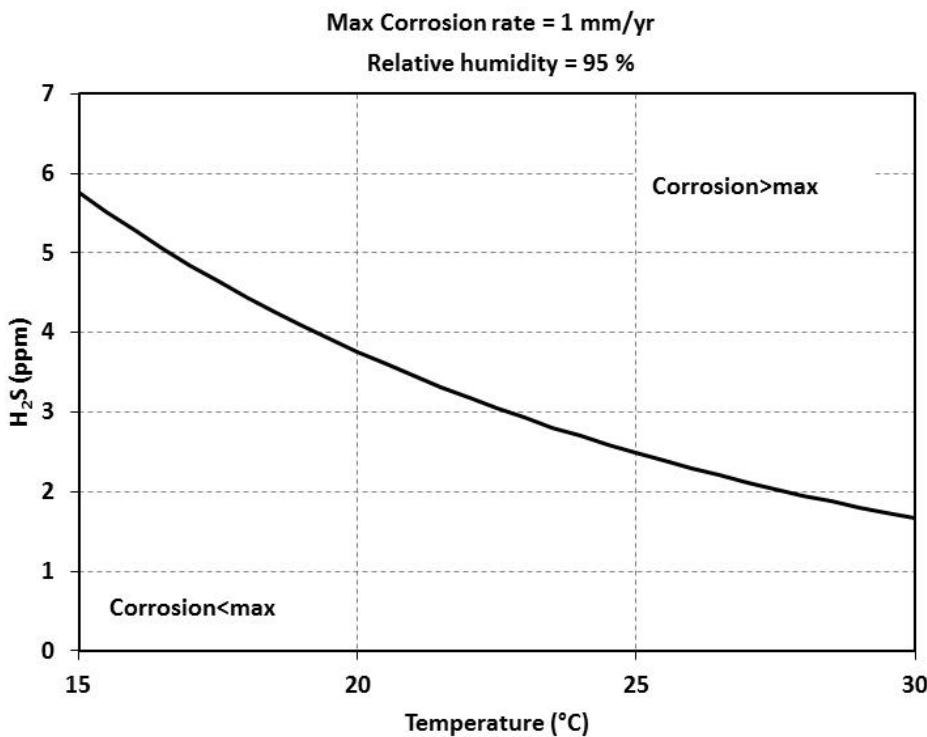


Figure 161. Excel spread sheet results showing the H₂S /temperature region that will produce rates of corrosion of <1mm/year at 95% humidity (desired corrosion behaviour applies at temperature/H₂S conditions below the curve).

6.7 Summary of Activity 4 outcomes

A detailed physical understanding of how the corrosion of concrete sewer pipe evolves over time has been developed using observations made in the laboratory and field work programs as well as insights gained from a survey of industry data and the scientific literature.

The insights gained have been used to model the corrosion process and develop a series of equations for predicting concrete sewer pipe service life.

Main corrosion milestones have also been identified. A summary of the time-wise evolution of the corrosion cycle is as follows:

- Abiotic corrosion (pipe installation to $t_{pH=9}$)
 - No biological activity due to high alkalinity of pipe surface
 - Corrosion involves weak inorganic acids generated from dissolved H₂S and CO₂
 - Only the most basic minerals (such as portlandite and C-S-H) are attacked
 - Attack is limited to a zone within 0.3mm of the pipe surface

- There is no loss of mass at this stage but surface pH declines rapidly
 - This stage of the corrosion cycle only lasts a matter of months
- First signs of life ($t_{pH=9}$ to $t_{pH=6}$)
 - Microbial and fungal colonisation of the pipe surface commences
 - Beginning of successive waves of bacterial colonisation
 - Neutrophilic sulphur oxidising bacteria appear and production of sulphuric acid begins along with some carboxylic acids
 - There is still no significant loss of mass but fine layers of crystalline gypsum can be found on pipe surface
 - Surface pH is still falling but less rapidly
 - When the surface pH falls to pH=6 the “incubation period” ends
 - Time spent in the incubation period ranges from several months to several years depending on the aggressiveness of the site.
- Initiation of corrosion losses ($t_{pH<6}$)
 - More aggressive bacteria which can tolerate a lower pH environment succeed neutrophilic bacteria.
 - Formation of a porous, soft corrosion product layer commences on the pipe surface
 - Visible biology on the pipe surface now includes dark ropey braided hyphae interspersed with nodules of pure sulphur.
 - Mass loss commences at pH=6. Mass loss accumulates linearly with time (i.e. a constant corrosion rate at each site).
- Advanced corrosion ($t>>t_{pH=6}$)
 - Corrosion losses accumulate at a constant rate until the pipe fails
 - The presence of the corrosion product layer has no impact on corrosion activity.

A better understanding of the geometry of the corrosion process was also developed. The main features are:

- Acid generation occurs at the exposed surface of the corrosion product layer where most of the bacterial activity takes place.
- Diffusion of acid through the corrosion product layer is rapid due to the highly porous nature of the layer.
- Once the acid reaches the sound concrete it is rapidly consumed in neutralisation reactions taking place there. Consequently there is little diffusion of acid into the sound concrete structure and the reaction front is sharp and well defined.

A one dimensional phenomenological model of the corrosion process has been developed. The main features of the model are:

- The model geometry is based on the spatial understanding of the corrosion process developed earlier.
- The model incorporates diffusional processes as well as corrosion reaction and oxidation kinetics
- The complexity of the model means that there is no analogue solution to the model and consequently it was solved using a numerical approach (Finite element)

- The only unknowns in the model were the oxidation and corrosion reaction rate constants which were determined by calibrating the model with field and laboratory corrosion loss data and pH profiling observations.
- The results indicate that the overall corrosion process is controlled by the rate at which H₂S is oxidised at the exposed surface of the corrosion product layer.
- The phenomenological model predicted the rates of corrosion at the Perth and Melbourne field sites to within 1.5mm/yr of the observed values.
- The model also successfully predicted the constant accumulation of mass loss over time.
- The primary insight that H₂S oxidation is the rate determining step in the corrosion process was used in the formulation of the concrete sewer pipe service life prediction tool.

An analysis of the impact of environmental parameters was also completed. A summary of the findings is as follows:

- H₂S gas phase concentration
 - An analysis of industry and Sp1A data as well as kinetic studies of H₂S oxidation all point to the following relationship:

$$CR \propto [H_2S]_{gas}^{0.5}$$

- Sewer gas temperature
 - Little data was available however studies of the impact of temperature on the action of some sulphur oxidising bacteria in the scientific literature indicate the following:

$$CR \propto e^{(-30,000/(R \times (T+273.15)))}$$

- Sewer humidity
 - Studies carried out by Melbourne Water in the 1980's and field study results from the Perth Bibra Lake site both indicate that corrosion activity is sensitive to the concrete moisture content which in turn is determined by the sewer gas humidity and pore size distribution of the concrete.
 - Theoretical calculations combined with an analysis of the pore structure of concretes used in this study indicate the following relationship:

$$CR \propto \frac{(1 - 0.01245 \times RH\%)}{(0.0955 \times RH\% - 9.8044)}$$

- Temperature of the sewer pipe wall
 - If the sewer pipe is different in temperature to the sewer headspace gases this will affect the concrete moisture content and hence the rate of corrosion.
 - The relationship between the wall temperature and corrosion rate are complex but analysis of the physics involved indicates that the impact may

be considerable in some circumstances particularly when sewer pipe temperatures are driving pore gas humidities towards saturation.

- For example if the pipe temperature is 1°C colder than the sewer gas (at 96% RH) corrosion rates are predicted to be 70% higher than if the two are at the same temperature.

A concrete service life prediction tool was developed from the insights into the corrosion process gained from the field and laboratory work, industry and scientific data pool as well as phenomenological modelling of the sewer pipe corrosion process. The tool estimates the service life of a concrete sewer pipe for a given set of local environmental conditions, (time averaged local sewer gas phase temperature, humidity and H₂S concentration).

- The service life is calculated from:

$$\text{Service life (years)} = \frac{CD_{t=0}}{CR} + t_{in}$$

- Where $CD_{t=0}$ is the depth of concrete cover over the metal reinforcement at the time of installation (mm); CR is the rate of corrosion, (mm/yr), and t_{in} is the incubation time (years).
- If temperature, humidity and H₂S concentration are known t_{in} and CR can be estimated using the following:

$$t_{in}(\text{years}) = 1.24e - 10 \times [H_2S]^{-0.8} \times \frac{(0.0955 \times RH\% - 9.8044)}{(1 - 0.01245 \times RH\%)} \times e^{(56,000/(8.314 \times (T+273)))} + 0.91$$

$$CR (\text{mm/yr}) = 458000 \times [H_2S]^{0.5} \times \frac{(1 - 0.01245 \times RH\%)}{(0.0955 \times RH\% - 9.8044)} \times e^{(-30,000/(8.314 \times (T+273)))}$$

- Where $[H_2S]$ is the concentration of H₂S in the sewer gas (ppm); $RH\%$ is the sewer gas relative humidity (%) and T is the sewer gas temperature (°C). All values are the best estimates for the average values expected at the sewer site in question
- The estimated error in the prediction of CR is 1.5mm/yr.
- If only the H₂S concentration is known t_{in} and CR can be estimated using the following expressions:

$$t_{in} (\text{years}) = 1.62 - 0.083 \times \ln[H_2S]$$

$$CR (\text{mm/yr}) = 0.56 \times [H_2S]^{0.5}$$

- This last expression is formulated on evidence provided from an analysis of industry corrosion data.
- It was noted however that the truncated expression for calculating CR will significantly underestimate corrosion rates if the humidity in the sewer is significantly above 95%.

- An excel spread sheet has been developed to allow calculation of the service life for a given input of H₂S, temperature, humidity and depth of concrete cover.
- The spread sheet returns the date of the estimated first signs of corrosion, service lifespan and the range of possible end-of-service-life dates
- Additional spread sheets have been added that will calculate the temperature/humidity/H₂S combinations that will provide an environment where corrosion rates are less than a maximum rate (specified by the user).
- The excel spread sheets are available through the SCORe project knowledge management system.

7 Practical Outcomes and Conclusion

1. The primary practical outcome of the present project is a first version of an excel based application tool that allows users without detailed background in sewer pipe corrosion to predict the likely service life of given sewer pipe for which temperature, humidity and H₂S gas concentration conditions are known or can be estimated.
2. The same excel based application tool can be used to determine the optimal sewer operating conditions satisfying pre-specified corrosion losses for given exposure periods.
3. A model of sewer pipe corrosion has been developed. The model shows that there is a short incubation period followed by a long-term steady linear corrosion rate. The theory for both parts of the model has been developed. It is based on current understanding of sewer corrosion processes and also on the better understanding obtained during the present project.
4. The available data and the model show that the corrosion product layer that forms over the sound concrete sewer wall has insignificant influence on the rate of concrete corrosion. As a result, washing of sewer walls to remove corrosion product is unlikely to have a significant long-term effect but may slow corrosion activity temporarily by removing bacterial growth and altering the surface pH of the pipe.
5. The oxidation of H₂S on the exposed surface of the corrosion product layer plays a critical, rate-controlling, role in the corrosion of concrete. Theoretical considerations and an analysis of field observations, show that the rate of corrosion is proportional to the square root of the concentration of H₂S in the sewer gas. Thus a quadrupling of the H₂S concentration causes a doubling of the corrosion rate.
6. Typically, H₂S is absorbed by the concrete of the sewer wall. As a result the application of a low permeability protective coating to large sections of a sewer line is likely to significantly decrease the ability of the sewer line as a whole to absorb H₂S gas. As a result H₂S levels in the sewer gas will increase thereby increasing corrosion in the remaining unlined sections of the sewer line.
7. Increased average temperatures in sewers can be assumed to increase the rate of corrosion and follow the classical Arrhenius relationship. This means that the corrosion rate increases by 50% for every 10°C rise in temperature.
8. Corrosion is very sensitive to the moisture content of the sewer wall concrete. Ventilation strategies that lower sewer humidity and thereby dry out sewer walls will have a significant impact on corrosion rates. Corrosion activity is significantly inhibited if relative humidities fall below 90%.

9. Differences in temperature between the sewer gas and the sewer pipe wall are likely to have an influence on corrosion activity. Specifically, sewers in cold ground are likely to experience relatively more corrosion as warm sewer gases condense on the interior surfaces of the pipe and thereby increase concrete moisture levels.

8 Recommendations for future work

The pool of data used to construct the models and form the conclusions outlined above was limited. Consequently more data (specifically temperature, humidity and H₂S concentration data coupled to corrosion loss observations) would improve the confidence with which the models generated in this study could be applied.

Other recommendations for future work include:

- Continued recording of in situ corrosion losses in working sewers (as for example in traverse surveys).
 - Multiple surveys carried out periodically over the same locations however are necessary to build up a reasonable picture of corrosion trends.
 - Environmental data (temperature, humidity and H₂S concentration at a minimum) need to be gathered concurrently with the loss data to extract the full value from the loss survey.
- Monitoring of in-situ humidity levels.
 - While it is difficult to measure humidity in a sewer environment this study shows that the corrosion losses are heavily impacted by humidity levels. More data will help clarify the relationship between corrosion and humidity levels (and particularly humidity cycling) in sewers.
 - The link between concrete moisture content and humidity cycling also needs to be investigated as it is poorly understood.
- Monitoring of sewer pipe wall temperatures
 - The link between sewer pipe wall temperatures need to be ascertained as theoretical considerations indicate this could have a large impact on corrosion activity.
- Further investigation of the effect of the position around the sewer wall on corrosion needs to be undertaken.
 - The trials at Sydney which were in part set up to investigate this question had to be aborted before the issue of position could be adequately addressed.
- More coupon trials at more varied locations.
 - The Sp1B field trials conducted at Melbourne and Perth were very successful however they only generated corrosion data at four sets of environmental conditions thereby limiting the combination of temperature/humidity and H₂S condition combinations examined. Similar trials conducted at more varied locations will help better understand the corrosion process and reduce the level of uncertainty in the corrosion prediction model.

9 Appendices

The following pages list much of the data accumulated in the Sp1B project.

Appendix I. NGRS Corrosion Loss Data

Location	Manhole ID	Corrosion Loss Observed (mm)															
		1997 Losses			2004 Losses			2009 Losses			2011 Losses						
			all	roof	wall		all	roof	wall		all	roof	wall		all	roof	wall
Tangerine St	S11MH1	40	27.5			Lined				Lined				Lined			
Cnr hercules and Tangerine St	S11MH2	15	5	50						Lined				Lined			
Hercules St	S11MH3	5	5	35						Lined				Lined			
Cnr Morse and Mitchell St	S11MH4	5	5	50						Lined				Lined			
River Rd	S11MH5	5	5	20						Lined				Lined			
Wattle Ave	S11MH6	2	2	15						Lined				Lined			
Villawood Public School	S11MH7	5	5											Lined			
8 Curringa Rd	S11MH8	5	10											Lined			
Tuncooee Rd	S11MH9	15	10	20		Lined								Lined			
Landsdowne Pk (1)	S10MH10	10	10	20										Lined			
Landsdowne Pk (2)	S10MH11	10	15	20										Lined			
Landsdowne Pk (3)	S10MH12	10	10	20										Lined			
Landsdowne Pk (4)	S10MH13	10	10	15										Lined			
Landsdowne Pk (5)	S10MH14	10	10	15										Lined			
Landsdowne Pk (6)	S10MH15	10	10	20										Lined			
Landsdowne Pk (7)	S9MH16	10	10	20										Lined			
Lucinda Ave (1)	S9MH17	10	10	20										Lined			
Lucinda Ave (2)	S9MH18	7.5	7.5	20										Lined			
Caroline Crescent	S9MH19	10	10	7.5										Lined			
					17.5									Lined			

NGRS Corrosion Loss Data (Cont)

Location	Manhole ID	1997 Losses			Corrosion Loss Observed (mm)			2009 Losses			2011 Losses		
		all	roof	wall	all	2004 Losses	wall	all	roof	wall	all	roof	wall
Whitmore Ave (1)	S9MH20	10			17.5							Lined	
		10			17.5							Lined	
Whitmore Ave (2)	S9MH21	10			17.5							Lined	
		10			17.5							Lined	
Marsden St (1)	S9MH21A	10			17.5							Lined	
		10			17.5							Lined	
Marsden St (2)	S9MH22	10			10							Lined	
		10			17.5							Lined	
Amaroo Ave	S9MH23	10			17.5							Lined	
		10			17.5							Lined	
15 Keswick St	S9MH24	10			Lined							Lined	
		15			Lined							Lined	
Keswick St	S8MH25	15			Lined							Lined	
		20			20							25	25
Marion St	S8MH25A	20			12.5	15	10	25.0			25	25	25
		10			12.5	15	10	17.5					
Birch St	S8MH26	10			12.5							Lined	
		7.5			12.5							Lined	
Cnr Birch and Allingham St	S8MH27	5			7.5	10	5					Lined	
		5			7.5	10	5					Lined	
Galasso tile factory	S8MH28	5			7.5			17.5	18.5	16.5		Lined	
		10			10			13.0	13.0	13.0		Lined	
Harley St	S7MH29	5			12.5			17.0	19.0	15.0		Lined	
		10			12.5			16.0	17.0	15.0		Lined	
Bankstown airport (1)	S7MH30	10			12.5			13.0	15.0	11.0		Lined	
		10			12.5			13.0	15.0	11.0		Lined	
Bankstown airport (2)	S7MH30A	10			12.5			13.8	15.0	12.5		Lined	
		5			12.5			14.0	15.8	12.1		Lined	
Kinch reserve	S7MH31	3			12.5			15.0	17.5	12.5		Lined	
		3			12.5			13.8	14.5	13.0		Lined	
Deverall Pk	S7MH32	3			12.5			14.2	15.6	12.8		Lined	
		3			12.5			13.2	13.6	12.9		Lined	
Access Rd to trotting track	S7MH33	3			10							Lined	
		3			10							Lined	
Leighton's yard (1)	S7MH34	5			10							Lined	
		5			10							Lined	
Leighton's yard (2)	S7MH35	5			12.5							Lined	
		5			5							25	25

NGRS Corrosion Loss Data (Cont)

Location	Manhole ID	Corrosion Loss Observed (mm)															
		1997 Losses			2004 Losses			2009 Losses			2011 Losses						
		all	roof	wall		all	roof	wall		all	roof	wall		all	roof	wall	
Edgar St	S7MH36	5			12.5				14.5	16.1	12.9	25	25	25			
		5			12.5				13.2	15.4	10.9	25	25	25			
MacDonalds, River Rd	S6MH37	5			12.5				15.1	16.4	13.8	25	25	25			
		5			12.5				15.4	17.9	12.9	25	25	25			
73 MacKenzie Rd	S6MH38	5			12.5	20	5								Lined		
		20			12.5	20	5								Lined		
83 MacKenzie Rd	S6MH39	25			12.5	20	5								Lined		
		11.5	20	3	12.5	20	5								Lined		
37 Archnold St	S5MH40	11.5	20	3	12.75	22.5	3								Lined		
		11.5	20	3	11.5	20	3								Lined		
9 Cahors Rd	S5MH41	11.5	20	3	12.75	22.5	3								Lined		
		6.5	10	3	6.5	10	3								Lined		
42 Cahors Rd	S5MH42	3	3	3	13.75	17.5	10								Lined		
		4	5	3	17.5	25	10								Lined		
Arab Rd	S5MH43	11.5	20	3	13.75	17.5	10								Lined		
		11.5	20	3	13.75	17.5	10								Lined		
2 Alice St	S5MH44	11.5	20	3	16.25	17.5	15		20.8	17.5	24.0				Lined		
		9	15	3	25	35	15		19.5	12.0	27.0				Lined		
End of Alice St	S5MH45	9	15	3	27.5	40	15		26.3	16.1	36.6				Lined		
		6.5	10	3	16.25	22.5	10		25.7	14.8	36.6				Lined		
7 Burley Rd	S4MH46	6.5	10	3	11.25	10	12.5								Lined		
		4	3	5	17.5	22.5	12.5								Lined		
U/S Salt pan Ck aqueduct	S4MH47	10	15	5	17.5	22.5	12.5								Lined		
		Cement lined steel pipe			Cement lined steel pipe												
D/S Salt Pan aqueduct	S3MH1	10	15	5	22.5	25	20										
		10	15	5	22.5	25	20										
Elwin St	S3MH2	9	15	3	25	30	20										
		5	7	3	27.5	35	20										
Clarke St	S3MH3	3	3	3	26.25	30	22.5										
		3	3	3	26.25	30	22.5										
Johnstone St	S3MH4	10	15	5					39.7	36.9	42.5						
		7.5	10	5					43.2	39.2	47.1						
Forest Rd	S3MH5	10	15	5					38.0	33.0	43.1						
		10	15	5					39.0	35.4	42.6						
Roberts Ave U/S aqueduct	S3MH6	5	5	5													
		3	3	3													
Roberts Ave aqueduct (1)	S3MH7	3	3	3	17.5	20	15										
		3	3	3	17.5	20	15										

NGRS Corrosion Loss Data (Cont)

Location	Manhole ID	1997 Losses			Corrosion Loss Observed (mm)			2009 Losses			2011 Losses		
		all	roof	wall	all	roof	wall	all	roof	wall	all	roof	wall
Roberts Ave aqueduct (2)	S3MH8	3	3	3	20	20	20						
		3	3	3	20	20	20						
Roberts Ave aqueduct (3)	S3MH9	5	7	3	22.5	25	20	30.4	26.8	34.1			
		10	15	5	25	30	20	34.8	31.9	37.7			
Acacia St U/S aqueduct	S3MH10	3	3	3	25	25	25						
		5	5	5	25	25	25						
Acacia St D/S aqueduct	S3MH11	5	5	5	35	40	30	34.6	29.6	39.5			
		10	15	5	35	40	30	35.5	28.0	43.0			
River Rd U/S Aqueduct	S3MH12	5	5	5	20	20	20						
		5	5	5	20	20	20						
River Rd D/S Aqueduct	S3MH13	12.5	20	5	32.5	40	25	31.7	25.1	38.2			
		12.5	20	5	32.5	40	25	31.9	27.3	36.5			
Ada St	S3MH14	12.5	20	5	25	30	20	30.0	27.5	32.5			
		12.5	20	5	25	30	20	28.1	25.9	30.3			
Renown Park	S3MH15	12.5	20	5	22.5	25	20	32.8	28.6	37.1			
		12.5	20	5	30	40	20	37.3	35.3	39.4			
Jellicoe St	S2MH16	15	25	5	27.5	30	25	38.9	36.9	41.0			
		15	25	5	20	25	15	42.0	39.8	44.2			
Oatley bay Ck aqueduct (1)	S2MH17	6.5	10	3	17.5	25	10						
		6.5	10	3	17.5	25	10						
Oatley bay Ck aqueduct (2)	S2MH18	17.5	20	15	15	20	10						
		17.5	20	15	15	20	10						
Oatley bay Ck aqueduct (3)	S2MH19	10	15	5	32.5	40	25	41.9	39.8	44.1			
		12.5	15	10				41.8	38.8	44.8			
West St	S2MH20	12.5	15	10				35.8	32.3	39.2			
		15	20	10				42.2	40.9	43.4			
Blake St	S1MH21	10	15	5	35	40	30	33.1	31.3	34.8			
		10	15	5	35	40	30	30.8	29.4	32.1			
Kensington Rd	S1MH22	12.5	20	5	35	40	30						
		12.5	20	5	35	40	30						
Gladstone St	S1MH23	12.5	20	5	35	40	30	42.2	40.0	44.4			
		12.5	20	5	35	40	30	40.3	38.1	42.5			
Catherine St	S1MH24	10	15	5	17.5	25	10						
		10	15	5	17.5	25	10						
Muddy Ck Aqueduct (1)	S1MH25	6.5	10	3	20	20	20						
		6.5	10	3	20	20	20						
Muddy Ck Aqueduct (2)	S1MH26	6.5	10	3	20	20	20						

NGRS Corrosion Data (Cont)

Location	Manhole ID	1997 Losses			Corrosion Loss Observed			2009 Losses			2011 Losses						
		all	roof	wall	all	roof	wall	all	roof	wall	all	roof	wall				
Subway Rd	S1MH27	12.5	20	5	25	25	25	67.5	63.8	71.3	67.5	63.8	71.3				
		12.5	20	5	35	40	30	75.0	73.3	76.7							
Chapel St	S1MH28	11.5	20	3	35	40	30	60.6	59.0	62.3	60.6	59.0	62.3				
		11.5	20	3	35	40	30	56.8	54.0	59.6							
George St	S1MH29	11.5	20	3	35	40	30	56.0	54.0	58.0	56.0	54.0	58.0				
		11.5	20	3	35	40	30	46.9	44.4	49.4							
Shaaron Walk	S1MH30	9	15	3	20	20	20	50.8	48.3	53.3	50.8	48.3	53.3				
		9	15	3	20	20	20										
Terry St	S1MH31	11.5	20	3	27.5	30	25	49.6	46.3	53.0	49.6	46.3	53.0				
		11.5	20	3	30	35	25										
Tantalon St	S1MH32	12.5	20	5	35	40	30	40.5	40.0	40.9	40.5	40.0	40.9				
		12.5	20	5	40	50	30										
Bellvue St reserve	S1MH33	15	25	5	30	30	30	41.5	41.0	42.0	41.5	41.0	42.0				
		15	25	5	30	30	30										
Eve St	S1MH34	12.5	20	5	27.5	25	30	39.5	39.0	40.0	39.5	39.0	40.0				
		25	20	30	27.5	25	30										
Barton Pk (1)	S1MH35	5.25	7.5	3	22.5	25	20	Lined	Lined	Lined	Lined	Lined	Lined				
		5.25	7.5	3	22.5	25	20										
Barton Pk (2)	S1MH36	5.25	7.5	3	13.75	17.5	10	Lined	Lined	Lined	Lined	Lined	Lined				
		5.25	7.5	3	13.75	17.5	10										
Barton Pk (3)	S1MH37	6.5	10	3	13.75	17.5	10	Lined	Lined	Lined	Lined	Lined	Lined				
		6.5	10	3	13.75	17.5	10										
Barton Pk (4)	S1MH38	15	20	10	13.75	17.5	10	Lined	Lined	Lined	Lined	Lined	Lined				
		25	25	25	Lined	Lined	Lined										
Eve St Merging Chamber	S1MH39	25	25	25													

Appendix II. NGRS Calculated corrosion rates

Location	Manhole No.	Corrosion rate (mm/yr)			
		<1997	1997-2004	2004-2009	2009-2011
Tangerine St	S11MH1	1.29 0.89			
Cnr hercules and Tangerine St	S11MH2	0.48 0.16	5.00 6.43		
Hercules St	S11MH3	0.16 0.16	4.29 4.29		
Cnr Morse and Mitchell St	S11MH4	0.16 0.16	6.43 2.14		
River Rd	S11MH5	0.16 0.16	2.14 0.71		
Wattle Ave	S11MH6	0.06 0.06	1.86 1.86		
Villawood Public School	S11MH7	0.16 0.16	0.00 0.00		
8 Curringa Rd	S11MH8	0.16 0.32	0.00 0.00		
Tuncooee Rd	S11MH9	0.48 0.32		1.43	
Landsdowne Pk (1)	S10MH10	0.32 0.32		1.43 1.43	
Landsdowne Pk (2)	S10MH11	0.32 0.48		1.43 0.00	
Landsdowne Pk (3)	S10MH12	0.32 0.32		1.43 0.71	
Landsdowne Pk (4)	S10MH13	0.32 0.32		0.71 0.71	
Landsdowne Pk (5)	S10MH14	0.32 0.32		1.43 1.43	
Landsdowne Pk (6)	S10MH15	0.32 0.32		1.43 1.43	
Landsdowne Pk (7)	S9MH16	0.31 0.31		1.43 1.43	
Lucinda Ave (1)	S9MH17	0.31 0.31		1.43 1.43	
Lucinda Ave (2)	S9MH18	0.23 0.23		1.79 1.79	
Caroline Crescent	S9MH19	0.31 0.31		0.00 1.07	

NGRS Calculated corrosion rates (Cont).

Location	Manhole No.	Corrosion rate (mm/yr)			
		<1997	1997-2004	2004-2009	2009-2011
Whitmore Ave (1)	S9MH20	0.31 0.31	1.07 1.07		
Whitmore Ave (2)	S9MH21	0.31 0.31	1.07 1.07		
Marsden St (1)	S9MH21A	0.31 0.31	1.07 1.07		
Marsden St (2)	S9MH22	0.31 0.31	0.00 1.07		
Amaroo Ave	S9MH23	0.31 0.31	1.07 1.07		
15 Keswick St	S9MH24	0.31 0.47			
Keswick St	S8MH25	0.47			
Marion St	S8MH25A	0.63 0.63 0.31	0.00 0.00 0.36	1.00 1.00	0.00 3.75
Birch St	S8MH26	0.31 0.23	0.36 0.71		
Cnr Birch and Allingham St	S8MH27	0.16 0.16	0.36 0.36		
Galasso tile factory	S8MH28	0.16 0.31	0.36 0.00	2.00 0.60	
Harley St	S7MH29	0.15 0.30	1.07 0.36	0.90 0.70	
Bankstown airport (1)	S7MH30	0.30 0.30	0.36 0.36	0.10 0.10	
Bankstown airport (2)	S7MH30A	0.30 0.15	0.36 1.07	0.25 0.29	
Kinch reserve	S7MH31	0.09 0.09	1.36 1.36	0.50 0.25	
Deverall Pk	S7MH32	0.09 0.09	1.36 1.36	0.34 0.14	
Access Rd to trotting track	S7MH33	0.09 0.09	1.00 1.00		
Leighton's yard (1)	S7MH34	0.15 0.15	0.71 0.71		
Leighton's yard (2)	S7MH35	0.15 0.15	1.07 0.00		
Edgar St	S7MH36	0.15 0.15	1.07 1.07	0.40 0.13	5.25 5.92

NGRS Calculated corrosion rates (Cont).

Location	Manhole No.	Corrosion rate (mm/yr)			
		<1997	1997-2004	2004-2009	2009-2011
MacDonalds, River Rd	S6MH37	0.15 0.15	1.07 1.07	0.51 0.58	4.97 4.79
73 MacKenzie Rd	S6MH38	0.15 0.61	1.07 0.00		
83 MacKenzie Rd	S6MH39	0.76 0.35	0.00 0.14		
37 Archbold St	S5MH40	0.34 0.34	0.18 0.00		
9 Cahors Rd	S5MH41	0.34 0.19	0.18 0.00		
42 Cahors Rd	S5MH42	0.09 0.12	1.54 1.93		
Arab Rd	S5MH43	0.34 0.34	0.32 0.32		
2 Alice St	S5MH44	0.34 0.26	0.68 2.29	0.90 -1.10	
End of Alice St	S5MH45	0.26 0.19	2.64 1.39	-0.23 1.89	
7 Burley Rd	S4MH46	0.19 0.12	0.68 1.93		
U/S Salt pan Ck aqueduct	S4MH47	0.29 0.00	1.07		
D/S Salt Pan aqueduct	S3MH1	0.21 0.21	1.79 1.79		
Elwin St	S3MH2	0.19 0.10	2.29 3.21		
Clarke St	S3MH3	0.06 0.06	3.32 3.32		
Johnstone St	S3MH4	0.21 0.16	0.00 0.00		
Forest Rd	S3MH5	0.21 0.21	0.00 0.00		
Roberts Ave U/S aqueduct	S3MH6	0.10 0.06	0.00 0.00		
Roberts Ave aqueduct (1)	S3MH7	0.06 0.06	2.07 2.07		
Roberts Ave aqueduct (2)	S3MH8	0.06 0.06	2.43 2.43		
Roberts Ave aqueduct (3)	S3MH9	0.10 0.21	2.50 2.14	1.59 1.96	

NGRS Calculated corrosion rates (Cont).

Location	Manhole No.	Corrosion rate (mm/yr)			
		<1997	1997-2004	2004-2009	2009-2011
Acacia St U/S aqueduct	S3MH10	0.06 0.10	3.14 2.86		
Acacia St D/S aqueduct	S3MH11	0.10 0.21	4.29 3.57	-0.09 0.11	
River Rd U/S Aqueduct	S3MH12	0.10 0.10	2.14 2.14		
River Rd D/S Aqueduct	S3MH13	0.26 0.26	2.86 2.86	-0.16 -0.13	
Ada St	S3MH14	0.26 0.26	1.79 1.79	1.00 0.63	
Renown Park	S3MH15	0.26 0.26	1.43 2.50	2.07 1.47	
Jellicoe St	S2MH16	0.27 0.27	1.79 0.71	2.29 4.40	
Oatley bay Ck aqueduct (1)	S2MH17	0.12 0.12	1.57 1.57		
Oatley bay Ck aqueduct (2)	S2MH18	0.32 0.32	0.00 0.00		
Oatley bay Ck aqueduct (3)	S2MH19	0.18 0.23	3.21 0.00	1.89	
West St	S2MH20	0.23 0.27	0.00 0.00		
Blake St	S1MH21	0.18 0.18	3.57 3.57	-0.38 -0.85	
Kensington Rd	S1MH22	0.23 0.23	3.21 3.21		
Gladstone St	S1MH23	0.23 0.23	3.21 3.21	1.44 1.06	
Catherine St	S1MH24	0.18 0.18	1.07 1.07		
Muddy Ck Aqueduct (1)	S1MH25	0.12 0.12	1.93 1.93		
Muddy Ck Aqueduct (2)	S1MH26	0.12 0.12	1.93 1.93		
Subway Rd	S1MH27	0.23 0.23	1.79 3.21	8.50 8.00	
Chapel St	S1MH28	0.21 0.21	3.36 3.36	5.13 4.35	
George St	S1MH29	0.21 0.21	3.36 3.36	4.20 2.38	

NGRS Calculated corrosion rates (Cont).

Location	Manhole No.	Corrosion rate (mm/yr)			
		<1997	1997-2004	2004-2009	2009-2011
Shaaron Walk	S1MH30	0.16 0.16	1.57 1.57		
Terry St	S1MH31	0.21 0.21	2.29 2.64	4.17	
Tantalon St	S1MH32	0.23 0.23	3.21 3.93	2.93 0.09	
Bellvue St reserve	S1MH33	0.27 0.27	2.14 2.14	2.30 1.90	
Eve St	S1MH34	0.23 0.45	2.14 0.36		
Barton Pk (1)	S1MH35	0.10 0.10	2.46 2.46		
Barton Pk (2)	S1MH36	0.10 0.10	1.21 1.21		
Barton Pk (3)	S1MH37	0.12 0.12	1.04 1.04		
Barton Pk (4)	S1MH38	0.27 0.45	0.00		
Eve St Merging Chamber	S1MH39	0.45			

Appendix III. Historical SWSOOS2 Losses and corrosion rates

Location	Corrosion Losses Observed (mm) [38]						
	1966	1969	1971	1974	1977	1986	1997
Upstream of Botany (above ground)	0	0	1	1	1	2	15
Botany Rd	1	1	2	3	5	25	40
Hill St to Railway	0	0	0	1	1	2	20
Railway to Perry St	1	1	6	6	20	30	105

Location	Corrosion rates (mm/yr)						
	1966-1969	1969-1971	1971-1974	1974-1977	1977-1986	1986-1997	average
Upstream of Botany	0.0	0.5	0.0	0.0	0.1	1.2	0.3
Botany Rd	0.0	0.5	0.3	0.7	2.2	1.4	0.8
Hill St to Railway	0.0	0.0	0.3	0.0	0.1	1.6	0.3
Railway to Perry St	0.0	2.5	0.0	4.7	1.1	6.8	2.5

Appendix IV. SWSOOS1 corrosion losses

Location	Corrosion loss observations (mm)											
	1997 Losses			2007 Losses			2009 Losses		2012 Losses			
	all	roof	wall	all	roof	wall	all	roof	wall	all	roof	wall
Eve St Merge Chamber	3	lined	3	25	lined	25						
Opposite golf course (+142m)	3	lined	3	25	lined	25						
Opposite golf course (+227m)	3	lined	3	24	lined	24						
Flow monitoring station Arncliffe (+298m)	3	lined	3	22.5	lined	22.5						
Cooks River Aqueduct (+411m)	4.5	6	3	35	25	45						
Midway along muddy ck aqueduct	10	10	10	33.75	35	32.5						
Airport Land 1 (+485m)	10.5	6	15	36.25	40	32.5						
Airport Land on bend airport rising main (+513m)	12	12	12	36.25	32.5	40						
Airport opposite East-west runway (+627m)	2	2	2	36.25	32.5	40						
Just past east west runway (+712m)	2	2	2	25			25					
2nd past east west runway	2	2	2	15			15					
Upstream of silt traps	2	2	2	25			25					
Just before silt pits by Penstock gates (817m)	6	6	6	35			35					
Airport Silt traps	6	6	6	30			30					
Downstream of silt trap	6	6	6	27.5			27.5					
2nd downstream of silt trap	lined			Lined								
3rd downstream of silt trap	lined			Lined								
4th downstream of silt trap	lined			Lined								
5th downstream of silt trap	lined			Lined								
6th downstream of silt trap	lined			Lined								
7th downstream of silt trap	lined			Lined								
8th downstream of silt trap	lined			Lined								
9th downstream of silt trap	lined			Lined								
10th downstream of silt trap	lined			Lined								
11th downstream of silt trap	lined			Lined								
Upstream of runway deviation	12	12	12									
1st in runway deviation	12	12	12									
	12	12	12									

Observed Losses for SWSOOS1 line (cont).

Location	Corrosion loss observations (mm)											
	1997 Losses			2007 Losses			2009 Losses			2012 Losses		
	all	roof	wall	all	roof	wall	all	roof	wall	all	roof	wall
2nd in runway deviation	10	10	10									
	10	10	10									
3rd in runway deviation	6	6	6									
	6	6	6									
Downstream of runway deviation	12	12	12									
	12	12	12									
2nd D/S of runway deviations	16.5	20	13									
	20	25	15									
3rd D/S of runway deviations	20	25	15	Lined								
	20	25	15	Lined								
4th D/S of runway deviations	22	27	17	Lined								
	25	30	20	Lined								
5th D/S of runway deviations	25	30	20	Lined								
	25	30	20	Lined								
6th D/S of runway deviations	20	25	15	Lined								
	15	20	10	Lined								
Cross connection				Lined								
				Lined								
Cooks River Syphon SPS 38				Lined								
Downstream of syphon	12.5	15	10									
	10	10	10	Lined								
2nd downstream of syphon	15	15	15	Lined								
	15	15	15	Lined								
Mill ponds 1	12	12	12	Lined								
	12	12	12	Lined								
Mill ponds 2				Lined								
Crossover past southern cross dve	15	15	15	Lined								
	6	6	6	Lined								
First past water	6	6	6	Lined								
	9	12	6	Lined								
Approaching Hale st	6	6	6	Lined								
	6	6	6	Lined								
Hale St 1	6	6	6	Lined								
	6	6	6	Lined								
Hale St 2	9	12	6	Lined								
	9	12	6	Lined								
Hale and Underwood	6	6	6	Lined								
	6	6	6	Lined								
Hale and Chegwyn												
Hale and Botany Rd	6	6	6	Lined								
	6	6	6	Lined								
Hale and Botany Rd 2	8	6	10	Lined								
	8	6	10	Lined								
Hastings and Cranbrook	8	6	10	Lined								
	8	6	10	Lined								
Hastings and Tenterden	8	6	10	Lined								
	8	6	10	Lined								
1st past Tenderden	8	6	10							50		
	8	6	10							50		
	8	6	10							35		

Observed Losses for SWSOOS1 line (cont).

Location	Corrosion loss observations (mm)											
	1997 Losses			2007 Losses			2009 Losses			2012 Losses		
	all	roof	wall	all	roof	wall	all	roof	wall	all	roof	wall
2nd past Tenderden	8	6	10							13.5	20	7
	10	10	10							13.5	20	7
3rd past Tenderden	8	6	10							lined		
	8	6	10							lined		
4th past Tenderden										lined		
										lined		
William and Swinbourne st							45			50		
							45			50		
Wilson and Swinbourne St - Site 6 H2S monitor							50			50		
							50			60		
Stephen and Swinbourne St	17.5	25	10				35			50		
	17.5	25	10				35			50		
end of swinbourne st	12.5	15	10				35			50		
	12.5	15	10				35			50		
next to rail line	10	10	10							lined		
	10	10	10							lined		
on east side of rail line	10	10	10							50		
	10	10	10							50		
Orica plant 1										lined		
										lined		
Orica plant 2	17.5	25	10							lined		
	17.5	25	10							lined		
Orica plant 3							50			50		
							50			50		
Orica plant 4							50			50		
							50			50		
Orica plant 5	20	30	10				35			50		
	20	30	10				35			50		
Orica plant 6	15	20	10				45			45		
	15	20	10				45			80		
Orica plant 7							45			50		
							45			50		
Between Denison and Rhodes st 1	10	10	10				45			60		
	10	10	10				45			60		
Between Denison and Rhodes st 2							45			70		
							45			70		
Between Rhodes and Bunnerong 1	10	10	10				50			50		
							50			70	90	50
Between Rhodes and Bunnerong 1							25			45		
							25			45		
east of Bunnerong	15	20	10				25			60		
	15	20	10				25			60		
Howell Ave	8	6	10									
	8	6	10									
Duant Ave and Knowles Ave										35		
										35		
Pozieres ave												

Observed Losses for SWSOOS1 line (cont).

Location	Corrosion loss observations (mm)														
	1997 Losses			2007 Losses			2009 Losses			2012 Losses					
	all	roof	wall		all	roof	wall		all	roof	wall		all	roof	wall
Off end of landers Ave	8	6	10										50		
	8	6	10										40		
Near lawson St															
Off Kain Ave	6.5	3	10										50		
	6.5	3	10										50		
Cromwell Pl	6.5	3	10						35				50		
	6.5	3	10						35				50		
Malabar STP	6.5	3	10										100		
	6.5	3	10										100		

Appendix V. Calculated corrosion rates for SWSOOS1

Location	Corrosion rate (mm/yr)		
	<1997	1997-2007	2009-2012
Eve St Merge Chamber	0.03 0.03	2.20 2.20	
Opposite golf course 1	0.03 0.03	2.10 1.95	
Opposite golf course 2	0.03 0.05	2.95 3.05	
Flow monitoring station Arncliffe	0.10 0.11	2.38 2.58	
Cooks River Aqueduct	0.12 0.02	2.43 3.43	
Midway along muddy ck aqueduct	0.05 0.05	2.30 1.30	
Airport Land 1	0.06 0.06	2.30 3.80	
Airport Land on bend airport rising main	0.18 0.18	2.90 2.40	
Airport opposite East-west runway (+627m)			
Just past east west runway (+712m)			
2nd past east west runway			
Upstream of silt traps			
Just before silt pits by Penstock gates (817m)			
Airport Silt traps			
Downstream of silt trap			
2nd downstream of silt trap	0.07		
3rd downstream of silt trap	0.07		
4th downstream of silt trap	0.07		
5th downstream of silt trap	0.07		
6th downstream of silt trap	0.11 0.15		
7th downstream of silt trap	0.15		
8th downstream of silt trap	0.15		
9th downstream of silt trap	0.15		
10th downstream of silt trap	0.15		
11th downstream of silt trap	0.15		
Upstream of runway deviation	0.15		
1st in runway deviation	0.15		

Calculated corrosion rates for SWSOOS1 (Cont).

Location	Corrosion rate (mm/yr)		
	<1997	1997-2007	2009-2012
2nd in runway deviation	0.12	0.12	
3rd in runway deviation	0.07	0.07	
Downstream of runway deviation	0.15	0.15	
2nd D/S of runway deviations	0.20	0.25	
3rd D/S of runway deviations	0.25	0.25	
4th D/S of runway deviations	0.27	0.31	
5th D/S of runway deviations	0.31	0.31	
6th D/S of runway deviations	0.25	0.19	
Cross connection			
Cooks River Syphon SPS 38			
Downstream of syphon	0.15	0.12	
2nd downstream of syphon	0.17	0.17	
Mill ponds 1	0.14	0.14	
Mill ponds 2			
Crossover past southern cross dve	0.17	0.07	
First past water	0.07	0.10	
Approaching Hale st	0.07	0.07	
Hale St 1	0.07	0.07	
Hale St 2	0.10	0.10	
Hale and Underwood	0.07	0.07	
Hale and Chegwyn			
Hale and Botany Rd	0.07	0.07	
Hale and Botany Rd 2	0.09	0.09	
Hastings and Cranbrook	0.09	0.09	
Hastings and Tenterden	0.09	0.09	
1st past Tenterden	0.09	0.09	
2nd past Tenterden	0.09	0.11	

Calculated corrosion rates for SWSOOS1 (Cont).

Location	Corrosion rate (mm/yr)		
	<1997	1997-2007	2009-2012
3rd past Tenderden	0.09		
	0.09		
4th past Tenderden			
William and Swinbourne st			1.67
			1.67
Wilson and Swinbourne St - Site 6 H2S monitor			0.00
			3.33
Stephen and Swinbourne St	0.20		5.00
	0.20		5.00
end of swinbourne st	0.14		5.00
	0.14		5.00
next to rail line	0.11		
	0.11		
on east side of rail line	0.11		
	0.11		
Orica plant 1			
Orica plant 2	0.20		
	0.20		
Orica plant 3			0.00
			0.00
Orica plant 4			0.00
			0.00
Orica plant 5	0.23		5.00
	0.23		5.00
Orica plant 6	0.17		0.00
	0.17		0.00
Orica plant 7			1.67
			1.67
Between Denison and Rhodes st 1	0.11		5.00
	0.11		5.00
Between Denison and Rhodes st 2			8.33
			8.33
Between Rhodes and Bunnerong 1	0.11		0.00
			6.67
Between Rhodes and Bunnerong 1			6.67
			5.00
east of Bunnerong	0.17		8.33
	0.17		8.33
Howell Ave	0.09		
	0.09		
Duant Ave and Knowles Ave			
Pozieres ave			
Off end of landers Ave	0.09		
	0.09		
Near lawson St			
Off Kain Ave	0.07		
	0.07		
Cromwell Pl	0.07		5.00
	0.07		5.00
Malabar STP	0.07		
	0.07		

Appendix VI. SWSOOS2 South cell corrosion losses

Location	Corrosion Loss Observations (mm)								
	1997 Losses			2007 Losses			all	roof	wall
	all	roof	wall	all	roof	wall			
Eve St Merge	17.5	15	20	37.5	25	50			
	12.5	10	15	37.5	25	50			
D/S of merging chamber (1)	13.5	12	15	37.5	25	50			
	13.5	12	15	37.5	25	50			
D/S of merging chamber (2)	12.5	10	15	37.5	25	50			
	12.5	10	15	37.5	25	50			
D/S of merging chamber (3)	17.5	15	20						
	17.5	15	20						
D/S of merging chamber (4)	25	25	25	35	25	45			
	25	25	25	35	25	45			
Muddy Ck Aqueduct (1)	25	25	25						
	15	20	10						
Muddy Ck Aqueduct (2)	20	20	20	30	25	35			
	20	20	20	30	25	35			
Muddy Ck Aqueduct (3)	17.5	15	20						
	17.5	15	20						
Muddy Ck Aqueduct (4)	17.5	15	20						
	17.5	15	20						
Muddy Ck Aqueduct (5)	17.5	15	20	57.5	50	65			
	17.5	15	20	45	50	40			
Muddy Ck Aqueduct (6)	17.5	15	20	40	45	35			
	17.5	15	20	40	45	35			
Muddy Ck Aqueduct (7)	17.5	15	20	30	25	35			
	17.5	15	20	30	25	35			
Cross connection	17.5	15	20	30	25	35			
	17.5	15	20	30	25	35			
U/S of airport silt pits									
D/S of airport silt pits (1)	20	20	20						
	20	20	20						
D/S of airport silt pits (2)	20	20	20						
	20	20	20						
D/S of airport silt pits (3)	17.5	15	20						
	17.5	15	20						
D/S of airport silt pits (4)	17.5	15	20						
	17.5	15	20						

Observed corrosion losses for SWSOOS2 South cell (cont)

Location	Corrosion Loss Observations (mm)					
	1997 Losses			2007 Losses		
	all	roof	wall	all	roof	wall
D/S of airport silt pits (5)	20	20	20			
	20	20	20			
D/S of airport silt pits (6)	20	20	20			
	20	20	20			
D/S of airport silt pits (7)	20	20	20			
	20	20	20			
D/S of airport silt pits (8)	15	10	20			
	15	10	20			
D/S of airport silt pits (9)	20	20	20			
	20	20	20			
D/S of airport silt pits (10)	20	20	20			
	20	20	20			
Runway deviation (1)	17.5	15	20			
	17.5	15	20			
Runway deviation (2)	17.5	15	20			
	17.5	15	20			
Runway deviation (3)	20	20	20			
	20	20	20			
D/S runway deviation (1)	20	20	20			
	20	20	20			
D/S runway deviation (2)	20	20	20			
	20	20	20			
D/S runway deviation (3)	20	20	20			
	20	20	20			
D/S runway deviation (4)	20	20	20			
	15	15	15			
D/S runway deviation (5)	10.5	6	15			
	10.5	6	15			
D/S runway deviation (6)	15	15	15			
	15	15	15			
Opposite SPS38		17.5	15	20	32.5	30
		17.5	15	20	32.5	30
					35	35

Observed corrosion losses for SWSOOS2 South cell (cont)

Location	Corrosion Loss Observations (mm)					
	1997 Losses			2007 Losses		
	all	roof	wall	all	roof	wall
D/S SPS38				32.5	30	35
				45		
Crossover in airport land	9	9	9	20	20	
	9	9	9	45		
Under General Holmes flyover	16	12	20	40	40	
	16	12	20			
U/S Hale St	12	12	12	35	35	
	12	12	12	30	30	30
22-24 Booralee St	16	12	20	40		
	16	12	20	50		
Adjacent Booralee St	16	12	20	20		
	16	12	20	20		
Rear of 1 - Building 9 Hale St	16	12	20	20		
	16	12	20	20		
Rear of 1 - Building 6 Hale St	16	12	20	30		
	16	12	20	45		
Rear of 1 Hale St	16	12	20	20		
	16	12	20	45		
30-34 the Esplanade	16	12	20	30		
	16	12	20	30		
13 The Esplanade	16	12	20	30		
	16	12	20	30		
Prior to Hayden Place	25	25	25	30		
	25	25	25	70		
Opposite Hayden Place	22.5	20	25	50		
	22.5	20	25	40		
Tupia St	25	25	25	40		
	25	25	25	60		
Opp Waratah St	25	25	25	60		
	25	25	25	70		
21 Dent St	25	25	25	70		
	30	30	30	85		
Hill St rear of vacant block	20	20	20	47.5	45	50
	20	20	20	35	35	
Hill St front of vacant block	20	20	20	50		
	20	20	20	40		
15-17 Greenfield	17.5	15	20	20	20	
	17.5	15	20	25	25	
1763-1765 Botany Rd	22.5	22.5	22.5	30		
	22.5	22.5	22.5	45		

Observed corrosion losses for SWSOOS2 South cell (cont)

Location	Corrosion Loss Observations (mm)					
	1997 Losses			2007 Losses		
	all	roof	wall	all	roof	wall
1767-1781 Botany Rd	20	20	20	30		
	20	20	20	30		
1801 Botany Rd	25	25	25	30		
	25	25	25	70		
Factory units Discovery Cove	25	25	25	50		
	37.5	50	25			
Railway fence Botany rd	47.5	70	25			
	47.5	70	25			
2-12 Beauchamp rd	55	80	30			
	55	80	30			
89 Beauchamp Rd	60	90	30			
	60	90	30			
7-98 Perry St	17.5	15	20			
	17.5	15	20			
22 Raymond Ave	65	100	30			
	65	100	30			
McAuley St	65	100	30			
	65	100	30			
83 Perry St	47.5	75	20			
	20	20	20			

Appendix VII. Calculated corrosion rates for SWSOOS2 South Cell

Location	Corrosion rate (mm/yr)	
	<1997	1997-2007
Eve St Merge	0.31	2.00
	0.22	2.50
D/S of merging chamber (1)	0.24	2.40
	0.24	2.40
D/S of merging chamber (2)	0.22	2.50
	0.22	2.50
D/S of merging chamber (3)	0.31	
	0.31	
D/S of merging chamber (4)	0.45	1.00
	0.45	1.00
Muddy Ck Aqueduct (1)	0.45	
	0.27	
Muddy Ck Aqueduct (2)	0.36	1.00
	0.36	1.00
Muddy Ck Aqueduct (3)	0.31	
	0.31	
Muddy Ck Aqueduct (4)	0.31	
	0.31	
Muddy Ck Aqueduct (5)	0.31	4.00
	0.31	2.75
Muddy Ck Aqueduct (6)	0.31	2.25
	0.31	2.25
Muddy Ck Aqueduct (7)	0.31	1.25
	0.31	1.25
Cross connection	0.31	1.25
	0.31	1.25
U/S of airport silt pits		
D/S of airport silt pits (1)	0.36	
	0.36	
D/S of airport silt pits (2)	0.36	
	0.36	
D/S of airport silt pits (3)	0.31	
	0.31	
D/S of airport silt pits (4)	0.31	
	0.31	
D/S of airport silt pits (5)	0.36	
	0.36	
D/S of airport silt pits (6)	0.36	
	0.36	
D/S of airport silt pits (7)	0.36	
	0.36	
D/S of airport silt pits (8)	0.27	
	0.27	
D/S of airport silt pits (9)	0.36	
	0.36	
D/S of airport silt pits (10)	0.36	
	0.36	
Runway deviation (1)	0.31	
	0.31	
Runway deviation (2)	0.31	
	0.31	
Runway deviation (3)	0.36	
	0.36	

Calculated corrosion rates for SWSOOS2 South Cell (Cont).

Location	Corrosion rate (mm/yr)	
	<1997	1997-2007
D/S runway deviation (1)	0.36	
	0.36	
D/S runway deviation (2)	0.36	
	0.36	
D/S runway deviation (3)	0.36	
	0.36	
D/S runway deviation (4)	0.36	
	0.27	
D/S runway deviation (5)	0.19	
	0.19	
D/S runway deviation (6)	0.27	
	0.27	
Opposite SPS38	0.31	1.50
	0.31	1.50
D/S SPS38		3.25
		4.50
Crossover in airport land	0.16	1.10
	0.16	3.60
Under General Holmes flyover	0.29	2.40
	0.29	
U/S Hale St	0.21	2.30
	0.21	1.80
22-24 Booralee St	0.29	2.40
	0.29	3.40
Adjacent Booralee St	0.29	0.40
	0.29	0.40
Rear of 1 - Building 9 Hale St	0.29	0.40
	0.29	0.40
Rear of 1 - Building 6 Hale St	0.29	1.40
	0.29	2.90
Rear of 1 Hale St	0.29	0.40
	0.29	2.90
30-34 the Esplanade	0.29	1.40
	0.29	1.40
13 The Esplanade	0.29	1.40
	0.29	1.40
Prior to Hayden Place	0.45	0.50
	0.45	4.50
Opposite Hayden Place	0.40	2.75
	0.40	1.75
Tupia St	0.45	1.50
	0.45	3.50
Opp Waratah St	0.45	3.50
	0.45	4.50
21 Dent St	0.45	4.50
	0.54	5.50
Hill St rear of vacant block	0.36	2.75
	0.36	1.50
Hill St front of vacant block	0.36	3.00
	0.36	2.00
15-17 Greenfield	0.31	0.25
	0.31	0.75
1763-1765 Botany Rd	0.40	0.75
	0.40	2.25
1767-1781 Botany Rd	0.36	1.00

Calculated corrosion rates for SWSOOS2 South Cell (Cont).

Location	Corrosion rate (mm/yr)	
	<1997	1997-2007
1801 Botany Rd	0.36	1.00
	0.45	0.50
	0.45	4.50
Factory units Discovery Cove	0.45	2.50
	0.67	
Railway fence Botany rd	0.85	
	0.85	
2-12 Beauchamp rd	0.98	
	0.98	
89 Beauchamp Rd	1.07	
	1.07	
7-98 Perry St	0.31	
	0.31	
22 Raymond Ave	1.16	
	1.16	
McAuley St	1.16	
	1.16	
83 Perry St	0.85	
	0.36	

Appendix VIII. SWSOOS2 North Cell corrosion losses

Location	Corrosion Loss Observations (mm)					
	1997 Losses			2007 Losses		
	all	roof	wall	all	roof	wall
Eve St Merge	10.5	6	15	32.5	25	40
	10.5	6	15	30	25	35
D/S of merging chamber (1)	8	6	10	30	25	35
	8	6	10	30	25	35
D/S of merging chamber (2)	8	6	10	27.5	15	40
	8	6	10	35	20	50
D/S of merging chamber (3)	8	6	10			
	8	6	10			
D/S of merging chamber (4)	17.5	15	20	30	20	40
	17.5	15	20	37.5	25	50
Muddy Ck Aqueduct (1)	11.5	3	20			
	11.5	3	20			
Muddy Ck Aqueduct (2)	11.5	3	20	32.5	25	40
	11.5	3	20	32.5	25	40
Muddy Ck Aqueduct (3)	6.5	3	10			
	6.5	3	10			
Muddy Ck Aqueduct (4)	13	6	20			
	13	6	20			
Muddy Ck Aqueduct (5)	13	6	20	37.5	30	45
	13	6	20	37.5	30	45
Muddy Ck Aqueduct (6)	6.5	3	10	35	25	45
	6.5	3	10	35	25	45
Muddy Ck Aqueduct (7)	6.5	3	10	33.8	28	40
	6.5	3	10	33.8	28	40
D/S of aqueduct	6.5	3	10	33.8	28	40
	6.5	3	10	33.8	28	40
Cross connection	9	6	12	Lined		
	9	6	12	Lined		
U/S of airport silt pits				Lined		
				Lined		
D/S of airport silt pits (1)	7.5	3	12	Lined		
	7.5	3	12	Lined		
D/S of airport silt pits (2)	13	6	20	Lined		
	13	6	20	Lined		
D/S of airport silt pits (3)	9	6	12	Lined		
	9	6	12	Lined		
D/S of airport silt pits (4)	9	6	12	Lined		
	9	6	12	Lined		
D/S of airport silt pits (5)	15	10	20	Lined		
	15	10	20	Lined		
D/S of airport silt pits (6)	15	10	20	Lined		
	15	10	20	Lined		
D/S of airport silt pits (7)	16	12	20	Lined		
	16	12	20	Lined		
D/S of airport silt pits (8)	8	6	10	Lined		
	8	6	10	Lined		
D/S of airport silt pits (9)	9	6	12	Lined		
	9	6	12	Lined		
D/S of airport silt pits (10)	10.5	6	15	Lined		
	10.5	6	15	Lined		
Runway deviation (1)	16	12	20	Lined		
	16	12	20	Lined		

Observed corrosion Losses for SWSOOS2 North Cell (Cont).

Location	Corrosion Loss Observations (mm)					
	1997 Losses			2007 Losses		
	all	roof	wall	all	roof	wall
Runway deviation (2)	8.75	7.5	10		Lined	
	8.75	7.5	10		Lined	
Runway deviation (3)	3	3	3		Lined	
	3	3	3		Lined	
D/S runway deviation (1)	16	12	20		Lined	
	16	12	20		Lined	
D/S runway deviation (2)	12	12	12		Lined	
	12	12	12		Lined	
D/S runway deviation (3)	12	12	12		Lined	
	12	12	12		Lined	
D/S runway deviation (4)	10	10	10		Lined	
	10	10	10		Lined	
D/S runway deviation (5)	10	12	8		Lined	
	10	12	8		Lined	
D/S runway deviation (6)	11	12	10		Lined	
	11	12	10		Lined	
Opposite SPS38	17.5	15	20			
D/S SPS38	15	15	15	35	35	
	15	15	15	35	35	
Between siphon and crossover				35	35	
				35	35	
Crossover in airport land	15	15	15	35	35	
	15	15	15	35	35	
Under General Holmes flyover	8	10	6	30	30	
	8	10	6	35	35	
U/S Hale St	10.5	15	6	40		
	10.5	15	6	40		
22-24 Booralee St	15	15	15	40		
	15	15	15	40		
Adjacent Booralee St	17.5	15	20	40		
	17.5	15	20	40		
Rear of 1 - Building 9 Hale St	15	15	15	45		
	15	15	15	45		
Rear of 1 - Building 6 Hale St	20	20	20	50		
	20	20	20	50		
Rear of 1 Hale St	15	15	15	40		
	15	15	15	40		
30-34 the Esplanade	16	12	20	40		
	16	12	20	35		
13 The Esplanade	17.5	15	20	35		
	17.5	15	20	35		
Prior to Hayden Place	20	20	20	30		
	20	20	20	30		
Opposite Hayden Place	15	15	15	60		
	15	15	15	60		
Tupia St	25	25	25	65		
	25	25	25	75		
Opp Waratah St	25	25	25	45		
	25	25	25	60		
21 Dent St	30	30	30	70		
	50	50	50	90		

Observed corrosion Losses for SWSOOS2 North Cell (Cont).

Location	Corrosion Loss Observations (mm)					
	1997 Losses			2007 Losses		
	all	roof	wall	all	roof	wall
Hill St rear of vacant block	30	30	30	45		
	30	30	30	45		
Hill St front of vacant block	25	25	25	50		
	25	25	25	20		
15-17 Greenfield	20	20	20	20		
	20	20	20	30		
1763-1765 Botany Rd	20	20	20	50		
	20	20	20	50		
1767-1781 Botany Rd	20	20	20	20		
	20	20	20	20		
1801 Botany Rd	22.5	20	25	15		
	22.5	20	25	15		
Factory units Discovery Cove	22.5	20	25		Lined	
	22.5	20	25		Lined	
Railway fence Botany rd	30	30	30		Lined	
	30	30	30		Lined	
2-12 Beauchamp rd	40	50	30		Lined	
	40	50	30		Lined	
89 Beauchamp Rd	45	60	30		Lined	
	45	60	30		Lined	
7-98 Perry St	20	20	20		Lined	
	20	20	20		Lined	
22 Raymond Ave	35	35	35		Lined	
	50	50	50		Lined	
McAuley St	35	35	35		Lined	
	42.5	50	35		Lined	
83 Perry St	47.5	75	20		Lined	
	20	20	20		Lined	
115 Perry St					Lined	
					Lined	
523 Bunnerong Rd	25	25	25	50		
	25	25	25	50		
Gwydir Ave				50		
				50		
1 Barwon Cres	22.5	25	20	50		
	22.5	25	20	50		
Lawson St	25	25	25			
	25	25	25			
Landy St	20	25	15			
	17.5	20	15			

Appendix IX. Calculated corrosion rates for SWSOOS2 North Cell

Location	Corrosion rate (mm/yr)	
	<1997	1997-2007
Eve St Merge	0.19	2.20
	0.19	1.95
D/S of merging chamber (1)	0.14	2.20
	0.14	2.20
D/S of merging chamber (2)	0.14	1.95
	0.14	2.70
D/S of merging chamber (3)	0.14	
	0.14	
D/S of merging chamber (4)	0.31	1.25
	0.31	2.00
Muddy Ck Aqueduct (1)	0.21	
	0.21	
Muddy Ck Aqueduct (2)	0.21	2.10
	0.21	2.10
Muddy Ck Aqueduct (3)	0.12	
	0.12	
Muddy Ck Aqueduct (4)	0.23	
	0.23	
Muddy Ck Aqueduct (5)	0.23	2.45
	0.23	2.45
Muddy Ck Aqueduct (6)	0.12	2.85
	0.12	2.85
Muddy Ck Aqueduct (7)	0.12	2.73
	0.12	2.73
D/S of aqueduct	0.12	2.73
	0.12	2.73
Cross connection	0.16	
	0.16	
U/S of airport silt pits		
D/S of airport silt pits (1)	0.13	
	0.13	
D/S of airport silt pits (2)	0.23	
	0.23	
D/S of airport silt pits (3)	0.16	
	0.16	
D/S of airport silt pits (4)	0.16	
	0.16	
D/S of airport silt pits (5)	0.27	
	0.27	
D/S of airport silt pits (6)	0.27	
	0.27	
D/S of airport silt pits (7)	0.29	
	0.29	
D/S of airport silt pits (8)	0.14	
	0.14	
D/S of airport silt pits (9)	0.16	
	0.16	
D/S of airport silt pits (10)	0.19	
	0.19	
Runway deviation (1)	0.29	
	0.29	

Calculated corrosion rates for SWSOOS2 North Cell (Cont).

Location	Corrosion rate (mm/yr)	
	<1997	1997-2007
Runway deviation (2)	0.16	
	0.16	
Runway deviation (3)	0.05	
	0.05	
D/S runway deviation (1)	0.29	
	0.29	
D/S runway deviation (2)	0.21	
	0.21	
D/S runway deviation (3)	0.21	
	0.21	
D/S runway deviation (4)	0.18	
	0.18	
D/S runway deviation (5)	0.18	
	0.18	
D/S runway deviation (6)	0.20	
	0.20	
Opposite SPS38	0.31	
D/S SPS38	0.27	2.00
	0.27	2.00
Between siphon and crossover		3.50
		3.50
Crossover in airport land	0.27	2.00
	0.27	2.00
Under General Holmes flyover	0.14	2.20
	0.14	2.70
U/S Hale St	0.19	2.95
	0.19	2.95
22-24 Booralee St	0.27	2.50
	0.27	2.50
Adjacent Booralee St	0.31	2.25
	0.31	2.25
Rear of 1 - Building 9 Hale St	0.27	3.00
	0.27	3.00
Rear of 1 - Building 6 Hale St	0.36	3.00
	0.36	3.00
Rear of 1 Hale St	0.27	2.50
	0.27	2.50
30-34 the Esplanade	0.29	2.40
	0.29	1.90
13 The Esplanade	0.31	1.75
	0.31	1.75
Prior to Hayden Place	0.36	1.00
	0.36	1.00
Opposite Hayden Place	0.27	4.50
	0.27	4.50
Tupia St	0.45	4.00
	0.45	5.00
Opp Waratah St	0.45	2.00
	0.45	3.50
21 Dent St	0.54	4.00
	0.89	4.00

Calculated corrosion rates for SWSOOS2 North Cell (Cont).

Location	Corrosion rate (mm/yr)	
	<1997	1997-2007
Hill St rear of vacant block	0.54	1.50
	0.54	1.50
Hill St front of vacant block	0.45	2.50
	0.45	-0.50
15-17 Greenfield	0.36	0.00
	0.36	1.00
1763-1765 Botany Rd	0.36	3.00
	0.36	3.00
1767-1781 Botany Rd	0.36	0.00
	0.36	0.00
1801 Botany Rd	0.40	
	0.40	
Factory units Discovery Cove	0.40	
	0.40	
Railway fence Botany rd	0.54	
	0.54	
2-12 Beauchamp rd	0.71	
	0.71	
89 Beauchamp Rd	0.80	
	0.80	
7-98 Perry St	0.36	
	0.36	
22 Raymond Ave	0.63	
	0.89	
McAuley St	0.63	
	0.76	
83 Perry St	0.85	
	0.36	
115 Perry St		
523 Bunnerong Rd	0.45	2.50
	0.45	2.50
Gwydir Ave		5.00
		5.00
1 Barwon Cres	0.40	2.75
	0.40	2.75
Lawson St	0.45	
	0.45	
Landy St	0.36	
	0.31	

Appendix X. NSOOS Corrosion losses

Location	Corrosion Loss Observed (mm)														
	1993 Losses			2007 Losses			2008 Losses			2009 Losses			2010 Losses		
	all	roof	wall		all	roof	wall		all	roof	wall		all	roof	wall
30 Briens Rd Northmead													2		
Campbell St													2		
48 Caprera Rd													15		15
19 Walter Pl													15		15
Lake Parramatta Reserve (1)													15		
Lake Parramatta Reserve (2)													15		
38 Alanas St													15		
18 greens Rd													35		
2 Conway Pl													35		
4 Bellos Rd													18.8	7.5	30
57 Kissing Pt Rd	50												22.5	15	30
Station St	15												22.5	15	30
90 Kissing Pt Rd	10												22.5	15	30
Elder Rd	10												22.5	15	30
159 Park Rd	10												22.5	15	30
22 Baronbali St	10												22.5	15	30
Kirby St	10												35	35	
12 Ronald St	10												50	50	
59 Ulm St	10												50	50	
163 Spurway St	10												60	60	
Bartlett St	10												60	60	
4 Chester Pl	10												35	35	
Cowells lane	10												2.5	2.5	
Cowells lane (2)	10												2.5	2.5	
36 William St	10														

Observed Losses for NSOOS line (cont).

Location	Corrosion Loss Observed (mm)									2009 Losses			2010 Losses			
	1993 Losses			2007 Losses			2008 Losses				all	roof	wall		all	roof
		all	roof	wall		all	roof	wall		all	roof	wall		all	roof	wall
31 Marsden Rd		10								20	20					
		15								50	50					
3 Eulalia St		20								45	45					
		20								50	50					
Maze Pk		20														
		20														
152 Darvall Rd		20								40	50	30				
		20								50	50					
1 Mirool St		20								50	50					
		20								10	10					
4 Shaftsbury Rd		20								20	20					
		20								30	30	30				
Dickson Ave		10								50	50					
		10								60	60					
Market St		10								40	40					
		10								5	5					
Wollwoths Carpark		10														
		10														
West Pde		15								20	20					
		15								40	40					
Herbert St		20														
		20														
25 Herbert St		20								20	20					
		20								30	30					
Falconer St		20								40	40					
		10								20	20					
Linton Ave		10								50	60	40				
		10								40	40					
Griffiths Ave		10								5	5					
		10								5	5					
33 Shepherd St		10								5	5					
		10								30	30					
34 Belmore St		10								5	5					
		10								80	80					
721 Victoria Pde		10								5	5					
		10														
59 Princes St		10								5	5					
		10								80	80					
Linley Way		10								5	5					
		10								50	50					
43 Charles St		10								60	60					
		10								30	30					
Arnold St		10								47.5	55	40				
		10								40	40					
Curtis St		10								30	30					
		10														
Tyagarah Pk Aqueduct W		15														
		15														
Tyagarah Pk Aqueduct E		10								50	30	70				
		10								60	60					
Spencer St		10								100	100					
		10								50	50					
Peel Pk		10								50	50					
		10								35	35					
43 Western Cres		10								50	50					
		10								40	40					
26 Hepburn Ave		10								20	20					
		10								55	55					
Pittwater Rd		10								50	50					
		10								100	100					
Mars St		10								40	40					
		10								50	50					
5A Milling St		10								50	50					
		10														

Observed Losses for NSOOS line (cont).

Location	Corrosion Loss Observed (mm)									2009 Losses			2010 Losses			
	1993 Losses			2007 Losses			2008 Losses				all	roof	wall		all	roof
		all	roof	wall		all	roof	wall		all	roof	wall		all	roof	wall
Augustine St		10								50	50					
		10								100	100					
Boronia Pk		10								50	50					
		10								50	50					
Prince St		15								40	40					
		15								30	30					
120 High St		15								50	50					
		25								80	80					
West Lane Cove Siphon house (1)		40														
		40														
West Lane Cove Siphon house (2)																
East Lane Cove Siphon House		25								27.5	35	20				
		25								15	15	15				
Burns Bay Aqueduct W		20								15	15	15				
		20								32.5	50	15				
Burns Bay Aqueduct E		25								32.5	50	15				
		25								15						
Riverview College		10								27.5	40	15				
		10								10						
Riverview St		10								32.5	50	15				
		10								20						
104 Tambourine Bay Rd		10								31.3	50	12.5				
		10								15						
15 Kallaroo St		10								21.3	30	12.5				
		10								20						
Dettman Ave		10								40	50	30				
		10								20						
33 Kenneth St		10								20						
		12								15		15				
Woodford Bay		12								15						
		12								27.5	30	25				
12 Private Rd		10								20						
		10								45	75	15				
Gore Creek Aqueduct U/S		10														
		25														
Gore Ck Aqueduct D/S		25								50	25	75				
		10								50	25	75				
28 Carlotta St		10								40						
		10								60	100	20				
10 Vista St		12								50	75	25				
		18								50	75	25				
4 Russell St		15								50						
		15								50	75	25				
Carlyle St		15								40						
		15								65	100	30				
387 Pacific Hwy		15								25						
		15								37.5	50	25				
135 West St		15								60						
		15								52.5	75	30				
Ernest St		15								65						
		15								52.5	75	30				
Cammeray Golf Course (1)		15								50						
		15								52.5	75	30				
Cammeray Golf Course (2)		15								125						
		15								40	40	40				

Observed Losses for NSOOS line (cont).

Location	Corrosion Loss Observed (mm)														
	1993 Losses			2007 Losses			2008 Losses			2009 Losses			2010 Losses		
	all	roof	wall		all	roof	wall		all	roof	wall		all	roof	wall
161 Young St	25														
Brightmore Res. Aqueduct U/S	30														
Brightmore Res. Aqueduct D/S	20														
5th Ave	20								43.8	62.5	25				
Quakers Hat Bay Aqueduct U/S	20								20						
Quakers Hat Bay Aqueduct	20								43.8	62.5	25				
4 Central Ave	20														
Upper Split Rd	20														
Split Siphon House	60														
Clontarf Siphon House	60														
Clontarf Aqueduct	10														
Amiens Rd	15														
Ernest Rd	25														
Jackson St	25														
Burton St	25														
Kings and Lauderdale	20														
Ashley St	20														
9 George St	20														
15 Eustace St	20														

Appendix XI. NSOOS calculated corrosion rates

Location	Corrosion rate (mm/yr)	
	<1993	1993-2007,8,9
57 Kissing Pt Rd	0.79	
	0.24	
Station St	0.16	
	0.16	
90 Kissing Pt Rd	0.16	0.31
	0.16	0.00
Elder Rd	0.16	0.00
	0.16	0.00
159 Park Rd	0.16	0.00
	0.16	0.63
22 Baronbali St	0.16	0.00
	0.16	0.00
Kirby St	0.16	0.31
	0.16	
12 Ronald St	0.16	
	0.16	
59 Ulm St	0.16	0.31
	0.16	0.00
163 Spurway St	0.16	1.25
	0.16	1.25
Bartlett St	0.16	1.25
	0.16	0.00
4 Chester Pl	0.16	0.31
	0.16	0.00
Cowells lane	0.16	
	0.16	
Cowells lane (2)	0.16	1.25
	0.16	0.00
36 William St	0.16	1.25
	0.16	0.31
31 Marsden Rd	0.16	0.63
	0.24	2.19
3 Eulalia St	0.32	1.56
	0.32	1.88
Maze Pk	0.32	
	0.32	
152 Darvall Rd	0.32	1.25
	0.32	1.88
1 Mirool St	0.32	1.88
	0.32	-0.63
4 Shaftsbury Rd	0.32	0.00
	0.32	0.63
Dickson Ave	0.16	2.50
	0.16	3.13
Market St	0.16	1.88
	0.16	-0.31
Wollwoths Carpark	0.16	
	0.16	
West Pde	0.24	0.31
	0.24	1.56
Herbert St	0.32	
	0.32	
25 Herbert St	0.32	
	0.32	0.00
Falconer St	0.32	0.63
	0.16	1.88

NSOOS calculated corrosion rates (Cont).

Location	Corrosion rate (mm/yr)	
	<1993	1993-2007,8,9
Linton Ave	0.16	0.63
	0.16	2.50
Griffiths Ave	0.16	1.88
	0.16	-0.31
33 Shepherd St	0.16	-0.31
	0.16	-0.31
34 Belmore St	0.16	1.25
	0.16	-0.31
721 Victoria Pde	0.16	4.38
	0.16	-0.31
59 Princes St	0.16	
	0.16	-0.31
Linley Way	0.16	4.38
	0.16	-0.31
43 Charles St	0.16	2.50
	0.16	3.13
Arnold St	0.16	1.25
	0.16	2.34
Curtis St	0.16	1.88
	0.16	1.25
Tyagarah Pk Aqueduct W	0.24	
	0.24	
Tyagarah Pk Aqueduct E	0.16	
	0.16	2.50
Spencer St	0.16	3.13
	0.16	5.63
Peel Pk	0.16	2.50
	0.16	2.50
43 Western Cres	0.16	2.50
	0.16	1.56
26 Hepburn Ave	0.16	2.50
	0.16	1.88
Pittwater Rd	0.16	0.63
	0.16	2.81
Mars St	0.16	2.50
	0.16	5.63
5A Milling St	0.16	1.88
	0.16	2.50
Augustine St	0.16	2.50
	0.16	5.63
Boronia Pk	0.16	2.50
	0.16	2.50
Prince St	0.24	1.56
	0.24	0.94
120 High St	0.24	2.19
	0.40	3.44
West Lane Cove Siphon house (1)	0.63	
	0.63	
West Lane Cove Siphon house (2)		
East Lane Cove Siphon House	0.40	
	0.40	0.17
Burns Bay Aqueduct W	0.32	-0.33
	0.32	-0.33
Burns Bay Aqueduct E	0.40	0.50
	0.40	0.50
Riverview College	0.16	0.33
	0.16	1.17
Riverview St	0.16	0.00
	0.16	1.50
104 Tambourine Bay Rd	0.16	0.67
	0.16	1.42

NSOOS calculated corrosion rates (Cont).

Location	Corrosion rate (mm/yr)	
	<1993	1993-2007,8,9
15 Kallaroo St	0.16	0.33
	0.16	0.75
Dettman Ave	0.16	0.67
	0.16	2.00
33 Kenneth St	0.16	0.67
	0.19	0.20
Woodford Bay	0.19	0.20
	0.19	1.03
12 Private Rd	0.16	0.67
	0.16	2.33
Gore Creek Aqueduct U/S	0.16	
	0.40	
Gore Ck Aqueduct D/S	0.40	1.67
	0.16	2.67
28 Carlotta St	0.16	2.00
	0.16	3.33
10 Vista St	0.19	2.53
	0.29	2.13
4 Russell St	0.23	2.33
	0.23	2.33
Carlyle St	0.23	1.67
	0.23	3.33
387 Pacific Hwy	0.23	0.67
	0.23	1.50
135 West St	0.23	3.00
	0.23	2.50
Ernest St	0.23	3.33
	0.23	2.50
Cammeray Golf Course (1)	0.23	2.33
	0.23	2.50
Cammeray Golf Course (2)	0.22	7.33
	0.22	1.67
161 Young St	0.37	
	0.37	
Brightmore Res. Aqueduct U/S	0.45	
	0.45	
Brightmore Res. Aqueduct D/S	0.30	
	0.30	1.58
5th Ave	0.30	0.00
	0.22	1.92
Quakers Hat Bay Aqueduct U/S	0.30	
	0.30	3.33
Quakers Hat Bay Aqueduct	0.30	2.00
	0.30	2.00
4 Central Ave	0.30	0.00
	0.30	2.00
Upper Split Rd	0.30	0.67
	0.30	0.67
Split Siphon House	0.90	
	0.90	
Clontarf Siphon House	0.15	
	0.22	1.79
Clontarf Aqueduct	0.37	0.36
	0.37	1.79
Amiens Rd	0.37	1.79
	0.37	3.57
Ernest Rd	0.37	3.21
	0.37	3.93
Jackson St	0.30	2.14
	0.30	2.14
Burton St	0.30	2.14
	0.30	2.14
Kings and Lauderdale	0.30	
	0.30	
Ashley St	0.30	1.43
	0.30	1.43
9 George St	0.30	1.43
	0.30	
15 Eustace St	0.30	2.14

Appendix XII. Summary of NGRS environmental data

	Site 1 LTM Summary					
	Av H2S	90% H2S	95%H2S	Av T	90% T	95% T
2000	13.4	32.9	40.3	25.1	26.7	27.1
2001						
2002						
2003						
2004	6.8	15.9	22.5	20.0	25.2	26.5
2005	9.9	25.5	39.7	24.1	28.3	29.1
2006	10.7	27.6	40.6	21.3	27.1	28.2
2007	9.5	23.6	34.5	21.0	26.1	26.6
2008	3.3	8.6	13.0	19.1	26.3	27.7
2009	1.3	1.7	5.1	21.4	27.1	28.4
2010	1.8	2.0	5.2	21.8	27.2	28.3

	Site 2 LTM Summary					
	Av H2S	90% H2S	95%H2S	Av T	90% T	95% T
2000						
2001						
2002						
2003						
2004	2.1	4.7	5.7	20.8	25.9	27.3
2005	1.4	3.2	3.9	23.8	28.1	28.8
2006	1.0	2.6	3.3	22.9	27.8	28.8
2007	1.2	3.0	6.7	22.5	27.6	28.6
2008	0.9	2.0	2.5	22.2	27.4	28.6
2009						
2010						

	Site 3 LTM Summary					
	Av H2S	90% H2S	95%H2S	Av T	90% T	95% T
2000						
2001						
2002						
2003						
2004	1.1	3.1	4.0	19.9	25.1	26.4
2005	0.7	2.1	3.4	22.4	27.2	28.8
2006	1.5	3.7	9.8	21.2	27.0	28.6
2007	1.2	3.0	6.2	21.7	26.8	28.3
2008	0.8	1.6	2.1	20.8	25.9	27.4
2009						
2010						

Summary of NGRS environmental data (Cont).

Salt pan OCU Summary

	Inlet			Outlet			Av T	90% T	95% T
	Av H2S	90% H2S	95%H2S	Av H2S	90% H2S	95%H2S			
2004	9.0	19.0	22.1	0.7	1.4	1.6	32.8	42.2	45.0
2005	8.0	14.0	20.0	0.2	0.6	1.2	30.3	36.0	40.7
2006	5.7	14.0	19.0	0.4	0.9	1.1	29.3	37.3	40.6
2007	5.7	14.4	19.6	0.1	0.5	0.7	29.4	38.2	41.1
2008	3.7	7.9	10.4	0.3	0.4	0.4	25.2	32.3	36.2

West St OCU Summary

	Inlet			Outlet			Av T	90% T	95% T
	Av H2S	90% H2S	95%H2S	Av H2S	90% H2S	95%H2S			
2004	2.2	6.3	8.3	0.3	0.6	0.6	28.1	37.8	41.8
2005	15.8	50.0	50.0	0.4	0.7	1.2	26.5	35.9	41.6
2006	6.4	17.4	25.1	0.5	0.9	2.1	27.3	37.3	41.8
2007	5.6	11.8	14.8	0.5	1.0	1.2	28.7	39.1	44.3
2008	7.2	16.1	20.3	0.3	0.6	1.0	27.1	37.6	42.4

Eve St OCU Summary

	Inlet			Outlet			Av T	90% T	95% T
	Av H2S	90% H2S	95%H2S	Av H2S	90% H2S	95%H2S			
2004	2.3	6.9	9.1				28.1	39.0	41.9
2005	9.5	27.4	43.8				28.9	40.3	43.7
2006	13.6	38.0	49.4				29.6	40.0	43.2
2007	4.8	10.8	16.6				30.2	41.0	44.1
2008	4.2	11.2	14.6				26.1	38.0	41.7

Summary of NGRS environmental data (Cont).

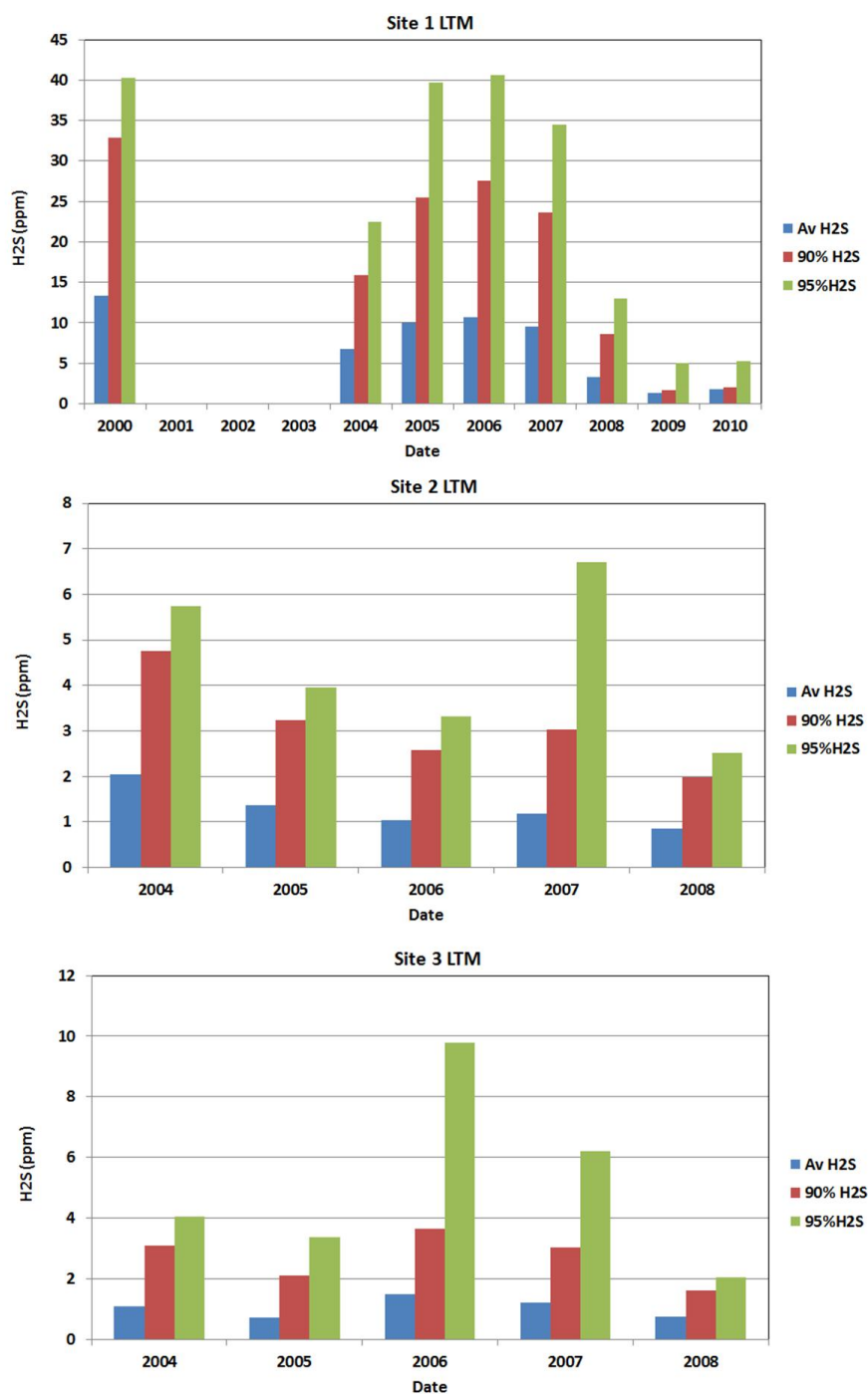


Figure 162. H₂S levels recorded at the three NGRS long term monitoring sites.

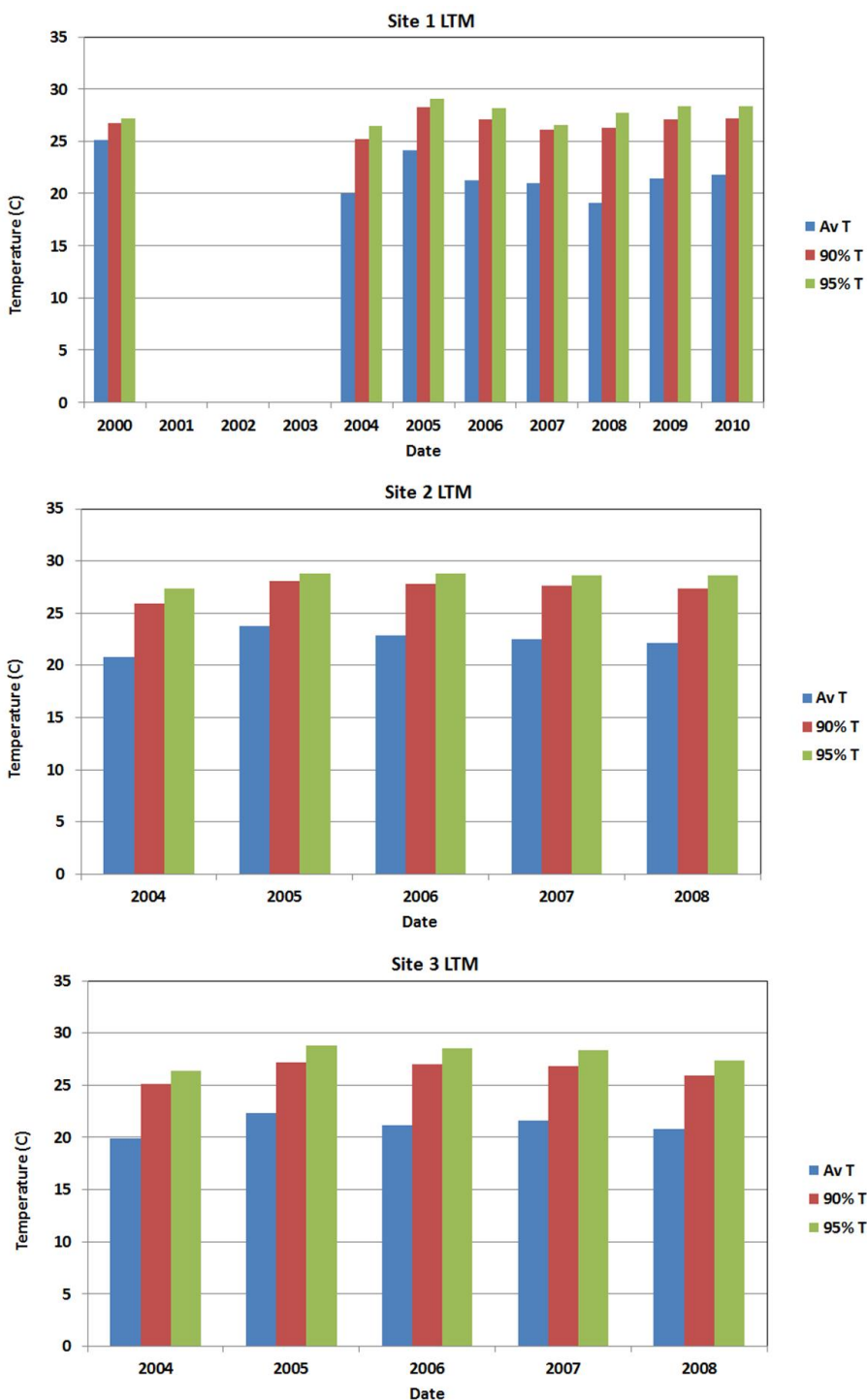


Figure 163. Gas temperature recorded at the three NGRS long term monitoring sites.

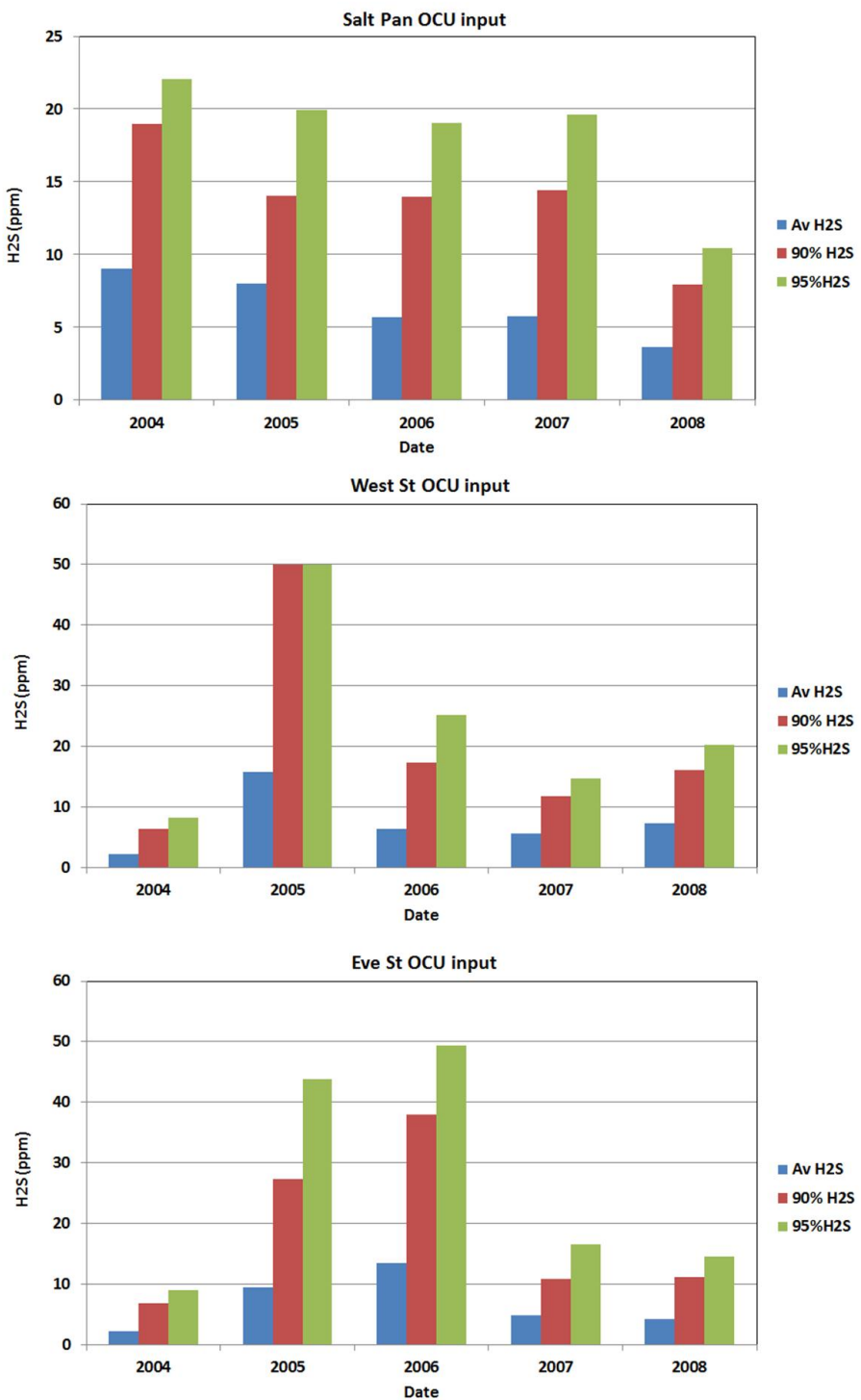


Figure 164. Inlet H₂S levels recorded at the three NGRS OCU stations.

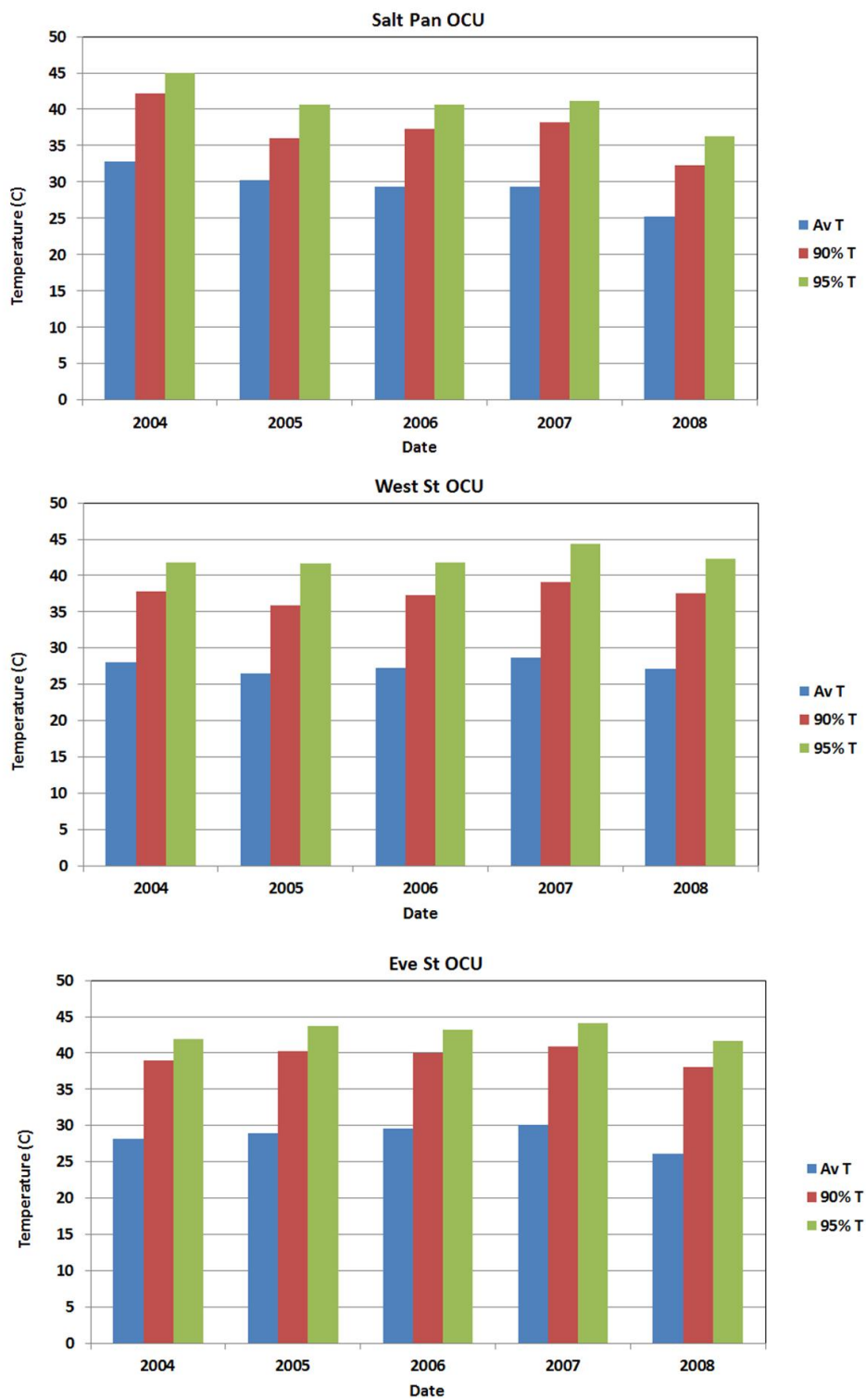


Figure 165. Temperatures logged at the three NGRS OCU stations.

Appendix XIII. Summary of SWSOOS environmental data

Table 21. Summary of H₂S data recorded at 3 long term monitoring sites on the SWSOOS lines.

Site 6 LTM Summary						
	Av H ₂ S	90% H ₂ S	95%H ₂ S	Av T	90% T	95% T
2004	1.1	2.6	3.5	21.9	27.5	34.0
2005	0.3	0.7	1.1	24.9	29.5	31.3
2006	0.2	0.5	0.7	22.0	29.5	30.4
2007	1.3	3.4	4.8	22.7	28.9	30.2
2008	1.9	4.4	5.4	21.6	28.3	30.0
2009	1.9	3.9	5.2	23.0	26.0	26.3

Site 7 LTM Summary						
	Av H ₂ S	90% H ₂ S	95%H ₂ S	Av T	90% T	95% T
2005	1.6	3.9	5.9	24.7	31.4	32.1
2006	1.4	3.8	6.2	31.5	33.0	33.5

Site 9 LTM Summary						
	Av H ₂ S	90% H ₂ S	95%H ₂ S	Av T	90% T	95% T
2004	1.1	3.1	4.0	19.9	25.1	26.4
2005	0.7	2.1	3.4	22.4	27.2	28.8
2006	1.7	3.7	6.5	21.9	27.8	28.9
2007	0.6	2.1	3.0	20.5	27.7	29.3
2008	16.3	30.9	63.4	20.4	25.3	26.2
2009	9.1	22.2	37.1	23.0	28.8	29.8
2010	2.5	5.0	6.9	22.3	28.7	30.1

Summary of SWSOOS environmental data (Cont).

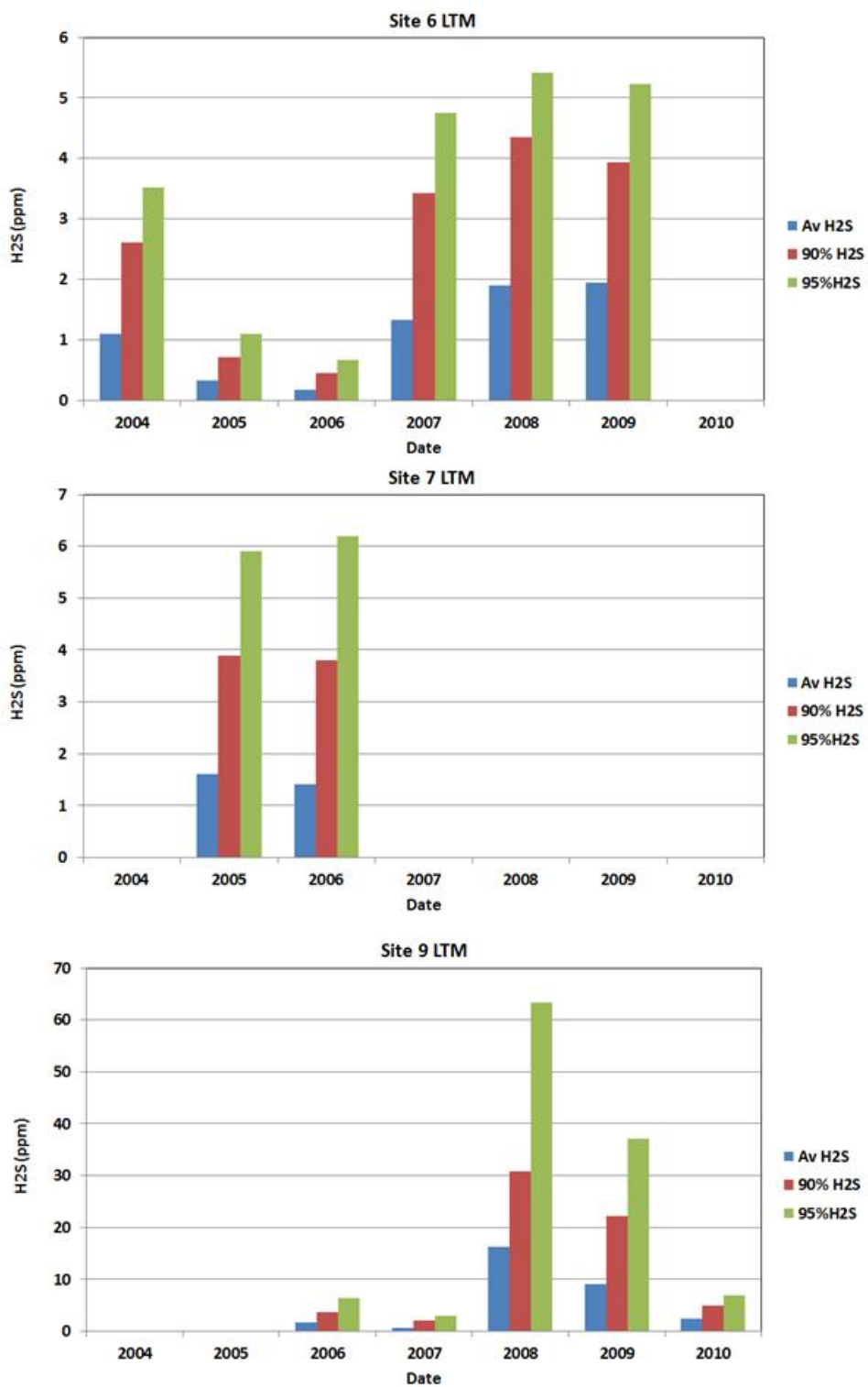


Figure 166. Annual averages of SWSOOS H₂S levels.

Summary of SWSOOS environmental data (Cont).

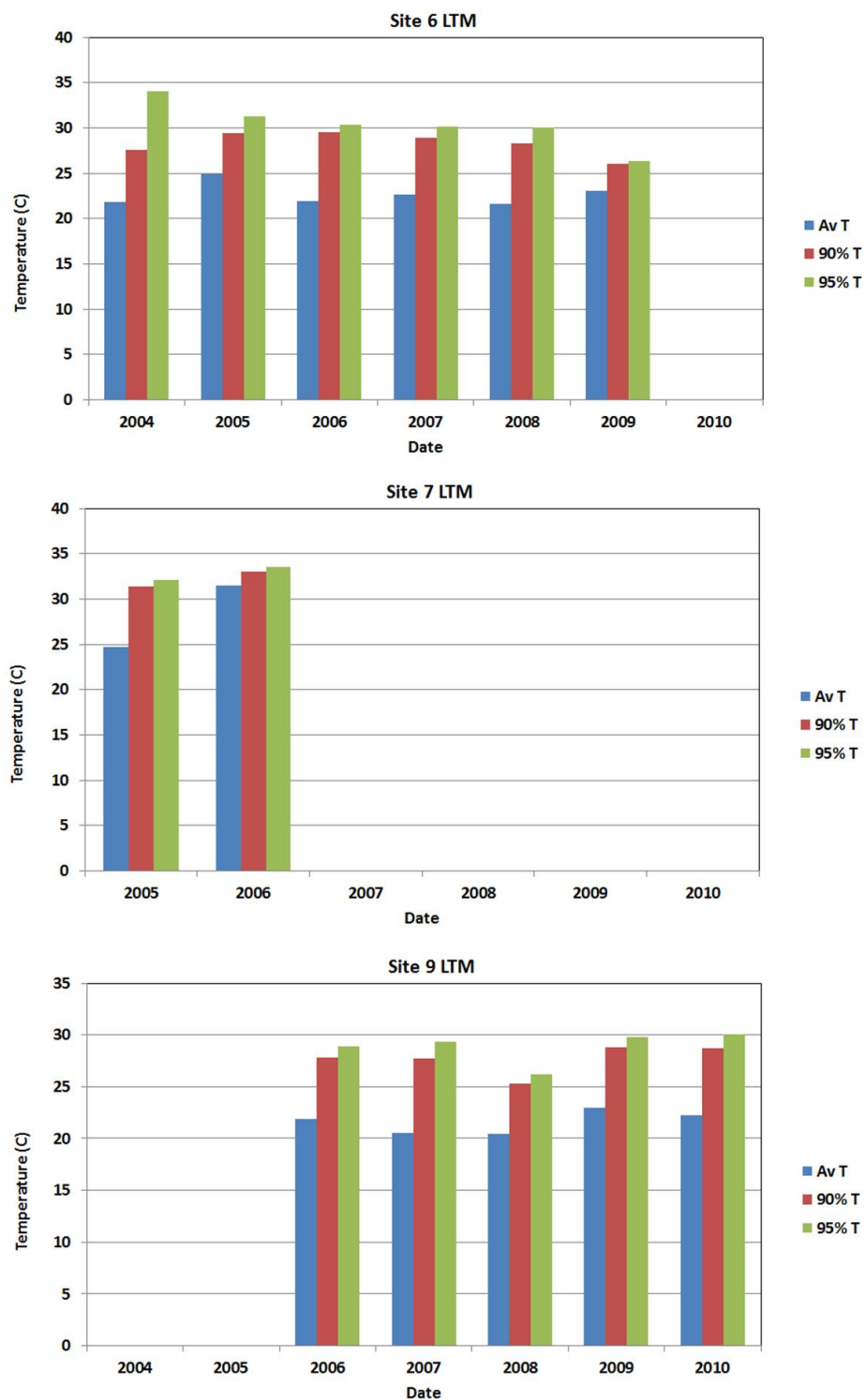


Figure 167. Annual averages of sewer gas temperatures recorded at three SWSOOS long term monitoring sites.

Appendix XIV. Summary of NSOOS environmental data

Table 22. Annual averages of NSOOS environmental data

Site 2 Tulong Ave LTM Summary						
	Av H2S	90% H2S	95%H2S	Av T	90% T	95% T
2009	3.8	7.2	9.6	21.9	25.0	26.3
2010	3.3	6.1	7.3	21.5	24.6	25.0
2011	2.9	5.8	7.0	21.1	24.5	25.0
2012	3.0	6.6	8.4	21.0	23.0	23.4
Site 3 Kissing Pt Rd LTM Summary						
	Av H2S	90% H2S	95%H2S	Av T	90% T	95% T
2009	19.0	49.6	73.9	22.2	25.1	26.0
2010	13.6	28.4	47.0	21.2	24.6	25.1
2011	8.5	20.2	32.1	20.7	25.0	25.3
2012	7.3	20.8	33.1	21.1	23.5	23.7
Site 4 Spencer St LTM Summary						
	Av H2S	90% H2S	95%H2S	Av T	90% T	95% T
2009	9.6	20.0	26.0	22.6	26.3	27.1
2010	3.6	7.2	9.9	21.6	26.5	27.5
2011	4.2	8.6	11.0	21.6	27.7	30.0
2012	5.5	14.0	17.9	21.5	24.5	25.0
Site 5 Burns Bay Aqueduct LTM Summary						
	Av H2S	90% H2S	95%H2S	Av T	90% T	95% T
2009	9.9	23.5	30.8	22.0	25.1	25.8
2010	11.2	24.7	32.5	21.7	25.8	26.6
2011	10.7	21.6	28.6	20.0	25.1	25.9
2012	13.8	31.9	41.8	19.8	23.3	23.7
Site 6 Primrose Pk LTM Summary						
	Av H2S	90% H2S	95%H2S	Av T	90% T	95% T
2009	7.8	15.6	18.6	20.0	22.6	22.9
2010	5.2	11.8	14.6	22.8	24.6	24.7
2011	18.4	38.6	46.3	20.3	23.5	24.3
2012	24.7	52.7	68.3	20.8	22.5	22.6
Site 7 Brightmore Res LTM Summary						
	Av H2S	90% H2S	95%H2S	Av T	90% T	95% T
2009	27.6	61.5	77.3	21.4	25.3	25.8
2010	45.1	100.5	122.5	24.1	25.3	25.6
2011	34.5	74.6	97.2	21.2	25.6	26.4
2012	36.8	77.4	110.1	21.4	24.6	25.0
Site 8 Spit Syphon LTM Summary						
	Av H2S	90% H2S	95%H2S	Av T	90% T	95% T
2009	7.5	14.3	20.3	20.2	23.9	24.6
2010	2.9	6.6	9.5	19.9	24.4	25.0
2011	3.7	7.6	11.2	19.8	24.3	24.9
2012	2.9	5.7	6.6	19.7	22.8	23.3
Site 9 Eustace St LTM Summary						
	Av H2S	90% H2S	95%H2S	Av T	90% T	95% T
2009	4.5	9.1	11.0	20.5	23.4	23.7
2010	3.2	6.4	8.2	21.3	24.2	24.9
2011	3.6	7.1	8.4	20.5	23.9	24.1
2012	4.3	8.0	9.2	21.0	22.9	23.1

Summary of NSOOS environmental data (Cont).

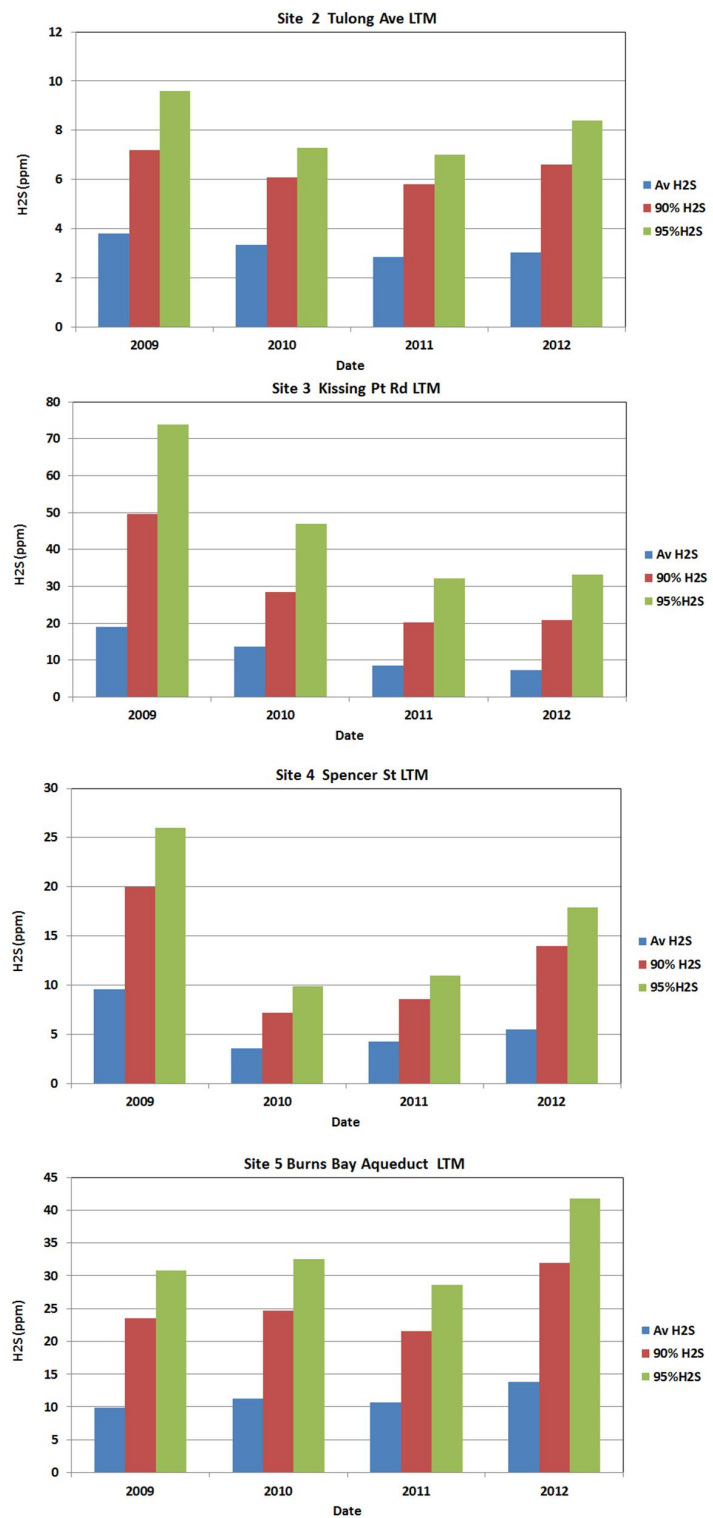


Figure 168. NSOOS H₂S annual averages - LTM sites 2-5.

Summary of NSOOS environmental data (Cont).

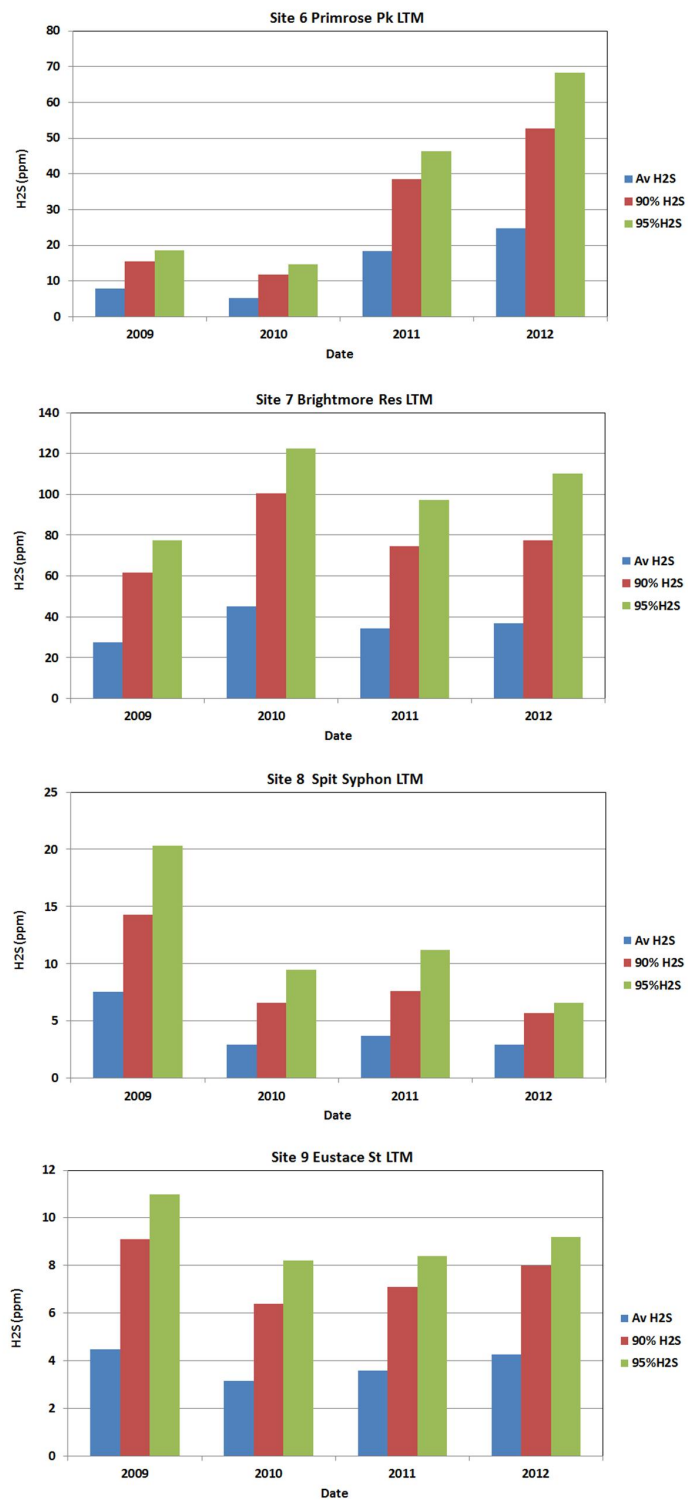


Figure 169. NSOOS H₂S annual averages - LTM sites 6-9

Summary of NSOOS environmental data (Cont).

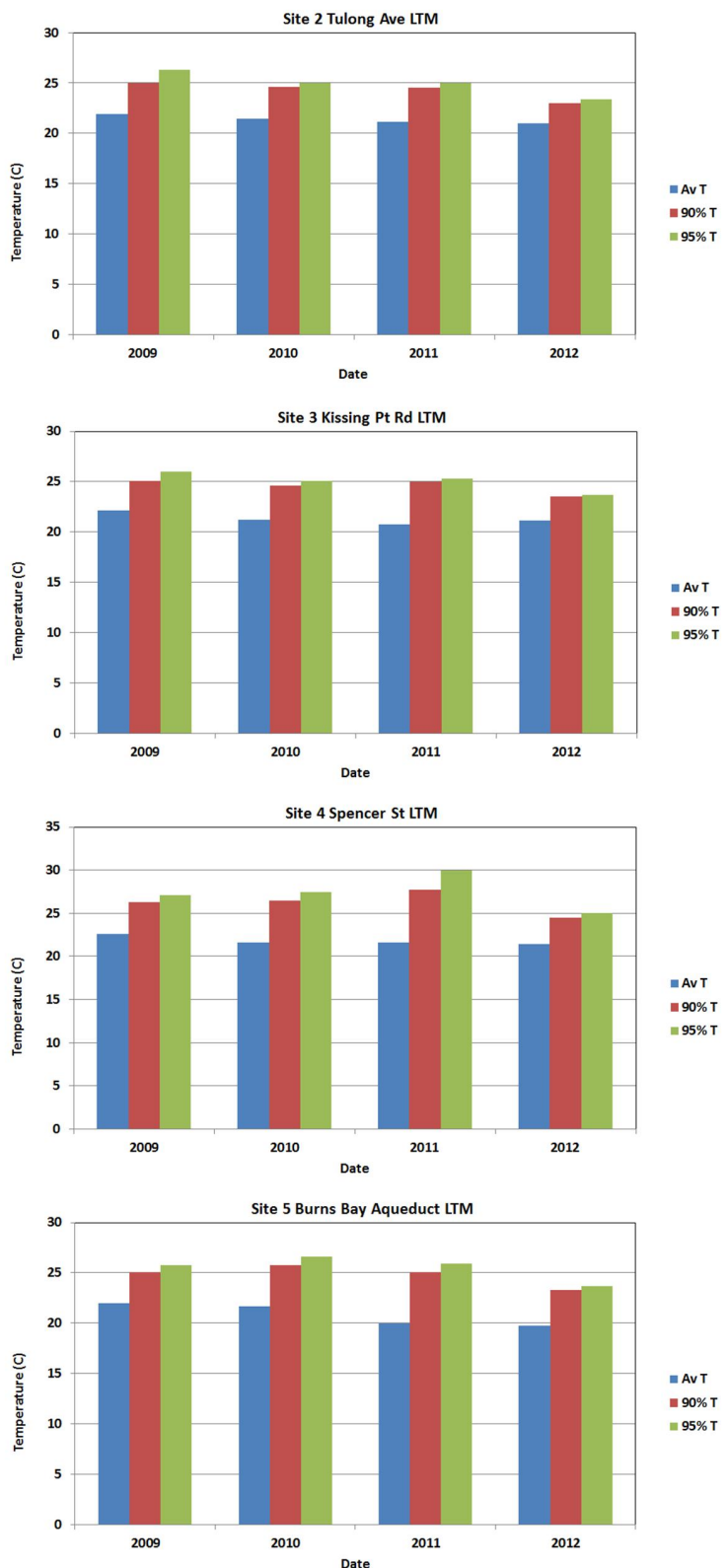


Figure 170. NSOOS gas temperature annual averages - LTM sites 2-5.

Summary of NSOOS environmental data (Cont).

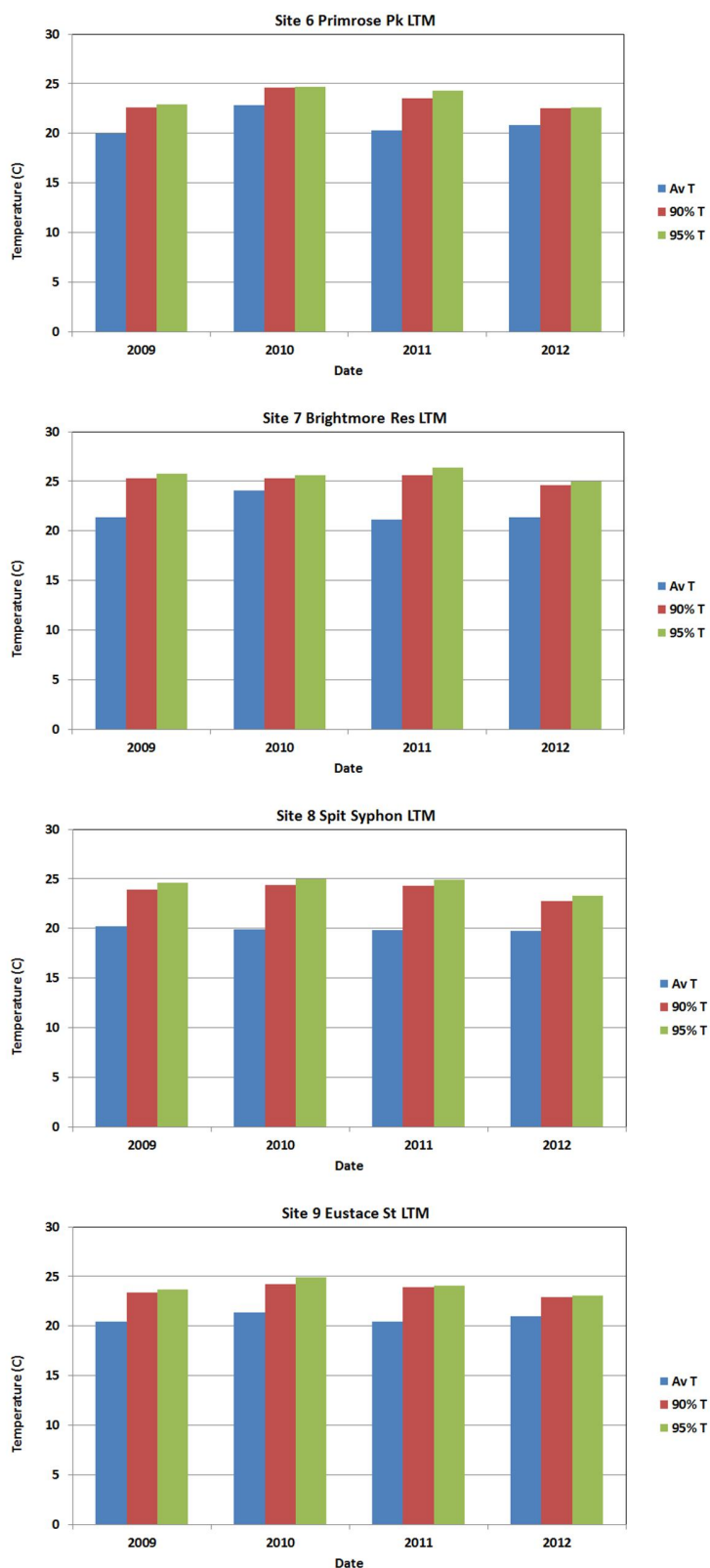


Figure 171. NSOOS gas temperature annual averages - LTM sites 6-9.

Appendix XV. Melbourne Water SETS Corrosion pin data

Table 23. Location and duration of Melbourne Water corrosion pin measurements.

Location	Commencement of monitoring	End of monitoring	Number of measurements
SETS			
SETMH4 Heathers Rd Shaft	26/8/1998	17/11/2008	5
SETMH7 Spring Vale Rd Shaft	28/8/1998	18/11/2008	5
SETMH11 Dandenong Rd Shaft	28/8/1998	19/11/2008	5
SETMH15 Pitt St Shaft	1/9/1998	25/11/2008	5
SETMH20 Albion St Shaft	31/8/1998	24/11/2008	4 (+1 incomplete)
SETMH24 Barnsbury St Shaft	2/9/1998	26/11/2008	5
WTS			
WTSMH2 Shallow conduit	2/10/1997	1/7/2008	14
WTSMH9 Shallow conduit	2/10/1997	3/7/2008	13
WTSMH2 Hacketts St Shaft	28/7/1997	26/8/2008	12
WTSMH25 Laverton Base Shaft	28/7/1997	3/2/2000	6
WTSMH30 Dohertys Rd Shaft	28/7/1997	11/7/2008	13
WTSMH32 Smith St Shaft	28/7/1997	19/9/2008	13

Melbourne SETS Corrosion pin data (Cont).

SET MH4 Heathers Road Shaft

Raw data (mm)									
		Stations							
(1)	26/08/1998	1	2	3	4	5	6	7	8
Point 1	66	61	47	58	63	56	46	45	
Point 2	84	77	44	67	76	63	46	61	
Point 3	91	84	42	71	76	65	46	69	
Point 4	86	83	40	70	66	62	44	70	
Point 5	68	77	37	64	42	53	41	64	
Point 6		61	35	56		40	43	48	
average =		79.0	73.8	40.8	64.3	64.6	56.5	44.3	59.5
Stdev =		11.3	10.4	4.4	6.2	13.9	9.3	2.1	10.6
Average= 59.9 Stdev = 14.9									
(2)	20/04/2000	1	2	3	4	5	6	7	8
Point 1	66	61	47	58	64	51	46	59	
Point 2	83	76	44	68	76	64	46	72	
Point 3	90	84	42	72	77	65	46	79	
Point 4	86	84	40	71	65	62	44	80	
Point 5	68	77	39	63	42	53	43	70	
Point 6		61	37	57		39	43	58	
average =		78.6	73.8	41.5	64.8	64.8	55.7	44.7	69.7
Stdev =		10.9	10.5	3.6	6.5	14.1	10.0	1.5	9.5
Average= 61.3 Stdev = 15.1									
(3)	30/05/2002	1	2	3	4	5	6	7	8
Point 1	67	62	47	61	65	58	48	60	
Point 2	85	76	45	69	76	64	47	73	
Point 3	91	85	42	73	77	65	47	81	
Point 4	87	85	40	72	66	62	45	80	
Point 5	69	77	40	64	42	53	42	70	
Point 6		64	39	57		39	45	58	
average =		79.8	74.8	42.2	66.0	65.2	56.8	45.7	70.3
Stdev =		11.0	9.9	3.2	6.4	14.1	9.8	2.2	9.7
Average= 62.2 Stdev = 15.1									
(4)	30/11/2006	1	2	3	4	5	6	7	8
Point 1	67	62	47	60	65	60	50	60	
Point 2	85	75	45	70	75	65	47	75	
Point 3	90	86	42	72	77	65	46	81	
Point 4	85	86	42	72	65	63	45	80	
Point 5	70	77	42	65	44	55	42	70	
Point 6		65	39	55		40	45	60	
average =		79.4	75.2	42.8	65.7	65.2	58.0	45.8	71.0
Stdev =		10.2	10.1	2.8	7.0	13.1	9.6	2.6	9.4
Average= 62.5 Stdev = 14.8									
(5)	17/11/2008	1	2	3	4	5	6	7	8
Point 1	65	60	48	61	66	61	46	60	
Point 2	84	75	45	71	77	66	47	75	
Point 3	90	85	41	70	78	65	46	81	
Point 4	85	85	42	73	68	65	46	80	
Point 5	71	80	42	66	47	57	43	72	
Point 6		65		57		41		61	
average =		79.0	75.0	43.6	66.3	67.2	59.2	45.6	71.5
Stdev =		10.5	10.5	2.9	6.3	12.5	9.5	1.5	9.1
Average= 63.8 Stdev = 14.4									

Melbourne SETS Corrosion pin data (Cont).

SET MH7

Springvale rd shaft

Raw data (mm)

(1) 28/08/1998

Stations

	1	2	3	4	5	6	7	8
Point 1	58	55	38	54	58	52	38	51
Point 2	73	71	36	66	74	64	35	63
Point 3	78	80	35	76	78	72	33	70
Point 4	70	82	33	77	71	72	30	71
Point 5	51	77	30	71	51	66	27	65
Point 6		64	29	60		54	25	54
average =	66.0	71.5	33.5	67.3	66.4	63.3	31.3	62.3
Stdev =	11.2	10.4	3.5	9.1	11.4	8.6	4.9	8.2

Average= 57.3
Stdev = 17.2

(2) 19/04/2000

Stations

	1	2	3	4	5	6	7	8
Point 1	60	54	38	54	58	54	37	51
Point 2	75	70	38	67	75	66	35	63
Point 3	79	79	35	76	79	74	32	70
Point 4	72	80	33	77	71	74	30	70
Point 5	53	75	32	72	52	67	28	64
Point 6		62	34	59		54	25	54
average =	67.8	70.0	35.0	67.5	67.0	64.8	31.2	62.0
Stdev =	10.9	10.3	2.5	9.4	11.5	9.0	4.4	8.0

Average= 57.8
Stdev = 17.0

(3) 29/05/2002

Stations

	1	2	3	4	5	6	7	8
Point 1	58	56	37	53	58	53	38	52
Point 2	74	71	36	67	75	65	35	65
Point 3	79	80	34	76	80	73	34	70
Point 4	71	81	31	77	72	72	30	70
Point 5	53	75	30	72	54	66	28	65
Point 6		62	36	60		55	28	55
average =	67.0	70.8	34.0	67.5	67.8	64.0	32.2	62.8
Stdev =	11.0	10.0	2.9	9.5	11.2	8.4	4.1	7.6

Average= 57.9
Stdev = 17.0

(4) 30/11/2006

Stations

	1	2	3	4	5	6	7	8
Point 1	57	61	41	52	57	54	43	51
Point 2	75	70	40	66	75	66	36	62
Point 3	76	80	39	73	76	73	35	71
Point 4	71	82	33	75	71	72	33	70
Point 5	53	75	31	72	56	72	29	66
Point 6		62	36	60		56	28	54
average =	66.4	71.7	36.7	66.3	67.0	65.5	34.0	62.3
Stdev =	10.7	8.9	4.0	8.9	9.8	8.5	5.4	8.3

Average= 58.4
Stdev = 16.0

(5) 18/11/2008

Stations

	1	2	3	4	5	6	7	8
Point 1	55	55	41	52	58	54	43	51
Point 2	74	71	38	67	79	66	36	62
Point 3	81	80	35	77	78	73	35	73
Point 4	73	82	35	80	73	72	33	74
Point 5	54	80	35	75		72	29	69
Point 6		70		65		56	28	59
average =	67.4	73.0	36.8	69.3	72.0	65.5	34.0	64.7
Stdev =	12.2	10.2	2.7	10.3	9.7	8.5	5.4	9.0

Average= 60.2
Stdev = 16.9

Melbourne SETS Corrosion pin data (Cont).

SET MH11 Centre Dandenong Rd Shaft

(1) 28/08/1998

Raw data (mm)								
	Stations							
	1	2	3	4	5	6	7	8
Point 1	60	60	44	59	62	56	41	55
Point 2	76	75	54	82	80	74	40	69
Point 3	76	87	60	99	86	86	39	76
Point 4	68	87	66	104	76	87	37	75
Point 5	44	79	70	100	52	79	38	70
Point 6		66	82	91		67	35	60
average =	64.8	75.7	62.7	89.2	71.2	74.8	38.3	67.5
Stdev =	13.4	11.0	13.2	16.7	13.9	11.9	2.2	8.4

Average= 68.0
Stdev = 17.8

(2) 18/04/2000

Stations								
	1	2	3	4	5	6	7	8
Point 1	60	57	45	59	61	67	41	54
Point 2	77	75	54	82	79	80	39	69
Point 3	79	87	60	99	86	89	38	77
Point 4	68	87	66	105	76	90	37	76
Point 5	44	81	73	100	53	81	40	70
Point 6		67	83	91		66	39	60
average =	65.6	75.7	63.5	89.3	71.0	78.8	39.0	67.7
Stdev =	14.3	11.9	13.6	16.9	13.6	10.4	1.4	9.0

Average= 68.8
Stdev = 18.0

(3) 23/05/2002

Stations								
	1	2	3	4	5	6	7	8
Point 1	61	59	45	61	64	61	40	56
Point 2	77	75	55	82	80	75	40	69
Point 3	80	88	60	101	88	87	37	77
Point 4	69	87	67	105	77	88	40	77
Point 5	45	80	74	100	55	80	40	71
Point 6		66	83	93		65	37	61
average =	66.4	75.8	64.0	90.3	72.8	76.0	39.0	68.5
Stdev =	14.1	11.6	13.6	16.5	13.2	11.2	1.5	8.5

Average= 69.1
Stdev = 17.9

(4) 30/11/2006

Stations								
	1	2	3	4	5	6	7	8
Point 1	60	60	45	62	65	65	44	60
Point 2	80	75	53	83	80	75	40	70
Point 3	80	85	65	104	90	85	40	75
Point 4	70	85	70	110	75	88	40	75
Point 5	50	80	70	100	50	80	40	75
Point 6		70	85	93		68	38	67
average =	68.0	75.8	64.7	92.0	72.0	76.8	40.3	70.3
Stdev =	13.0	9.7	14.1	17.4	15.2	9.2	2.0	6.1

Average= 70.0
Stdev = 17.7

(5) 19/11/2008

Stations								
	1	2	3	4	5	6	7	8
Point 1	65	60	45	63	60	65	40	56
Point 2	80	75	52	80	77	75	41	71
Point 3	87	85	60	100	85	86	36	80
Point 4	85	85	76	104	80	86	36	86
Point 5	60	80		100	60	80	40	78
Point 6		70		91		81	36	
average =	75.4	75.8	58.3	89.7	72.4	78.8	38.2	74.2
Stdev =	12.2	9.7	13.3	15.7	11.7	7.9	2.4	11.5

Average= 70.7
Stdev = 18.3

Melbourne SETS Corrosion pin data (Cont).

SET MH15 Pitt St shaft

Raw data (mm)								
(1)	1/09/1998	Stations						
		1	2	3	4	5	6	7
Point 1		57	52	37	51	57	51	36
Point 2		74	68	35	65	71	65	36
Point 3		76	77	35	72	71	71	37
Point 4		63	78	33	72	58	72	37
Point 5		40	71	45	62	31	65	38
Point 6			58	34	46		52	39
		average =	62.0	67.3	36.5	61.3	57.6	62.7
		Stdev =	14.6	10.4	4.4	10.8	16.3	9.1
							1.2	11.5
		Average= 56.6 Stdev = 15.7						
(2)	18/04/2000	Stations						
		1	2	3	4	5	6	7
Point 1		57	52	37	52	57	52	36
Point 2		75	68	35	66	72	66	37
Point 3		77	77	35	73	72	72	37
Point 4		63	78	34	72	59	72	38
Point 5		40	71	48	62	31	66	38
Point 6			57	37	47		52	38
		average =	62.4	67.2	37.7	62.0	58.2	63.3
		Stdev =	15.0	10.6	5.2	10.6	16.8	9.2
							0.8	11.0
		Average= 57.1 Stdev = 15.6						
(3)	24/05/2002	Stations						
		1	2	3	4	5	6	7
Point 1		57	52	35	52	58	53	36
Point 2		75	70	35	66	72	67	37
Point 3		78	78	34	73	73	72	37
Point 4		63	78	34	72	60	73	38
Point 5		38	70	49	62	31	66	39
Point 6			60	35	50		52	39
		average =	62.2	68.0	37.0	62.5	58.8	63.8
		Stdev =	16.0	10.3	5.9	9.8	17.0	9.2
							1.2	11.1
		Average= 57.3 Stdev = 15.9						
(4)	30/11/2006	Stations						
		1	2	3	4	5	6	7
Point 1		60	54	35	54	60	54	36
Point 2		75	70	35	67	73	67	37
Point 3		82	78	33	75	73	72	37
Point 4		64	78	33	75	60	72	38
Point 5		40	70	44	62	35	64	38
Point 6			62	36	53		54	39
		average =	64.2	68.7	36.0	64.3	60.2	63.8
		Stdev =	16.1	9.4	4.1	9.8	15.5	8.2
							1.0	11.2
		Average= 57.9 Stdev = 16.0						
(5)	25/11/2008	Stations						
		1	2	3	4	5	6	7
Point 1		62	55	36	56	62	55	35
Point 2		77	71	33	65	71	67	36
Point 3		82	77	36	73	76	72	35
Point 4		61	76	35	72	62	72	35
Point 5		40	70	46	59	36	65	38
Point 6			62		53		54	62
		average =	64.4	68.5	37.2	63.0	61.4	64.2
		Stdev =	16.4	8.5	5.1	8.4	15.4	8.0
							1.3	12.5
		Average= 58.9 Stdev = 15.8						

Melbourne SETS Corrosion pin data (Cont).

SET MH20 Albion St Shaft

Raw data (mm)

(1) 31/08/1998

	Stations							
	1	2	3	4	5	6	7	8
Point 1	63	56	37	57	64	58	37	57
Point 2	81	73	36	79	83	77	37	75
Point 3	83	83	35	90	84	88	36	84
Point 4	67	84	33	90	69	86	37	82
Point 5	34	74	32	80	34	79	37	72
Point 6		64	30	63		63	37	55
average =	65.6	72.3	33.8	76.5		36.8	70.8	
Stdev =	19.7	10.9	2.6	13.8		0.4	12.3	

Average= 62.1
Stdev = 20.2

(2) 14/04/2000

	Stations							
	1	2	3	4	5	6	7	8
Point 1	63	55	37	59	64	59	37	56
Point 2	82	73	36	81	83	78	37	75
Point 3	83	83	35	91	85	87	36	84
Point 4	67	86	34	90	69	85	37	82
Point 5	34	82	31	81	75	77	37	72
Point 6		66	31	64		61	38	55
average =	65.8	74.2	34.0	77.7		37.0	70.7	
Stdev =	19.9	12.0	2.5	13.3		0.6	12.5	

Average= 63.3
Stdev = 20.1

(3) 27/05/2002

	Stations							
	1	2	3	4	5	6	7	8
Point 1	64	56	38	57	66	63	38	56
Point 2	83	73	36	81	85	81	39	74
Point 3	83	83	35	93	85	90	37	84
Point 4	67	86	33	96	72	90	38	82
Point 5	34	81	32	90	39	79	37	72
Point 6		67	30	72		65	37	55
average =	66.2	74.3	34.0	81.5		37.7	70.5	
Stdev =	20.0	11.4	2.9	14.9		0.8	12.5	

Average= 63.8
Stdev = 21.1

(4) 30/11/2006

	Stations							
	1	2	3	4	5	6	7	8
Point 1	65	60	37	57	65	64	37	57
Point 2	86	75	35	81	85	85	41	76
Point 3	80	85	35	90	85	92	38	85
Point 4	74	85	33	94	70	94	38	82
Point 5	35	80	32	92	35	83	37	73
Point 6	64	31	70			65	39	56
average =	68.0	74.8	33.8	80.7		38.3	71.5	
Stdev =	20.0	10.7	2.2	14.6		1.5	12.4	

Average= 64.3
Stdev = 21.3

(5) 24/11/2008

	Stations							
	1	2	3	4	5	6	7	8
Point 1	60	55	35	55	bottom	bottom	36	58
Point 2	80	73	35	75	3 pins	3 pins	35	75
Point 3	83	85	35	85	cut off!	cut off!	34	84
Point 4	67	85	32	85			37	81
Point 5	39	80	33	75			37	70
Point 6	65			55				53
average =	65.8	73.8	34.0	71.7		35.8	70.2	
Stdev =	17.7	12.0	1.4	13.7		1.3	12.4	

Average= 59.8
Stdev = 20.0

Note data from 24/11/2008 excluded from analysis as incomplete

Melbourne SETS Corrosion pin data (Cont).

SET MH24 Barnsbury St

Raw data (mm)								
(1)	2/09/1998	Stations						
		1	2	3	4	5	6	7
Point 1		61	55	37	54	62	52	35
Point 2		83	75	35	73	82	72	38
Point 3		87	87	36	83	89	81	41
Point 4		73	89	38	83	70	79	42
Point 5		41	83	37	79	36	71	46
Point 6			67	37	58		55	49
		average =	69.0	76.0	36.7	71.7	41.8	73.7
		Stdev =	18.6	13.1	1.0	12.7	5.1	13.8
(2)	13/02/2000	Stations						
		1	2	3	4	5	6	7
Point 1		61	54	38	54	62	54	35
Point 2		84	75	36	73	82	74	38
Point 3		87	87	37	82	89	82	41
Point 4		72	89	38	83	70	79	42
Point 5		41	84	38	75	34	71	45
Point 6			67	38	58		55	48
		average =	69.0	76.0	37.5	70.8	41.5	73.3
		Stdev =	18.7	13.6	0.8	12.2	4.7	13.6
(3)	20/05/2002	Stations						
		1	2	3	4	5	6	7
Point 1		63	53	37	53	60	56	35
Point 2		85	75	36	72	82	76	37
Point 3		90	87	37	82	86	83	40
Point 4		73	90	38	83	70	79	42
Point 5		40	83	38	75	35	71	45
Point 6			67	40	57		54	50
		average =	70.2	75.8	37.7	70.3	41.5	73.3
		Stdev =	19.9	14.0	1.4	12.6	5.5	13.5
(4)	30/11/2006	Stations						
		1	2	3	4	5	6	7
Point 1		63	60	37	56	62	60	35
Point 2		82	80	37	75	81	77	40
Point 3		87	90	36	85	87	85	40
Point 4		72	90	36	85	70	82	42
Point 5		42	83	40	75	35	74	45
Point 6			67	42	60		55	52
		average =	69.2	78.3	38.0	72.7	42.3	76.3
		Stdev =	17.8	12.3	2.4	12.3	5.8	13.8
(5)	26/11/2008	Stations						
		1	2	3	4	5	6	7
Point 1		82	60	35	57	62	60	38
Point 2		82	81	38	78	83	78	41
Point 3		87	90	37	87	87	86	40
Point 4		75	90	40	85	72	83	40
Point 5		42	84	40	75	38	77	46
Point 6			66		61		54	60
		average =	73.6	78.5	38.0	73.8	41.0	76.8
		Stdev =	18.2	12.6	2.1	12.4	3.0	14.6

Appendix XVI. Melbourne Water SETS Corrosion rate graphs

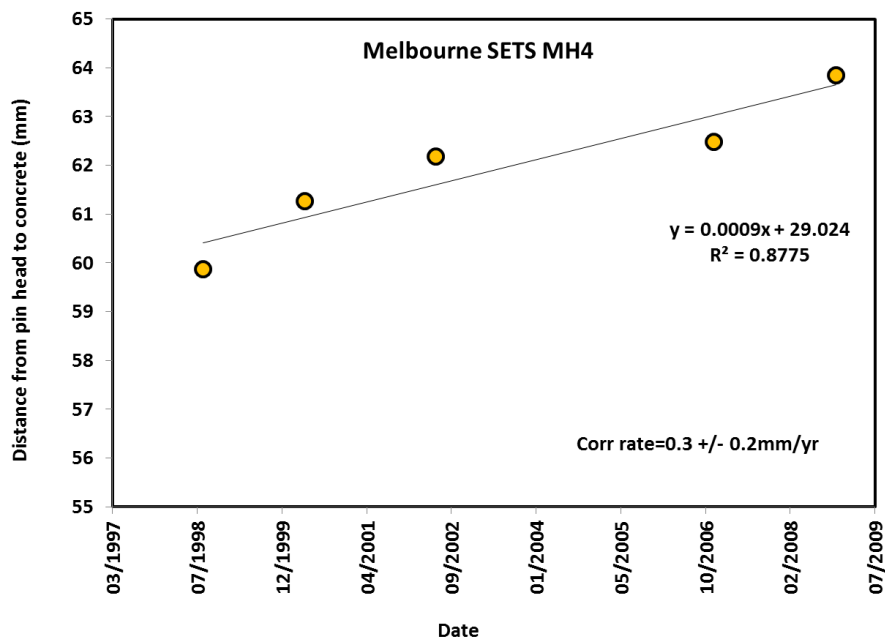


Figure 172. Erosion pin corrosion losses at Melbourne SETSMH4.

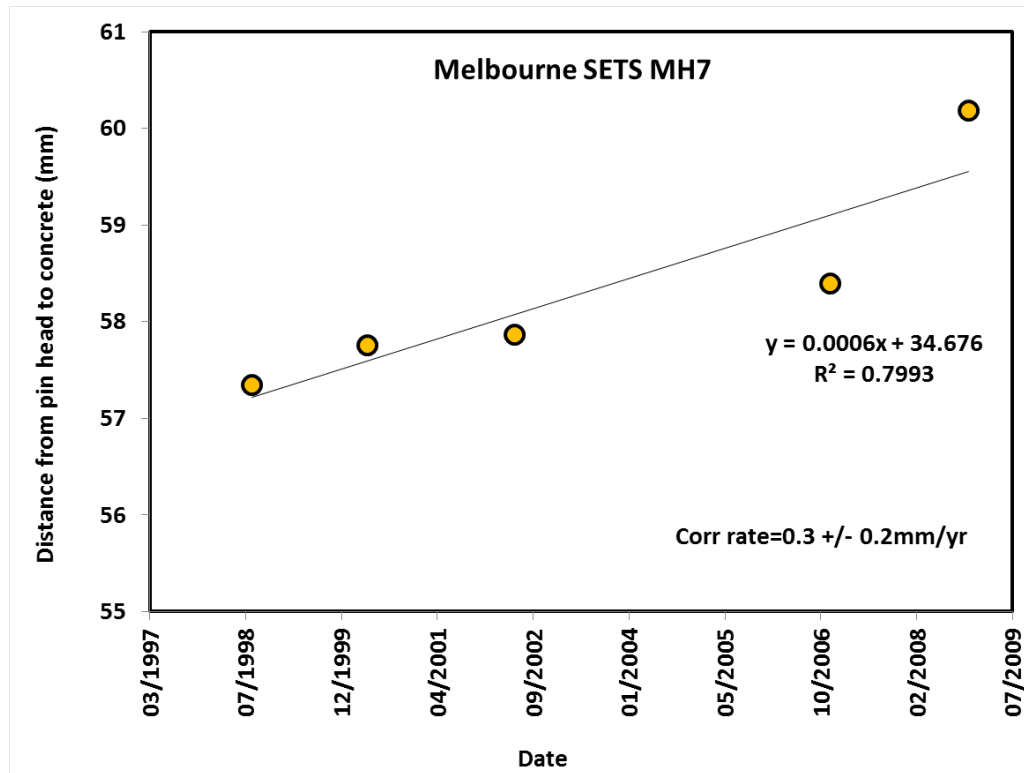


Figure 173. Erosion pin corrosion losses at Melbourne SETSMH7.

Melbourne Water SETS Corrosion rate graphs (cont).

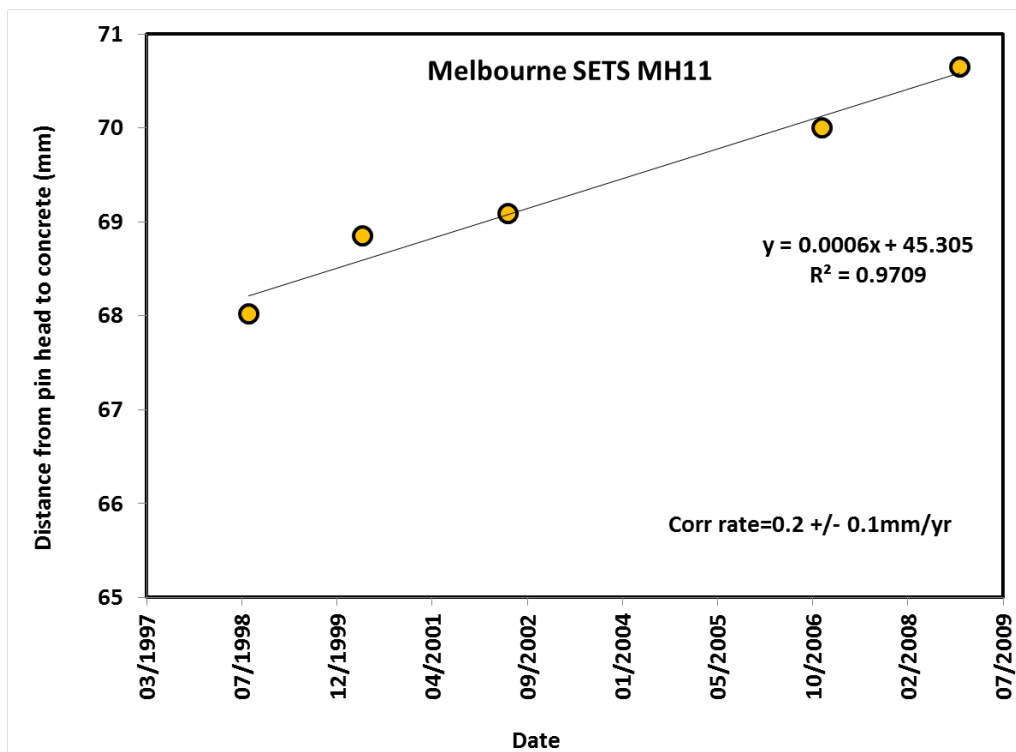


Figure 174. Erosion pin corrosion losses at Melbourne SETSMH11.

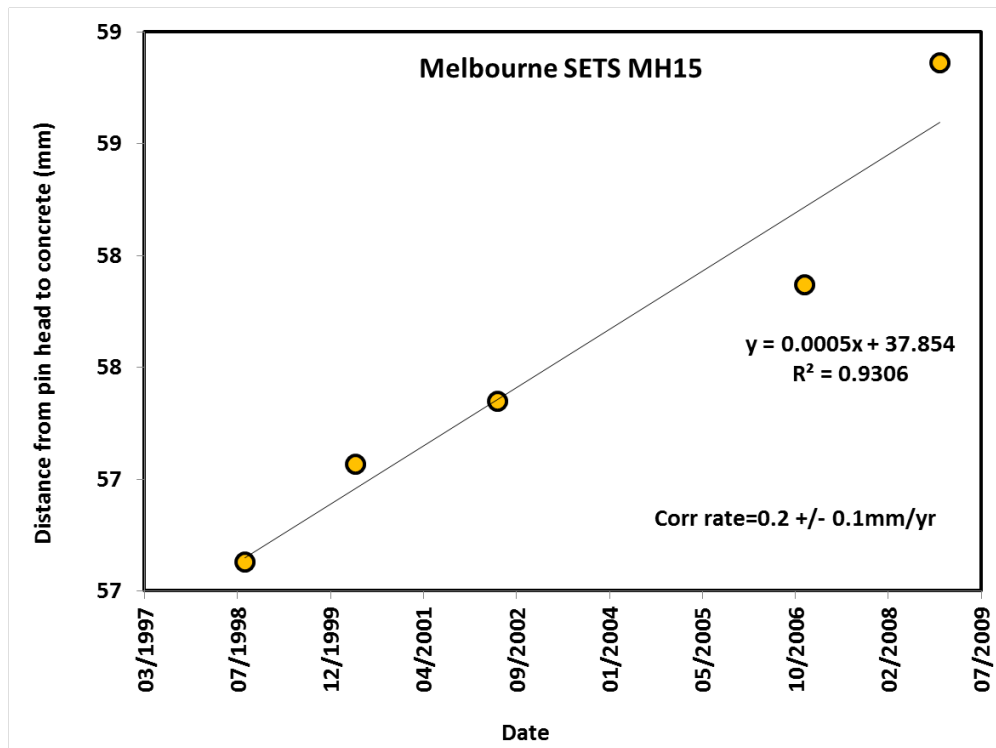


Figure 175. Erosion pin corrosion losses at Melbourne SETSMH15.

Melbourne Water SETS Corrosion rate graphs (cont).

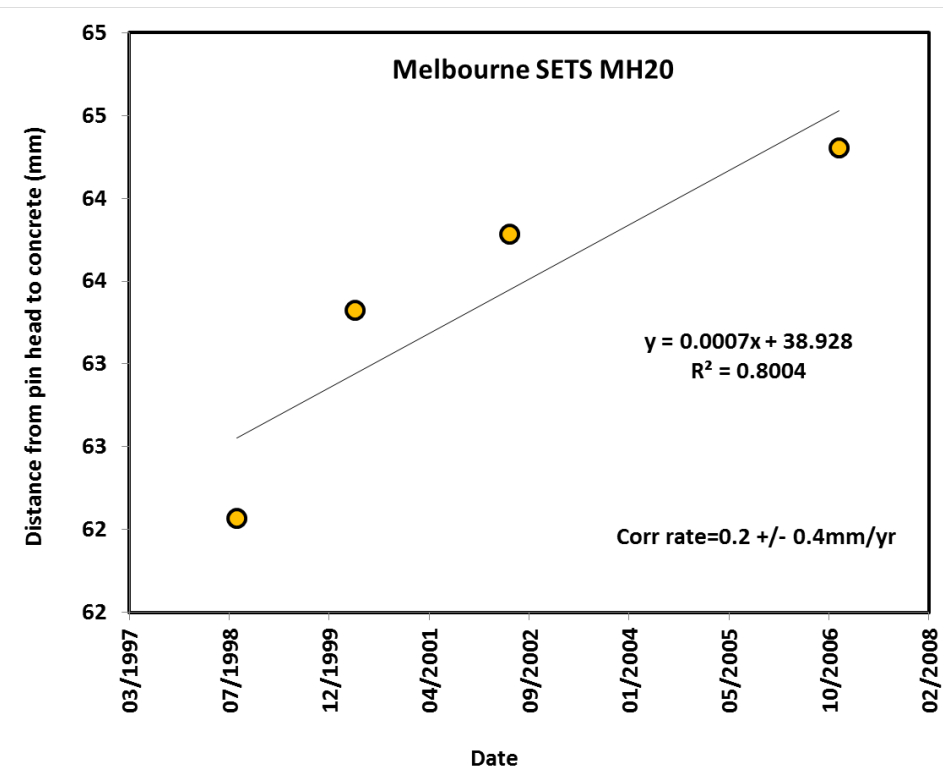


Figure 176. Erosion pin corrosion losses at Melbourne SETSMH20.

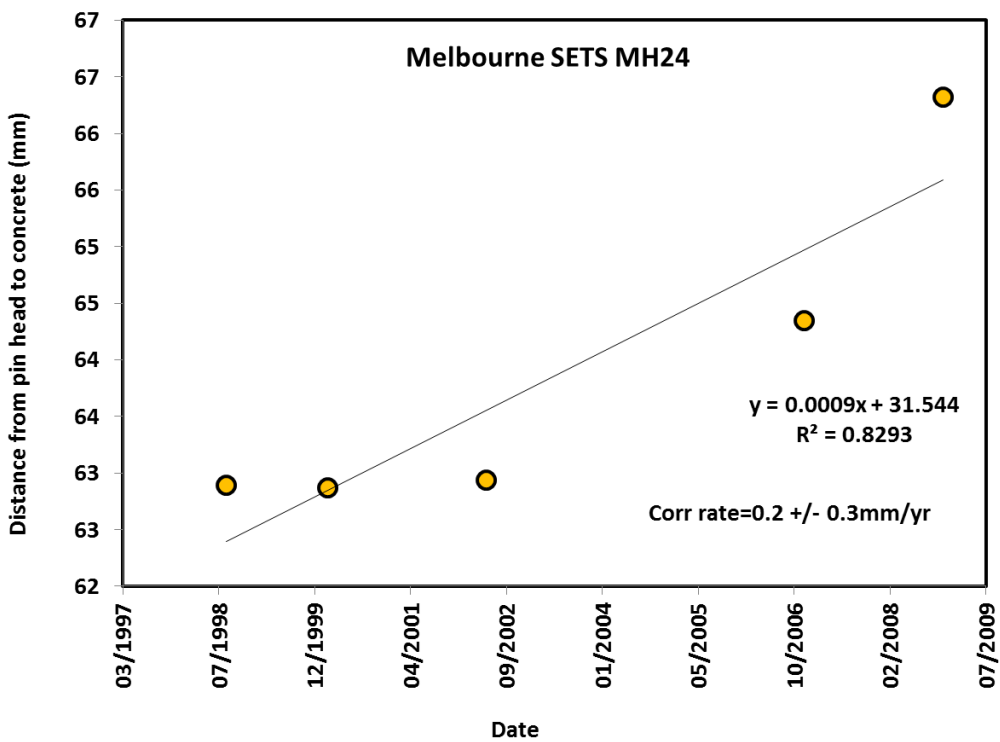


Figure 177. Erosion pin corrosion losses at Melbourne SETSMH24.

Appendix XVII. Melbourne Water WTS Corrosion pin data

WTS MH2 Shallow conduit		Raw data (mm)							
(1)	2/10/1997	Stations							
		1	2	3	4	5	6	7	8
Point 1	88	77	54	86	90	67	60	63	
Point 2	114	93	57	101	99	83	68	83	
Point 3	123	99	67	107	127	86	67	96	
Point 4	130	94	60	104	124	101	70	88	
Point 5	120	100	69	101	117	98	69	102	
Point 6	92	93	70	96	102	80	55	94	
average =	111.2	92.7	62.8	99.2	109.8	85.8	64.8	87.7	Average= 89.3
Stdev =	17.2	8.3	6.7	7.4	15.0	12.4	6.0	13.8	Stdev = 20.3
(2) 11/02/1998		Stations							
		1	2	3	4	5	6	7	8
Point 1	89	84	55	86	86	65	63	65	
Point 2	116	97	65	98	90	79	69	84	
Point 3	124	102	67	104	127	98	67	95	
Point 4	125	107	67	121	122	101	72	88	
Point 5	108	107	72	110	119	93	72	103	
Point 6	92	99	72	101	104	82	67	92	
average =	109.0	99.3	66.3	103.3	108.0	86.3	68.3	87.8	Average= 91.1
Stdev =	15.6	8.5	6.3	11.8	17.3	13.6	3.4	12.9	Stdev = 19.4
(3) 28/03/1998		Stations							
		1	2	3	4	5	6	7	8
Point 1	88	86	54	82	85	65	62	65	
Point 2	116	96	65	106	90	73	65	86	
Point 3	126	104	69	110	125	99	73	95	
Point 4	113	107	62	122	123	101	72	88	
Point 5	109	107	72	110	115	93	72	102	
Point 6	99	99	72	98	103	82	68	97	
average =	108.5	99.8	65.7	104.7	106.8	85.5	68.7	88.8	Average= 91.1
Stdev =	13.4	8.1	6.9	13.5	16.9	14.6	4.5	13.1	Stdev = 19.5
(4) 15/04/1998		Stations							
		1	2	3	4	5	6	7	8
Point 1	91	83	53	86	85	70	62	66	
Point 2	118	92	68	103	100	72	68	85	
Point 3	127	102	66	107	127	100	73	100	
Point 4	134	107	65	121	123	102	71	93	
Point 5	108	108	70	112	114	94	68	98	
Point 6	100	99	71	102	103	81	72	95	
average =	113.0	98.5	65.5	105.2	108.7	86.5	69.0	89.5	Average= 92.0
Stdev =	16.4	9.6	6.5	11.7	15.7	14.1	4.0	12.6	Stdev = 20.1
(5) 1/06/1998		Stations							
		1	2	3	4	5	6	7	8
Point 1	88	81	56	84	90	76	63	67	
Point 2	116	92	65	101	112	73	65	84	
Point 3	125	102	70	109	130	98	71	100	
Point 4	134	104	70	116	126	101	71	97	
Point 5	109	107	69	106	118	94	71	102	
Point 6	100	97	75	98	105	83	72	93	
average =	112.0	97.2	67.5	102.3	113.5	87.5	68.8	90.5	Average= 92.4
Stdev =	16.7	9.5	6.5	11.0	14.7	11.8	3.8	13.2	Stdev = 19.7

Melbourne WTS Corrosion pin data (Cont).

WTS MH2 Shallow conduit

(6)	27/01/1999	Stations <table border="1" style="width: 100%; border-collapse: collapse;"> <thead> <tr> <th></th><th>1</th><th>2</th><th>3</th><th>4</th><th>5</th><th>6</th><th>7</th><th>8</th></tr> </thead> <tbody> <tr><td>Point 1</td><td>92</td><td>77</td><td>51</td><td>82</td><td>91</td><td>65</td><td>62</td><td>69</td></tr> <tr><td>Point 2</td><td>114</td><td>93</td><td>62</td><td>99</td><td>98</td><td>71</td><td>60</td><td>85</td></tr> <tr><td>Point 3</td><td>124</td><td>94</td><td>64</td><td>100</td><td>128</td><td>97</td><td>73</td><td>101</td></tr> <tr><td>Point 4</td><td>129</td><td>95</td><td>60</td><td>116</td><td>123</td><td>100</td><td>71</td><td>102</td></tr> <tr><td>Point 5</td><td>107</td><td>96</td><td>69</td><td>109</td><td>121</td><td>93</td><td>71</td><td>97</td></tr> <tr><td>Point 6</td><td>97</td><td>97</td><td>71</td><td>98</td><td>104</td><td>84</td><td>71</td><td>94</td></tr> <tr> <td>average =</td><td>110.5</td><td>92.0</td><td>62.8</td><td>100.7</td><td>110.8</td><td>85.0</td><td>68.0</td><td>91.3</td></tr> <tr> <td>Stdev =</td><td>14.7</td><td>7.5</td><td>7.1</td><td>11.5</td><td>15.2</td><td>14.4</td><td>5.5</td><td>12.5</td></tr> </tbody> </table>		1	2	3	4	5	6	7	8	Point 1	92	77	51	82	91	65	62	69	Point 2	114	93	62	99	98	71	60	85	Point 3	124	94	64	100	128	97	73	101	Point 4	129	95	60	116	123	100	71	102	Point 5	107	96	69	109	121	93	71	97	Point 6	97	97	71	98	104	84	71	94	average =	110.5	92.0	62.8	100.7	110.8	85.0	68.0	91.3	Stdev =	14.7	7.5	7.1	11.5	15.2	14.4	5.5	12.5
	1	2	3	4	5	6	7	8																																																																											
Point 1	92	77	51	82	91	65	62	69																																																																											
Point 2	114	93	62	99	98	71	60	85																																																																											
Point 3	124	94	64	100	128	97	73	101																																																																											
Point 4	129	95	60	116	123	100	71	102																																																																											
Point 5	107	96	69	109	121	93	71	97																																																																											
Point 6	97	97	71	98	104	84	71	94																																																																											
average =	110.5	92.0	62.8	100.7	110.8	85.0	68.0	91.3																																																																											
Stdev =	14.7	7.5	7.1	11.5	15.2	14.4	5.5	12.5																																																																											
(7)	27/01/2000	<table border="1" style="width: 100%; border-collapse: collapse;"> <thead> <tr> <th></th><th>1</th><th>2</th><th>3</th><th>4</th><th>5</th><th>6</th><th>7</th><th>8</th></tr> </thead> <tbody> <tr><td>Point 1</td><td>92</td><td>80</td><td>67</td><td>84</td><td>90</td><td>72</td><td>62</td><td>76</td></tr> <tr><td>Point 2</td><td>116</td><td>94</td><td>63</td><td>100</td><td>103</td><td>71</td><td>61</td><td>89</td></tr> <tr><td>Point 3</td><td>120</td><td>100</td><td>69</td><td>110</td><td>130</td><td>97</td><td>73</td><td>100</td></tr> <tr><td>Point 4</td><td>131</td><td>101</td><td>61</td><td>119</td><td>123</td><td>103</td><td>70</td><td>108</td></tr> <tr><td>Point 5</td><td>109</td><td>97</td><td>69</td><td>110</td><td>120</td><td>94</td><td>66</td><td>94</td></tr> <tr><td>Point 6</td><td>100</td><td>90</td><td>73</td><td>95</td><td>105</td><td>82</td><td>69</td><td>88</td></tr> <tr> <td>average =</td><td>111.3</td><td>93.7</td><td>67.0</td><td>103.0</td><td>111.8</td><td>86.5</td><td>66.8</td><td>92.5</td></tr> <tr> <td>Stdev =</td><td>14.1</td><td>7.8</td><td>4.4</td><td>12.6</td><td>15.0</td><td>13.5</td><td>4.7</td><td>11.0</td></tr> </tbody> </table>		1	2	3	4	5	6	7	8	Point 1	92	80	67	84	90	72	62	76	Point 2	116	94	63	100	103	71	61	89	Point 3	120	100	69	110	130	97	73	100	Point 4	131	101	61	119	123	103	70	108	Point 5	109	97	69	110	120	94	66	94	Point 6	100	90	73	95	105	82	69	88	average =	111.3	93.7	67.0	103.0	111.8	86.5	66.8	92.5	Stdev =	14.1	7.8	4.4	12.6	15.0	13.5	4.7	11.0
	1	2	3	4	5	6	7	8																																																																											
Point 1	92	80	67	84	90	72	62	76																																																																											
Point 2	116	94	63	100	103	71	61	89																																																																											
Point 3	120	100	69	110	130	97	73	100																																																																											
Point 4	131	101	61	119	123	103	70	108																																																																											
Point 5	109	97	69	110	120	94	66	94																																																																											
Point 6	100	90	73	95	105	82	69	88																																																																											
average =	111.3	93.7	67.0	103.0	111.8	86.5	66.8	92.5																																																																											
Stdev =	14.1	7.8	4.4	12.6	15.0	13.5	4.7	11.0																																																																											
(8)	15/03/2001	<table border="1" style="width: 100%; border-collapse: collapse;"> <thead> <tr> <th></th><th>1</th><th>2</th><th>3</th><th>4</th><th>5</th><th>6</th><th>7</th><th>8</th></tr> </thead> <tbody> <tr><td>Point 1</td><td>99</td><td>83</td><td>55</td><td>94</td><td>93</td><td>74</td><td>70</td><td>81</td></tr> <tr><td>Point 2</td><td>120</td><td>100</td><td>64</td><td>108</td><td>98</td><td>83</td><td>71</td><td>92</td></tr> <tr><td>Point 3</td><td>128</td><td>100</td><td>71</td><td>120</td><td>125</td><td>98</td><td>76</td><td>102</td></tr> <tr><td>Point 4</td><td>130</td><td>95</td><td>60</td><td>127</td><td>122</td><td>113</td><td>74</td><td>112</td></tr> <tr><td>Point 5</td><td>108</td><td>99</td><td>71</td><td>115</td><td>128</td><td>99</td><td>75</td><td>102</td></tr> <tr><td>Point 6</td><td>108</td><td>100</td><td>75</td><td>100</td><td>104</td><td>81</td><td>78</td><td>96</td></tr> <tr> <td>average =</td><td>115.5</td><td>96.2</td><td>66.0</td><td>110.7</td><td>111.7</td><td>91.3</td><td>74.0</td><td>97.5</td></tr> <tr> <td>Stdev =</td><td>12.4</td><td>6.7</td><td>7.6</td><td>12.4</td><td>15.1</td><td>14.5</td><td>3.0</td><td>10.5</td></tr> </tbody> </table>		1	2	3	4	5	6	7	8	Point 1	99	83	55	94	93	74	70	81	Point 2	120	100	64	108	98	83	71	92	Point 3	128	100	71	120	125	98	76	102	Point 4	130	95	60	127	122	113	74	112	Point 5	108	99	71	115	128	99	75	102	Point 6	108	100	75	100	104	81	78	96	average =	115.5	96.2	66.0	110.7	111.7	91.3	74.0	97.5	Stdev =	12.4	6.7	7.6	12.4	15.1	14.5	3.0	10.5
	1	2	3	4	5	6	7	8																																																																											
Point 1	99	83	55	94	93	74	70	81																																																																											
Point 2	120	100	64	108	98	83	71	92																																																																											
Point 3	128	100	71	120	125	98	76	102																																																																											
Point 4	130	95	60	127	122	113	74	112																																																																											
Point 5	108	99	71	115	128	99	75	102																																																																											
Point 6	108	100	75	100	104	81	78	96																																																																											
average =	115.5	96.2	66.0	110.7	111.7	91.3	74.0	97.5																																																																											
Stdev =	12.4	6.7	7.6	12.4	15.1	14.5	3.0	10.5																																																																											
(9)	8/05/2002	<table border="1" style="width: 100%; border-collapse: collapse;"> <thead> <tr> <th></th><th>1</th><th>2</th><th>3</th><th>4</th><th>5</th><th>6</th><th>7</th><th>8</th></tr> </thead> <tbody> <tr><td>Point 1</td><td>100</td><td>85</td><td>69</td><td>90</td><td>93</td><td>65</td><td>70</td><td>82</td></tr> <tr><td>Point 2</td><td>120</td><td>100</td><td>65</td><td>98</td><td>97</td><td>69</td><td>63</td><td>91</td></tr> <tr><td>Point 3</td><td>127</td><td>101</td><td>72</td><td>114</td><td>124</td><td>102</td><td>77</td><td>101</td></tr> <tr><td>Point 4</td><td>135</td><td>108</td><td>61</td><td>123</td><td>122</td><td>105</td><td>77</td><td>113</td></tr> <tr><td>Point 5</td><td>123</td><td>100</td><td>73</td><td>113</td><td>127</td><td>99</td><td>74</td><td>108</td></tr> <tr><td>Point 6</td><td>110</td><td>102</td><td>77</td><td>100</td><td>104</td><td>82</td><td>78</td><td>98</td></tr> <tr> <td>average =</td><td>119.2</td><td>99.3</td><td>69.5</td><td>106.3</td><td>111.2</td><td>87.0</td><td>73.2</td><td>98.8</td></tr> <tr> <td>Stdev =</td><td>12.5</td><td>7.6</td><td>5.8</td><td>12.3</td><td>14.9</td><td>17.5</td><td>5.8</td><td>11.3</td></tr> </tbody> </table>		1	2	3	4	5	6	7	8	Point 1	100	85	69	90	93	65	70	82	Point 2	120	100	65	98	97	69	63	91	Point 3	127	101	72	114	124	102	77	101	Point 4	135	108	61	123	122	105	77	113	Point 5	123	100	73	113	127	99	74	108	Point 6	110	102	77	100	104	82	78	98	average =	119.2	99.3	69.5	106.3	111.2	87.0	73.2	98.8	Stdev =	12.5	7.6	5.8	12.3	14.9	17.5	5.8	11.3
	1	2	3	4	5	6	7	8																																																																											
Point 1	100	85	69	90	93	65	70	82																																																																											
Point 2	120	100	65	98	97	69	63	91																																																																											
Point 3	127	101	72	114	124	102	77	101																																																																											
Point 4	135	108	61	123	122	105	77	113																																																																											
Point 5	123	100	73	113	127	99	74	108																																																																											
Point 6	110	102	77	100	104	82	78	98																																																																											
average =	119.2	99.3	69.5	106.3	111.2	87.0	73.2	98.8																																																																											
Stdev =	12.5	7.6	5.8	12.3	14.9	17.5	5.8	11.3																																																																											
(10)	14/08/2003	<table border="1" style="width: 100%; border-collapse: collapse;"> <thead> <tr> <th></th><th>1</th><th>2</th><th>3</th><th>4</th><th>5</th><th>6</th><th>7</th><th>8</th></tr> </thead> <tbody> <tr><td>Point 1</td><td>95</td><td>87</td><td>70</td><td>95</td><td>94</td><td>68</td><td>75</td><td>87</td></tr> <tr><td>Point 2</td><td>120</td><td>102</td><td>69</td><td>100</td><td>102</td><td>72</td><td>63</td><td>95</td></tr> <tr><td>Point 3</td><td>130</td><td>105</td><td>72</td><td>120</td><td>131</td><td>105</td><td>77</td><td>101</td></tr> <tr><td>Point 4</td><td>135</td><td>110</td><td>62</td><td>125</td><td>122</td><td>107</td><td>77</td><td>115</td></tr> <tr><td>Point 5</td><td>123</td><td>100</td><td>73</td><td>114</td><td>127</td><td>99</td><td>76</td><td>110</td></tr> <tr><td>Point 6</td><td>110</td><td>104</td><td>77</td><td>103</td><td>104</td><td>85</td><td>78</td><td>98</td></tr> <tr> <td>average =</td><td>118.8</td><td>101.3</td><td>70.5</td><td>109.5</td><td>113.3</td><td>89.3</td><td>74.3</td><td>101.0</td></tr> <tr> <td>Stdev =</td><td>14.5</td><td>7.8</td><td>5.0</td><td>11.9</td><td>15.3</td><td>16.9</td><td>5.6</td><td>10.2</td></tr> </tbody> </table>		1	2	3	4	5	6	7	8	Point 1	95	87	70	95	94	68	75	87	Point 2	120	102	69	100	102	72	63	95	Point 3	130	105	72	120	131	105	77	101	Point 4	135	110	62	125	122	107	77	115	Point 5	123	100	73	114	127	99	76	110	Point 6	110	104	77	103	104	85	78	98	average =	118.8	101.3	70.5	109.5	113.3	89.3	74.3	101.0	Stdev =	14.5	7.8	5.0	11.9	15.3	16.9	5.6	10.2
	1	2	3	4	5	6	7	8																																																																											
Point 1	95	87	70	95	94	68	75	87																																																																											
Point 2	120	102	69	100	102	72	63	95																																																																											
Point 3	130	105	72	120	131	105	77	101																																																																											
Point 4	135	110	62	125	122	107	77	115																																																																											
Point 5	123	100	73	114	127	99	76	110																																																																											
Point 6	110	104	77	103	104	85	78	98																																																																											
average =	118.8	101.3	70.5	109.5	113.3	89.3	74.3	101.0																																																																											
Stdev =	14.5	7.8	5.0	11.9	15.3	16.9	5.6	10.2																																																																											

Melbourne WTS Corrosion pin data (Cont).

WTS MH2 Shallow conduit

(11) 2/08/2004

	Stations							
	1	2	3	4	5	6	7	8
Point 1	92	91	87	85	90	75	85	95
Point 2	108	101	70	101	113	72	83	93
Point 3	120	103	72	107	118	96	75	95
Point 4	127	112	61	122	123	100	75	115
Point 5	131	107	73	115	127	100	70	110
Point 6	112	104	78	104	104	90	80	100
average =	115.0	103.0	73.5	105.7	112.5	88.8	78.0	101.3
Stdev =	14.2	7.0	8.6	12.7	13.6	12.5	5.7	9.1

Average= 97.2
Stdev = 17.7

(12) 22/09/2005

	Stations							
	1	2	3	4	5	6	7	8
Point 1	92	90	85	83	90	90	90	95
Point 2	107	101	72	104	111	72	95	92
Point 3	118	105	72	108	123	95	75	94
Point 4	126	115	72	123	123	101	75	114
Point 5	131	115	72	112	128	103	75	106
Point 6	116	102	79	102	105	93	80	100
average =	115.0	104.7	75.3	105.3	113.3	92.3	81.7	100.2
Stdev =	14.0	9.5	5.5	13.2	14.3	11.1	8.8	8.4

Average= 98.5
Stdev = 16.9

(13) 13/12/2006

	Stations							
	1	2	3	4	5	6	7	8
Point 1	102	97	77	97	95	96	86	86
Point 2	125	102	77	105	120	97	72	100
Point 3	135	110	70	120	130	115	90	105
Point 4	143	120	70	125	134	116	82	120
Point 5	135	105	72	115	132	106	85	117
Point 6	112	107	81	110	102	100	84	103
average =	125.3	106.8	74.5	112.0	118.8	105.0	83.2	105.2
Stdev =	15.6	7.8	4.5	10.2	16.6	8.9	6.1	12.3

Average= 103.9
Stdev = 19.1

(14) 1/07/2008

	Stations							
	1	2	3	4	5	6	7	8
Point 1	103	99	78	98	95	96	86	86
Point 2	125	102	78	105	120	98	73	101
Point 3	136	111	71	121	131	115	91	106
Point 4	145	121	71	125	134	116	82	121
Point 5	135	105	72	114	133	107	85	118
Point 6	114	107	82	101	103	101	85	104
average =	126.3	107.5	75.3	110.7	119.3	105.5	83.7	106.0
Stdev =	15.6	7.8	4.6	11.0	16.7	8.6	6.0	12.6

Average= 104.3
Stdev = 19.1

Melbourne WTS Corrosion pin data (Cont).

WTS MH9 Shallow conduit

Raw data (mm)

(1) 2/10/1997

	Stations							
	1	2	3	4	5	6	7	8
Point 1	86	82	74	85	91	90	79	81
Point 2	120	96	80	93	110	95	76	101
Point 3	130	96	80	100	128	104	70	104
Point 4	131	104	71	106	122	115	67	110
Point 5	109	95	70	107	107	116	78	108
Point 6	97	68	70	96	84	112	72	93
average	112.2	90.2	74.2	97.8	107.0	105.3	73.7	99.5
Stdev =	18.2	13.0	4.8	8.3	17.1	10.9	4.8	10.9

Average 95.0
Stdev = 17.6

(2) 5/02/1998

	Stations							
	1	2	3	4	5	6	7	8
Point 1	100	86	76	75	92	97	75	77
Point 2	120	96	78	91	105	105	76	101
Point 3	130	99	76	104	126	118	65	105
Point 4	131	101	78	104	122	113	66	107
Point 5	110	98	72	101	103	113	75	105
Point 6	96	80	71	91	83	110	72	95
average	114.5	93.3	75.2	94.3	105.2	109.3	71.5	98.3
Stdev =	14.9	8.4	3.0	11.2	16.7	7.4	4.8	11.3

Average 95.2
Stdev = 17.5

(3) 15/04/1998

	Stations							
	1	2	3	4	5	6	7	8
Point 1	100	81	77	81	91	97	76	81
Point 2	120	96	78	95	107	106	80	103
Point 3	130	98	80	105	126	118	72	105
Point 4	131	103	78	104	126	116	67	110
Point 5	110	99	71	101	107	113	78	104
Point 6	96	80	70	95	87	107	72	95
average	114.5	92.8	75.7	96.8	107.3	109.5	74.2	99.7
Stdev =	14.9	9.8	4.1	8.9	16.6	7.8	4.8	10.3

Average 96.3
Stdev = 17.1

(4) 1/06/1998

	Stations							
	1	2	3	4	5	6	7	8
Point 1	100	87	77	86	93	92	77	92
Point 2	119	97	78	91	107	106	77	101
Point 3	132	98	80	107	127	118	76	105
Point 4	131	103	78	108	123	116	67	110
Point 5	116	95	74	102	106	118	78	104
Point 6	96	81	70	95	86	115	72	95
average	115.7	93.5	76.2	98.2	107.0	110.8	74.5	101.2
Stdev =	15.1	8.0	3.6	8.9	16.1	10.2	4.2	6.7

Average 97.1
Stdev = 17.1

(5) 27/01/1999

	Stations							
	1	2	3	4	5	6	7	8
Point 1	82	82	81	91	91	91	83	83
Point 2	118	97	82	96	109	100	77	103
Point 3	130	102	84	98	126	96	74	105
Point 4	130	108	82	105	123	113	74	114
Point 5	116	95	82	104	106	115	76	112
Point 6	94	65	70	95	86	108	72	94
average	111.7	91.5	80.2	98.2	106.8	103.8	76.0	101.8
Stdev =	19.6	15.6	5.1	5.4	16.2	9.7	3.8	11.7

Average 96.3
Stdev = 16.5

Melbourne WTS Corrosion pin data (Cont).

WTS MH9 Shallow conduit

(6) 27/01/2000

	Stations							
	1	2	3	4	5	6	7	8
Point 1	100	90	90	98	120	98	85	103
Point 2	124	96	90	91	129	104	83	106
Point 3	126	95	89	108	130	115	75	110
Point 4	130	101	83	111	130	118	80	112
Point 5	112	95	99	103	114	115	81	116
Point 6	90	68	83	93	88	105	85	104
average	113.7	90.8	89.0	100.7	118.5	109.2	81.5	108.5
Stdev =	16.0	11.7	5.9	8.1	16.3	7.9	3.8	5.0

Average 101.5
Stdev = 15.7

(7) 14/03/2001

	Stations							
	1	2	3	4	5	6	7	8
Point 1	99	97	95	102	101	99	95	99
Point 2	131	106	95	90	134	105	87	113
Point 3	134	104	96	104	129	124	76	117
Point 4	141	117	87	115	120	122	83	116
Point 5	117	103	94	102	115	121	83	116
Point 6	108	85	92	94	87	111	86	94
average	121.7	102.0	93.2	101.2	114.3	113.7	85.0	109.2
Stdev =	16.3	10.6	3.3	8.7	17.7	10.3	6.2	10.0

Average 105.0
Stdev = 15.5

(8) 9/05/2002

	Stations							
	1	2	3	4	5	6	7	8
Point 1	102	99	93	105	111	104	89	102
Point 2	139	112	100	111	134	111	84	109
Point 3	147	106	94	109	135	121	87	129
Point 4	137	118	96	119	120	122	89	130
Point 5	136	108	99	108	104	113	79	117
Point 6	111	101	94	94	88	121	94	95
average	128.7	107.3	96.0	107.7	115.3	115.3	87.0	113.7
Stdev =	17.8	7.0	2.9	8.2	18.2	7.2	5.1	14.3

Average 108.9
Stdev = 16.1

(9) 15/08/2003

	Stations							
	1	2	3	4	5	6	7	8
Point 1	118	105	100	120	132	117	100	110
Point 2	141	118	100	117	147	120	102	150
Point 3	128	120	100	128	140	132	87	132
Point 4	152	125	105	124	120	122	91	130
Point 5	141	117	105	116	105	126	96	143
Point 6	120	118	118	95	87	117	95	130
average	133.3	117.2	104.7	116.7	121.8	122.3	95.2	132.5
Stdev =	13.5	6.6	7.0	11.5	22.7	5.8	5.6	13.7

Average 118.0
Stdev = 16.6

(10) 3/08/2004

	Stations							
	1	2	3	4	5	6	7	8
Point 1	116	110	103	110	130	111	100	111
Point 2	131	115	101	111	151	121	100	121
Point 3	131	123	100	110	132	130	105	125
Point 4	151	130	85	122	121	130	100	131
Point 5	140	110	102	113	100	131	95	130
Point 6	120	110	106	94	90	105	95	111
average	131.5	116.3	99.5	110.0	120.7	121.3	99.2	121.5
Stdev =	12.8	8.4	7.4	9.1	22.4	11.1	3.8	8.9

Average 115.0
Stdev = 15.2

Melbourne WTS Corrosion pin data (Cont).

WTS MH9 Shallow conduit
 (11) 23/09/2005

	Stations							
	1	2	3	4	5	6	7	8
Point 1	126	116	105	105	130	111	105	115
Point 2	150	130	105	117	160	129	100	122
Point 3	130	140	110	119	144	130	92	131
Point 4	160	135	110	131	115	140	90	127
Point 5	150	123	110	125	105	135	100	125
Point 6	120	117	100	95	85	130	105	124
average	139.3	126.8	106.7	115.3	123.2	129.2	98.7	124.0
Stdev =	16.1	9.8	4.1	13.2	27.2	9.8	6.4	5.4

Average 120.4
 Stdev = 17.5

(12) 14/12/2006

	Stations							
	1	2	3	4	5	6	7	8
Point 1	125	126	110	115	139	115	115	120
Point 2	160	132	105	121	157	132	110	124
Point 3	160	135	115	130	142	135	100	135
Point 4	165	142	121	135	126	145	112	127
Point 5	144	120	121	124	107	142	107	127
Point 6	130	118	121	95	87	132	111	134
average	147.3	128.8	115.5	120.0	126.3	133.5	109.2	127.8
Stdev =	17.0	9.2	6.8	14.1	25.6	10.5	5.2	5.8

Average 126.1
 Stdev = 16.6

(13) 3/07/2008

	Stations							
	1	2	3	4	5	6	7	8
Point 1	130	130	110	117	170	110	95	130
Point 2	150	140	115	127	170	140	112	140
Point 3	170	135	114	140	150	143	114	150
Point 4	170	150	120	130	140	150	114	125
Point 5	150	135	130	135	110	145	114	141
Point 6	137	120	130	114	90	130	114	137
average	151.2	135.0	119.8	127.2	138.3	136.3	110.5	137.2
Stdev =	16.5	10.0	8.5	10.1	32.5	14.5	7.6	8.8

Average 131.9
 Stdev = 18.6

Melbourne WTS Corrosion pin data (Cont).

WTS MH2 Hacketts Rd shaft - Deep tunnel

Raw data (mm)

(1) 28/07/1997

	Stations							
	1	2	3	4	5	6	7	8
Point 1	25	59	54	55	59	54	53	56
Point 2	49	71	59	59	67	57	56	64
Point 3	64	76	60	62	69	57	56	65
Point 4	78	79	64	62	75	59	61	63
Point 5	76	73	67	60	60	57	63	60
Point 6		57	66	54		48	64	37
average =	58.4	69.2	61.7	58.7	66.0	55.3	58.8	57.5
Stdev =	22.0	9.1	4.9	3.4	6.6	3.9	4.4	10.6

Average 60.6
Stdev = 9.8

(2) 11/02/1998

	Stations							
	1	2	3	4	5	6	7	8
Point 1	25	60	53	58	62	56	53	56
Point 2	50	71	60	60	68	58	56	65
Point 3	64	76	60	63	72	60	57	67
Point 4	79	80	64	63	75	59	61	65
Point 5	77	74	68	60	61	60	62	59
Point 6		57	67	56		48	65	37
average =	59.0	69.7	62.0	60.0	67.6	56.8	59.0	58.2
Stdev =	22.3	9.2	5.5	2.8	6.1	4.6	4.4	11.2

Average 61.5
Stdev = 9.9

(3) 17/04/1998

	Stations							
	1	2	3	4	5	6	7	8
Point 1	22	60	53	55	63	56	55	56
Point 2	50	72	60	60	70	60	58	65
Point 3	64	78	63	62	71	60	58	67
Point 4	80	82	66	65	76	59	65	66
Point 5	77	76	69	61	62	60	64	60
Point 6		58	73	57		50	65	37
average =	58.6	71.0	64.0	60.0	68.4	57.5	60.8	58.5
Stdev =	23.7	9.9	7.0	3.6	5.9	4.0	4.4	11.3

Average 62.3
Stdev = 10.5

(4) 2/06/1998

	Stations							
	1	2	3	4	5	6	7	8
Point 1	23	61	54	57	63	55	55	56
Point 2	51	72	60	60	70	57	56	64
Point 3	64	77	62	60	71	59	55	66
Point 4	80	82	64	63	74	59	65	66
Point 5	77	75	66	60	60	57	63	60
Point 6		61	71	57		50	64	38
average =	59.0	71.3	62.8	59.5	67.6	56.2	59.7	58.3
Stdev =	23.2	8.6	5.7	2.3	5.9	3.4	4.8	10.7

Average 61.7
Stdev = 10.2

(5) 2/02/1999

	Stations							
	1	2	3	4	5	6	7	8
Point 1	23	60	54	58	63	57	54	57
Point 2	51	73	61	62	67	61	57	64
Point 3	64	77	65	65	70	60	59	68
Point 4	80	84	69	63	74	59	64	69
Point 5	77	78	71	62	59	57	65	60
Point 6		63	75	57		49	67	38
average =	59.0	72.5	65.8	61.2	66.6	57.2	61.0	59.3
Stdev =	23.2	9.3	7.5	3.1	5.9	4.3	5.1	11.4

Average 62.8
Stdev = 10.5

Melbourne WTS Corrosion pin data (Cont).

WTS MH2 Hacketts Rd shaft - Deep tunnel

(6) 4/02/2000

	Stations							
	1	2	3	4	5	6	7	8
Point 1	26	60	55	58	63	56	55	87
Point 2	49	73	60	62	67	59	56	62
Point 3	65	77	62	66	67	60	60	66
Point 4	78	83	62	62	76	60	63	63
Point 5	77	75	69	62	61	58	65	58
Point 6		58	73	62		50	66	40
average =	59.0	71.0	63.5	62.0	66.8	57.2	60.8	62.7
Stdev =	21.9	9.9	6.5	2.5	5.8	3.8	4.6	15.1

Average 62.9
Stdev = 10.4

(7) 20/03/2001

	Stations							
	1	2	3	4	5	6	7	8
Point 1	28	61	57	61	66	62	63	57
Point 2	72	73	65	67	67	63	60	62
Point 3	87	78	74	68	72	59	60	72
Point 4	76	89	76	65	80	60	66	73
Point 5	66	81	75	62	61	58	69	69
Point 6		65	77	63		50	68	42
average =	65.8	74.5	70.7	64.3	69.2	58.7	64.3	62.5
Stdev =	22.5	10.4	8.0	2.8	7.2	4.6	3.9	11.8

Average 66.2
Stdev = 10.6

(8) 14/05/2002

	Stations							
	1	2	3	4	5	6	7	8
Point 1	29	59	54	64	70	64	64	61
Point 2	77	71	59	69	67	67	60	71
Point 3	87	80	62	70	79	67	66	76
Point 4	77	89	66	69	82	62	66	73
Point 5	65	76	71	65	61	59	74	65
Point 6		69	74	56		54	69	47
average =	67.0	74.0	64.3	65.5	71.8	62.2	66.5	65.5
Stdev =	22.6	10.2	7.5	5.2	8.6	5.0	4.7	10.6

Average 67.0
Stdev = 10.2

(9) 18/08/2003

	Stations							
	1	2	3	4	5	6	7	8
Point 1	31	59	56	66	70	66	65	61
Point 2	78	75	62	69	68	70	60	73
Point 3	90	81	64	71	79	71	68	78
Point 4	78	90	67	70	84	65	69	74
Point 5	67	80	72	67	63	61	76	66
Point 6	62	69	75	57	68	56	70	47
average =	67.7	75.7	66.0	66.7	72.0	64.8	68.0	66.5
Stdev =	20.4	10.7	6.9	5.1	7.9	5.6	5.3	11.3

Average 68.4
Stdev = 10.1

(10) 5/08/200

	Stations							
	1	2	3	4	5	6	7	8
Point 1	66	73	82	71	71	70	70	67
Point 2	83	70	91	73	70	65	60	71
Point 3	82	72	90	76	82	66	64	77
Point 4	80	76	81	74	81	62	64	75
Point 5	30	78	71	70	66	61	80	75
Point 6								
average =	68.2	73.8	83.0	72.8	74.0	64.8	67.6	73.0
Stdev =	22.4	3.2	8.1	2.4	7.1	3.6	7.8	4.0

Average 72.2
Stdev = 10.1

Melbourne WTS Corrosion pin data (Cont).

WTS MH2 Hacketts Rd shaft - Deep tunnel

(11) 26/09/20

	Stations							
	1	2	3	4	5	6	7	8
Point 1	75	78	82	78	71	70	78	75
Point 2	95	79	96	80	70	68	69	78
Point 3	70	80	98	75	84	70	69	85
Point 4	90	79	85	80	89	63	65	80
Point 5	45	78	71	72	78	65	89	79
Point 6	45	80		70	80	69	90	80
average =	70.0	79.0	86.4	75.8	78.7	67.5	76.7	79.5
Stdev =	21.4	0.9	11.0	4.2	7.4	2.9	10.8	3.3

Average 76.5
Stdev = 10.6

(12) 26/08/20

	Stations							
	1	2	3	4	5	6	7	8
Point 1	76	78	83	79	72	71	78	76
Point 2	96	79	97	80	71	69	70	79
Point 3	71	81	99	76	84	71	70	86
Point 4	91	80	86	81	89	64	66	81
Point 5	46	79	72	73	79	66	89	80
Point 6	46	81		70	81	70	91	80
average =	71.0	79.7	87.4	76.5	79.3	68.5	77.3	80.3
Stdev =	21.4	1.2	11.0	4.3	6.9	2.9	10.6	3.3

Average 77.3
Stdev = 10.5

Melbourne WTS Corrosion pin data (Cont).

WTS MH25 Laverton base shaft - deep tunnel

Raw data (mm)										
		Stations								
		1	2	3	4	5	6	7	8	
(1)	28/07/1997	Point 1	101	95	82	89	86	88	79	95
		Point 2	113	105	81	93	93	89	82	106
		Point 3	105	104	82	96	89	90	83	110
		Point 4	89	104	79	97	84	88	83	104
		Point 5	60	94	79	94	69	84	81	96
		Point 6		84	81	89		77	78	79
		average =	93.6	97.7	80.7	93.0	84.2	86.0	81.0	98.3
		Stdev =	20.7	8.3	1.4	3.4	9.1	4.9	2.1	11.1
(2)	11/02/1998	Point 1	101	95	81	89	90	87	80	95
		Point 2	113	106	80	92	93	88	83	107
		Point 3	105	105	80	97	91	90	83	108
		Point 4	89	104	79	97	84	89	82	103
		Point 5	60	94	81	95	72	86	80	96
		Point 6		84	79	90		80	80	80
		average =	93.6	98.0	80.0	93.3	86.0	86.7	81.3	98.2
		Stdev =	20.7	8.6	0.9	3.5	8.5	3.6	1.5	10.4
(3)	20/04/1998	Point 1	100	97	81	88	87	91	80	98
		Point 2	111	105	81	93	95	92	83	108
		Point 3	105	105	81	98	93	93	83	109
		Point 4	91	103	80	97	84	90	82	105
		Point 5	61	95	80	94	72	89	81	95
		Point 6		85	81	91		79	79	79
		average =	93.6	98.3	80.7	93.5	86.2	89.0	81.3	99.0
		Stdev =	19.6	7.8	0.5	3.7	9.1	5.1	1.6	11.3
(4)	3/06/1998	Point 1	100	98	86	89	90	91	84	98
		Point 2	110	103	83	93	97	92	82	107
		Point 3	105	107	84	98	93	90	83	110
		Point 4	90	105	82	98	84	90	82	105
		Point 5	62	92	80	95	72	89	81	95
		Point 6		81	81	90		80	80	78
		average =	93.4	97.7	82.7	93.8	87.2	88.7	82.0	98.8
		Stdev =	19.0	9.8	2.2	3.9	9.7	4.4	1.4	11.7
(5)	3/02/1999	Point 1	103	91	80	90	90	90	79	98
		Point 2	114	105	79	92	93	91	83	108
		Point 3	106	105	82	99	91	91	83	109
		Point 4	87	103	82	98	84	93	81	106
		Point 5	61	96	77	94	71	87	82	95
		Point 6		85	79	89		89	78	77
		average =	94.2	97.5	79.8	93.7	85.8	90.2	81.0	98.8
		Stdev =	21.0	8.3	1.9	4.1	8.9	2.0	2.1	12.1
(6)	3/02/2000	Point 1	80	88	79	90	89	90	88	101
		Point 2	95	90	83	93	97	93	89	108
		Point 3	94	93	82	99	94	90	90	109
		Point 4	88	93	82	99	88	95	85	109
		Point 5	70	94	85	97	71	88	86	96
		Point 6		88	84	91		85	85	85
		average =	85.4	91.0	82.5	94.8	87.8	90.2	87.2	101.3
		Stdev =	10.5	2.7	2.1	4.0	10.1	3.5	2.1	9.6

Melbourne WTS Corrosion pin data (Cont).

WTS MH25 Laverton base shaft - deep tunnel

(7) 30/03/2001

	Stations							
	1	2	3	4	5	6	7	8
Point 1	110	99	86	89	94	91	91	106
Point 2	118	105	86	94	98	96	87	114
Point 3	111	112	83	100	95	99	88	116
Point 4	97	110	83	101	91	98	81	110
Point 5	62	100	89	100	69	95	87	94
Point 6		95	86	93		84	84	86
average =	99.6	103.	85.5	96.2	89.4	93.8	86.3	104.3
Stdev =	22.3	6.7	2.3	4.9	11.7	5.6	3.4	11.9

Average 94.8
Stdev = 11.6

(8) 22/05/2002

	Stations							
	1	2	3	4	5	6	7	8
Point 1	111	101	91	92	94	94	90	101
Point 2	118	106	87	98	97	95	86	110
Point 3	114	115	89	100	98	98	86	115
Point 4	97	109	83	100	88	94	89	114
Point 5	61	100	89	100	77	92	83	103
Point 6		95	88	94		91	87	84
average =	100.2	104.	87.8	97.3	90.8	94.0	86.8	104.5
Stdev =	23.3	7.1	2.7	3.5	8.6	2.4	2.5	11.5

Average 95.7
Stdev = 11.1

(9) 19/08/2003

	Stations							
	1	2	3	4	5	6	7	8
Point 1	113	100	92	94	96	95	92	104
Point 2	119	107	88	99	97	95	87	109
Point 3	116	117	90	101	99	97	89	117
Point 4	97	110	83	102	86	96	89	116
Point 5	61	100	89	100	78	93	87	105
Point 6		96	89	96	95	93	89	86
average =	101.2	105.	88.5	98.7	91.8	94.8	88.8	106.2
Stdev =	24.0	7.8	3.0	3.1	8.1	1.6	1.8	11.3

Average 96.8
Stdev = 11.1

(10) 6/08/2004

	Stations							
	1	2	3	4	5	6	7	8
Point 1	112	107	102	92	103	95	92	92
Point 2	114	112	94	103	90	103	96	120
Point 3	116	117	93	108	90	100	92	115
Point 4	105	115	85	107	88	100	90	121
Point 5	76	105	86	104	77	92	92	111
Point 6		100	91	98		92	90	94
average =	104.6	109.	91.8	102.0	89.6	97.0	92.0	108.8
Stdev =	16.5	6.5	6.2	6.0	9.2	4.6	2.2	12.8

Average 99.5
Stdev = 11.0

(11) 27/09/2005

	Stations							
	1	2	3	4	5	6	7	8
Point 1	116	112	102	92	103	99	94	92
Point 2	115	115	99	103	90	115	96	120
Point 3	118	119	100	112	95	110	97	120
Point 4	110	120	85	110	90	100	94	120
Point 5	80	110	86	109	90	94	94	115
Point 6		100	91	100		92	92	100
average =	107.8	112.	93.8	104.3	93.6	101.7	94.5	111.2
Stdev =	15.8	7.3	7.5	7.6	5.7	9.0	1.8	12.2

Average 102.
Stdev = 11.1

(12) 17/09/2008

	Stations							
	1	2	3	4	5	6	7	8
Point 1	116	113	103	93	103	100	94	92
Point 2	116	115	100	104	90	116	97	120
Point 3	118	120	100	113	96	111	97	121
Point 4	111	122	87	111	91	101	95	121
Point 5	80	111	86	109	91	94	95	115
Point 6		100	91	100		93	93	100
average =	108.2	113.	94.5	105.0	94.2	102.5	95.2	111.5
Stdev =	16.0	7.8	7.4	7.6	5.4	9.2	1.6	12.5

Average 103.
Stdev = 11.2

Melbourne WTS Corrosion pin data (Cont).

WTS MH30 Doherty's Rd - deep tunnel

Raw data (mm)											
		Stations									
		1	2	3	4	5	6	7	8		
(1)	28/07/1997	Point 1	50	42	34	41	42	39	35	41	
		Point 2	58	54	32	46	45	43	37	50	
		Point 3	53	60	31	48	44	44	35	57	
		Point 4	39	65	29	46	37	43	36	59	
		Point 5	19	61	34	43	26	40	40	54	
		Point 6		52	29	39		34	38	45	
		average =	43.8	55.7	31.5	43.8	38.8	40.5	36.8	51.0	
		Stdev =	15.5	8.2	2.3	3.4	7.8	3.7	1.9	7.0	
									Average= 42.8 Stdev = 10.0		
(2)	11/02/1998	Point 1	51	43	35	42	43	40	36	42	
		Point 2	58	54	34	46	45	43	38	51	
		Point 3	54	61	33	48	45	48	38	55	
		Point 4	39	67	31	46	38	44	35	61	
		Point 5	20	66	36	43	27	40	41	55	
		Point 6		55	29	40		35	39	45	
		average =	44.4	57.7	33.0	44.2	39.6	41.7	37.8	51.5	
		Stdev =	15.4	9.0	2.6	3.0	7.6	4.4	2.1	7.0	
									Average= 43.8 Stdev = 10.1		
(3)	16/04/1998	Point 1	51	42	35	42	43	40	36	41	
		Point 2	58	55	34	48	47	45	38	50	
		Point 3	53	61	33	49	45	46	38	57	
		Point 4	39	67	31	47	39	44	36	60	
		Point 5	20	66	36	44	26	40	40	56	
		Point 6		55	29	40		35	38	47	
		average =	44.2	57.7	33.0	45.0	40.0	41.7	37.7	51.8	
		Stdev =	15.2	9.2	2.6	3.6	8.4	4.1	1.5	7.1	
									Average= 44.0 Stdev = 10.2		
(4)	3/06/1998	Point 1	50	42	35	42	43	40	35	43	
		Point 2	60	54	33	46	46	43	38	51	
		Point 3	55	61	33	49	45	45	35	57	
		Point 4	39	65	30	46	38	40	35	60	
		Point 5	21	62	36	42	26	40	40	56	
		Point 6		54	29	40		34	37	46	
		average =	45.0	56.3	32.7	44.2	39.6	40.3	36.7	52.2	
		Stdev =	15.5	8.3	2.7	3.4	8.2	3.7	2.1	6.7	
									Average= 43.4 Stdev = 10.1		
(5)	27/01/1999	Point 1	48	42	35	41	42	43	36	41	
		Point 2	62	53	34	47	46	45	37	51	
		Point 3	66	60	32	49	44	46	37	57	
		Point 4	56	65	31	47	37	44	37	60	
		Point 5	26	62	34	43	25	40	42	56	
		Point 6		53	29	40		35	38	46	
		average =	51.6	55.8	32.5	44.5	38.8	42.2	37.8	51.8	
		Stdev =	15.8	8.3	2.3	3.7	8.4	4.1	2.1	7.3	
									Average= 44.3 Stdev = 10.3		

Melbourne WTS Corrosion pin data (Cont).

WTS MH30 Doherty's Rd - deep tunnel

(6)

2/02/2000

	Stations							
	1	2	3	4	5	6	7	8
Point 1	52	44	34	41	50	40	36	42
Point 2	58	55	33	47	52	43	37	50
Point 3	52	60	31	48	48	46	37	58
Point 4	40	66	29	47	39	44	36	60
Point 5	19	61	33	43	26	40	45	60
Point 6		54	28	39		45	37	48
average = 44.2 56.7 31.3 44.2 43.0 43.0 38.0 53.0								
Stdev = 15.5 7.6 2.4 3.7 10.7 2.5 3.5 7.5								

Average= 44.2
Stdev = 10.3

(7)

29/03/2001

	Stations							
	1	2	3	4	5	6	7	8
Point 1	49	46	35	45	44	43	39	44
Point 2	64	58	34	48	47	44	40	54
Point 3	67	64	33	51	44	46	40	63
Point 4	55	70	32	48	39	44	39	64
Point 5	26	71	42	45	25	41	51	58
Point 6		60	30	39		35	42	50
average = 52.2 61.5 34.3 46.0 39.8 42.2 41.8 55.5								
Stdev = 16.3 9.2 4.1 4.1 8.8 3.9 4.6 7.7								

Average= 46.7
Stdev = 11.4

(8)

28/05/2002

	Stations							
	1	2	3	4	5	6	7	8
Point 1	51	45	37	45	45	45	38	45
Point 2	65	59	37	48	47	45	41	54
Point 3	68	65	36	50	46	47	40	64
Point 4	60	70	36	48	39	44	43	67
Point 5	28	69	45	45	28	42	48	59
Point 6		60	37	40		34	41	50
average = 54.4 61.3 38.0 46.0 41.0 42.8 41.8 56.5								
Stdev = 16.1 9.2 3.5 3.5 7.9 4.6 3.4 8.4								

Average= 47.7
Stdev = 10.9

(9)

21/08/2003

	Stations							
	1	2	3	4	5	6	7	8
Point 1	50	45	32	46	46	46	40	49
Point 2	62	50	39	49	47	49	42	59
Point 3	66	67	35	52	47	48	41	67
Point 4	59	71	36	48	39	44	49	63
Point 5	27	70	33	46	30	50	52	65
Point 6		60	34	40		42	42	55
average = 52.8 60.5 34.8 46.8 41.8 46.5 44.3 59.7								
Stdev = 15.6 10.9 2.5 4.0 7.4 3.1 4.9 6.8								

Average= 48.5
Stdev = 11.0

(10)

9/08/2004

	Stations							
	1	2	3	4	5	6	7	8
Point 1	60	51	38	45	46	50	42	51
Point 2	70	52	37	51	45	51	45	60
Point 3	66	66	33	51	46	50	43	65
Point 4	61	73	35	50	45	48	43	70
Point 5		73	41	47	40	45	51	65
Point 6		66	34	40		40	45	52
average = 64.3 63.5 36.3 47.3 44.4 47.3 44.8 60.5								
Stdev = 4.6 9.8 2.9 4.3 2.5 4.2 3.3 7.7								

Average= 50.6
Stdev = 10.9

Melbourne WTS Corrosion pin data (Cont).

WTS MH30 Doherty's Rd - deep tunnel
 (11) 30/09/2005

	Stations							
	1	2	3	4	5	6	7	8
Point 1	60	56	50	51	45	52	50	50
Point 2	70	62	45	56	50	50	50	60
Point 3	66	70	42	55	50	50	50	65
Point 4	61	75	40	53	48	50	50	70
Point 5		75	40	50	50	50	47	62
Point 6		70	33	42	0	45	42	54
average = 64.3 68.0 41.7 51.2 40.5 49.5 48.2 60.2								
Stdev = 4.6 7.6 5.7 5.0 19.9 2.3 3.3 7.3								

Average= 52.4
 Stdev = 12.5

(12) 4/01/2007

	Stations							
	1	2	3	4	5	6	7	8
Point 1	60	52	50	45	60	47	45	80
Point 2	70	60	46	53	56	50	44	51
Point 3	73	70	41	56	43	51	44	71
Point 4	65	76	39	50	51	51	43	70
Point 5	31	74	41	46	50	46	64	67
Point 6		69	34	40		36	43	54
average = 59.8 66.8 41.8 48.3 52.0 46.8 47.2 65.5								
Stdev = 16.8 9.1 5.6 5.8 6.4 5.7 8.3 11.0								

Average= 53.4
 Stdev = 12.3

(13) 11/07/2008

	Stations							
	1	2	3	4	5	6	7	8
Point 1	61	70	45	60	55	57	51	65
Point 2	71	74	47	60	52	55	50	65
Point 3	75	75	42	55	54	55	47	73
Point 4	72	80	40	54	47	55	49	73
Point 5	40	84	40	50	44	50	45	65
Point 6		70		47		35		65
average = 63.8 75.5 42.8 54.3 50.4 51.2 48.4 67.7								
Stdev = 14.3 5.6 3.1 5.2 4.7 8.3 2.4 4.1								

Average= 57.3
 Stdev = 12.3

Melbourne WTS Corrosion pin data (Cont).

WTS MH32 Smith St shaft - Deep tunnel

Raw data (mm)									
		Stations							
(1)	28/07/1997	1	2	3	4	5	6	7	8
Point 1	48	42	30	36	40	35	29	39	
Point 2	71	61	34	44	48	42	31	55	
Point 3	79	75	38	49	53	46	33	65	
Point 4	66	79	39	50	49	46	34	68	
Point 5	44	74	44	48	42	45	36	66	
Point 6		64	46	43		42	40	56	
average =		61.6	65.8	38.5	45.0	46.4	42.7	33.8	58.2
Stdev =		15.0	13.6	6.0	5.2	5.3	4.2	3.9	10.8

Raw data (mm)									
		Stations							
(2)	11/02/1998	1	2	3	4	5	6	7	8
Point 1	48	42	30	36	40	35	29	39	
Point 2	71	61	34	44	48	43	31	55	
Point 3	79	75	38	49	53	46	33	65	
Point 4	66	79	39	50	49	46	35	68	
Point 5	44	74	44	48	42	45	35	66	
Point 6		64	46	43		42	41	56	
average =		61.6	65.8	38.5	45.0	46.4	42.8	34.0	58.2
Stdev =		15.0	13.6	6.0	5.2	5.3	4.2	4.1	10.8

Raw data (mm)									
		Stations							
(3)	16/04/1998	1	2	3	4	5	6	7	8
Point 1	49	39	29	35	42	36	30	42	
Point 2	72	60	34	43	50	43	34	60	
Point 3	79	75	39	49	53	49	35	66	
Point 4	67	78	40	51	50	50	39	70	
Point 5	45	75	42	49	44	47	33	64	
Point 6		65	44	51		45	44	55	
average =		62.4	65.3	38.0	46.3	47.8	45.0	35.8	59.5
Stdev =		14.8	14.6	5.5	6.3	4.6	5.1	5.0	10.0

Raw data (mm)									
		Stations							
(4)	3/06/1998	1	2	3	4	5	6	7	8
Point 1	49	42	30	36	42	34	30	41	
Point 2	72	62	34	44	47	39	30	60	
Point 3	78	75	37	48	53	49	33	65	
Point 4	65	78	40	50	50	46	24	70	
Point 5	44	74	42	48	41	47	35	64	
Point 6		63	43	51		45	44	55	
average =		61.6	65.7	37.7	46.2	46.6	43.3	32.7	59.2
Stdev =		14.6	13.3	5.0	5.5	5.1	5.7	6.7	10.2

Raw data (mm)									
		Stations							
(5)	27/01/1999	1	2	3	4	5	6	7	8
Point 1	48	42	30	36	40	35	29	39	
Point 2	71	61	34	44	48	41	30	55	
Point 3	77	75	38	49	52	45	32	64	
Point 4	65	79	40	50	48	46	34	68	
Point 5	44	75	44	48	41	44	35	66	
Point 6		65	46	43		41	42	56	
average =		61.0	66.2	38.7	45.0	45.8	42.0	33.7	58.0
Stdev =		14.4	13.7	6.0	5.2	5.1	4.0	4.7	10.7

Melbourne WTS Corrosion pin data (Cont).

WTS MH32 Smith St shaft - Deep tunnel

(6) 1/02/2000

	Stations							
	1	2	3	4	5	6	7	8
Point 1	50	43	31	37	40	35	29	40
Point 2	71	62	35	45	48	42	31	55
Point 3	78	75	39	50	52	46	30	64
Point 4	66	79	41	51	49	47	35	68
Point 5	44	74	46	48	43	45	36	65
Point 6		63	49	43		42	38	55
average =	61.8	66.0	40.2	45.7	46.4	42.8	33.2	57.8
Stdev =	14.3	13.2	6.7	5.2	4.8	4.4	3.7	10.3

Average= 49.0
Stdev = 13.5

(7) 26/03/2001

	Stations							
	1	2	3	4	5	6	7	8
Point 1	49	43	31	37	40	35	29	40
Point 2	72	61	35	45	48	41	31	55
Point 3	78	76	37	49	52	45	33	64
Point 4	66	79	40	51	49	47	34	69
Point 5	44	75	44	49	42	45	35	66
Point 6		64	45	43		42	41	56
average =	61.8	66.3	38.7	45.7	46.2	42.5	33.8	58.3
Stdev =	14.7	13.5	5.4	5.2	5.0	4.3	4.1	10.6

Average= 49.0
Stdev = 13.7

(8) 4/06/2002

	Stations							
	1	2	3	4	5	6	7	8
Point 1	51	43	31	37	40	36	29	39
Point 2	73	62	35	45	49	42	31	54
Point 3	80	76	39	49	52	46	33	64
Point 4	69	78	40	51	51	46	34	69
Point 5	44	74	47	49	43	45	36	67
Point 6		63	45	44		42	48	59
average =	63.4	66.0	39.5	45.8	47.0	42.8	35.2	58.7
Stdev =	15.2	13.1	6.0	5.1	5.2	3.8	6.7	11.1

Average= 49.6
Stdev = 13.7

(9) 26/08/2003

	Stations							
	1	2	3	4	5	6	7	8
Point 1	51	44	32	38	41	36	30	40
Point 2	74	63	35	45	49	42	32	56
Point 3	81	76	38	50	53	46	34	65
Point 4	69	78	41	51	52	47	34	70
Point 5	45	76	47	49	44	45	37	67
Point 6		64	45	45		43	49	59
average =	64.0	66.8	39.7	46.3	47.8	43.2	36.0	59.5
Stdev =	15.4	12.9	5.8	4.8	5.2	4.0	6.8	10.9

Average= 50.2
Stdev = 13.7

Melbourne WTS Corrosion pin data (Cont).

WTS MH32 (10)	Smith St shaft - Deep tunnel 10/08/2004	Stations							
		1	2	3	4	5	6	7	8
Point 1		52	45	32	37	42	35	31	41
Point 2		71	63	35	45	51	43	33	57
Point 3		77	75	40	51	51	48	35	66
Point 4		69	78	41	52	54	47	35	68
Point 5		43	72	46	50	45	45	38	70
Point 6			63	45	45		42	49	60
average =		62.4	66.0	39.8	46.7	48.6	43.3	36.8	60.3
Stdev =		14.3	12.0	5.5	5.6	4.9	4.7	6.4	10.7

Average= 50.3
Stdev = 13.1

(11)	1/10/2005	Stations							
		1	2	3	4	5	6	7	8
Point 1		50	50	32	40	45	40	40	42
Point 2		72	65	35	47	50	45	40	60
Point 3		80	80	40	54	55	50	40	68
Point 4		70	80	44	54	55	50	39	70
Point 5		45	74	50	50	50	50	39	70
Point 6			64	49	47		47	49	60
average =		63.4	68.8	41.7	48.7	51.0	47.0	41.2	61.7
Stdev =		15.1	11.6	7.3	5.3	4.2	4.0	3.9	10.7

Average= 52.7
Stdev = 12.7

(12)	5/01/2007	Stations							
		1	2	3	4	5	6	7	8
Point 1		50	50	31	39	45	40	40	42
Point 2		71	64	35	47	50	45	40	59
Point 3		78	80	40	53	54	50	40	68
Point 4		70	80	43	53	54	49	38	70
Point 5		45	74	49	50	50	49	39	70
Point 6			63	49	46		47	49	59
average =		62.8	68.5	41.2	48.0	50.6	46.7	41.0	61.3
Stdev =		14.4	11.7	7.3	5.3	3.7	3.7	4.0	10.8

Average= 52.3
Stdev = 12.6

(13)	19/09/2008	Stations							
		1	2	3	4	5	6	7	8
Point 1		51	51	33	42	46	41	41	44
Point 2		73	65	36	49	51	45	41	61
Point 3		82	83	43	55	56	51	42	68
Point 4		72	82	42	56	56	51	40	71
Point 5		47	74	55	51	51	50	40	71
Point 6			65	50	48		47	42	62
average =		65.0	70.0	43.2	50.2	52.0	47.5	41.0	62.8
Stdev =		15.2	12.2	8.3	5.1	4.2	4.0	0.9	10.2

Average= 53.8
Stdev = 12.9

Appendix XVIII. Melbourne Water WTS Corrosion rate graphs

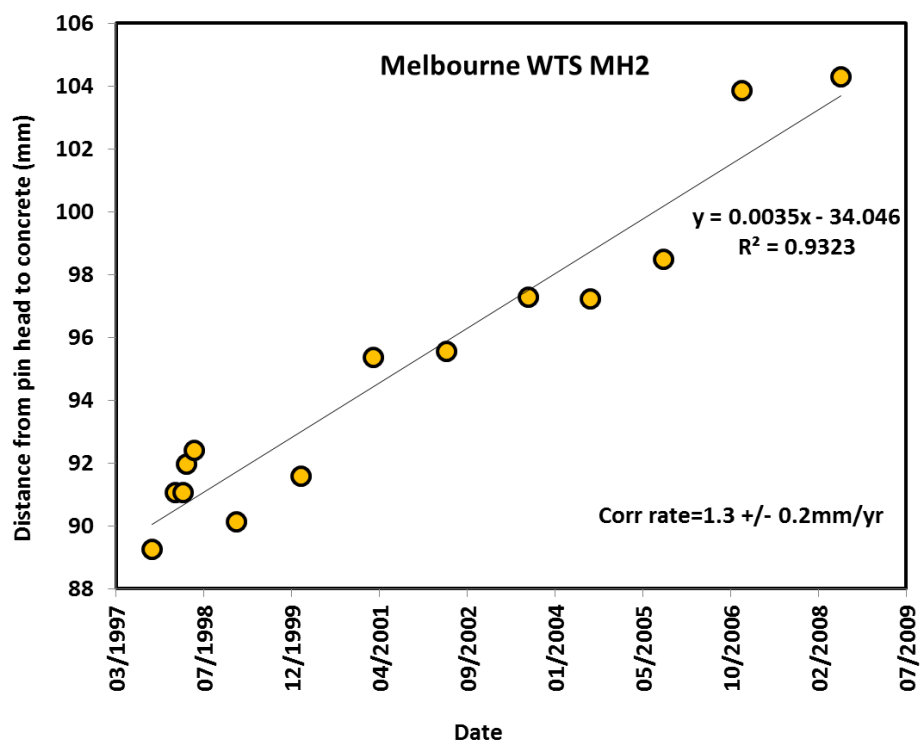


Figure 178. Erosion pin corrosion losses at Melbourne WTSMH2.

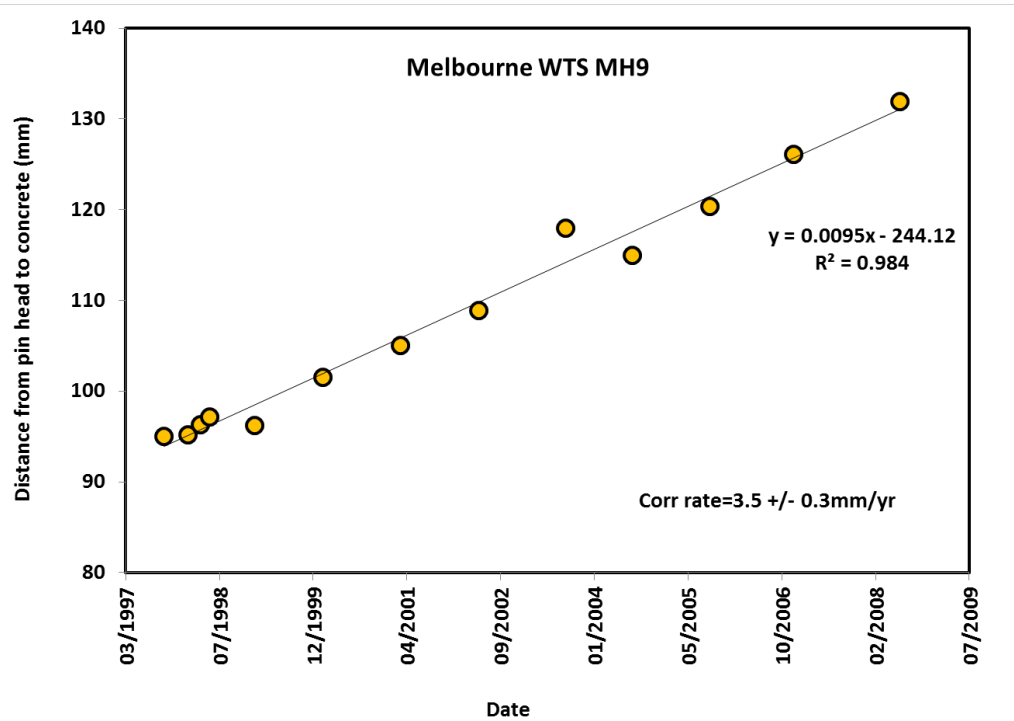


Figure 179. Erosion pin corrosion losses at Melbourne WTSMH9.

Melbourne Water WTS Corrosion rate graphs (Cont).

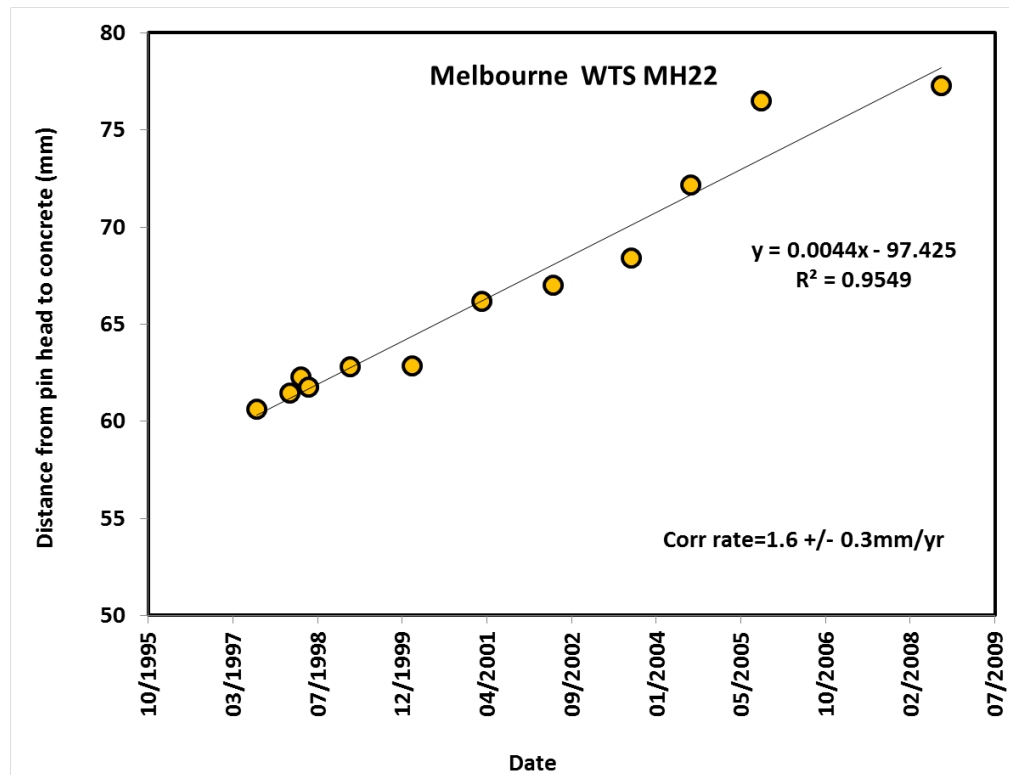


Figure 180. Erosion pin corrosion losses at Melbourne WTS MH22.

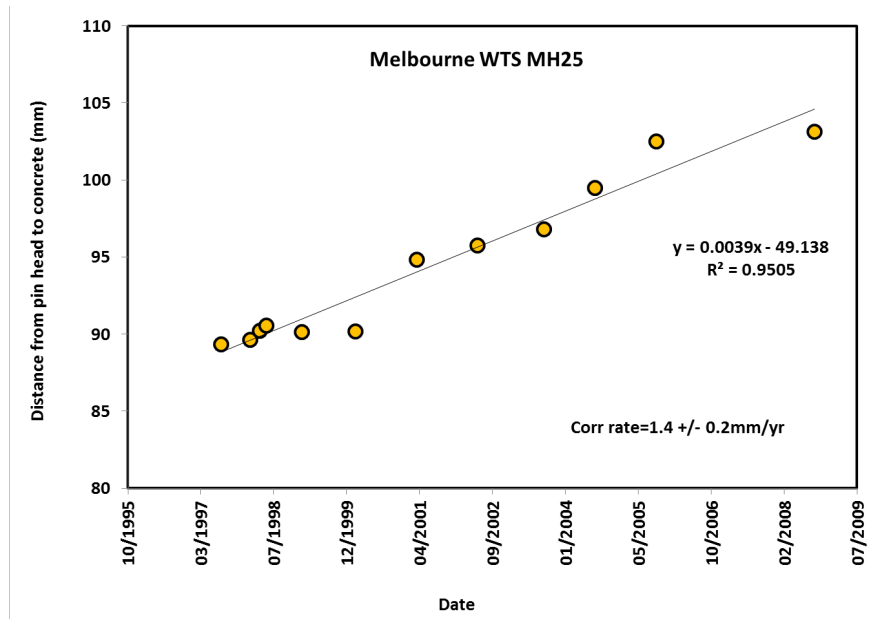


Figure 181. Erosion pin corrosion losses at Melbourne WTS MH25.

Melbourne Water WTS Corrosion rate graphs (Cont).

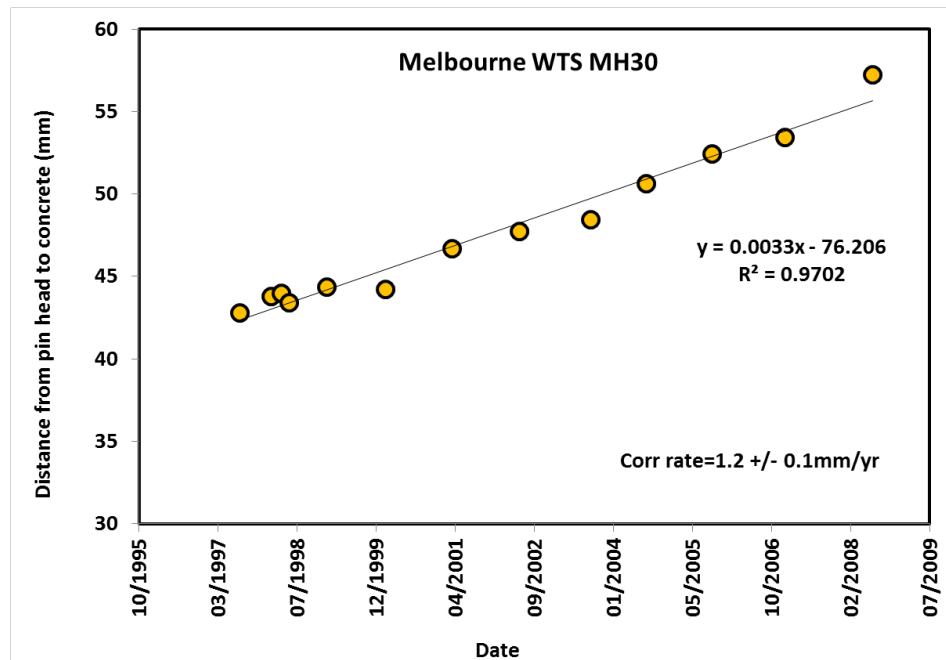


Figure 182. Erosion pin corrosion losses at Melbourne WTSMH30.

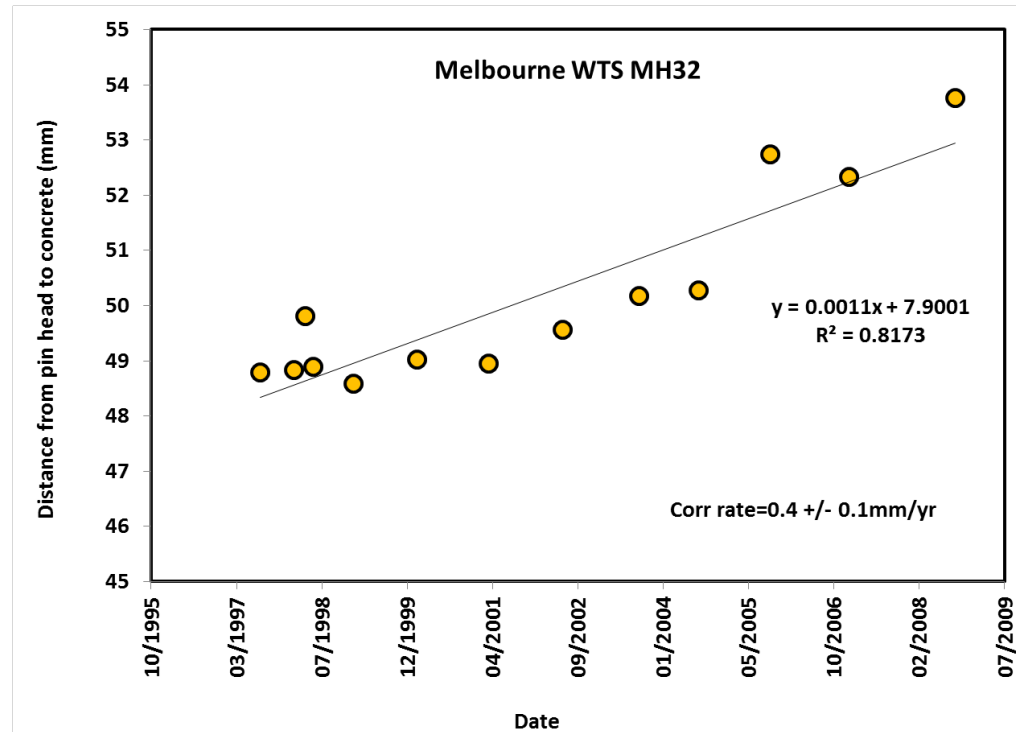


Figure 183. Erosion pin corrosion losses at Melbourne WTSMH32.

Appendix XIX. Summary of Melbourne WTS observed environmental data

Table 24. Summary of Melbourne WTS environmental data for the period 2 Jan - 13 Feb 2013

Site	Av H ₂ S	90% H ₂ S	95% H ₂ S	Av T	90% T	95% T
WTS MH2	8.2	11.1	11.6	23.0	23.4	23.5
WTS MH6	8.2	11.4	12	22.8	23.6	23.9
WTS MH7	6.4	9.1	9.6	23.0	23.8	24.1
WTS MH9	6.8	9.6	10	23.5	23.8	23.9
WTS MH14	12.0	15.5	16.2	22.9	23.2	23.3
WTS MH18	12.0	15.5	16.2	22.9	23.2	23.3
WTS MH21	3.4	5.8	6.2	20.3	20.8	20.9
WTS MH23	1.5	3.1	3.5	21.9	22.2	22.3
WTS MH29	0.2	0.3	0.5	26.3	27.5	27.9
WTS MH31	3.9	8.7	10.1	22.3	22.6	22.7
WTS MH33	0.7	1.6	1.8	24.1	24.7	24.8

Appendix XX. Schedule of returned environmental data

Years 2009-2010

Schedule of returned environmental data (Cont).

Years 2011

Schedule of returned environmental data (Cont).

Years 2012

Schedule of returned environmental data (Cont).

Year 2013

		Environmental reporting																																															
		Jan-13				Feb-13				Mar-13				Apr-13				May-13				Jun-13				Jul-13				Aug-13				Sep-13				Oct-13				Nov-13				Dec-13			
		1	2	3	4	1	2	3	4	1	2	3	4	1	2	3	4	1	2	3	4	1	2	3	4	1	2	3	4	1	2	3	4	1	2	3	4	1	2	3	4								
Sydney South arm	H2S																																																
	Air T																																																
	RH																																																
Sydney North arm	H2S																																																
	Air T																																																
	RH																																																
Melbourne SETS	H2S																																																
	Air T																																																
	RH																																																
Melbourne WTS	H2S																																																
	Air T																																																
	RH																																																
Perth MS	H2S																																																
	Air T																																																
	RH																																																
Perth Bibra Lake	H2S																																																
	Air T																																																
	RH																																																

Appendix XXI. Sp1B New coupon field data

Table 25. New coupon field data collected from Sydney field sites.

Site	time	Surface pH		Corrosion Losses (mm)		Corrosion Layer Depth (mm)	
		Average	Std Dev.	Average	Std Dev.	Average	Std Dev.
Control samples	0	10.3		0.00	0.00	0.00	0.00
	6	9.73	0.38	0.00	0.00	0.00	0.00
	12	10.03	0.27	0.00	0.00	0.00	0.00
	18.1	9.87	0.43	0.00	0.00	0.00	0.00
	31.2	9.94	0.08	0.00	0.00	0.00	0.00
<hr/>							
Sydney North roof	0.0	10.3		0.00	0.00	0.04	0.00
	8.8	7.53	0.2	0.05	0.05	0.05	0.09
	12.0	6.87	0.34	0.05	0.19	0.31	0.06
	24.0	6.92	0.54	0.06	0.02	0.18	0.03
<hr/>							
Sydney South roof	0.0	10.3	0	0.00	0.00	0.04	0.00
	8.8	7.23	0.11	0.03	0.08	0.06	0.05
	12.0	5.98	0.67	0.18	0.11	0.36	0.06
	24.0	6.66	0.49	0.14	0.03	0.21	0.08
<hr/>							
Sydney South wall	0.0	10.3		0.00	0.00	0.04	0.00
	8.8	7.53	0.17	0.04	0.24	0.05	0.15
	12.0	7.46	0.30	0.16	0.12	0.23	0.04
	24.0	7.70	0.11	0.17	0.09	0.23	0.17

New coupon field data collected from the Sp1B field samples (cont).

Table 26. New coupon field data collected from Melbourne field sites.

Site	time	Surface pH		Corrosion Losses (mm)		Corrosion Layer Depth (mm)	
		Average	Std Dev.	Average	Std Dev.	Average	Std Dev.
Melbourne SETS	0.0	10.3		0.0	0.0	0.04	0.0
	7.5	8.77	0.10	0.15	0.10	0.19	0.13
	12.6	8.44	0.26	0.02	0.11	0.12	0.08
	18.3	6.37	0.28	0.07	0.13	0.12	0.14
	24.4	6.42	0.24	0.05	0.03	0.24	0.10
	31.1	5.24	0.61	0.31	0.39	0.46	0.09
	39.4	4.95	0.04	0.83	0.07	1.38	0.04
<hr/>							
Melbourne WTS	0.0	10.3		0.00	0.00	0.04	0.0
	7.1	8.00	0.57	0.12	0.10	0.02	0.17
	12.2	6.62	1.15	0.91	0.48	0.77	0.20
	18.0	4.84	0.40	1.46	0.67	1.33	0.20
	24.0	5.17	0.88	3.84	1.07	2.31	1.24
	33.7	3.33	0.30	9.79	3.66	3.63	0.73
	39.0	3.21	0.17	11.60	1.30	3.63	0.66

New coupon field data collected from the Sp1B field samples (cont).

Table 27. New coupon field data collected from Perth field sites.

Site	time	Surface pH		Corrosion Losses (mm)		Corrosion Layer Depth (mm)	
		Average	Std Dev.	Average	Std Dev.	Average	Std Dev.
Perth MS	0.0	10.3		0.00	0.00	0.04	0.0
	7.1	6.95	0.97	0.20	0.07	0.48	0.22
	13.9	4.66	0.07	5.96	1.69	2.96	0.93
	19.3	4.27	0.14	8.69	5.20	6.21	1.49
	26.3	3.14	0.10	15.92	1.39	7.63	0.26
	31.4	2.35	0.46	23.32	3.00	8.44	1.40
	37.8	2.48	0.16	30.40	1.32	9.01	0.29
<hr/>							
Perth Bibra lake	0.0	10.3		0.00	0.00	0.04	0.0
	5.9	9.03	0.37	0.10	0.23	0.30	0.43
	12.7	5.93	0.43	0.33	0.19	0.25	0.07
	18.1	4.20	0.11	1.90	0.57	2.41	0.45
	25.1	3.76	0.13	3.46	0.87	2.86	1.01
	30.3	3.96	0.26	6.74	1.55	4.91	1.09
	36.6	3.02	0.75	7.30	1.54	3.30	1.50

Appendix XXII. Sp1B Old coupon field data

Table 28. Old coupon field data collected from Sydney field sites.

Site	time	Surface pH		Corrosion Losses (mm)		Corrosion Layer Depth (mm)	
		Average	Std Dev.	Average	Std Dev.	Average	Std Dev.
Control samples	0	8.2		0.00	0.00	0.00	0.00
	6	7.90	0.07	0.00	0.00	0.00	0.00
	12	8.00	0.26	0.00	0.00	0.00	0.00
	18.1	7.49	0.52	0.00	0.00	0.00	0.00
	31.2	7.45	0.00	0.00	0.00	0.00	0.00
Sydney North roof	0.0	8.2		0.00	0.00	2.05	0.00
	8.8	4.20	0.01	0.34	0.76	1.55	0.91
	12.0	3.92	0.15	1.25	2.01	2.80	0.84
	24.0	4.30	0.19	0.24	0.04	0.90	0.57
Sydney South roof	0.0	8.2	0	0.00	0.00	2.05	0.00
	8.8	4.11	0.25	-0.16	0.38	1.13	0.98
	12.0	3.79	0.18	2.01	1.60	3.45	0.91
	24.0	4.10	0.06	-0.51	0.88	4.56	0.00
Sydney South wall	0.0	8.2		0.00	0.00	2.05	0.00
	8.8	5.36	0.83	1.02	0.26	1.54	0.49
	12.0	4.11	0.22	1.01	1.11	1.81	0.87
	24.0	6.24	0.65	0.40	0.47	0.02	0.39

Old coupon field data collected from the Sp1B field samples (cont).

Table 29. Old coupon field data collected from Melbourne field sites.

Site	time	Surface pH		Corrosion Losses (mm)		Corrosion Layer Depth (mm)	
		Average	Std Dev.	Average	Std Dev.	Average	Std Dev.
Melbourne SETS	0.0	8.2		0.0	0.0	2.1	0.0
	7.5	6.07	0.57	1.03	1.19	3.01	1.11
	12.6	4.41	0.06	-0.10	0.85	0.47	0.28
	18.3	3.68	0.22	1.34	1.29	1.15	0.55
	24.4	3.72	0.19	-0.48	0.04	0.72	0.45
	31.1	3.44	0.12	3.90	3.65	5.12	3.54
	39.4	4.03	0.10	4.82	0.86	3.30	0.79
<hr/>							
Melbourne WTS	0.0	8.2		0.00	0.00	2.05	0.00
	7.1	3.51	0.14	2.28	2.04	3.01	1.11
	12.2	3.67	0.40	5.06	0.91	0.47	0.28
	18.0	3.48	0.30	11.06	1.19	1.15	0.55
	24.0	3.58	0.30	14.98	6.33	0.72	0.45
	33.7	2.74	0.21	19.15	4.60	5.12	3.54
	39.0	3.08	0.21	19.02	3.32	3.30	0.79

Old coupon field data collected from the Sp1B field samples (cont).

Table 30. Old coupon field data collected from Perth field sites.

Site	time	Surface pH		Corrosion Losses (mm)		Corrosion Layer Depth (mm)	
		Average	Std Dev.	Average	Std Dev.	Average	Std Dev.
Perth MS	0.0	8.2		0.00	0.00	2.05	0.00
	7.1	3.71	0.51	6.39	2.09	3.18	0.69
	13.9	4.01	0.15	12.63	0.77	6.83	2.02
	19.3	3.63	0.20	18.74	3.44	5.97	0.89
	26.3	2.94	0.13	24.71	2.30	4.12	1.16
	31.4	2.20	0.26	27.86	3.68	8.57	4.69
	37.8	2.35	0.33	30.72	4.94	6.56	0.23
<hr/>							
Perth Bibra lake	0.0	8.2		0.00	0.00	2.05	0.00
	5.9	3.76	0.09	0.78	1.73	2.88	2.52
	12.7	4.67	0.76	2.33	1.47	4.74	2.21
	18.1	3.33	0.04	5.38	5.49	4.05	2.45
	25.1	2.98	0.73	14.16	4.02	6.64	0.97
	30.3	3.65	0.30	12.51	3.38	7.39	0.28
	36.6	3.06	0.37	15.50	3.63	9.40	0.50

10 References

- [1] E. Hewayde, M. Nehdi, E. Allouche, G. Nakhla, Effect of Mixture Design Parameters and Wetting-Drying Cycles on Resistance of Concrete to Sulfuric Acid Attack, *Journal of Materials in Civil Engineering*, 19 (2007) 155-163.
- [2] E. Hewayde, M. Nehdi, E. Allouche, G. Nakhla, Effect of geopolymer cement on microstructure, compressive strength and sulphuric acid resistance of concrete, *Magazine of Concrete Research*, 58 (2006) 321-331.
- [3] L. Zhang, P. De Schryver, B. De Gusseme, W. De Muynck, N. Boon, W. Verstraete, Chemical and biological technologies for hydrogen sulfide emission control in sewer systems: A review, *Water research*, 42 (2008) 1-12.
- [4] R. Sydney, E. Esfandi, S. Surapaneni, Control Concrete Sewer Corrosion via the Crown Spray Process, *Water Environment Research*, 68 (1996) 338-347.
- [5] W.M. Olmstead, H. Hamlin, Converting portions of the Los Angles outfall sewer into a septic tank, *Engineering news*, 44(19) (1900) 317-318.
- [6] F.D. Bowlus, A.P. Banta, Control of anaerobic decomposition in sewage transportation, *Water Works Sewerage*, 79 (1932) 369.
- [7] F.M. Lea, C.H. Desch, *The chemistry of cement and concrete*, Edward Arnold, London, England, 1936.
- [8] C.D. Parker, The corrosion of concrete 1. The isolation of a species of bacterium associated with the corrosion of concrete exposed to atmospheres containing hydrogen sulphides, *The Australian journal of experimental biology and medical science*, 23 (1945) 81-90.
- [9] C.D. Parker, The corrosion of concrete 2. The function of *Thiobacillus concretivorus* (nov. spec.) in the corrosion of concrete exposed to atmospheres containing hydrogen sulphides, *The Australian journal of experimental biology and medical science*, 23 (1945) 91-98.
- [10] R. Pomeroy, F.D. Bowlus, Progress report on sulfide control research, *Sewage Works Journal*, 18 (1946) 597-640.
- [11] D. Kelly, A. Wood, Reclassification of some species of *Thiobacillus* to the newly designated genera *Acidithiobacillus* gen. nov., *Halothiobacillus* gen. nov. and *Thermithiobacillus* gen. nov, *Int J Syst Evol Microbiol*, 50 (2000) 511-516.
- [12] K.B. Tator, Preventing hydrogen sulfide and microbially influenced corrosion in wastewater facilities. , *Materials Performance*, 42 (2003) 32-37.
- [13] J.D. Gu, T.E. Ford, N.S. Berke, R. Mitchell, Biodeterioration of concrete by the fungus *Fusarium*, *International Biodeterioration & Biodegradation*, 41 (1998) 101-109.
- [14] W. Sand, T. Dumas, S. Marcdargent, Tests for biogenic sulfuric acid corrosion in a simulation chamber confirm the on-site performance of calcium aluminate-based concretes in sewage applications., in: K.D.

Basham (Ed.) Infrastructure: New materials and methods of repair - Proceedings of the Third Materials Engineering Conference, ASCE, New York, NY, 1992, pp. 35-55.

[15] D. Nica, J.L. Davis, L. Kirby, G. Zuo, D.J. Roberts, Isolation and characterization of microorganisms involved in the biodeterioration of concrete in sewers, International Biodeterioration & Biodegradation, 46 (2000) 61-68.

[16] S. Okabe, M. Odagiri, T. Ito, H. Satoh, Succession of Sulfur-Oxidizing Bacteria in the Microbial Community on Corroding Concrete in Sewer Systems., Applied and Environmental Microbiology, 73 (2007) 971-980.

[17] K.S. Cho, T. Mori, A Newly Isolated Fungus Participates in the Corrosion of Concrete Sewer Pipes, Water Science and Technology, 31 (1995) 263-271.

[18] H.S. Jensen, Hydrogen sulfide induced concrete corrosion of sewer networks, in: Section of Environmental Engineering, Aalborg University, 2009, pp. 67.

[19] H.S. Jensen, A.H. Nielsen, T. Hvítved-Jacobsen, J. Vollertsen, Modeling of Hydrogen Sulfide Oxidation in Concrete Corrosion Products from Sewer Pipes, Water Environment Research, 81 (2009) 365-373.

[20] J. Vollertsen, A.H. Nielsen, H.S. Jensen, T. Wium-Andersen, T. Hvítved-Jacobsen, Corrosion of concrete sewers - The kinetics of hydrogen sulfide oxidation., Science of the Total Environment, 394 (2008) 162-170.

[21] A.P. Joseph, J. Keller, H. Bustamante, P.L. Bond, Surface neutralization and H₂S oxidation at early stages of sewer corrosion: Influence of temperature, relative humidity and H₂S concentration, Water Research, 46 (2012) 4235-4245.

[22] A. Bielefeldt, M.G.D. Gutierrez-Padilla, S. Ovtchinnikov, J. Silverstein, M. Hernandez, Bacterial Kinetics of Sulfur Oxidizing Bacteria and Their Biodeterioration Rates of Concrete Sewer Pipe Samples, Journal of Environmental Engineering, 136 (2010) 731-738.

[23] H.S. Jensen, P.N.L. Lens, J.L. Nielsen, K. Bester, A.H. Nielsen, T. Hvítved-Jacobsen, J. Vollertsen, Growth kinetics of hydrogen sulfide oxidizing bacteria in corroded concrete from sewers, Journal of Hazardous Materials, 189 (2011) 685-691.

[24] H. Satoh, M. Odagiri, T. Ito, S. Okabe, Microbial community structures and in situ sulfate-reducing and sulfur-oxidizing activities in biofilms developed on mortar specimens in a corroded sewer system, Water research, 43 (2009) 4729-4739.

[25] R.L. Islander, J.S. Devinny, F. Mansfeld, A. Postyn, S. Hong, Microbial Ecology of Crown Corrosion in Sewers, Journal of Environmental Engineering-Asce, 117 (1991) 751-770.

[26] D.J. Roberts, D. Nica, G. Zuo, J.L. Davis, Quantifying microbially induced deterioration of concrete: initial studies, International Biodeterioration & Biodegradation, 49 (2002) 227-234.

[27] P.A. Wells, R.E. Melchers, Factors involved in the long term corrosion of concrete sewers (Paper 54), in: Conference Proceedings Corrosion and Prevention 2009: The Management of Infrastructure Deterioration, Coffs Harbour, Australia, 2009.

[28] R.E. Melchers, P.A. Wells, Modelling the long term corrosion of reinforced concrete sewers, in: 7th IWA Leading-Edge Conference on Water and Wastewater Technologies, Phoenix, Arizona, USA, 2-4 June 2010, 2009.

- [29] P.A. Wells, R.E. Melchers, Microbial corrosion of sewer pipe in australia - initial field results, in: 18th International Corrosion Conference, Perth, W.A., Australia, 2011, pp. Paper no. 183.
- [30] T. Wells, R.E. Melchers, An observation-based model for corrosion of concrete sewers under aggressive conditions., Cement and Concrete Research, (submitted) (2013).
- [31] W. Goodman, North Georges River submain section 1-3. Traverse report. Sydney Water Corporation internal report., 1997.
- [32] W. Goodman, North Georges River submain Salt Pan Creek aqueduct. Traverse report. Sydney Water Corporation internal report., 1997.
- [33] W. Goodman, North Georges River submain section 4-11. Traverse report. Sydney Water corporation internal report., 1997.
- [34] Sewer Assessment Specialists Pty Ltd, North Georges River submain sections 1-3. Traverse report 2004. Sydney Water Corporation internal report., 2004.
- [35] Sewer Assessment Specialists Pty Ltd, North Georges River submain sections 4 to 11. Traverse report 2004. Sydney Water Corporation internal report., 2004.
- [36] SAS TTI Joint Venture, North Georges River submain sections 1 to 3, 5 to 8 & 11. Traverse report. Sydney Water Report No. SWSOOS-077, 2009.
- [37] S.T.J. Venture, North Georges River submain sections 4-10. Traverse report. Sydney Water report No. SWSOOS-109, 2011.
- [38] W. Goodman, Structures and Reservoirs AWT Engineering, SWSOOS No. 2 SPS 38 to Malabar STP, December 1997.
- [39] W. Goldman, Structures and Reservoirs Group Engineering Consulting, SWSOOS, Merging Chamber to Cooks River Syphons traverse report. August 1997.
- [40] W. Goodman, SWSOOS No. 1, SPS 38 to Malabar STP travers report. September 1997., September 1997.
- [41] Kellogg Brown and Root Pty Ltd, Sewer traverse report SWSOOS 1 &2 North and South. Eve Street merging chamber to Airport Silt Pits. November 2007.
- [42] Kellogg Brown and Root Pty Ltd, Sewer traverse report SWSOOS 1 & 2 North and South. Airport Silt Pits to Cooks River Siphon., Nov 2007.
- [43] SAS TTI Joint Venture, SWSOOS No. 1 SPS38 to Malabar STP. Traverse report. June 2009.
- [44] Kellogg Brown and Root Pty Ltd, Southern and Western Suburbs Ocean outfall sewer SWSOOS No. 1 Syphon to STP. March 2012.
- [45] Kellogg Brown and Root Pty Ltd, Sewer traverse report. SWSOOS 2 North and South. Cooks River Siphon to Barwon Crescent. November 2007.
- [46] W.J. Goodman, NSOOS Sections 1 to 10 Summary of inspection reports 1993, 1993.

[47] Kellogg Brown and Root Pty Ltd, NSOOS from Clontarf Siphon House to Eustace St, Manly. Sewer Traverse report. March 2007.

[48] SAS TTI Joint Venture, NSOOS Sections 3,4 and 5 traverse report. Report No. NSOOS-093., 2007.

[49] Kellogg Brown and Root Pty Ltd, NSOOS - Sections 6-7 Sewer traverse report. SWC report Number: NSOOS-108, 2009.

[50] Kellogg Brown and Root Pty Ltd, NSOOS Section 8 Amplification Tunnels Sewer Traverse report. SWC report Number: NSOOS 130, 2011.

[51] Melbourne Water, Western trunk sewer corrosion control. Operational Strategy report. Report 323/250/0004., 1986.

[52] R. Morton, R. Caballero, C.-L. Chen, J. Redner, Study of sulfide generation and concrete corrosion of sanitary sewers, Sanitation Districts of Los Angeles County Carson, California, 1989.

[53] Hampton roads sanitation project, Basics on corrosion in wastewater collection and treatment systems., 2005.

[54] D. Apgar, J. Witherspoon, C. Easter, S. Bassari, C. Dillon, E. Torres, R.P.G. Bowker, R. Corsi, S. Davidson, P. Wolstenholme, B. Forbes, C. Quigley, M. Ward, J. Joyce, R. Morton, J. Weiss, R. Stuetz, Minimization of Odours and Corrosion in Collection Systems, Phase I. Report No. 04-CTS-1., Water Environmental Research Foundation (WERF), Alexandria, VA, USA, 2007.

[55] T. Mori, T. Nonaka, K. Tazaki, M. Koga, Y. Hikosaka, S. Noda, Interactions of nutrients, moisture and pH on microbial corrosion of concrete sewer pipes., Water research, 26 (1992) 29-37.

[56] E. Hudon, S. Mirza, D. Frigon, Biodeterioration of Concrete Sewer Pipes: A State-of-the-Art and Research Needs, Journal of Pipeline Systems Engineering and Practice, (2010).

[57] A.H.Y. Nielsen, C., T. Hvitved-Jacobsen, J. Vollertsen, Simulation of sulfide buildup in wastewater and atmosphere of sewer networks., Water Science and Technology, 52 (2005) 201-208.

[58] E. Vincke, Biogenic sulfuric acid corrosion of concrete: microbial interaction, simulation and prevention, in: Faculteit Landbouwkundige en Toegepaste Biologische, Wetenschappen, 2002.

[59] W. Sand, E. Bock, Biodeterioration of Mineral Materials by Microorganisms - Biogenic Sulfuric and Nitric-Acid Corrosion of Concrete and Natural Stone, Geomicrobiology Journal, 9 (1991) 129-138.

[60] B.I. Cayford, P.G. Dennis, J. Keller, G.W. Tyson, P.L. Bond, High-Throughput Amplicon Sequencing Reveals Distinct Communities within a Corroding Concrete Sewer System, Applied and Environmental Microbiology, 78 (2012) 7160-7162.

[61] H. Fujimoto, F. Mishina, K. Onishi, K. Miyaguchi, Evaluation of Sulfuric Acid Resistant Mortar as a Corrosion Protection Method for Sewerage Facilities, in: Third International Conference on Sustainable Construction Materials and Technologies, Kyoto, Japan, 2013.

[62] P.D. Franzmann, C.M. Haddad, R.B. Hawkes, W.J. Robertson, J.J. Plumb, Effects of temperature on the rates of iron and sulfur oxidation by selected bioleaching Bacteria and Archaea: Application of the Ratkowsky equation, Minerals Engineering, 18 (2005) 1304-1314.

- [63] A. Allahverdi, F. Škvara, Acidic corrosion of hydrated cement based materials. Part 2. Kinetics of the phenomenon and mathematical models., Ceramics - Silikáty, 44 (2000) 152-160.
- [64] C. Buisman, P. Uspeert, A. Janssen, G. Lettinga, Kinetics of chemical and biological sulphide oxidation in aqueous solutions, Water research, 24 (1990) 667-671.
- [65] V. Baroghel-Bouny, Water vapour sorption experiments on hardened cementitious materials Part 1: Essential tool for analysis of hygral behaviour and its relation to pore structure., Cement and Concrete Research, 37 (2007) 414-437.
- [66] A.H. Nielsen, J. Vollertsen, T. Hvitved-Jacobsen, Determination of Kinetics and Stoichiometry of Chemical Sulfide Oxidation in Wastewater of Sewer Networks, Environ Sci Technol, 37 (2003) 3853-3858.
- [67] F.J. Millero, S. Hubinger, M. Fernandez, S. Garnett, Oxidation of H₂S in seawater as a function of temperature, pH, and ionic strength, Environ Sci Technol, 21 (1987) 439-443.